Thermoluminescence of secondary glow peaks in carbon-doped aluminium oxide

Cleophace Seneza

Supervisor: Professor Makaiko L. Chithambo

A thesis submitted to

the Department of Physics and Electronics, Faculty of Science,

Rhodes University, in fulfilment of the requirements for the degree of

Master of Science

March 30, 2014

Abstract

Carbon-doped aluminium oxide, α-Al_2O_3 : C, is a highly sensitive luminescence dosimeter. The high sensitivity of α-Al_2O_3 : C has been attributed to large concentrations of oxygen vacancies, F and F^+ centres, induced in the material during its preparation. The material is prepared in a highly reducing atmosphere in the presence of carbon. In the luminescence process, electrons are trapped in F-centre defects as a result of irradiation of the material. Thermal or optical release of trapped electrons leads to emission of light, thermoluminescence (TL) or optically stimulated light (OSL) respectively. The thermoluminescence technique is used to study point defects involved in luminescence of α-Al_2O_3 : C. A glow curve of α-Al_2O_3 : C, generally, shows three peaks; the main dosimetric peak of high intensity (peak II) and two other peaks of lower intensity called secondary glow peaks (peaks I and III).

The overall aim of our work was to study the TL mechanisms responsible for secondary glow peaks in α-Al_2O_3 : C. The dynamics of charge movement between centres during the TL process was studied. The phototransferred thermoluminescence (PTTL) from secondary glow peaks was also studied.

The kinetic analysis of TL from secondary peaks has shown that the activation energy of peak I is 0.7 eV and that of peak III, 1.2 eV. The frequency factor, the frequency at which an electron attempts to escape a trap, was found near the range of the Debye vibration frequency. Values of the activation energy are consistent within a variety of methods used. The two peaks follow first order kinetics as confirmed by the T_M-T_{stop} method. A linear dependence of TL from peak I on dose is observed at various doses from 0.5 to 2.5 Gy. The peak position for peak I was also independent

on dose, further confirmation that peak I is of first order kinetics. Peak I suffers from thermal fading with storage with a half-life of about 120 s. The dependence of TL intensity for peak I increased as a function of heating rate from 0.2 to $6^{o}C\,s^{-1}$. In contrast to the TL intensity for peak I, the intensity of TL for peak III decreases with an increase of heating rate from 0.2 to $6^{o}C\,s^{-1}$. This is evidence of thermal quenching for peak III. Parameters $W = 1.48 \pm 0.10\,eV$ and $C = 4 \times 10^{13}$ of thermal quenching were calculated from peak III intensities at different heating rates. Thermal cleaning of peak III and the glow curve deconvolution methods confirmed that the main peak is actually overlapped by a small peak (labeled peak IIA). The kinetic analysis of peak IIA showed that it is of first order kinetics and that its activation energy is 1.0 eV. In addition, the peak IIA is affected by thermal quenching. Another secondary peak appears at 422°C (peak IV). However, the kinetic analysis of TL from peak IV was not studied because its intensity is not well defined. A heating rate of $0.4^{o}C\,s^{-1}$ was used after a dose of 3 Gy in kinetic analysis of peaks IIA and III.

The study of the PTTL showed that peaks I and II were regenerated under PTTL but peak III was not. Various effects of the PTTL for peaks I and II for different preheating temperatures in different samples were observed. The effect of annealing at 900°C for 15 minutes between measurements following each illumination time was studied. The effect of dose on secondary peaks was also studied in this work. The kinetic analysis of the PTTL intensity for peak I showed that its activation energy is 0.7 eV, consistent with the activation energy of the normal TL for peak I. The PTTL intensity from peak I fades rapidly with storage compared with the thermal fading from peak I of the normal TL. The PTTL intensity for peak I decreases as a function of heating rate. This decrease was attributed to thermal quenching. Thermal quenching was not observed in the case of the normal TL intensity. The cause of this contrast requires further study.

Dedicace

To my wife, *Marie Claire*, and our lovely children, *Bruno* and *Blandine*, whose constant love, encouragement and support have made this work possible.

Acknowledgements

This work is a fruit of many tasks handled by many people that their efforts and contributions are highly acknowledged.

My first grateful thanks to Professor Makaiko L. Chithambo, for accepting to supervise this scientific research day to day from the beginning to the end of my research programme. I would like to thank him, for his strong assistance and advice in doing experiments towards the quality of data collection. I give my deepest thanks to Professor Makaiko L. Chithambo, for guiding and encouraging me to have a good scientific writing. His supervision and techniques helped me achieve this scientific work.

Many thanks to the Department of Physics and Electronics, Rhodes University, Lecturers, Colleagues and friends, for their strong research support, collaboration and their scientific sharing of knowledge.

I would like to thank the Government of Rwanda, for supporting my study programme by giving me REB bursary that helped me undertake my MSc studies at Rhodes University.

I would like to acknowledge my family members; Mum, Dad, Sisters , Father and Mother-in-law, Brothers and Sisters-in-law; your constant encouragements and support are highly appreciated.

I give my grateful thanks to my wife, Marie Claire, to my children, Aldo Bruno and Mercy Blandine, your strong support, advice and encouragement have made this work possible.

May God bless you All!

Contents

List of Figures

List of Tables

Chapter 1

Introduction

1.1 Luminescence

Luminescence is the light emitted from irradiated solids, mostly insulators or semiconductors when exposed to ionizing radiation such as beta, alpha, gamma or X-ray irradiation. The ionization frees electrons which then move through the crystal lattice and may be trapped at imperfections within the lattice [1].

Trapped electrons can be thermally or optically released from the trap to recombine with charge carriers of the opposite sign that is, electron-hole recombination. In the recombination processes, the electron relaxes to emit back the absorbed radiation. The relaxation energy is released as light which is the luminescence. For this reason, the emission of light, usually in the visible spectrum, is termed as "luminescence" [2]. Non-radiative recombination may also be possible when the absorbed energy is released as thermal vibration of the lattice or phonons.

1.2 Defects in solids

Defects in solids may be defined as all kinds of imperfections such as impurities, interstitials and vacancies within the atomic structure of the solid [1]. Impurities refer to the random placement of foreign atoms into the crystal lattice structure. Vacancies are unoccupied sites or missing atoms in the lattice structure. Interstitials are irregu-

larly occupied sites. The most common type of defect are point defects which can be classified in two major categories depending on their origin: Intrinsic defects consist of vacancies and self interstitials. Extrinsic defects arise from substitutional or added impurity atoms in the lattice. Defects may also arise from interstitial impurities which are impurity atoms at irregular lattice sites. Radiation itself and transitional atoms in the lattice can also produce impurities. If defects are not present (in a perfect crystal), electrons are allowed to exist in certain discrete energy levels. These allowed energy levels are called delocalized energy bands, either valence band or conduction band. The separation of two consecutive delocalized energy bands is called the energy band gap or forbidden energy band. No electron is allowed to exist in the forbidden bands. The presence of point defects and their distributions in a material structure introduces local energy levels in the forbidden energy band [3]. These local energy levels host an anion vacancy or an excess anion. An anion vacancy may capture a free electron from the conduction band and thereby act as an electron trap. An excess anion may capture a free hole from the valence band and in that way act as a hole trap. If the defective level can return an electron or hole back to the band it came from, then the defect is called a "trap centre". The defective level where a charge carrier of opposite sign can be captured to produce electron-hole recombination is called a "recombination centre" [1].

1.3 Simple energy band model

The trapping and recombination process can be described in terms of electronic transitions between delocalized bands and localized bands [1, 2]. Figure 1.1 illustrates transitions of electrons in the luminescence process, equivalently to hole transitions. Ionizing radiation frees electrons to the conduction band and leaves behind free holes in the valence band. Free electrons in the conduction band can be captured at an electron trap (ET) and free holes at a hole trap (HT). A trapped electron or hole may be released from its trap by thermal or optical energy. When electrons are released from traps, they move via the conduction band and recombine with hole centres to

produce luminescence. In this process, the shallower level (electron level) is a "trap" and the other one (hole level) is a "recombination centre".

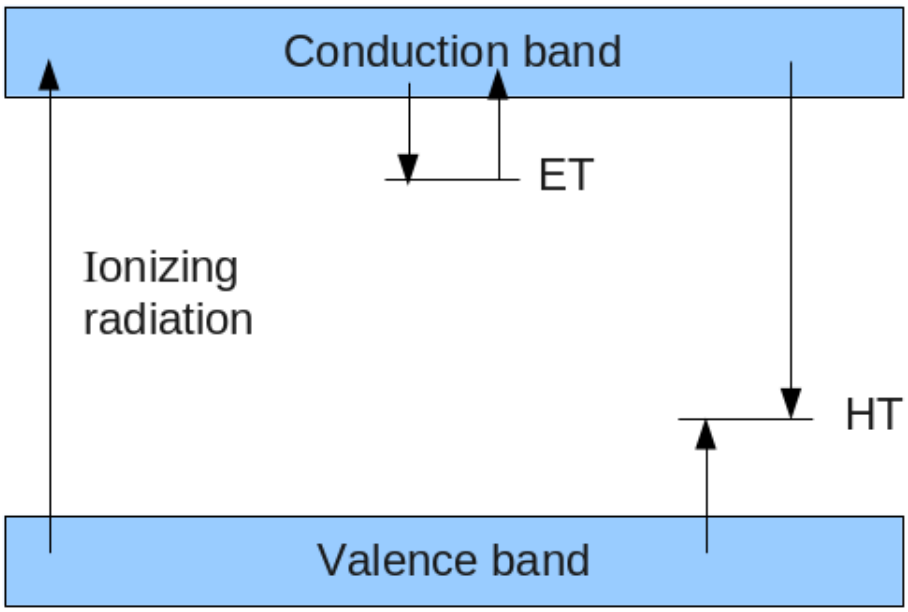

Figure 1.1: Energy band model for the trapping and recombination process leading to luminescence. ET and HT are electron trap and hole trap respectively [2].

1.4 Fluorescence and phosphorescence

The luminescence emission in an insulator can be classified as either fluorescence or phosphorescence. The classification depends on the lifetime and atomic mechanisms by which the luminescence is emitted [1, 2]. Figure 1.2 illustrates the luminescence emission resulting from electron transitions from the ground state g to the excited state e and back to g. Fluorescence is the radiation which follows the excitation of an electron from g to e and its subsequent return to g as shown in figure 1.2 (a). Phosphorescence is characterized by a delayed return of the electrons to the state g. The delay is due to a transition into and out of a metastable state m via the conduction band after the excitation has been removed as depicted in figure 1.2 (b). Fluorescence is observed for short lifetime less than 10^{-8} s while phosphorescence is characterized by longer lifetime

greater than 10^{-8} s. The fluorescence process is temperature independent while the phosphorescence process depends on temperature. The phosphorescence lifetime also depends on the physical parameter E which is called the "trap depth". The trap depth, also known as the potential barrier of the trap or activation energy, is a separation between metastable m and excited e state.

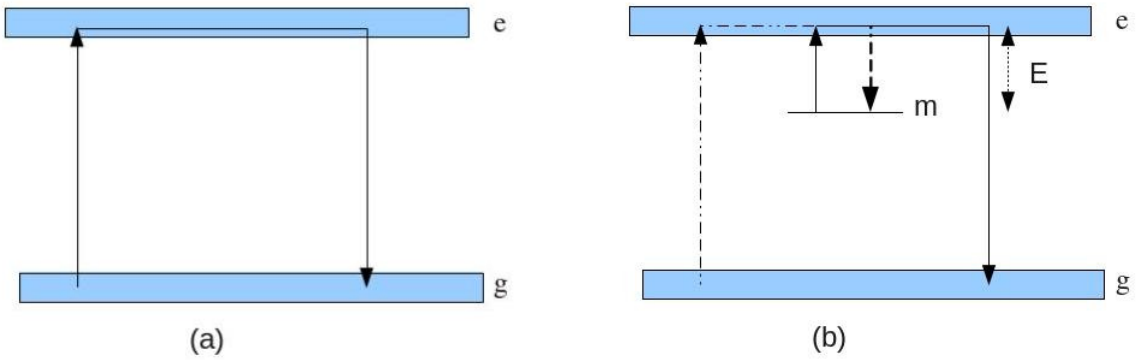

Figure 1.2: Energy transitions for fluorescence (a) and phosphorescence (b) processes [1].

1.4.1 Thermal stimulation of trapped charges

A trapped charge carrier, either an electron or a hole, at metastable level m may be released by thermal energy. The charge is likely to escape the barrier E if the external thermal energy is greater than or equal to E [4]. The probability per second to stimulate a trapped charge from a trap is given by

$$\mathrm{p(T)} = s \exp(-\mathrm{E/kT}) \tag{1.1}$$

where T is the temperature in Kelvin and s is called the frequency factor or pre-exponential factor or attempt-to-escape frequency [1, 2, 4]. The unit of s is s^{-1}. The frequency factor is related to the local lattice vibration frequency and entropy change associated with the charge release [3]. The vibration frequency is in the order between 10^{-12} and $10^{-14}\,\mathrm{s}^{-1}$ [2, 5]. The constant k, is called Boltzmann's constant ($k = 8.617 \times 10^{-5}$ eV K^{-1}). The rate of thermal excitation of electrons from level m back to e, if at a certain time t after thermal excitation there is a concentration of electrons n in level

m, can be written as [2]

$$-\mathrm{dn/dt} = \mathrm{np} = \mathrm{n}\, s \exp\left(-\mathrm{E/kT}\right) \tag{1.2}$$

where the negative sign implies a loss of electrons which gives rise to the phosphorescence. Using the Randall and Wilkins equation [2], for non-retrapping of charges, the intensity of the phosphorescence $I(t)$ is described as

$$\mathrm{I(t)} = -\eta\left(\mathrm{dn/dt}\right) = -\eta \mathrm{np} \tag{1.3}$$

where η is a constant. At constant temperature T, the simplest solution to the equation 1.3 indicates that the phosphorescence is an exponential decay given by

$$\mathrm{I} = \mathrm{I_o} \exp\left[s \exp\left(-\mathrm{E/kT}\right) \mathrm{t}\right] = \mathrm{I_o} \exp\left(-\mathrm{pt}\right) \tag{1.4}$$

where I_o shows the initial intensity at $t = t_o$. The intensity of phosphorescence has the lifetime τ (the mean time spent by an electron in the trap) of [1]

$$\tau = 1/\mathrm{p} = s^{-1} \exp\left(\mathrm{E/kT}\right). \tag{1.5}$$

1.4.2 Luminescence techniques

We consider the phosphorescence process where each trapped electron near the conduction band is associated with a trapped hole near the valence band as previously shown in figure 1.1. The lifetime τ for phosphorescence is very small leading to the luminescence even at room temperature T. Considering a trap which is stable at room temperature T (a trap having the potential barrier E such that $E > kT$) [6], the lifetime of trapped charges becomes large enough and they can stay in the trap for long periods. Subsequent thermal or optical stimulation can release some of the trapped charge carriers with an associated emission of light. The emission is either thermoluminescence (TL) or optically stimulated luminescence (OSL) respectively [2]. In TL

or OSL process, the increase of stimulating energy increases the possibility of eviction in accordance with equation 1.1. The evicted charges diffuse around the crystal. The diffusion time is very short and recombination can take place instantaneously. Optically stimulated luminescence (OSL) is a phenomenon in which the phosphorescence is stimulated by the absorption of radiation energy. OSL follows the same basic concepts as TL with some minor dissimilarities. In OSL, the stimulation energy is supplied by illumination or photons instead of heat. Therefore, in luminescence techniques, both TL and OSL can be applied for luminescence measurements. TL in α-$Al_2O_3 : C$ is the main focus in this thesis.

1.5 Thermoluminescence

Thermoluminescence (TL) is phosphorescence triggered by thermal energy after previous absorption of ionizing radiation [2]. TL is empirically observed by heating a previously irradiated dosimeter. The TL intensity emitted as a function of temperature is called a glow curve. The emission glow peaks characteristic of a glow curve are due to trapping centres at different trap depths. Initial irradiation stores TL energy in the crystal. The subsequent stimulation is due to temperature which is raised gradually at a constant rate as the specimen is heated. The temperature increases linearly as a function of time t as

$$\mathrm{T(t) = T_o + \beta\, t} \tag{1.6}$$

where $\beta = \mathrm{dT/dt}$ in K/s is the heating rate and T_o is the initial temperature.

1.5.1 Simple mathematical TL model

The simple model for TL process as reported by Chen and McKeever [2] is shown in figure 1.3 and consists of one trap and one recombination centre. After ionization, transition 1, free electrons may be trapped at the electron trap (downward arrow, transition 2). At the end of excitation, the initial concentrations of electrons in the trap and holes in the recombination centre are n_o and m_o, respectively and are equal.

During stimulation trapped electrons are released, transition 3, and recombine with holes at the recombination centre, transition 4. Each electron-hole recombination gives rise to an emitted photon, this is TL. In assumption of a simplified model, the number of electrons released per second is proportional to the total concentration of trapped electrons. This means that there is no retrapping of electrons from the conduction band. From these assumptions, the rate of production of emitted photons or intensity, $I(t)$ of TL is given by the following expression

$$\mathrm{I(t) = -dn/dt = -dm/dt = } s\ \mathrm{n\ exp(-E/kT)} \tag{1.7}$$

where the quantity $I(t)$ corresponds to the number of photons per unit volume per unit time. All other terms are as previously defined.

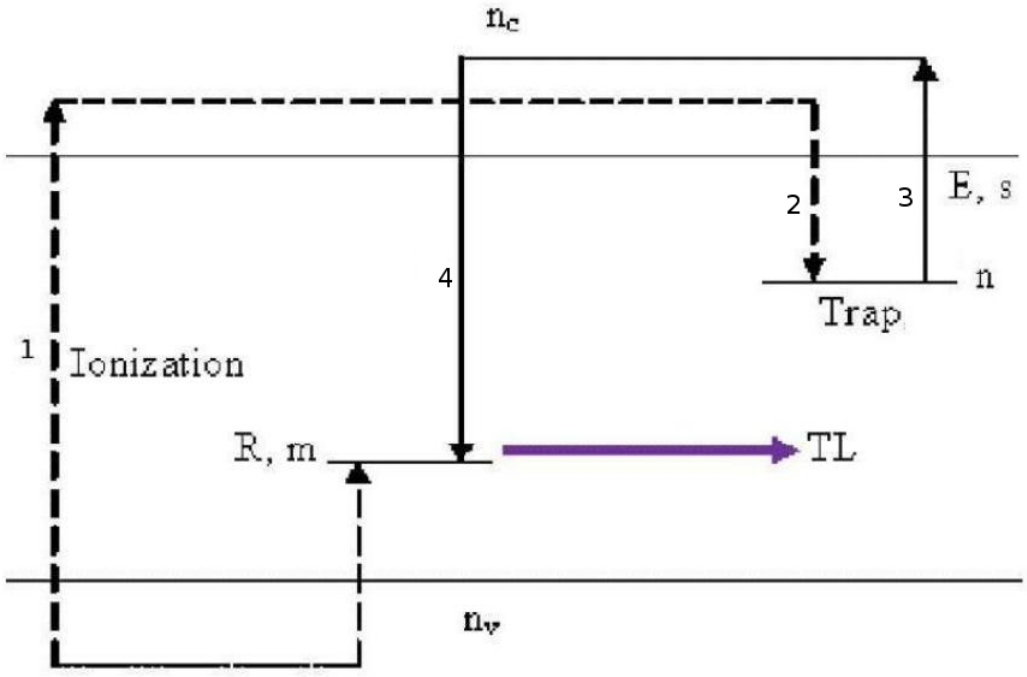

Figure 1.3: The simplest model for TL process [2]. E (eV) is an activation energy, s in s^{-1} is the frequency factor, n and m are the concentrations (m^{-3}) of electrons or holes at traps and recombination centres, respectively. R is the recombination centre, n_c and n_v are concentrations (m^{-3}) of electrons in the conduction band and holes in the valence band, respectively.

1.5.2 Kinetics of TL process

1.5.2.1 First order TL equation

The Randall and Wilkins equation (equation 1.7) as reviewed by Chen and McKeever [2] is known as the first-order TL equation. This implies the proportionality of TL intensity to the initial concentration of trapped electrons. For a first-order peak, the probability of retrapping is negligible compared with the probability of recombination. Assuming a linear heating rate β, the solution to the differential equation 1.7 yields:

$$\mathrm{I_{TL}(T)} = \mathrm{n_o}\, s\, \exp(-\mathrm{E/kT}) \exp\left[-\frac{s}{\beta}\int_{\mathrm{To}}^{\mathrm{T}} \exp(-\mathrm{E/k}\theta)\mathrm{d}\theta\right] \tag{1.8}$$

where θ is a temperature variable which disappears upon integration. The other parameters have their usual meanings as stated earlier. Equation 1.8 shows TL intensity of first order of kinetics.

1.5.2.2 Second order TL equation

In contrast to first order of kinetics, second order TL kinetics arise when the retrapping probability is high compared with the probability of recombination [1, 7]. The increase of retrapping of released electrons delays the TL at the initial part of a second order TL peak and leads to more thermaluminescence at the second half of the peak. This means that a second order TL peak is wider and more symmetric than a first order glow peak [2]. An expression for second order TL kinetics can be written as

$$\mathrm{I(t)} = -\mathrm{dn/dt} = s'\, \mathrm{n}^2 \exp(-\mathrm{E/kT}), \tag{1.9}$$

where $s' = s/N$ in $\mathrm{m^3\, s^{-1}}$ is the effective pre-exponential factor for second order of kinetics and N ($\mathrm{m^{-3}}$) is the total concentration of electron traps. The integration of equation 1.9 for linear heating rate yields

$$\mathrm{I_{TL}(T)} = \mathrm{n_o^2}\, s' \exp(-\mathrm{E/kT}) \left[1 + \frac{\mathrm{n_o}\, s'}{\beta}\int_{\mathrm{To}}^{\mathrm{T}} \exp(\mathrm{E/k}\theta)\mathrm{d}\theta\right]^{-2}. \tag{1.10}$$

1.5.2.3 General order TL equation

A TL equation for general order of kinetics was discussed by McKeever [1] and by Chen and McKeever [2]. For the general order equation, they considered intermediate order of kinetics between 1 and 2 resulting in

$$\mathrm{I(t)} = -\mathrm{dn/dt} = s'\,\mathrm{n^b}\exp(-\mathrm{E/kT}) \tag{1.11}$$

provided that $1 < b < 2$. The solution of equation 1.11 gives a TL intensity equation for general order of kinetics given by

$$\mathrm{I_{TL}(T)} = \mathrm{n_o}\,s''\exp(-\mathrm{E/kT})\left[1 + \frac{s''(\mathrm{b}-1)}{\beta}\int_{\mathrm{To}}^{\mathrm{T}}\exp(-\mathrm{E/k}\theta)\mathrm{d}\theta\right]^{\frac{-\mathrm{b}}{\mathrm{b}-1}}, \tag{1.12}$$

where $s'' = s'\mathrm{n_o^{b-1}}$ and it depends on b. For $b = 2$, the general order equation describes second order kinetics. If $b \longmapsto 1$, a first order TL equation emerges.

1.6 A brief summary of the research done on TL of α-$Al_2O_3 : C$

1.6.1 Necessity and justification of research

The thesis concerns the basic thermoluminescence (TL) mechanisms responsible for secondary glow peaks in α-$Al_2O_3 : C$, a highly sensitive luminescence dosimeter. To date, wide studies of TL in α-$Al_2O_3 : C$ have been mainly focused on the main peak of this material with few exceptions on the secondary ones exemplified in [8–11]. However, the features of the secondary TL peaks whose presence is revealed as TL at temperatures close to ambient as well as other weak intensity peaks present at relatively higher temperatures suggest in-depth studies for further development of the dosimetric applications of α-$Al_2O_3 : C$.

The choice of the thesis subject was to find an appropriate solution to these problems by providing a better understanding of the mechanisms involved in the TL process. In

addition, several TL analysis methods were used to identify the complexity of the TL characteristics in the material.

1.6.2 Purpose of thesis

The overall aim of our work was to study the TL mechanisms responsible for secondary glow peaks in α-$Al_2O_3 : C$. The dynamics of charge movement between centres during the TL process was studied. Additional analysis on phototransferred TL (PTTL) from secondary glow peaks was also studied. The specific objectives of the work are presented in six chapters as follows.

Chapter one defines the main concepts important for the TL analysis and introduces a simple model that describes the TL analysis process.

Chapter two describes six methods of kinetic analysis that allow to establish the fundamental kinetic parameters such as the activation energy, frequency factor and the order of kinetics.

Chapter three provides a mathematical description of PTTL in terms of the energy band theory of α-$Al_2O_3 : C$.

Chapter four describes the apparatus used to measure TL and provides a detailed description of the experimental procedures followed. The details include sample preparation by annealing and thermoluminescence read out. A brief description of the sample under study (α-$Al_2O_3 : C$) is also included in this chapter.

Chapter five discusses the experimental results in two parts. The first part compares the values of kinetic parameters for secondary TL peaks. Thermal quenching effect for the high temperature secondary peak, fading and dosimetric features of the low secondary peak are assessed. In the second part, the PTTL features from secondary peaks and determination of the same kinetic parameters for PTTL are provided. The dependence of the PTTL intensity from secondary peaks on illumination time is investigated for different temperatures of preheats following the irradiation. The PTTL data were attempted to fit the model of PTTL phenomenon.

Chapter six includes conclusion and suggestions for further research.

Chapter 2

Kinetic analysis

2.1 Introduction

The kinetic analysis of TL consists of extracting data from an experimental glow curve and using it to establish the trapping parameters of the traps in the sample material [1]. These parameters include the trap depth or activation energy E, frequency factor or attempt of electron to escape the trapping energy s, kinetic order b, etc. In the case of a simple first order peak, the initial concentration of trapped charge carriers n_0 can also be obtained from kinetic analysis. The dynamics of trapped charge carriers between centres is also studied [12]. The analysis consists of selecting the TL equation appropriate to a particular mathematical model. Various methods of kinetic analysis are used to calculate values of the trapping parameters. The next step is to discuss the applicability, reliability and validity of these methods to analyze the glow curve in the material under study. The calculated parameters are then applied to verify the coincidence of kinetic models with the experimental findings [2]. Kinetic parameters provide additional restrictions to refine the applicability and validity of the general model. This leads to some acceptance criteria or rejection of calculated parameters.

2.2 Evaluation of the frequency factor s

When E, b and temperature T_M at maximum intensity are known, the frequency factor s can be evaluated. The expression for evaluating s is obtained from the maximum condition of a kinetic order TL equation. This means that the derivative of a TL intensity, $I(T)$ at T_M is equal to zero, i.e

$$\left(\frac{\mathrm{dI(T)}}{\mathrm{dT}}\right)_{\mathrm{T_M}} = 0. \tag{2.1}$$

Rewriting the maximum condition for a first order peak (equation 1.8) we find

$$\frac{\mathrm{d}}{\mathrm{dT}}\left[\mathrm{n_0}\, s\, \exp(-\mathrm{E/kT})\exp\left(-\frac{s}{\beta}\int_{\mathrm{To}}^{\mathrm{T}}\exp(-\mathrm{E/k}\theta)\mathrm{d}\theta\right)\right]_{\mathrm{T_M}} = 0, \tag{2.2}$$

where θ is temperature variable and the other parameters are previously defined. Assuming a constant s, equation 2.2 yields

$$s\exp\left(-\mathrm{E/kT_M}\right) = \frac{\beta \mathrm{E}}{\mathrm{kT_M^2}}; \tag{2.3}$$

which gives a first order kinetics expression for s as

$$s = \frac{\beta \mathrm{E}}{\mathrm{kT_M^2}}\exp\left(\mathrm{E/kT_M}\right), \tag{2.4}$$

where β is a constant heating rate, E activation energy, k is Boltzmann's constant and T_M is the temperature at maximum intensity. Similarly, applying equation 2.1 to a general order TL equation yields after approximation [12]

$$s = \frac{\beta \mathrm{E}}{\mathrm{kT_M^2}}\exp\left(\mathrm{E/kT_M}\right)\left[(\mathrm{b}-1)\frac{2\mathrm{kT_M}}{\mathrm{E}}+1\right]^{-1}. \tag{2.5}$$

For $b = 1$, a first order expression emerges; for $b = 2$ the second order s expression is written as

$$s = \frac{\beta \mathrm{E}}{\mathrm{kT_M^2}}\exp\left(\mathrm{E/kT_M}\right)\left(\frac{2\mathrm{kT_M}}{\mathrm{E}}+1\right)^{-1}. \tag{2.6}$$

2.3 Methods of kinetic analysis

2.3.1 Initial rise methods

The initial rise method is a common way of evaluating the activation energy E of an isolated peak. The applicability of this method relies on the assumption that in the initial rise region of a peak, the concentration of trapped charge carriers is nearly constant [2]. Figure 2.1 shows an example of an initial rise region of a glow peak. The low temperature peak tail in this region increases up to a critical temperature T_C which is less than T_M. In this approximation T_C corresponds to a TL intensity I_C less than 15% of the maximum TL intensity I_M. The initial occupancies of traps and recombination centres are assumed to be constant only for a limited temperature range under T_C.

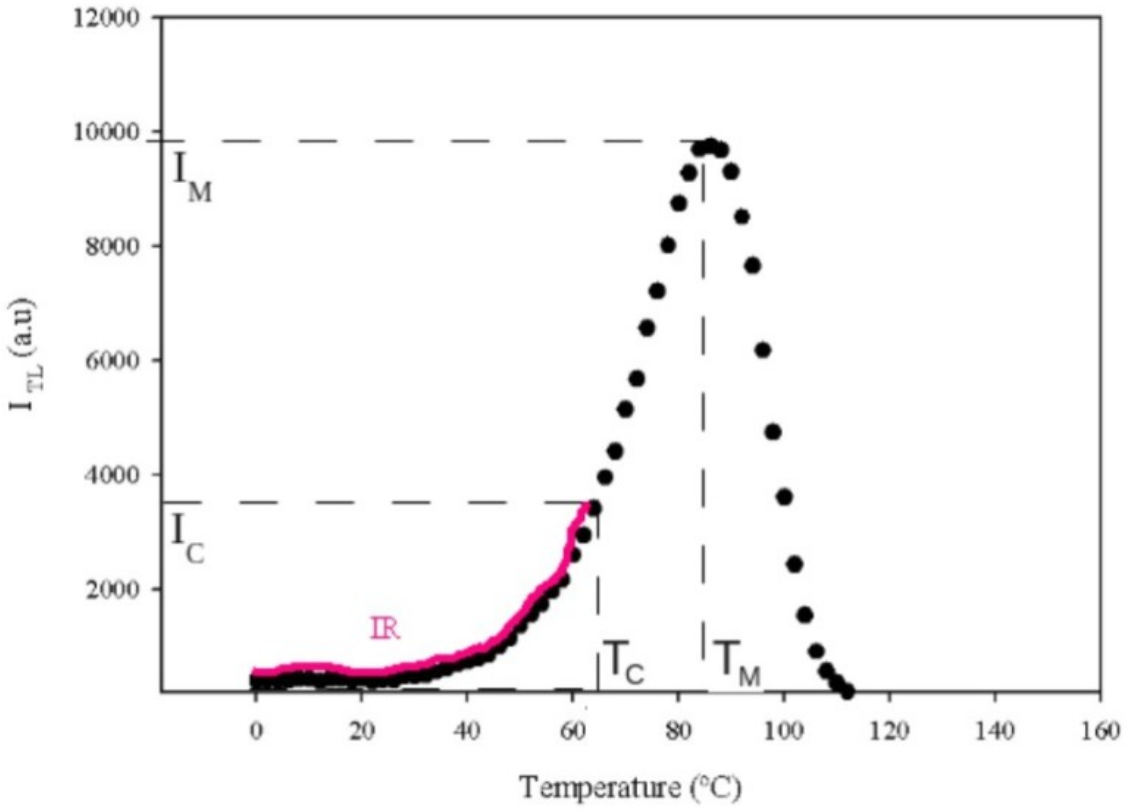

Figure 2.1: The initial rise (IR) region of a TL glow peak. The parameters I_M, I_C, T_C and T_M stand for the maximum TL intensity, TL intensity limit at less than 15% of I_M, critical temperature which corresponds to I_C and the maximum temperature, respectively.

The initial rise technique can be applied to the general order TL equation 1.12:

$$\mathrm{I(T)} = \underbrace{\left(\frac{s'}{\beta}\right) \mathrm{n_o^b} \exp(-\mathrm{E/kT})}_{\text{(A)}} \underbrace{\left[\beta + s'\, \mathrm{n_o^{b-1}(b-1)} \int_{\mathrm{To}}^{\mathrm{T}} \exp(-\mathrm{E/k}\theta)\mathrm{d}\theta\right]^{\frac{-\mathrm{b}}{\mathrm{b-1}}}}_{\text{(B)}}. \quad (2.7)$$

In the linear temperature rise portion, the term (B) of equation 2.7 changes slower than term (A) and can be approximated to unity [5]. In this case, the general order equation for the initial rise portion of a peak becomes

$$\mathrm{I(T)} = (s'/\beta)\, \mathrm{n_o^b} \exp(-\mathrm{E/kT}) \quad (2.8)$$

or commonly written as

$$\mathrm{I(T)} = \mathrm{Constant} \times \exp\left(-\mathrm{E/kT}\right), \quad (2.9)$$

where E is the activation energy, k is Boltzmann's constant and T is temperature. A plot of $\ln(I)$ against $1/kT$ yields a straight line. The activation energy is computed from the slope $(-E)$ of the straight line.

The validity and applicability of techniques used in the initial rise method may not be based only on the fitness of a straight line [1]. The values of E from the initial rise method remain true for some critical values of temperature up to T_C. T_C should correspond to an intensity between 10 and 15% of I_M. However, the literature [1] has shown that in some cases, equation 2.9 cannot be used even in this region for some glow peaks. The obtained values for E are less than the actual true values for E [13]. There may be several reasons for this including abrupt changes of charge carrier occupancies in the initial rise region for some glow peaks.

2.3.2 Peak shape method

The peak shape method is used to evaluate E, s and b. This method is based on geometrical shape of a glow peak. In contrast to the initial rise method, the peak shape

method is dependent on the order of kinetics. First order glow peaks are asymmetrical while second order peaks are nearly symmetrical in shape. E, s and b are calculated using three parameters τ, δ and ω shown in figure 2.2.

$$\tau = \mathrm{T_M} - \mathrm{T_1}, \tag{2.10}$$

$$\delta = \mathrm{T_2} - \mathrm{T_M}, \tag{2.11}$$

$$\omega = \mathrm{T_2} - \mathrm{T_1}, \tag{2.12}$$

where τ is the low temperature half width of a peak, δ is half width at the high temperature and ω the total half-intensity width. T_1 and T_2 are low and high temperatures corresponding to half-maximum intensity, respectively. T_M is the temperature at maximum intensity [2, 12]. The kinetic order b is a monotonic function of the geometrical or symmetrical factor written as

$$\mu_g = \delta/\omega. \tag{2.13}$$

Symmetry properties of a peak are used to distinguish between first and second order kinetics. For a first order peak ($b = 1$) $\mu_g = 0.42$ and for second, $b = 2$, $\mu_g = 0.52$. Chen derived a general order expression to calculate E as

$$\mathrm{E_\alpha} = \mathrm{c_\alpha}\left(\frac{\mathrm{kT_M^2}}{\alpha}\right) - \mathrm{b_\alpha}\left(2\mathrm{kT_M}\right) \tag{2.14}$$

where α can take the values of τ, δ and ω. The values of the factors c_α and b_α in equation 2.14 are shown below:

$\alpha = \tau$:

$$c_\tau = 1.51 + 3.0(\mu_g - 0.42) \text{ and } \mathrm{b_\tau} = 1.58 + 4.2(\mu_\mathrm{g} - 0.42) \tag{2.15}$$

$\alpha = \delta$:

$$c_\delta = 0.976 + 7.3(\mu_g - 0.42) \text{ and } \mathrm{b_\delta} = 0 \tag{2.16}$$

$\alpha = \omega$:

$$c_\omega = 2.52 + 10.2(\mu_g - 0.42) \text{ and } \mathrm{b_\omega} = 1.0. \tag{2.17}$$

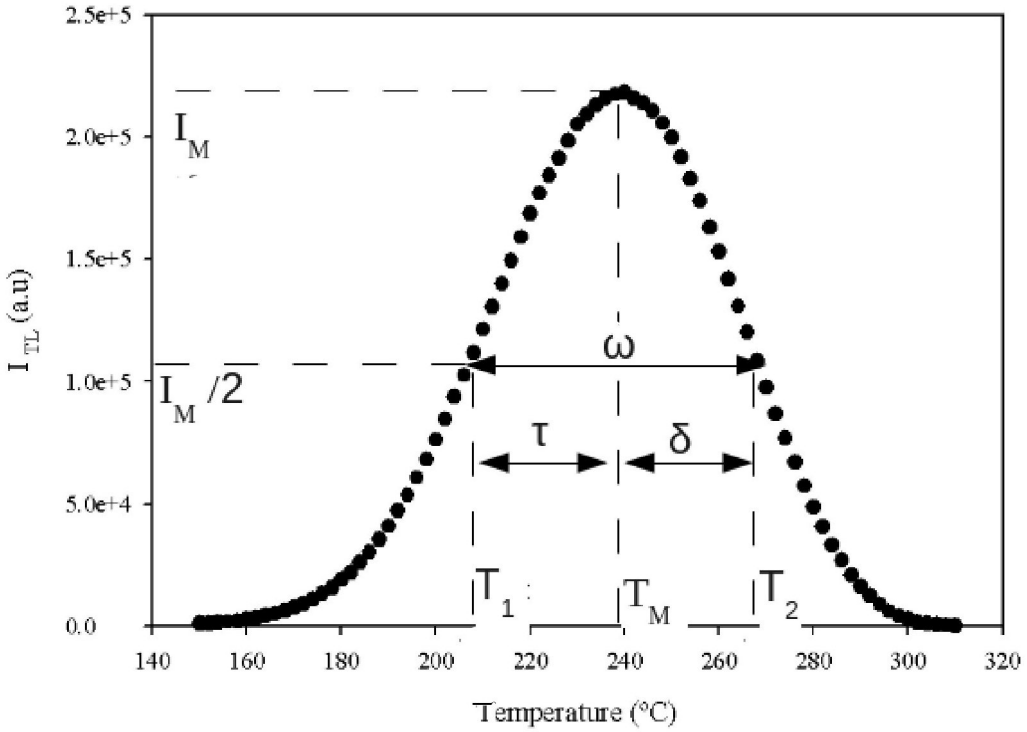

Figure 2.2: Three TL parameters τ, δ and ω used to evaluate E, s and b in a peak shape method [2, 12].

For a first order peak, $b = 1$ and $\mu_g = 0.42$, activation energy equations in the three forms of peak shape method become

$$\mathrm{E}_\tau = \frac{1.51\mathrm{kT}_\mathrm{M}^2}{\tau} - 1.58(2\mathrm{kT}_\mathrm{M}), \tag{2.18}$$

$$\mathrm{E}_\delta = \frac{0.976\mathrm{kT}_\mathrm{M}^2}{\delta}, \tag{2.19}$$

$$\mathrm{E}_\omega = \frac{2.52\mathrm{kT}_\mathrm{M}^2}{\omega} - 2\mathrm{kT}_\mathrm{M}. \tag{2.20}$$

For a second order, b = 2 and $\mu_g = 0.52$, we have the following equations:

$$\mathrm{E}_\tau = \frac{1.81\mathrm{kT}_\mathrm{M}^2}{\tau} - 2(2\mathrm{kT}_\mathrm{M}) \tag{2.21}$$

$$\mathrm{E}_{\delta} = \frac{1.71\mathrm{kT}_{\mathrm{M}}^2}{\delta} \tag{2.22}$$

$$\mathrm{E}_{\omega} = \frac{3.54\mathrm{kT}_{\mathrm{M}}^2}{\omega} - 2\mathrm{kT}_{\mathrm{M}}. \tag{2.23}$$

The frequency factor s can be calculated from equations 2.4 to 2.6 when E and b are obtained.

2.3.3 The variable heating rate method

The change in heating rate causes a shift in peak position T_M which is used in the variable heating rate or peak position method to calculate kinetic parameters [1, 2]. The method can rely on either two or several heating rates to compute the activation energy. Increasing the heating rate from β_1 to β_2 shifts the peak position from a low maximum temperature T_{M1} to a higher maximum temperature T_{M2}. Rewriting equation 2.4 from the first order kinetics expression for constant frequency factor s as

$$s = \frac{\beta \mathrm{E}}{\mathrm{kT}_{\mathrm{M}}^2} \exp\left(\mathrm{E}/\mathrm{kT}_{\mathrm{M}}\right), \tag{2.24}$$

we can obtain two heating rate equations as

$$\beta_1 = \left(s\ \mathrm{k}/\mathrm{E}\right)\ \mathrm{T}_{\mathrm{M1}}^2 \exp\left(-\mathrm{E}/\mathrm{kT}_{\mathrm{M1}}\right), \tag{2.25}$$

$$\beta_2 = \left(s\ \mathrm{k}/\mathrm{E}\right)\ \mathrm{T}_{\mathrm{M2}}^2 \exp\left(-\mathrm{E}/\mathrm{kT}_{\mathrm{M2}}\right). \tag{2.26}$$

From the two equations, we get the following expression for the activation energy

$$\mathrm{E} = \mathrm{k}\frac{\mathrm{T}_{\mathrm{M1}}\mathrm{T}_{\mathrm{M2}}}{\mathrm{T}_{\mathrm{M1}} - \mathrm{T}_{\mathrm{M2}}} \ln\left[\frac{\beta_1}{\beta_2}\left(\frac{\mathrm{T}_{\mathrm{M2}}}{\mathrm{T}_{\mathrm{M1}}}\right)^2\right]. \tag{2.27}$$

When several instead of two heating rates are used, the T_M value corresponding to each rate is noted. The dependence of β on T_M is found from equation 2.24 as

$$\ln\left(\frac{\mathrm{T_M^2}}{\beta}\right) = \ln\left(\frac{\mathrm{E}}{s\mathrm{k}}\right) + \frac{\mathrm{E}}{\mathrm{kT_M}}, \tag{2.28}$$

from which a plot of $\ln(T_M^2/\beta)$ versus $1/kT_M$ should be linear with slope E and intercept $\ln(E/sk)$. The activation energy E and the frequency factor s are calculated from the slope and intercept, respectively. The variable heating method is a good approximation for any order kinetics [1, 5] as it can be deduced from the following expression [1] by assuming that the frequency factor s is constant

$$\beta\mathrm{E/kT_M^2} = s\left[1 + (\mathrm{b}-1)2\mathrm{kT_M/E}\right]\exp\left(-\mathrm{E/kT_M}\right). \tag{2.29}$$

The general order term $[1 + (b-1)2kT_M/E]$ of equation 2.29 is approximately constant and close to unity so that the plot of $\ln(T_M^2/\beta)$ versus $1/kT_M$ provides a good value of E for any order kinetics b. Therefore, equation 2.28 is useful in various heating rates method independently of order kinetics.

2.3.4 Whole glow peak method

The previously stated methods use a limited number of data points. The initial rise method uses the low temperature rise portion; only three parameters T_1, T_2 and T_M are used for peak shape method and one point (T_M , I_M) in various heating rates method. In contrast, the whole glow peak method considers the whole area under a glow peak instead of one section of it [1]. The other name of whole glow curve method derived from first order TL equation is the "area method". Figure 2.3 shows the area $n(T)$ under the glow peak. Using the expression of TL intensity, equation 1.7 on an isolated peak, the area can be approximated by

$$\mathrm{n(T)} = \int_{\mathrm{to}}^{\mathrm{t}} \mathrm{I(t)dt} = (1/\beta)\int_{\mathrm{To}}^{\mathrm{T}} \mathrm{I(T)dT} \tag{2.30}$$

where $I(T)$ is the TL intensity of a glow peak at a constant heating rate $\beta = dT/dt$, t is time and T denotes the absolute temperature. For finite data points, the area becomes:

$$\mathrm{n(T)} = (1/\beta) \sum_{\mathrm{To}}^{\mathrm{T}} \mathrm{I}\Delta\mathrm{T} \tag{2.31}$$

where ΔT is a step or temperature interval used in sampling the TL data [5]. From general order kinetics, in the linear temperature rise, it can be shown that

$$\ln\left(\frac{\mathrm{I(T)}}{\mathrm{n^b}}\right) = \ln\left(\frac{s'}{\beta}\right) - \frac{\mathrm{E}}{\mathrm{kT}}, \tag{2.32}$$

where s' in $\mathrm{m}^{3(\mathrm{b}-1)}\,\mathrm{s}^{-1}$ is the effective frequency factor for general order kinetics [5]. From equation 2.32, a plot of $\ln\left(I(T)/n^b\right)$ versus $1/kT$ yields a straight line of a slope $(-E)$ and an intercept of $\ln\left(s'/\beta\right)$. E and s' are evaluated from the slope and the intercept of the best fit in a graph determined by a correct choice of b value.

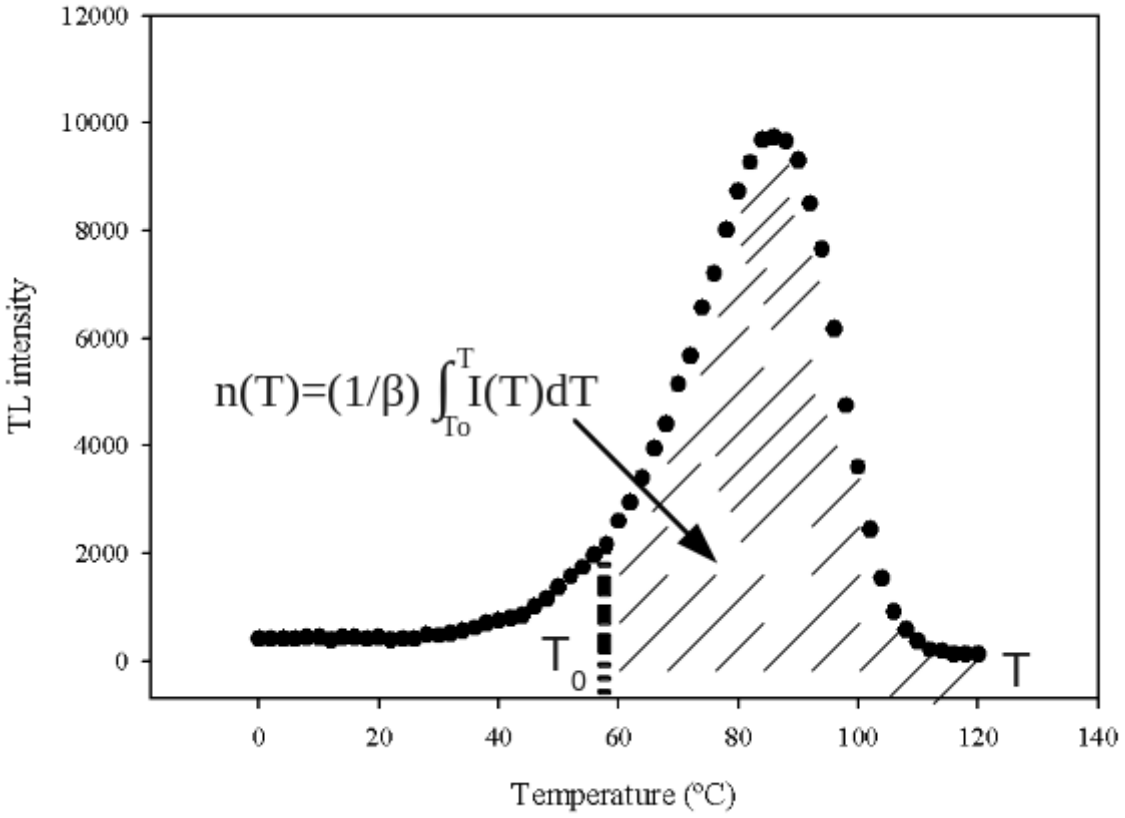

Figure 2.3: Whole glow peak method. The area under a glow peak is approximated to a total concentration n in shaded area beyond a certain temperature T_0 [1].

2.3.5 Glow curve deconvolution

The consistency of E, s and b values evaluated from previously stated methods can be checked by the glow curve deconvolution method. The method follows a number of steps [1]. Firstly, after determining the number and positions of peaks of the glow curve, the experimental glow curve is fitted with one or more of equations, 2.33 to 2.35 [14]. The values of E, s and b found from other methods are used as initial estimates in the fit. The computed curve is then compared with the actual experimental curve. Each of the parameters used is varied independently until a best fit is reached. The glow curve deconvolution method is regarded to be efficient if the computed values for the parameters closely agree with those obtained by other methods [1]. The analytical equations for TL peaks using this method are derived from the basic kinetic TL equations. The equations considers two measured experimental quantities, the maximum intensity I_M and the maximum temperature T_M, as follows

(a) For first order kinetics

$$\begin{aligned} \mathrm{I(T)} &= \mathrm{I_M} \exp\left[1 + \frac{\mathrm{E}}{\mathrm{kT}} \cdot \frac{\mathrm{T}-\mathrm{T_M}}{\mathrm{T_M}} - \frac{\mathrm{T}^2}{\mathrm{T_M^2}} \right. \\ &\quad \left. \times \exp\left(\frac{\mathrm{E}}{\mathrm{kT}} \frac{\mathrm{T}-\mathrm{T_M}}{\mathrm{T_M}}\right)\left(1 - \frac{2\mathrm{kT}}{\mathrm{E}}\right) - \frac{2\mathrm{kT_M}}{\mathrm{E}}\right] \end{aligned} \tag{2.33}$$

(b) The form of the second order kinetics

$$\begin{aligned} \mathrm{I(T)} &= 4\mathrm{I_M} \exp\left(\frac{\mathrm{E}}{\mathrm{kT}} \cdot \frac{\mathrm{T}-\mathrm{T_M}}{\mathrm{T_M}}\right) \\ &\quad \times \left[\frac{\mathrm{T}^2}{\mathrm{T_M^2}}\left(1 - \frac{2\mathrm{kT}}{\mathrm{E}}\right) \exp\left(\frac{\mathrm{E}}{\mathrm{kT}} \cdot \frac{\mathrm{T}-\mathrm{T_M}}{\mathrm{T_M}}\right) + 1 + \frac{2\mathrm{kT_M}}{\mathrm{E}}\right]^{-2} \end{aligned} \tag{2.34}$$

(c) Analytical equation for general order kinetics

$$\begin{aligned} \mathrm{I(T)} &= \mathrm{I_M b}^{\frac{\mathrm{b}}{\mathrm{b}-1}} \exp\left(\frac{\mathrm{E}}{\mathrm{kT}} \cdot \frac{\mathrm{T}-\mathrm{T_M}}{\mathrm{T_M}}\right)\left[1 + (\mathrm{b}-1)\frac{2\mathrm{kT_M}}{\mathrm{E}} \right. \\ &\quad \left. + (\mathrm{b}-1)\left(1 - \frac{2\mathrm{kT}}{\mathrm{E}}\right)\frac{\mathrm{T}^2}{\mathrm{T_M^2}} \times \exp\left(\frac{\mathrm{E}}{\mathrm{kT}} \cdot \frac{\mathrm{T}-\mathrm{T_M}}{\mathrm{T_M}}\right)\right]^{-\frac{\mathrm{b}}{\mathrm{b}-1}} \end{aligned} \tag{2.35}$$

The accuracy of these analytical TL equations is numerically expressed by calculating the figure of merit (FOM) [5] and the slowly varying quantity C_b for a very wide range of E and s [15]. The FOM is given by

$$\mathrm{FOM} = \frac{\sum_{\mathrm{p}} \mid \mathrm{y_{exp}} - \mathrm{y_{fit}} \mid}{\sum_{\mathrm{p}} \mathrm{y_{fit}}}, \tag{2.36}$$

where y_{exp} and y_{fit} are the experimental data and the values of the fitting function, respectively. $\mathrm{C_b}$ values can be evaluated from

$$\mathrm{C_b} = \left[\frac{\mathrm{b}}{1 + (\mathrm{b}-1)\Delta_{\mathrm{M}}}\right]^{-\frac{\mathrm{b}}{\mathrm{b}-1}}, \tag{2.37}$$

where $\Delta_M = (2kT_M)/E$, b is the order of kinetics , T_M is the temperature at the maximum intensity and E is the activation energy. The use of all analytical data is an advantage of the glow curve deconvolution method compared to other methods. However, some errors increase when the fitting is applied to separate closely spaced peaks. In some samples, $\alpha - \mathrm{Al_2O_3} : \mathrm{C}$ for example, the lower temperature glow peak is affected by phosphorescence and higher temperature peaks by thermal quenching and this may affect the accuracy of the fitting.

2.3.6 Isothermal analysis

Isothermal analysis is another method used to determine E, s and b values by plotting TL intensity versus time at constant temperature. The method consists of heating an irradiated sample to a specific temperature at which the phosphorescence decay can be observed [5]. The decay rate of trapped charge carriers is monitored from the luminescence measured as a function of time. This is phosphorescence decay. The plot of TL intensity versus time at constant temperature is called an isothermal decay curve. In the case of a first order peak, isothermal decay is described by an isothermal decay function of time t as

$$\mathrm{I(t)} = \mathrm{I_0} \exp\left[-s \exp\left(-\mathrm{E/kT}\right) \mathrm{t}\right], \tag{2.38}$$

where $I(t)$ is the luminescence intensity at time t and at constant temperature T; I_0 is the initial intensity at $t = t_0$, E denotes an activation energy and k is Boltzmann's constant. TL intensity has a lifetime of

$$\tau = s^{-1} \exp\left(\mathrm{E/kT}\right). \tag{2.39}$$

The plot of $\ln\left(I(t)/I_0\right)$ versus t is a straight line of slope

$$\mathrm{m} = s \exp\left(-\mathrm{E/kT}\right). \tag{2.40}$$

The activation energy can be evaluated from any two different slopes m_1 and m_2 measured at two constant temperatures T_1 and T_2 as:

$$\mathrm{E} = \mathrm{k}\,\frac{\mathrm{T_1 T_2}}{\mathrm{T_1 - T_2}} \ln\left(\frac{\mathrm{m_1}}{\mathrm{m_2}}\right). \tag{2.41}$$

If the decay is measured at several constant temperatures, a plot of $\ln(m)$ against $1/kT$ shows a straight line of slope $(-E)$ and intercept $\ln(s)$. The activation energy is obtained from the slope and the frequency factor is evaluated from intercept $\ln(s)$.

Isothermal analysis may be used to calculate the order kinetics b for a general order peak according to the following

$$\left(\mathrm{I/I_0}\right)^{(1-\mathrm{b})/\mathrm{b}} = 1 + \mathrm{n_0^{b-1}}(\mathrm{b}-1)\, s' \exp\left(-\mathrm{E/kT}\right) \mathrm{t}, \tag{2.42}$$

where I_0 and n_o are the initial intensity and initial concentration of trapped charges at $t = t_0$ respectively; $I(t)$ is the TL intensity at time t and s' $(\mathrm{m}^{3(\mathrm{b}-1)})$ denotes the pre-exponential frequency factor for general order kinetics. The rate of TL decay for general order kinetics depends on n_0 so that $I(t)$ does not always decay exponentially with time as shown by equation 2.42. So, a plot of $(I/I_0)^{(1-b)/b}$ against t will only yield a straight line when the correct value of b is used. Each such inserted value of b in the plot of $(I/I_o)^{(1-b)/b}$ against t corresponds to the slope $\mathrm{m} = \mathrm{n_0^{b-1}}(\mathrm{b}-1)\, s' \exp\left(-\mathrm{E/kT}\right)$. Furthermore, a plot of $\ln(m)$ against $1/kT$ gives a straight line of slope $(-E)$ and the

intercept $\ln\left((b-1)s'n_0^{b-1}\right)$. The activation energy is obtained from a slope while the effective frequency factor can be found from an intercept as follows

$$s'' = 1/(\mathrm{b}-1) \times \exp(\text{intercept}), \tag{2.43}$$

where $s'' = s'n_0^{(b-1)}$ is an experimental fitting parameter [5].

Chapter 3

Phototransfer

Phototransfer refers to the optical transfer of charge from populated traps or centres into empty or partially-filled traps. The transfer of charge by light may induce or increase the size of glow peaks associated with traps within the material [1]. The dynamics of charge transfer involved for this report considers trap concentrations and centres to be filled by electrons and holes, respectively. The aim of this chapter is to provide a mathematical description of phototransferred thermoluminescence in terms of the energy band theory of α-Al_2O_3 : C.

3.1 Phototransferred thermoluminescence

Phototransferred thermoluminescence (PTTL) is the thermoluminescence induced from shallow traps as a result of optical transfer of charges from deeper traps into them [1, 2]. PTTL is observed experimentally following a number of steps such as ionization, preheating, illumination and reheating of the sample [2]. Ionizing radiation produces free electrons which fill shallow and deep levels within the material under study. Illumination of the material with light of a certain wavelength then transfers charge from deep to shallower traps. Charges in shallow traps are removed by preheating to a specific temperature high enough to empty the shallow traps but not the deeper ones [16]. Subsequent heating at a controlled rate produces a new glow peak at the original position of the peak associated with the shallow trap. This is PTTL.

3.2 Models for phototransferred thermoluminescence

3.2.1 Simple model

Figure 3.1 shows the simplest model used to explain the PTTL feature. The model consists of one shallow trap (ST), one active deep trap (DT) and one radiative recombination centre [2]. After preheat, following irradiation and immediately before illumination, at time $t = 0$, the charge neutrality at the initial condition is

$$n_{10} = 0, \tag{3.1}$$

$$n_{20} = m_0. \tag{3.2}$$

where n_{10} and n_{20} are the initial concentrations of electrons in the shallow trap and deep trap respectively and m_0 is the initial concentration of holes in the recombination centre. During illumination, if thermal excitation is negligible, the transfer of electrons by light from the deep trap into the shallow trap may be described by the following rate equations [2]

$$\frac{\mathrm{dn_2}}{\mathrm{dt}} = \mathrm{n_C(N_2 - n_2)A_2 - n_2 f_2}, \tag{3.3}$$

$$\frac{\mathrm{dn_1}}{\mathrm{dt}} = \mathrm{n_C(N_1 - n_1)A_1 - n_1 f_1}, \tag{3.4}$$

$$\frac{\mathrm{dm}}{\mathrm{dt}} = -\mathrm{A_m m n_C}, \tag{3.5}$$

$$\frac{\mathrm{dn_C}}{\mathrm{dt}} = -\frac{\mathrm{dn_1}}{\mathrm{dt}} - \frac{\mathrm{dn_2}}{\mathrm{dt}} + \frac{\mathrm{dm}}{\mathrm{dt}}, \tag{3.6}$$

where N_1 and N_2 are the concentrations of available shallow and deep electron traps; f_1 and f_2 are the optical excitation rates out of the shallow and deep traps, respectively. A_1 and A_2 are the probabilities for trapping of free electrons in the shallow and deep traps respectively while A_m is the probability of a free electron recombining with a trapped hole at the recombination centre. The analytical solution to equations 3.3-3.6 is possible under certain assumptions [2]. The first assumption consists of existence of

a quasi-equilibrium situation, that is

$$|\frac{\mathrm{dn_C}}{\mathrm{dt}}| << |\frac{\mathrm{dm}}{\mathrm{dt}}| \text{ or } \frac{\mathrm{dn_C}}{\mathrm{dt}} \approx 0. \tag{3.7}$$

The second states that at the start of illumination, the optical excitation out of the shallow trap is negligible and there is no re-trapping of free electrons into the deep trap; that means

$$\mathrm{n_1 f_1} \approx 0 \text{ and } \mathrm{n_2 f_2} >> \mathrm{A_2(N_2 - n_2)n_C}. \tag{3.8}$$

With these assumptions, equations 3.3-3.5 become

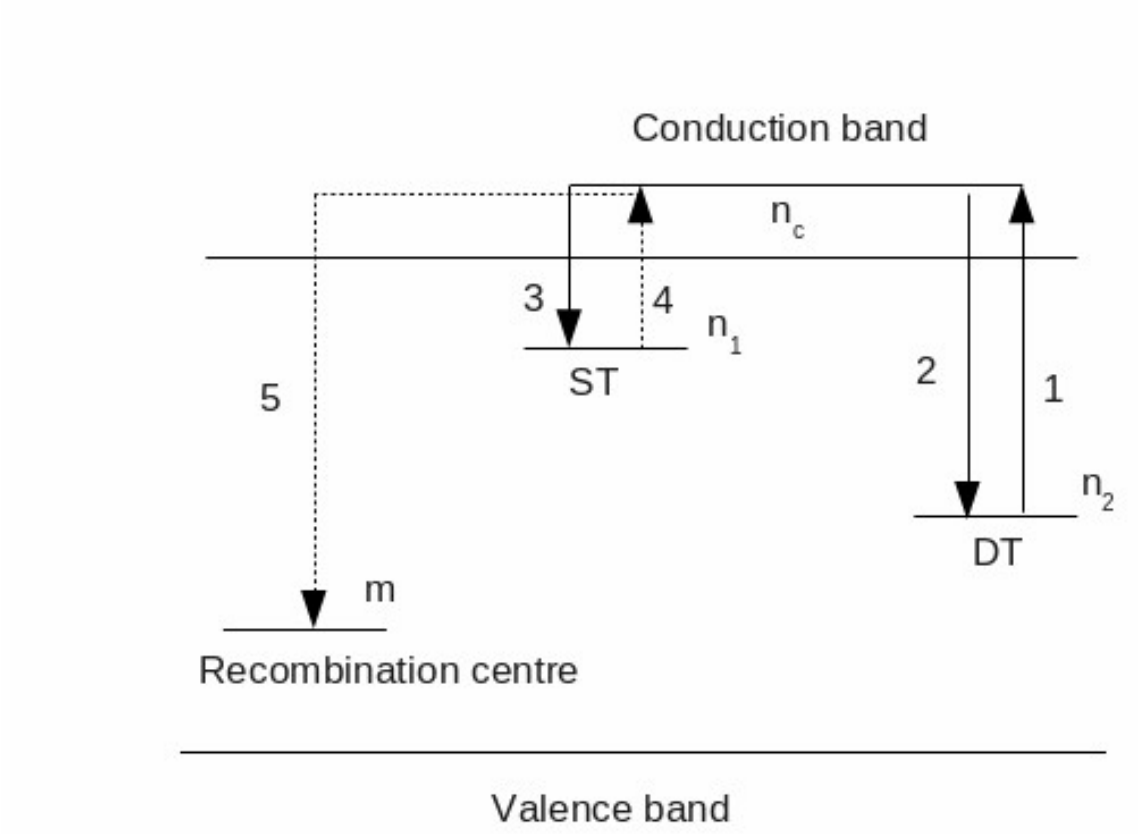

Figure 3.1: Simple model used for analysis of PTTL. n_1 and n_2 stand for the concentrations of electrons in the shallow trap (ST) and deep trap (DT) respectively, n_C and m are the concentrations of free electrons in the conduction band and of holes in the recombination centre, respectively. Transition 1 denotes optical excitation out of the deep electron trap. Some of the electrons are re-trapped into the deep trap (transition 2) others are transferred into the shallow trap via the conduction band, transition 3. In transition 5, trapped electrons are released by subsequent heating or illumination (transition 4) to recombine with holes at the recombination centre to produce PTTL.

$$\frac{dn_2}{dt} = -n_2 f_2, \tag{3.9}$$
$$\frac{dn_1}{dt} = n_C(N_1 - n_1)A_1, \tag{3.10}$$
$$\frac{dm}{dt} = -A_m m n_C, \tag{3.11}$$
$$\frac{dm}{dt} = \frac{dn_1}{dt} + \frac{dn_2}{dt}. \tag{3.12}$$

At the end of the illumination, equations 3.9-3.12 lead to the solutions:

$$n_2(t) = n_{20}\exp(-tf_2) \tag{3.13}$$
$$n_1(t) = N_1(1 - \exp(-bt)) \tag{3.14}$$
$$m(t) = m_0\exp(-t/\tau) \tag{3.15}$$

where $b = n_C A_m$ and $\tau = (n_C A_m)^{-1}$ are constants. The PTTL is, however, produced after subsequent heating following illumination. The heating can only stimulate trapped electrons from the shallow trap and thermal excitation from the deep trap is negligible. Therefore, during heating the rate equations of charge transfer are as follows [16]

$$\frac{dn_C}{dt} = -\frac{dn_1}{dt} - \frac{dn_2}{dt} + \frac{dm}{dt}, \tag{3.16}$$
$$\frac{dn_2}{dt} = n_C(N_2 - n_2)A_2, \tag{3.17}$$
$$\frac{dn_1}{dt} = n_C(N_1 - n_1)A_1 - n_1\gamma_1, \tag{3.18}$$
$$I(t) = -\frac{dm}{dt} = A_m m n_C. \tag{3.19}$$

where $I(t)$ is the intensity of the PTTL emission during heating and γ is the thermal excitation or thermal detrapping constant. The thermal excitation associated with the shallow trap is given by

$$\gamma_1 = s_1 \exp(-E_1/kT), \tag{3.20}$$

where s_1 and E_1 are the frequency factor and the activation energy associated with the shallow trap; T is the temperature in Kelvin and k is the Boltzmann's constant. On

assumption of quasi-equilibrium ($dn_C/dt \approx 0$), equation 3.16 can be written as [2]

$$\frac{\mathrm{dm}}{\mathrm{dt}} = \frac{\mathrm{dn_1}}{\mathrm{dt}} + \frac{\mathrm{dn_2}}{\mathrm{dt}}, \tag{3.21}$$

which can be integrated from initial to final values of concentrations n_1, n_2 and m to yield

$$\mathrm{m} - \mathrm{m_0} = \mathrm{n_1} - \mathrm{n_{10}} + \mathrm{n_2} - \mathrm{n_{20}}. \tag{3.22}$$

Substituting equations 3.17, 3.18 and 3.19 into 3.21, one can get

$$\mathrm{n_C} = \gamma_1 \mathrm{n_1} \times \left[\mathrm{A_1(N_1 - n_1) + A_2(N_2 - n_2) + A_m m}\right]^{-1}, \tag{3.23}$$

and substituting equation 3.23 into equation 3.19 we get

$$\mathrm{I(t) = -dm/dt = A_m \gamma_1 n_1 m} \times \left[\mathrm{A_1(N_1 - n_1) + A_2(N_2 - n_2) + A_m m}\right]^{-1}. \tag{3.24}$$

The simultaneous solution to the differential equations 3.17 and 3.19 leads to

$$\mathrm{N_2 - n_2 = (N_2 - n_{20})(m/m_0)^{A_2/A_m}}. \tag{3.25}$$

From equations 3.22 and 3.25, the differential equation 3.24 can be rewritten as

$$\mathrm{I_{PTTL}(t) = -dm/dt = \gamma_1 A_m m F(m)}. \tag{3.26}$$

The quantity F(m) is reported by Chen and McKeever [2] as

$$\mathrm{F(m) = \frac{(n_{10} + n_{20} - m_0 - N_2) + m + (N_2 - n_20)(m/m_0)^{A_2/A_m}}{A_1((N_1 + N_2 - n_{10} - n_{20} + m_0) + (A_m - A_1)(N_2 - A_1)(N_2 - n_{20})(m/m_0)^{A_2/A_m}}}, \tag{3.27}$$

where the set of parameters in the equation were previously defined. From theoretical background [2], equations 3.26 and 3.27 can only be analytically solved for various sets of given parameters. Using a heating rate $\beta = dT/T$ with assumptions of quasi-equilibrium for a negligible retrapping into shallow trap ($n_{10} << N_2 - n_{20}$) during

heating; equations 3.26 and 3.27 lead to the following

$$\mathrm{S_{PTTL}} = \int_{\mathrm{To}}^{\mathrm{T_f}} \mathrm{I_{PTTL}dT} \approx \frac{\mathrm{A_m m_0 n_{10}}}{\mathrm{A_2(N_2 - n_{20})}} \tag{3.28}$$

where S_{PTTL} is the measured PTTL intensity which can be defined as the integrated area under the PTTL peak from the initial to final temperatures T_o and T_f respectively. The time dependence of PTTL intensity can be analyzed using the above assumptions. Thus, equation 3.28 can be written as [2, 16].

$$\mathrm{S_{PTTL}} = \mathrm{C}\frac{\mathrm{m(t)n_1(t)}}{\mathrm{N_2 - n_2(t)}} \tag{3.29}$$

where C is a proportionality constant of integrated PTTL. Using equations 3.13, 3.14 and 3.15 into equation 3.29, one can get

$$\mathrm{S_{PTTL}(t)} = \mathrm{C}\frac{\exp(-\mathrm{t}/\tau)\mathrm{N_1}[1 - \exp(-\mathrm{bt})]}{\mathrm{N_2/n_{20}} - \exp(-\mathrm{f_2 t})} \tag{3.30}$$

For longer illumination, $t \longrightarrow \infty$, Chen and McKeever [2] showed that $n_2 \longrightarrow 0$ and $m \longrightarrow n_1$. It means that the PTTL intensity increases from zero to a maximum as

$$\mathrm{S_\infty} = \mathrm{C}\frac{\mathrm{n_{1\infty}}}{\mathrm{N_2}} \tag{3.31}$$

where $n_{1\infty}$ is the final concentration in the shallow trap at longer illumination $t = \infty$ and should be equal to the final concentration in the centre m_∞. This implies that the simple model used to explain the PTTL phenomenon shows an increase of PTTL intensity from zero to a maximum level with illumination time [2].

From our experimental data different behaviours of PTTL signal versus illumination time curves were observed. In contrast to the PTTL described using the simple model, some PTTL curves showed a peak shape structure and others a saturating exponential growth at longer illumination times. More details will be given in the sections to follow. Therefore, the simple model used to explain PTTL feature can be compared with other complex models for better understanding of the PTTL phenomenon.

3.2.2 General model

A number of publications [1, 2, 16–19] have discussed various forms of PTTL for different materials. The PTTL signal may go through a peak or have a saturating exponential growth at longer illumination times. Some PTTL intensity versus illumination time curves reach zero after long illumination times while others are described by a non-zero steady level [16]. Therefore, the assumptions made for the simple model may not always apply to particular experimental data from different samples. So, in a given sample, a complete analysis of the PTTL signal against illumination time curve can employ various models from which the real data can be fitted. Figure 3.2 shows an example of a general band model proposed by Bøtter-Jensen et al. [20] which can be used to explain a complete curve of the PTTL intensity versus illumination time [2]. An extra optically inactive deep trap, level 3, is added while an additional recombination centre R_2 provides a competing non-radiative recombination pathway. Thus, the

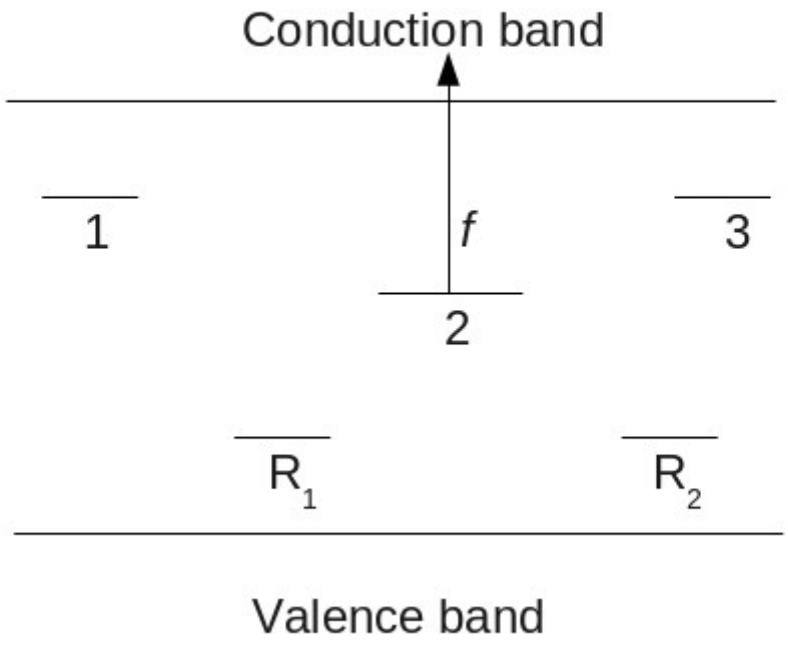

Figure 3.2: A general energy band model used to explain a PTTL peak with illumination time [2, 20]. Levels 1, 2 and 3 are the shallow trap, optically active and optically inactive deep traps, respectively; R_1 and R_2 are the radiative and non-radiative recombination centres, respectively. An upward arrow represents optically excited electrons from an optically active deep trap at a rate f.

charge neutrality condition becomes

$$\mathrm{n_1 + n_2 + n_3 = m_1 + m_2} \tag{3.32}$$

where n_1, n_2 and n_3 are the concentrations of electrons in the shallow, optically active and optically inactive deep traps; m_1 and m_2 are the concentrations of holes in the radiative and non-radiative recombination centres, respectively. Before illumination but immediately after preheat, the shallow trap is empty of electrons and the concentrations of electrons in the optically active and deep traps are equal to the number of holes in the recombination centres. During illumination, the observed PTTL growth with illumination corresponds to the increase in electrons filling into the shallow trap due to the optically emptying of electrons out of the deep trap. However, the increase of the PTTL signal may be followed by a decrease at long illumination times. This decrease of the PTTL intensity is caused by some of trapped charges that are optically lost from the shallow trap. Thus, under the assumption of quasi-equilibrium and negligible retrapping into deep trap during illumination the evolution of PTTL as a function of illumination time depends on the minimum available n_1 and m_1. From the above assumptions, an example of analytical function to explain PTTL phenomenon was suggested

$$\mathrm{S_{PTTL}(t) = \frac{Cf_2n_{20}}{f_1 - f_2}\left[\exp(-f_2 t) - \exp(-f_1 t)\right]} \tag{3.33}$$

where C is the proportionality constant, f_1 and f_2 are the rate constants of loss of electrons from shallow and deep traps respectively, and n_{20} is the initial electrons concentration in the optically active deep trap [16, 19]. Equation 3.33 was used to explain evolution of a PTTL peak [16, 19], example from quartz. However, experimental data where a decrease of a PTTL showed a non-zero steady state at long illumination times cannot always be explained by any of the above models. Thus, for PTTL phenomenon, an analytical function which can be used to explain a complete curve of PTTL peak depends essentially on experimental data and is subject to modification from sample to sample. For example, a general band model shown in figure 3.2 may be adapted to

the band model of α-Al_2O_3 : C in order to be used for analysis of PTTL behaviour in this material under study. Unlike the above model, the model for α-Al_2O_3 : C uses one recombination centre [21] from which a competing non-radiative recombination pathway is provided by an excited state which is between the 3P state and the conduction band.

Figure 3.3 shows the general energy band model of α-Al_2O_3 : C previously suggested by different authors [4, 9, 21, 22] used to describe PTTL phenomenon. The model involves charge transfer exchanges between shallow, main and intermediate electron traps which are associated with peak I, main peak and peak III, respectively. A deep electron trap and a deep hole trap compete for electron during illumination. The detailed mechanism of PTTL in α-Al_2O_3 : C using a general energy band model will be presented in the results section to follow.

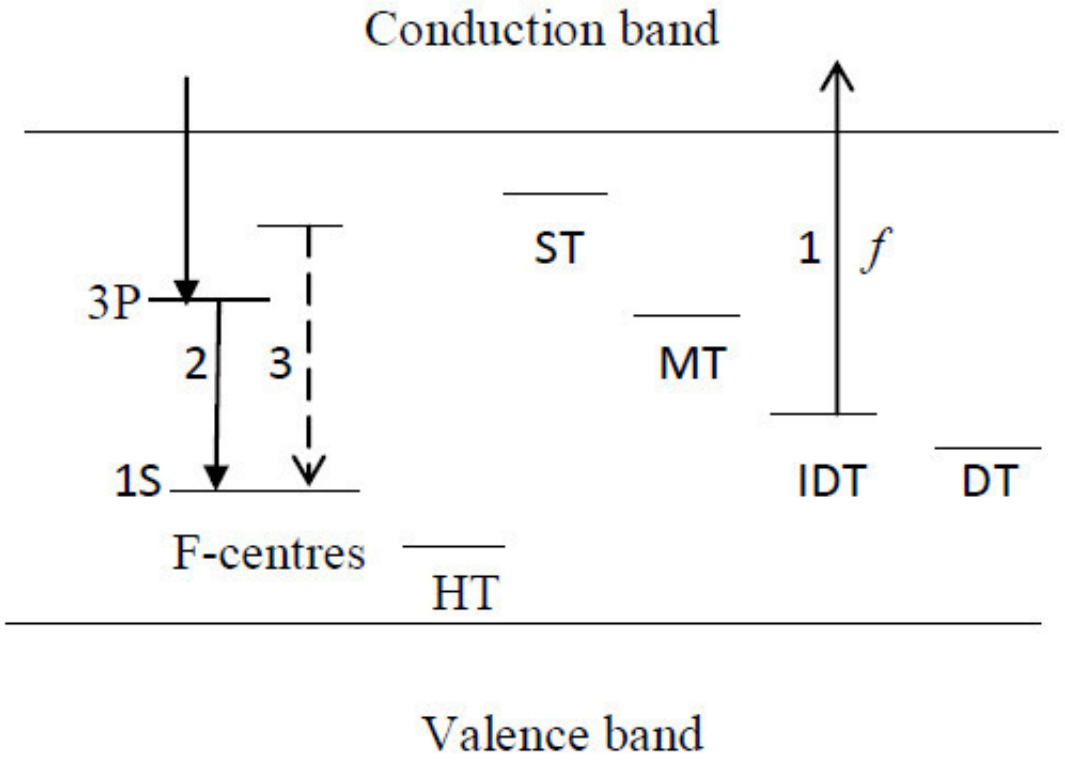

Figure 3.3: The general energy band model of α-Al_2O_3 : C which contains shallow, main and intermediate trap levels (ST, MT and IDT) while 3P is an excited state of F-centres and 1S the ground state F-centres. The optical excitation rate to the conduction band is given by f. Transitions 2 and 3 are radiative and non-radiative recombinations, respectively.

Chapter 4

Experimental procedures

In this chapter, we describe the apparatus used to measure thermoluminescence and we provide a detailed description of the experimental procedures followed. The details include sample preparation by annealing and thermoluminescence read out. A brief description of the sample under study (α-$Al_2O_3 : C$) is also included in this chapter.

4.1 Experimental apparatus

4.1.1 The Risø TL/OSL Luminescence Reader

Figure 4.1 shows the Risø TL/OSL DA-20 Luminescence Reader used to measure thermoluminescence in our study. Figure 4.2 shows a schematic diagram of an irradiator, heating system and light detectors of the Reader. Samples were placed on planchettes or sample holders, then on the sample carousel of the heating system. The irradiation is made at room temperature using a $^{90}Sr/^{90}Y$ beta source at dose rate of $0.1\,Gy\,s^{-1}$. During irradiation, the source faces the sample. When the source is not irradiating, it faces in opposite direction to the sample position. At the measurement position, samples are illuminated and heated. For measurements of phototransferred thermoluminescence, samples were illuminated by blue light from 470 nm blue light emitting diodes with the photon power of $80\,mW/cm^2$. The blue light has enough energy to transfer electrons from the deep electron traps to the shallower ones during illumination

times. Thermoluminescence was recorded from 30°C to 500°C at a constant heating rate between 0.1 and 5°C s^{-1} for doses between 0.5 up to 3 Gy. The thermoluminescence was detected by an EMI 9235QB photomultiplier tube via a Hoya U-340 filter with transmission band 250-390 nm FWHM. Nitrogen was used in all measurements of TL to prevent the oxidation of the sample heater and to improve thermal contact between sample holder and heater planchet. The temperature is given in ^oC unless otherwise stated.

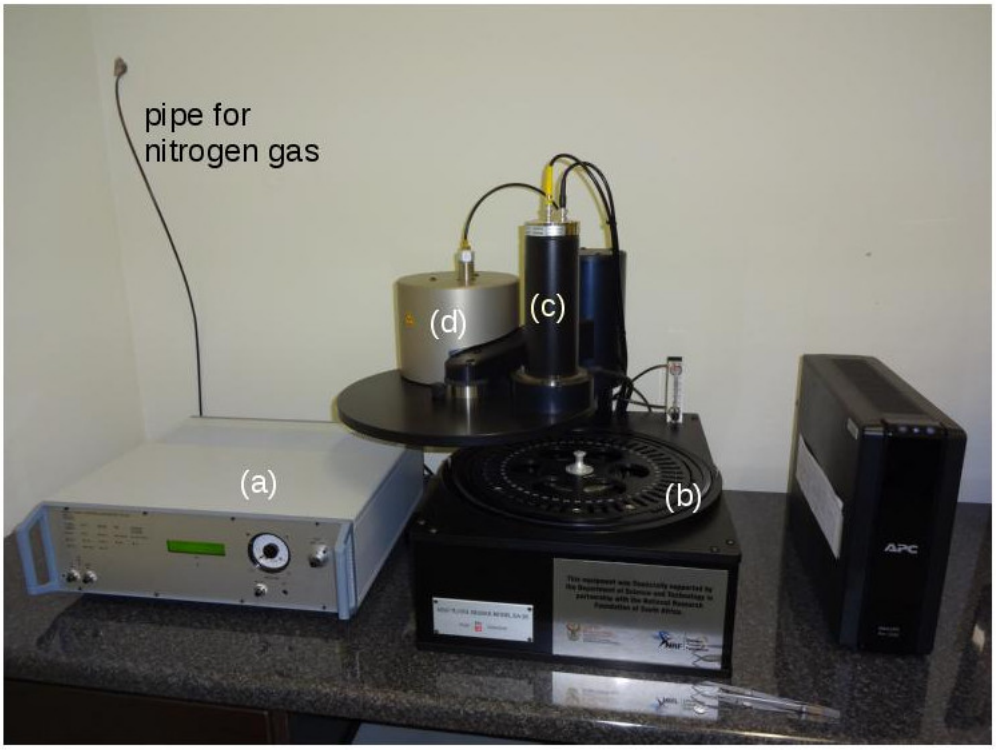

Figure 4.1: The Risø TL/OSL Luminescence Reader system, model DA-20. (a) The controller unit, (b) denotes the reader unit comprising the heating system and the lift mechanism, (c) is the photomultiplier and (d) is a $^{90}Sr/^{90}Y$ beta source.

4.1.2 The tube furnace

The tube furnace (DTP-563 DN-E Kiln control model) was used to anneal samples at 900°C for 15 minutes followed by rapid cooling in air. The purpose of annealing was to remove any residual charges present in deep traps. Figure 4.3 shows the tube furnace. The furnace can be heated at a rate of 167°C/hour from room temperature to 1260°C.

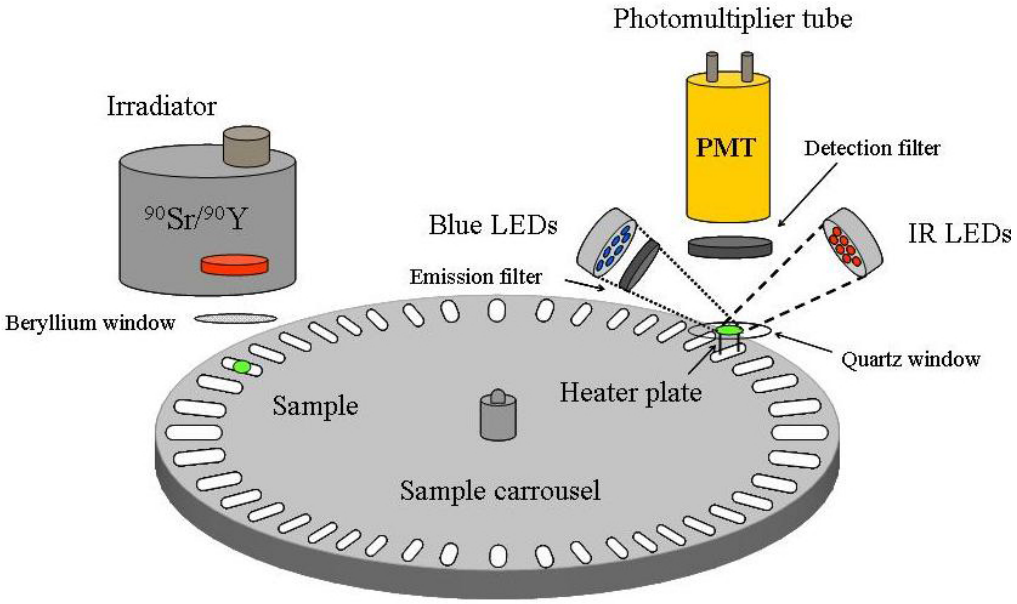

Figure 4.2: A schematic diagram of the reader system [23]. An irradiator is a ^{90}Sr/^{90}Y β source, the sample carousel and heater plate are components of the heating system; the light detection system comprises a photomultiplier tube and detection filters. Blue LED is used for optical simulation.

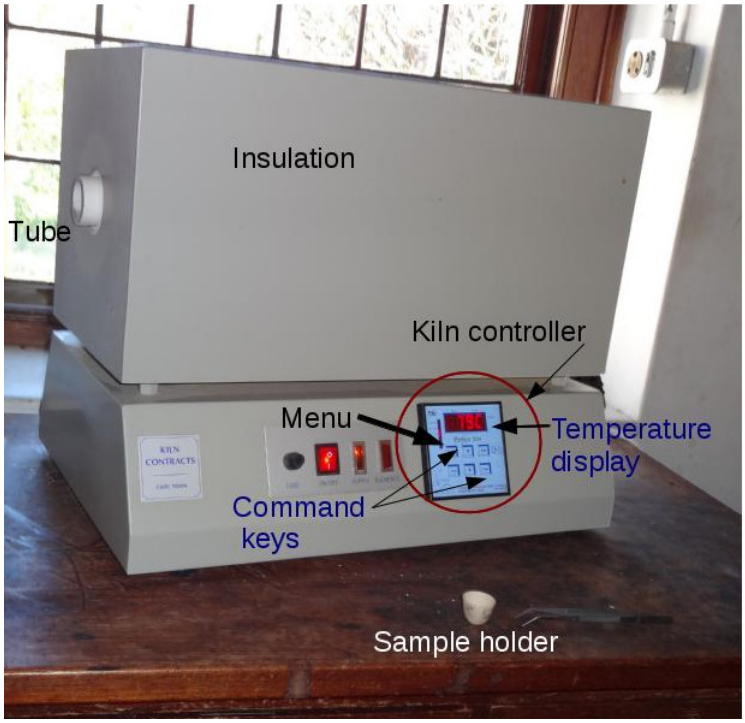

Figure 4.3: A tube furnace DTP-563 DN-E model. Once the furnace is connected to the main supply, the annealing temperature is set using the menu and setting keys. A ceramic pot was used to hold the sample during annealing.

4.1.2.1 The calibration of furnace

The coincidence of measured and set temperatures from the tube furnace was checked by calibrating the furnace. Figure 4.4 shows a plot of minimum and maximum temperatures as a function of set temperature. Experimentally, the displayed temperature oscillates between a maximum and a minimum about a set temperature. The minimum and the maximum temperatures overlap the set temperature with small deviations.

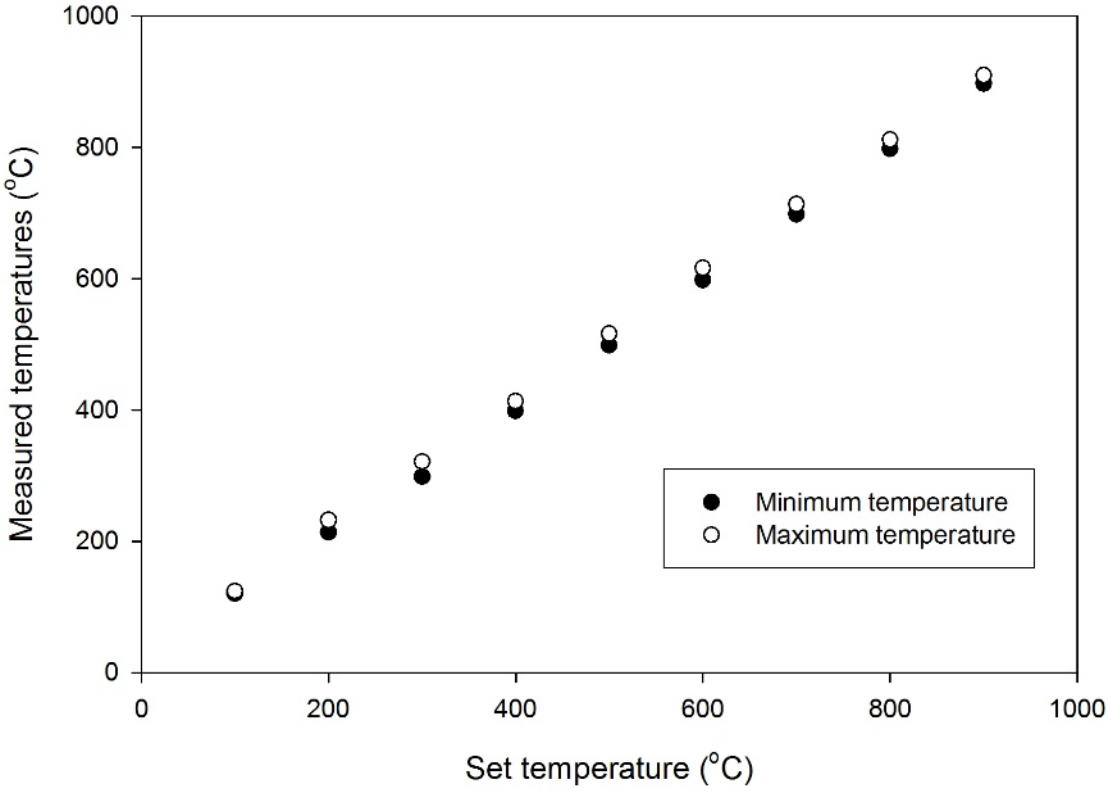

Figure 4.4: Minimum and maximum temperatures as a function of set temperature. It can be seen that the minimum and the maximum oscillate about the set temperature of the furnace with small deviation.

Figure 4.5 shows the mean temperature displayed on the controller versus set temperature. The residuals between the mean temperature and set temperature are shown on the top of figure 4.5. After calibration, the plot of residuals showed deviations in measurements ranging within 6.4°C of set temperature for temperature from 100°C to 900°C. Thus the mean temperatures measured from the furnace can be a good approximation to the set temperatures from the furnace.

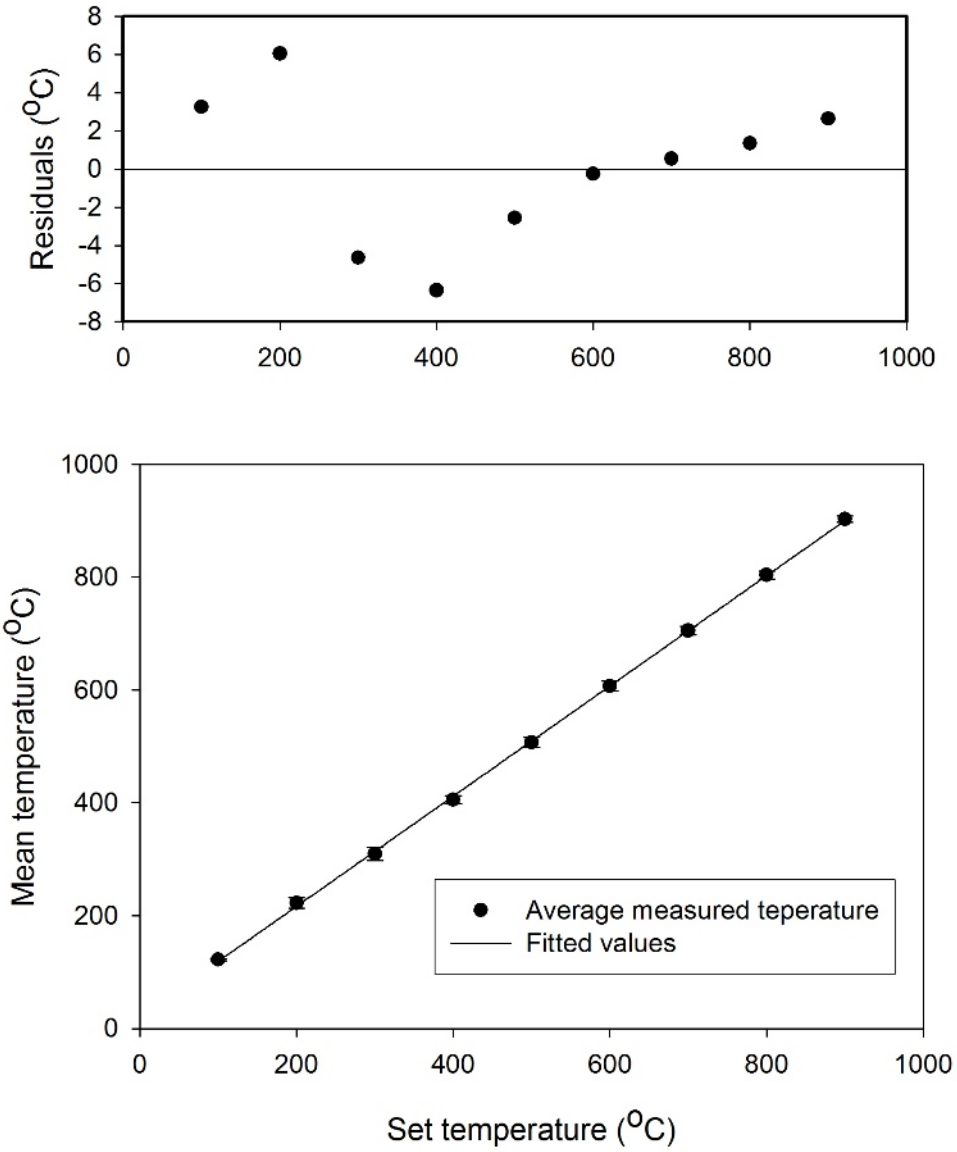

Figure 4.5: The average temperature from the minimum and the maximum temperatures measured from the furnace as a function of set temperature. As can be seen, residuals from the fit plotted as a function of set temperature showed small deviations of about 6.4°C.

4.2 Experimental samples

Samples used in this study were carbon-doped aluminium oxide (α-$Al_2O_3 : C$) discs of size 5 mm diameter and 1 mm thickness (Rexon TLD Systems, Ohio, U.S.A). These are largely used in luminescence dosimetry. α-$Al_2O_3 : C$ is a synthetically produced a ultra-sensitive luminescence dosimeter. Figure 4.6 shows the crystal structure of the material in a slightly distorted hexagonal O^{2-} ion sublattice with Al^{3+} ions situated in two out of three distorted octahedral (O_h symmetry) sites.

The high TL sensitivity of α-Al_2O_3 : C is associated with an increased concentration of oxygen vacancies during its growth in a highly reducing atmosphere in the presence of carbon [1, 4]. The formation of oxygen vacancies in the crystal arise from the substitution of O^{2-} by C^{4-} during its growth from which charge compensation are provided [3]. The most important point defects investigated in α-Al_2O_3 : C include a neutral F-centre (an O^{2-} ion vacancy is occupied by two-electrons) and an F^+-centre which arises from the occupancy of the vacancy by one-electron. The electrons involved in this process result from ionization in a previously irradiated material. The TL emission spectra of α-Al_2O_3 : C are dominated by an emission band between 410 and 420 nm [3, 4]. This band has been attributed to radiative transition caused by the relaxation of an electron from the excited 3P state to 1S ground state of the F-centre following

$$F^+ + e^- \Rightarrow F^* \Rightarrow F + h\nu_{410-420nm} \tag{4.1}$$

where F^* is the excited F centre. This relation means that an electron and the F^+ centre recombine to produce an excited F centre which relaxes to the ground state with the emission of a photon of a wavelength in the region 410-420 nm.

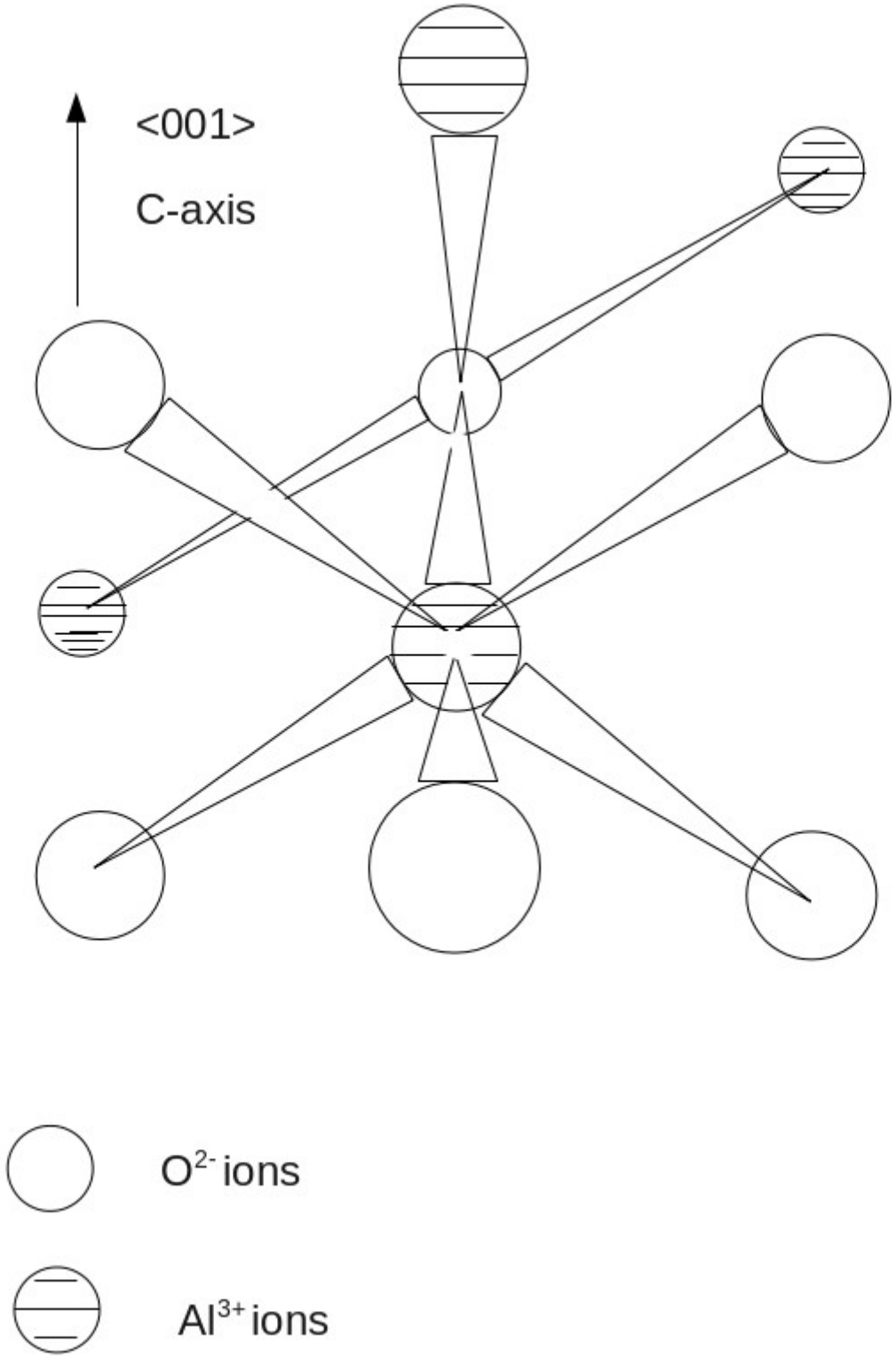

Figure 4.6: The crystal structure of α-Al_2O_3 : C in a slightly distorted hexagonal O^{2-} ion sublattice with Al^{3+} ions in octahedral sites [3].

Chapter 5

Results and discussion

5.1 Kinetic analysis of thermoluminescence of secondary glow peaks in α-$Al_2O_3 : C$

5.1.1 Thermoluminescence glow curves

Thermoluminescence glow curves were experimentally measured after heating samples from 30°C to 500°C following previous absorption of radiation. Samples used in thermoluminescence analysis showed three peaks; a dominant main peak of high intensity, usually used in dosimetry, and other two secondary peaks of low intensities. Figure 5.1 shows the main peak (peak II) at 186°C, the lower temperature secondary peak (peak I) at 46°C and the higher temperature secondary peak (peak III) at 314°C measured using a heating rate of $1^{\circ}\mathrm{C\,s^{-1}}$ after a beta dose of 0.5 Gy. This work focuses on the kinetic analysis of thermoluminescence of peaks I and III. Thermoluminescence was measured immediately after beta radiation to avoid fading of the TL signal at room temperature.

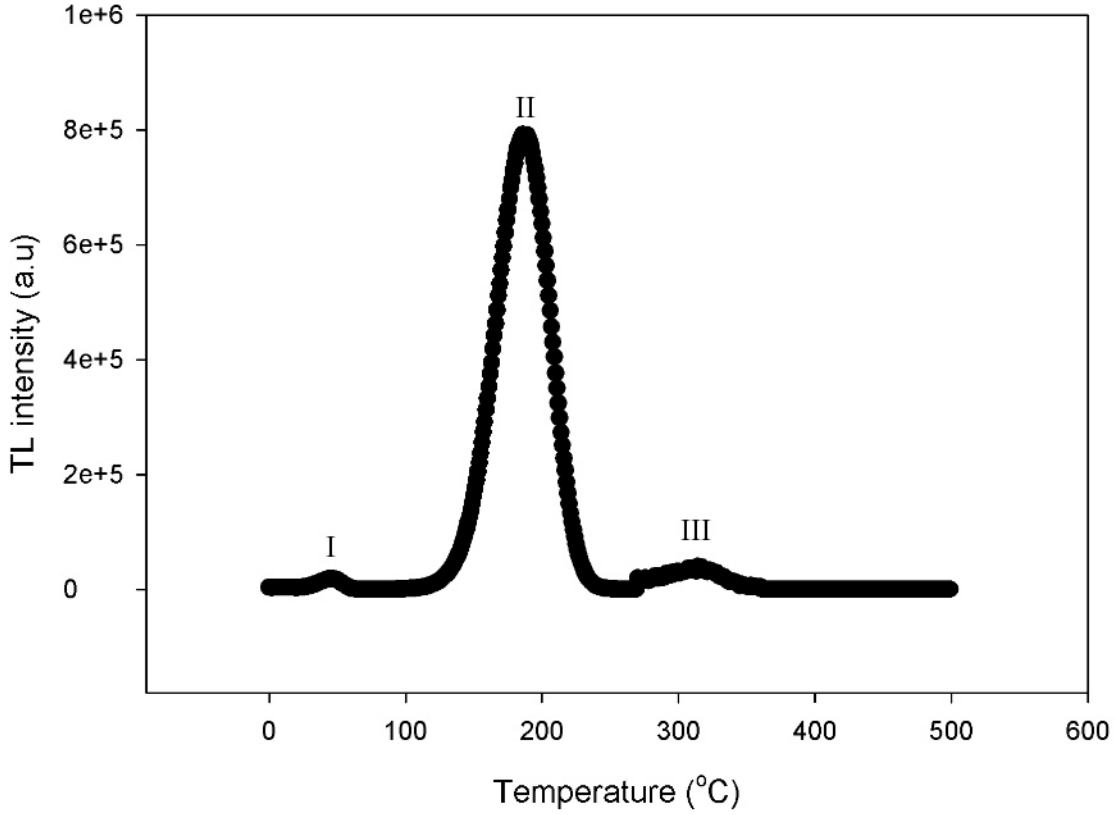

Figure 5.1: A thermoluminescence glow curve following heating to $1^{o}\mathrm{C\,s^{-1}}$ and a dose of 0.5 Gy. Data for peak III has been scaled up for better clarity.

5.1.2 Kinetic analysis of the low temperature secondary peak: peak I

The thermoluminescence for the low temperature secondary peak, peak I, was studied using a heating rate of $1^{o}\mathrm{C\,s^{-1}}$ for doses less than 2.5 Gy. The kinetic parameters associated with peak I were evaluated using six methods. These methods were the initial rise, whole curve, peak shape, variable heating rate, isothermal analysis and glow curve deconvolution methods. A variety of methods were used to check the validity and the reliability of the physical parameters from TL data for peak I. The order kinetics for peak I was assessed using the T_M-T_{stop} method [1, 5]. The order kinetics for peak I was further checked either by data from its dependence on doses or by using the isothermal analysis and the glow curve deconvolution methods.

5.1.2.1 The initial rise method

Figure 5.2 shows graph of $\ln(I)$ against $1/kT$ for a sample irradiated to 0.5 Gy using a heating rate of $1^{o}\mathrm{C\,s^{-1}}$. The activation energy was calculated from the slope of the best fit. The 15% rule of thumb [5] was not applied because TL data for peak I less than 15% of I_M corresponded to temperatures below 30°C. Different values of E evaluated using the initial rise method for different doses between 0.5 and 2.5 Gy are summarized in table 5.1 and, for clarity, in figure 5.3. As can be seen, E values are consistent. There was no real change of activation energy for peak I using the initial rise method at various doses from 0.5 to 2.5 Gy. The statistical scatter present may be due to the weak intensity of peak I and also due to inapplicability of the 15% rule of thumb. The average value of activation energy was $\mathrm{E} = 0.72 \pm 0.01\,\mathrm{eV}$. The corresponding frequency factor, on assumption of first order kinetics, was calculated as

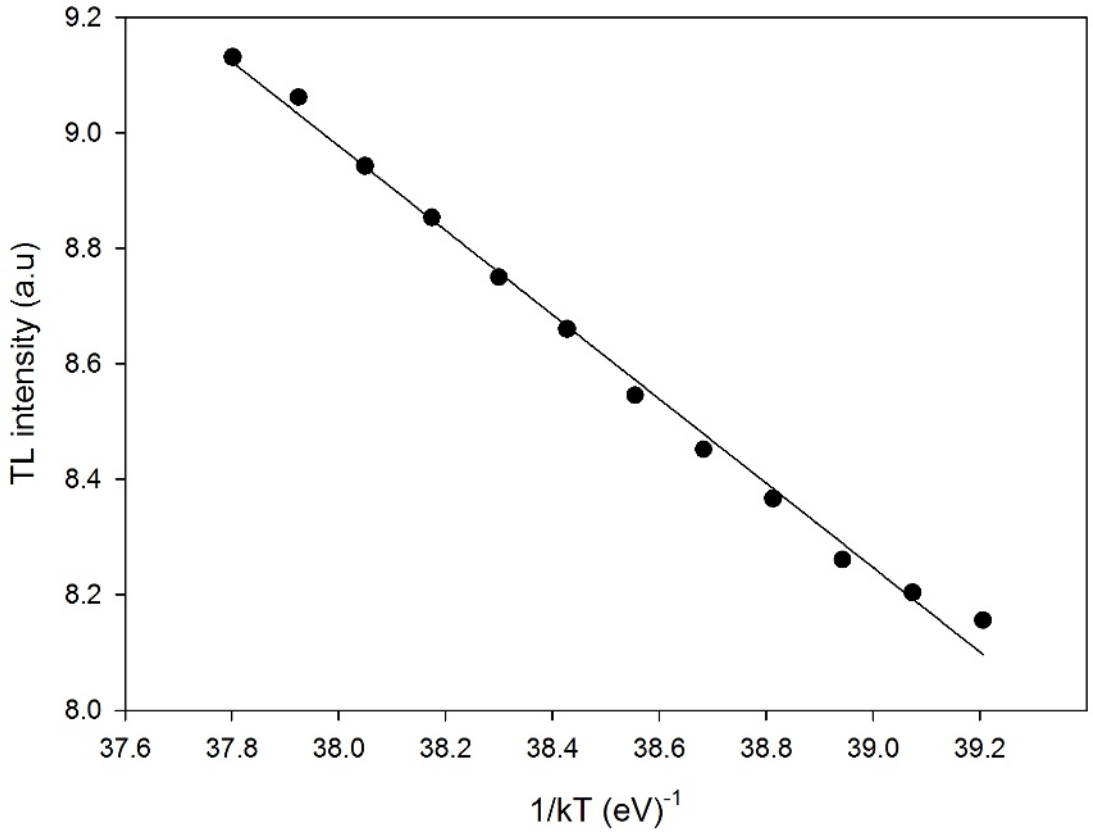

Figure 5.2: A plot of $\ln(I)$ versus $1/kT$ from the initial rise method for peak I. The sample was dosed to 0.5 Gy and TL measured at $1.0^{o}\mathrm{C\,s^{-1}}$. In this example, $\mathrm{E} = 0.73 \pm 0.02\,\mathrm{eV}$.

$s = 3 \times 10^{10}\,\mathrm{s}^{-1}$. The s value, the frequency at which an electron attempts to escape from a trap, is theoretically reasonable for being of the order of the Debye vibration frequency [5].

Table 5.1: The activation energy evaluated from the initial rise method for peak I.

β-dose (Gy)	E (eV)	Average E (eV)
0.5	0.73 ± 0.02	
1.0	0.73 ± 0.02	
1.5	0.73 ± 0.01	0.72 ± 0.01
2.0	0.70 ± 0.02	
2.5	0.72 ± 0.01	

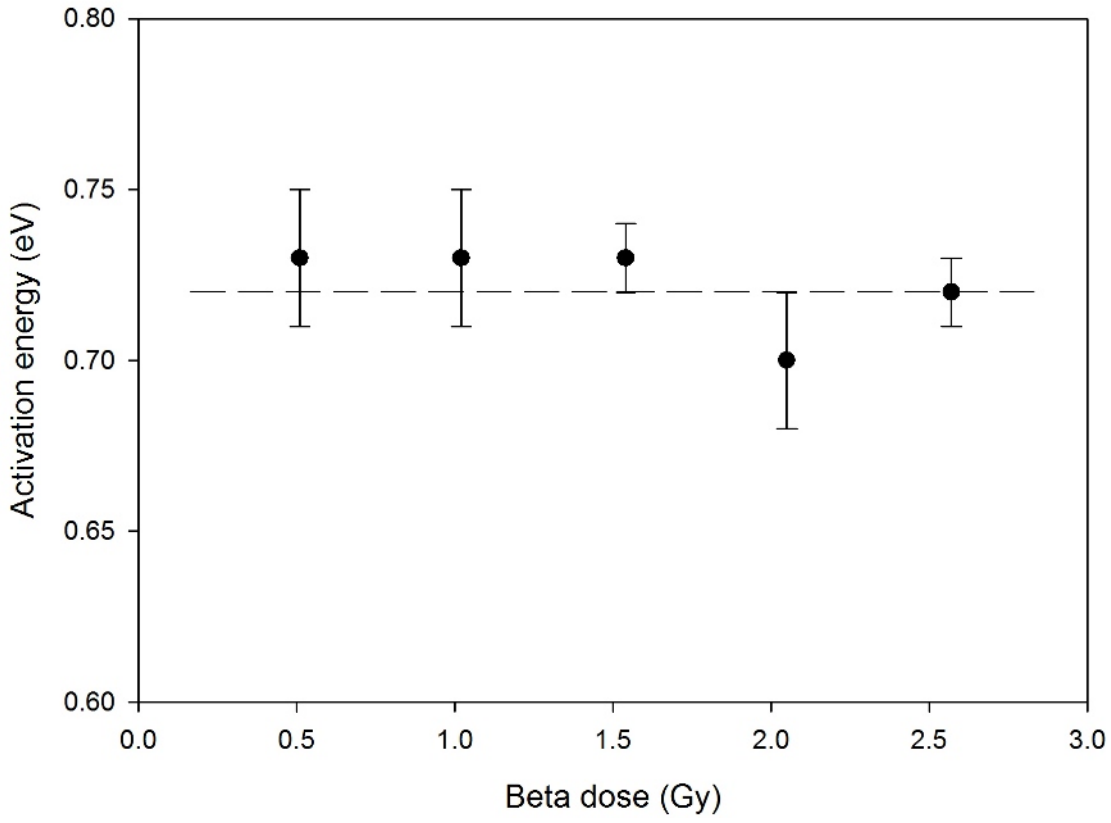

Figure 5.3: A graph of E versus dose for peak I. A straight line is inserted for clarity. The activation energy E is independent of dose.

5.1.2.2 The whole glow curve method

Thermoluminescence data for the whole of peak I were used in equation 2.32 to generate a graph of $\ln(I/n^b)$ against $1/kT$ presented in figure 5.4. Several straight lines were

obtained from the plots corresponding to various values of b between 0.9 and 1.2. The heating rate was $1^{\circ}\mathrm{C\,s^{-1}}$ and the sample was dosed to 0.5 Gy. The best option was for $b = 1$ from which an activation $\mathrm{E} = 0.90 \pm 0.02\,\mathrm{eV}$ was evaluated from the slope of the straight line. The y-intercept yielded a pre-exponential frequency factor for first order $s = 2 \times 10^{13}\,\mathrm{s^{-1}}$. Errors in the calculated E are attributed to the fact that peak I is partially-separated from other peaks. When applied to a well-resolved peak, the whole curve method can be expected to give a satisfactory estimation of kinetic parameters.

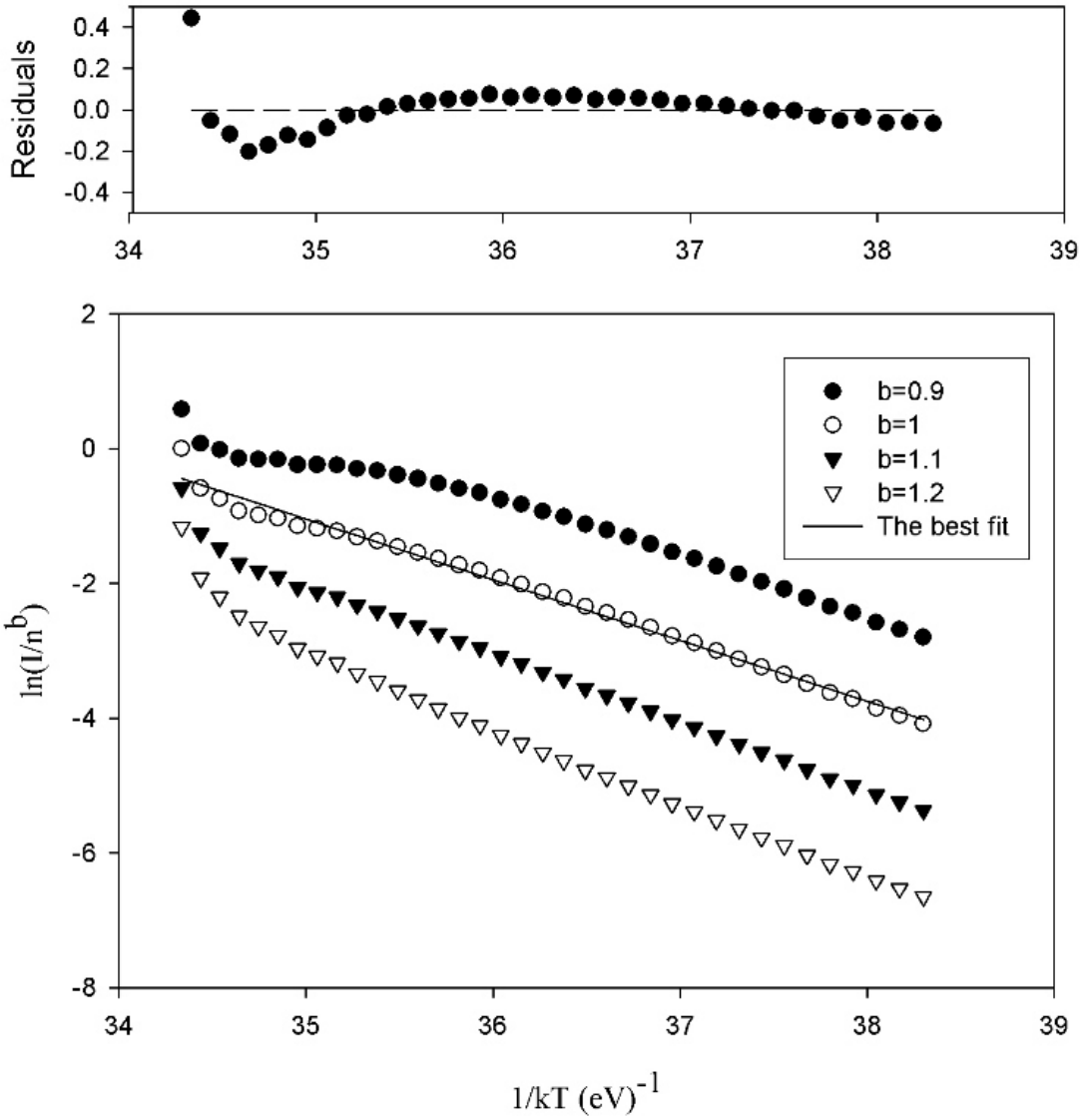

Figure 5.4: The whole curve method applied on peak I for TL measured at a heating rate of $1^{\circ}\mathrm{C\,s^{-1}}$ after dose of 0.5 Gy. The dependence of $\ln(I/n^b)$ on $1/kT$ for $b = 0.9$, 1, 1.1 and 1.2 yields several straight lines from which a plot of the residuals versus $1/kT$ shows the best option for $b = 1$. This suggests that first order kinetics apply for peak I.

5.1.2.3 The peak shape method

The peak shape method consisted of use of three parameters τ, δ and ω defined in equations 2.10, 2.11 and 2.12 measured from TL data for peak I. The maximum temperature appeared at 46°C independently of irradiation for beta dose between 0.5 and 2.5 Gy when a heating rate of $1^{o}\mathrm{C\,s^{-1}}$ was used. The results of activation energy evaluated using equation 2.14 in three forms of the peak shape method for doses between 0.5 and 2.5 Gy are shown in table 5.2. From the table, it can be seen that the kinetic parameters are consistent between different forms of the peak shape method. The average result of the symmetry factor μ_g for a variety of doses between 0.5 and 2.5 Gy was found to be 0.42 ± 0.03. This means that first order kinetics apply for peak I. Using a first order kinetics expression for the frequency factor s, equation 2.4, $s = 4.6 \times 10^{15}\,\mathrm{s^{-1}}$ was evaluated for E_ω and E_τ while for E_δ $s = 5.0 \times 10^{14}\,\mathrm{s^{-1}}$ was found. The values of E and s obtained using the peak shape method are consistent. However, E and s values calculated from the peak shape method are greater than the E and s values evaluated from the initial rise and the whole curve methods. The differences may be caused by imprecision in choice of temperatures for τ, δ and ω. Any resultant errors are propagated when calculating E and s. However, these values of E and s are comparable to the results previously reported by Mishra et al. [10] using the same method. In addition, as the initial rise method, the calculated activation energy using the peak shape method is essentially independent of dose. Figure 5.5 shows this result for E_ω.

Table 5.2: Comparison of activation energies calculated from three forms of the peak shape method for TL data from peak I using a heating rate of $1^{o}\mathrm{C\,s^{-1}}$ following various doses from 0.5 up to 2.5 Gy.

β-dose (Gy)	μ_g	E_ω (eV)	E_τ (eV)	E_δ (eV)
0.5	0.42 ± 0.03	1.05 ± 0.05	1.07 ± 0.07	1.01 ± 0.11
1.0	0.41 ± 0.03	1.04 ± 0.01	1.00 ± 0.06	0.93 ± 0.11
1.5	0.43 ± 0.03	1.09 ± 0.14	1.09 ± 0.09	1.08 ± 0.24
2.0	0.41 ± 0.03	1.04 ± 0.01	1.00 ± 0.06	0.93 ± 0.11
2.5	0.42 ± 0.03	1.05 ± 0.05	1.07 ± 0.07	0.99 ± 0.11
Average	$\mathbf{0.42 \pm 0.03}$	$\mathbf{1.05 \pm 0.05}$	$\mathbf{1.05 \pm 0.07}$	$\mathbf{0.99 \pm 0.14}$

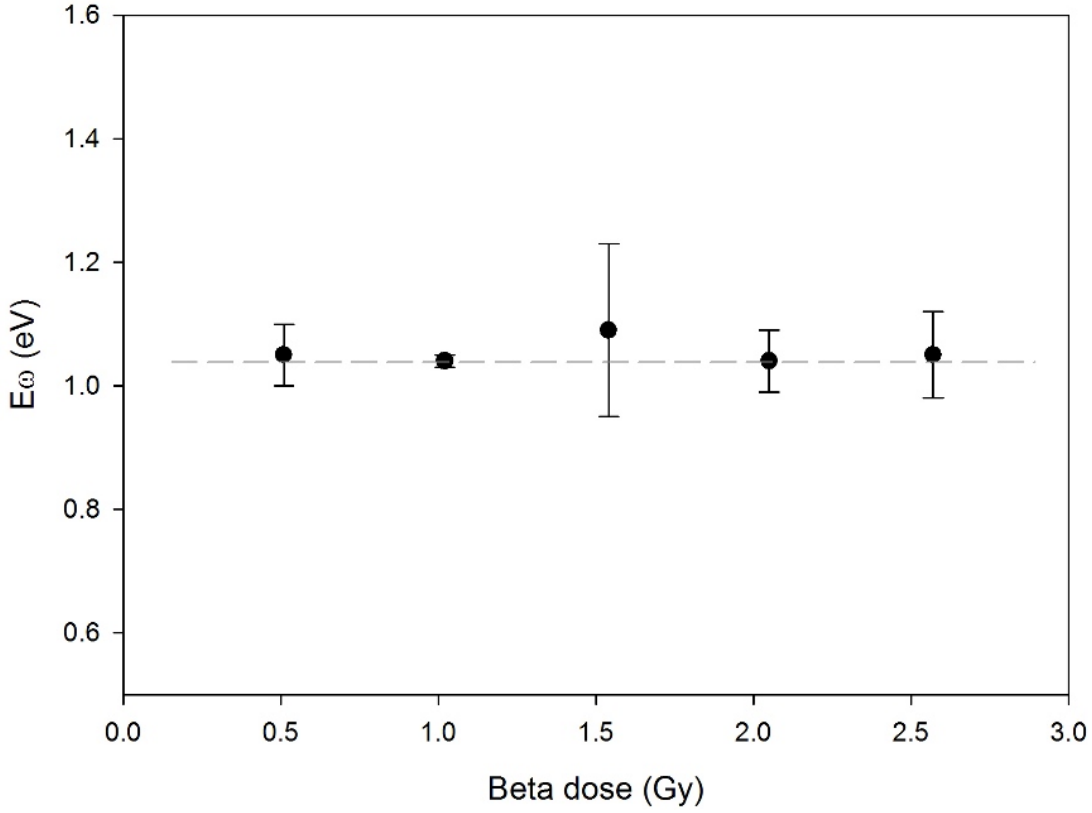

Figure 5.5: A plot of E_ω against beta dose for peak I using the peak shape method. The activation energy is independent of dose. The dashed line is only a visual guide.

5.1.2.4 The variable heating rate method

The variable heating rate method employed various heating rates between $0.1^{o}\mathrm{C\,s^{-1}}$ and $2^{o}\mathrm{C\,s^{-1}}$ at a beta dose of 0.5 Gy. Figure 5.6 shows a plot of $\ln\left(T_M^2/\beta\right)$ versus $1/kT_M$ from which the slope and intercept of the straight line yielded $\mathrm{E} = 0.72 \pm 0.04\,\mathrm{eV}$ and $s = 1.6 \times 10^{10}\,\mathrm{s^{-1}}$ respectively. For first order kinetics using equation 2.4, a similar value of $s = 2.7 \times 10^{10}\,\mathrm{s^{-1}}$ was calculated. The values of E and s calculated using the variable heating rate method are in a good agreement with E and s values from the initial rise and whole curve methods. Alternatively, pairs of heating rates were used in the formula in equation 2.27 and $\mathrm{E} = 0.85\,\mathrm{eV}$ was evaluated.

Figure 5.7 shows the dependence of TL intensity (in arbitrary units) on heating rate. As can be seen, the TL intensity increases monotonically as a function of a heating rate. The cause of this increase of TL intensity for peak I when the heating rate is increased is not well known.

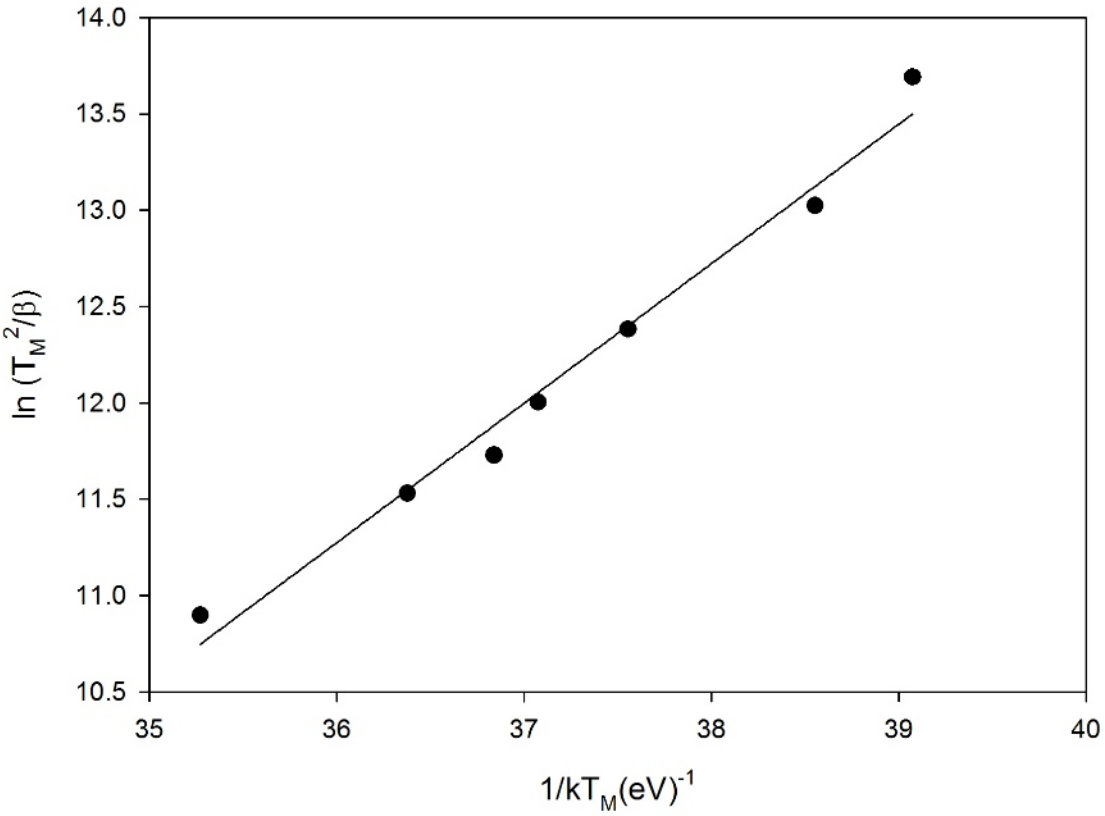

Figure 5.6: The dependence of $\ln(T_M^2/\beta)$ on $1/kT$ which was applied to determine values of E and s from TL data for peak I using heating rates between 0.1 and 2°C s^{-1} for TL corresponding to a beta dose of 0.5 Gy.

5.1.2.5 The isothermal analysis method

Unlike the previously stated methods from which the TL measurements employed linear heating from room temperature up to 500°C, the trapping parameters using isothermal analysis were calculated at different constant temperatures. Firstly, using a heating rate of 1°C s^{-1} after a dose of 0.5 Gy, a sample was heated to 30°C. The temperature was then kept constant during measurements of phosphorescence for a period of time t equals 80 s. The experiment was repeated five times with different temperatures with the initial constant temperature increased by ΔT = 1°C.

(a) Isothermal analysis using first order kinetics

Figure 5.8 (a) shows the luminescence decay as a function of time for peak I. The best fit to TL data using equation 2.38 is shown by a straight line through the data points. The assumption that first order kinetics apply for peak I was verified by plotting the

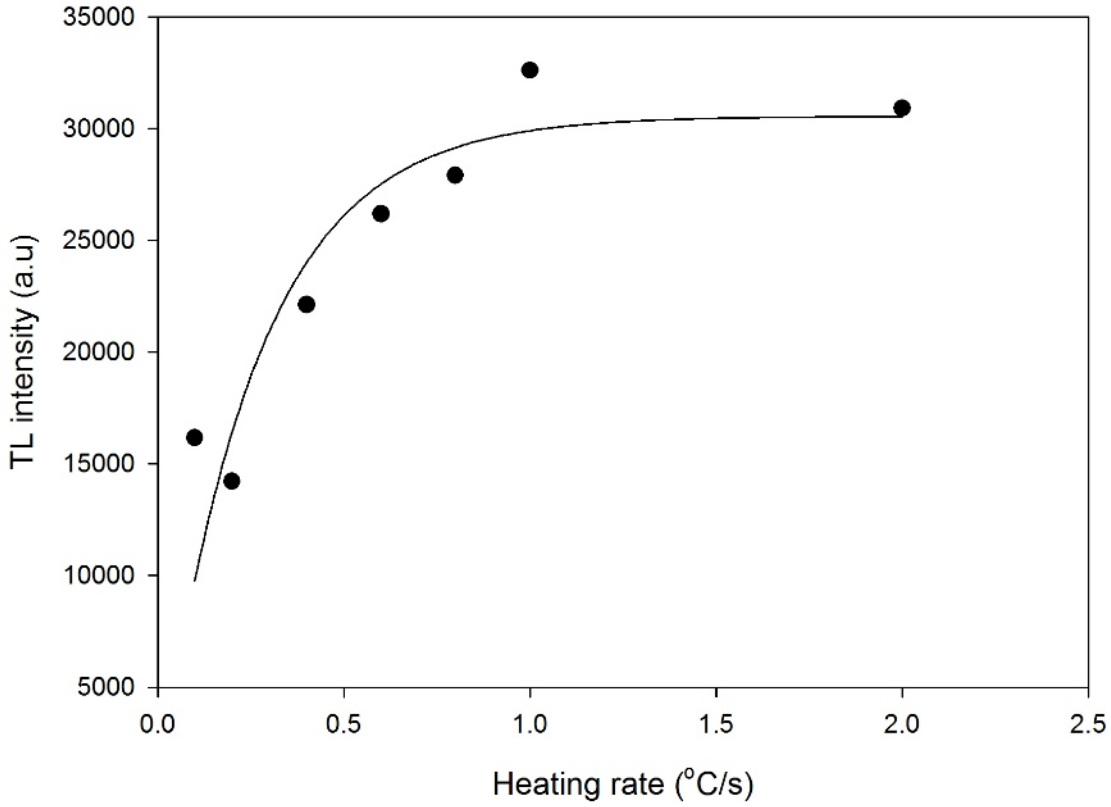

Figure 5.7: The effect of heating rate on TL intensity for peak I using various heating rates from 0.1 up to $2^{o}\mathrm{C\,s^{-1}}$ for a beta dose of 0.5 Gy. The solid line through data points is only a guide.

semi-log scale of iothermal TL intensity versus time. Figure 5.8 (b) shows a plot of $\ln(I/I_0)$ versus t at a constant temperature of 30°C. Various plots of $\ln(I_i/I_0)$ versus t for different constant temperatures $T_i = \{30, 31.32, 33, 34\}$ yielded several straight lines of slopes m_i. Figure 5.9 shows a plot of $\ln(slope)$ against $1/kT$ from which a slope $(-E)$ and intercept $\ln(s)$ gave $\mathrm{E} = 0.72 \pm 0.05\,\mathrm{eV}$ and $s = 2.6 \times 10^{10}\,\mathrm{s^{-1}}$ respectively. These values of E and s are consistent with E and s values calculated from the initial rise and variable heating rate methods.

Instead of several temperatures, we also used pairs of constant temperatures with their corresponding slopes into equation 2.41 to get an average activation energy of $\mathrm{E} = 0.74 \pm 0.1\,\mathrm{eV}$. Using the average value of $\mathrm{E} = 0.73\,\mathrm{eV}$ and $s \sim 10^{10}\mathrm{s}$ at room temperature (303 K) into equation 2.39, the mean lifetime of TL intensity for peak I was approximated to be about $\tau = 140\,\mathrm{s}$.

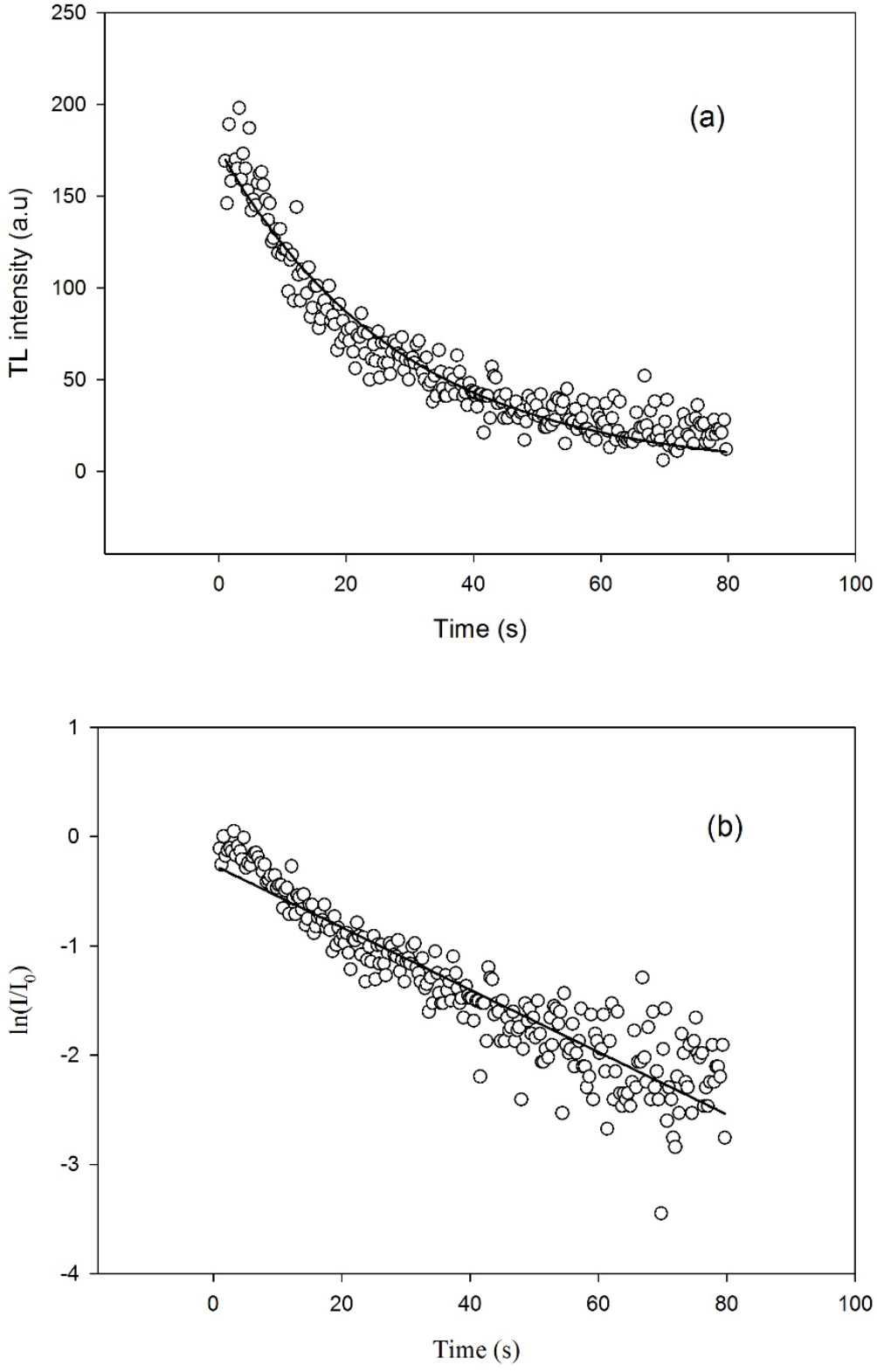

Figure 5.8: An exponential decay curve of TL for peak I at a constant temperature of 30°C (a). The continuous line through the data points is the best fit. A plot of $\ln(I)$ against t yielded a straight line (b), further confirmation that peak I follows first order kinetics.

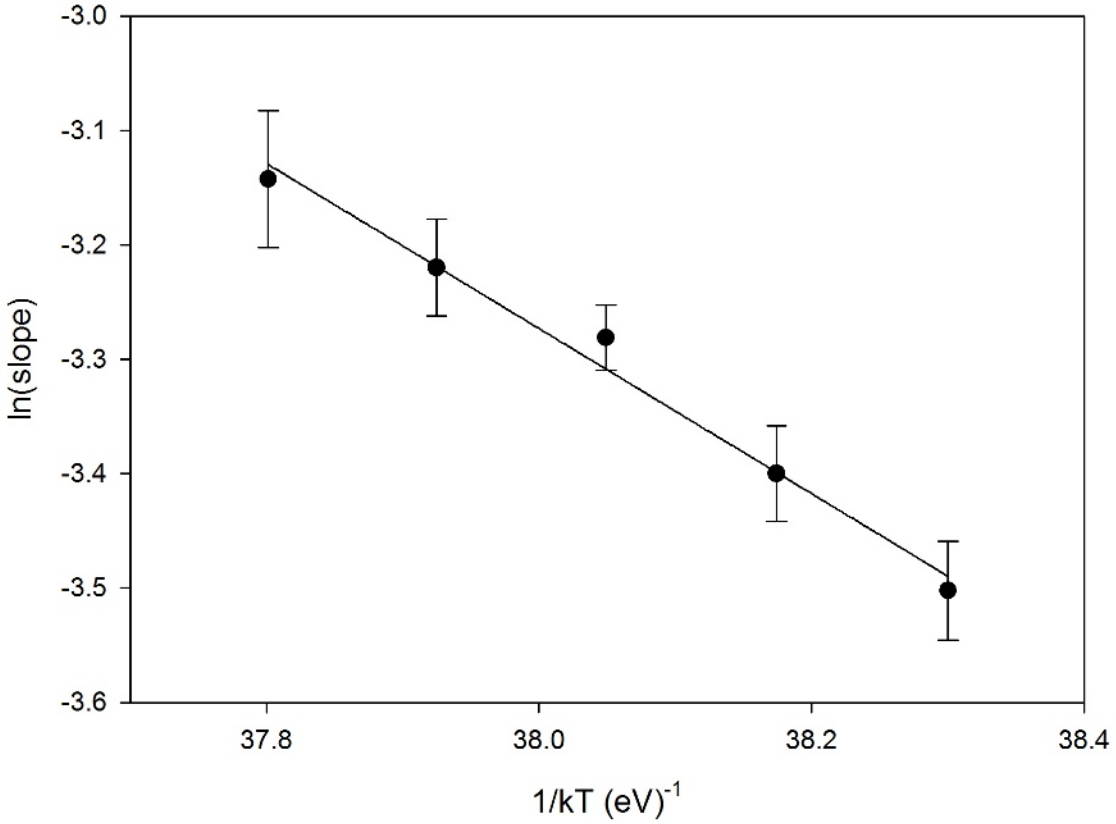

Figure 5.9: The isothermal analysis method for a first order peak I. Each data point is an average of five.

(b) Isothermal analysis using general order kinetics

A plot of $(I/I_0)^{(1-b)/b}$ against t from general order kinetics for isothermal analysis using equation 2.42 can give a straight of a slope m only for the correct value of order of kinetics b. For each constant temperature T_i, guesses for b_i from 0.9 to 1.3 were independently inserted in the plot. The slope m of a straight line from each graph was noted. The experiment was repeated four times for each constant temperature. Table 5.3 shows the results of the best fits for five different constant temperatures. As presented, b corresponded to the values between 0.9 and 1.1 which is close to first order kinetics ($b = 1$). The average of the best order kinetics for peak I, $b + \Delta b$, was found to be 1.06 ± 0.07 which means that the isothermal analysis agrees with previous methods that peak I follows first order kinetics.

Using the obtained order of kinetics to plot $(I/I_0)^{(1-b)/b}$ against t for each constant temperature, we noted slopes m_i from straight lines of the plots. Figure 5.10 (a)

shows an example of the dependence of $(I/I_0)^{(1-b)/b}$ on time at 30°C for $b = 1.1$. The procedure was repeated five times and then, the average slope, $m + \Delta m$, for each constant temperature was recorded. Figure 5.10 (b) shows a graph of $\ln(slope)$ versus $1/kT$ for five different constant temperatures used. The activation energy calculated from the best fit of $\ln(slope)$ was $\mathrm{E} = 0.83 \pm 0.06\,\mathrm{eV}$. The fitting parameter $s'' = 2 \times 10^{12}\,\mathrm{s}^{-1}$ was calculated from the intercept of the plot. In comparison, the average activation energy corresponding to the best fit using a decay equation for first order kinetics (equation 2.38) was less than that corresponding to the best fit using general order of kinetics, equation 2.42 and the best fit using these equations for first and general order kinetics show that first order kinetics can apply for peak I. The E values ($\mathrm{E} = 0.72 \pm 0.05\,\mathrm{eV}$ and $\mathrm{E} = 0.83 \pm 0.06\,\mathrm{eV}$) calculated using the isothermal analysis method are consistent with values of E from previously mentioned methods and are also in good agreement with reported values ($\mathrm{E} = 0.79\,\mathrm{eV}$ and $\mathrm{E} = 0.82\,\mathrm{eV}$ using isothermal analysis and variable heating rate methods respectively) by Kortov et al. [11].

Table 5.3: Values of b corresponding to different temperatures. The best fit to the function $(I/I_0)^{(1-b)/b}$ against t yielded orders of kinetics between 0.9 and 1.1.

Temperature (°C)	b_1	b_2	b_3	b_4	b_5	$b_i + \Delta b_i$
30	0.9	1.1	0.9	1.1	1.1	1.02 ± 0.10
31	1.1	1.1	1.1	1.1	1.1	1.10 ± 0.00
32	1.1	0.9	1.1	1.1	1.1	1.06 ± 0.08
33	0.9	1.1	1.1	1.1	1.1	1.06 ± 0.08
34	0.9	1.1	1.1	1.1	1.1	1.06 ± 0.08
Average						1.06 ± 0.07

5.1.2.6 The T_M-T_{stop} method

The T_M-T_{stop} method is one of the procedures used to find the number and position of component peaks of a complex glow curve [5, 24]. The order kinetics for peak I was assessed using the T_M-T_{stop} method. The procedure consisted firstly of preheating an irradiated sample from 30°C to 32°C. The complete glow curve was then measured from 30°C to 500°C using a heating rate of $1^{\circ}\mathrm{C\,s}^{-1}$ and the peak position T_M was noted. The experiment was repeated several times on the same sample, irradiated each

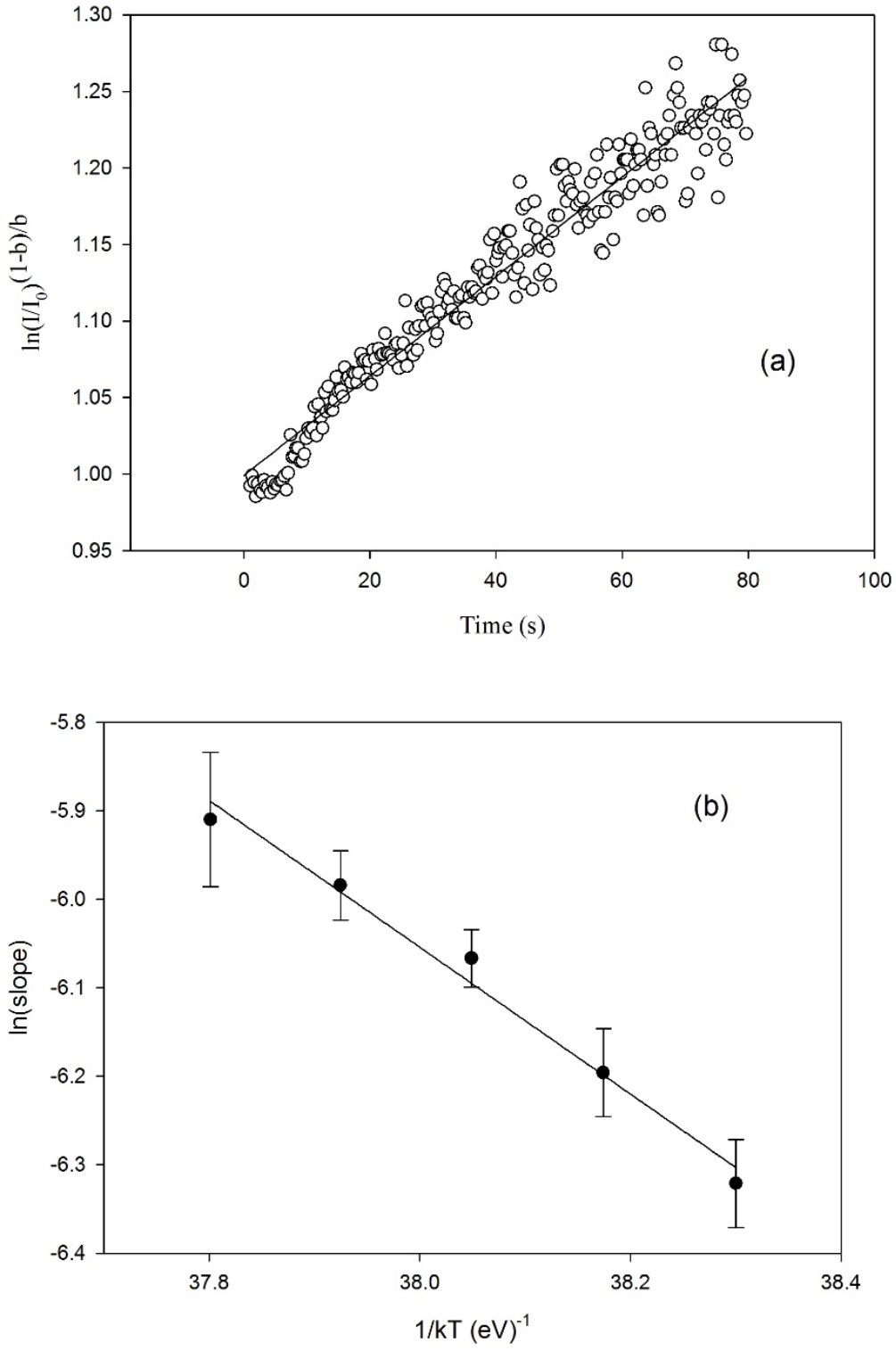

Figure 5.10: The dependence of $(I/I_0)^{(1-b)/b}$ on time at a constant temperature of 30°C for $b = 1.1$ from which a straight line of a slope m_i was obtained (a). An average of 5 slopes m for each temperature between 30 and 34°C was recorded.

time with the same dose of 0.5 Gy, with the T_{stop} increased in steps of $\Delta T_M = 2^oC$ from 32°C up to 42°C. T_M was plotted as a function of T_{stop} as depicted in figure 5.11. As can be seen from the plot, T_M is independent of T_{stop}. As discussed by Chithambo and Seneza [8] for this peak, such behaviour suggests that peak I is single and follows first order kinetics. The preheating to different T_{stop} temperatures changes the initial concentration of trapped charges without changing the position of the peak. In this kinetic process, the change in TL intensity is proportional to the change in the initial concentration of trapped electrons.

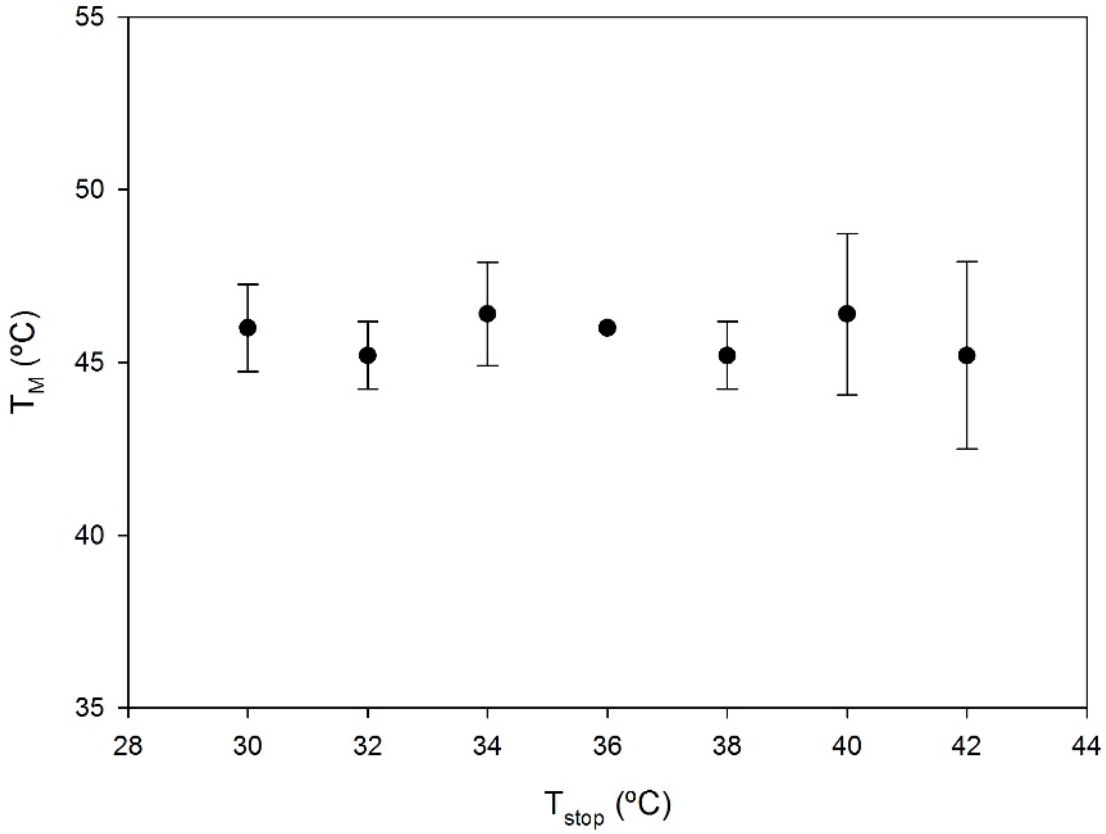

Figure 5.11: The plot of T_M against T_{stop} using TL data for peak I. As can be seen, the position of T_M is independent of T_{stop} from 30 to 42°C for TL measured using a heating rate of $1^oC\,s^{-1}$ in a sample dosed to 0.5 Gy.

5.1.2.7 Summary of the kinetic parameters for peak I

The values of the activation energy and frequency factor extracted from kinetic analysis of thermoluminescence data for peak I using the initial rise, whole curve, peak shape,

variable heating rate and the isothermal analysis methods are presented in table 5.4. The kinetic analysis suggested that peak I is of first order since the geometrical factor from the peak shape method is $\mu_g = 0.42$ and the order of kinetics $b \approx 1$ was determined using the whole curve and the isothermal analysis methods. The order of kinetics for peak I was also assessed using the T_M-T_{stop} method. The T_M-T_{stop} method showed peak I to be a single peak rather than being of the composite of many peaks. The position of the peak was independent of different preheats to T_{stop} temperatures.

The frequency with which trapped electrons attempt to escape the trap or the frequency factor is of the order of between $10^{10} - 10^{15}\,\mathrm{s}^{-1}$. These s values are physically reasonable as can be found in the range of the vibration frequency in the crystal lattice [5]. Clearly, the values of trapping parameters assessed using the above methods are consistent. They are also in good agreement with previously published values [10, 11]. However, the values of activation energy and frequency factor calculated using the peak shape and the whole curve methods appear to be greater than values obtained in other methods. As discussed earlier, calculations for the peak shape method, are affected by the estimation made in choosing temperatures corresponding to the half-maximum intensity used in this method. In addition, the whole curve method was only a good estimate for the evaluated activation energy since a well-resolved peak I was not achieved.

Table 5.4: The activation energy and frequency factor for peak I calculated from the initial rise, the variable heating rate, the peak shape, the whole curve and the isothermal analysis methods.

Method	E (eV)	s (s^{-1})
Initial rise	0.72 ± 0.01	3×10^{10}
Variable heating rate	0.72 ± 0.04	2.7×10^{10}
Peak shape in ω-form	1.05 ± 0.05	4.6×10^{15}
Peak shape in τ-form	1.05 ± 0.07	4.6×10^{15}
Peak shape in δ-form	0.99 ± 0.14	5×10^{14}
Whole curve	0.90 ± 0.02	2×10^{13}
Isothermal analysis	0.72 ± 0.05	2.6×10^{10}

5.1.3 Dosimetric properties of peak I

5.1.3.1 Fading characteristics of peak I

Thermal fading phenomenon can be explained as the loss of signal by heat either during irradiation or as the effect of delay between irradiation and readout [1]. Fading is prominent in shallow traps which are unstable metastable states. Fading features of TL for peak I in α-$Al_2O_3 : C$ were previously studied by Chithambo [9] to assess qualitatively if trapped electrons within the material can be lost without competitive re-trapping at electron traps. He concluded that the retrapping was negligible at the trap associated with peak I and more prominent at the trap associated with peak II.

Figure 5.12 shows the dependence of TL intensity on delay between irradiation and measurement for peak I. As can be seen, the TL intensity decreases as a function of time. Hence, the fading of peak I shows a significant loss of electrons at ambient temperatures. This decrease suggests that the retrapping of electrons at the electron trap associated with peak I is negligible as previously reported [9].

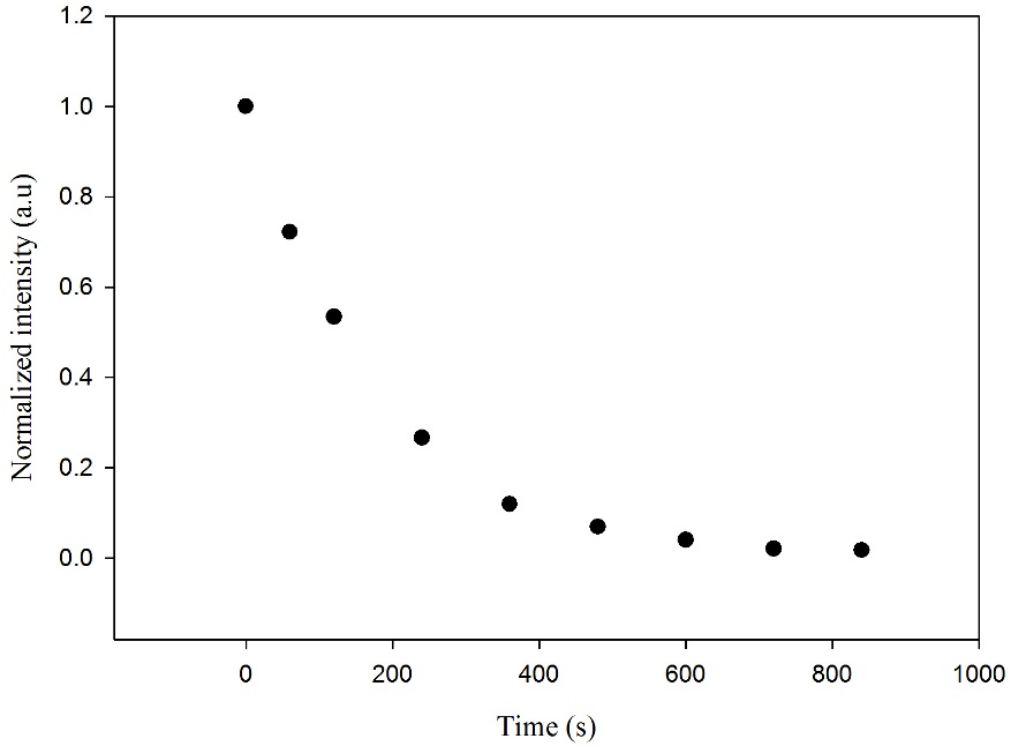

Figure 5.12: The TL intensity against delay between irradiation and readout for peak I. The TL was measured at $1^{o}\mathrm{C\,s^{-1}}$ after dosing to 0.5 Gy.

The loss of electrons can be experimentally explained in two ways to confirm the thermal fading of peak I. Some of the released electrons may recombine, either radiatively or non-radiatively, with holes in the recombination centres. Other released electrons may be trapped by competitor traps, the more stable traps, associated with peaks II and III. The radiative recombination of the released electrons at ambient temperature was assessed by measuring phosphorescence from an irradiated sample. First, the phosphorescence was measured using a decay time of 100 s from an irradiated sample without any preheating after a dose of 0.5 Gy. The results (figure 5.13; solid circles) showed phosphorescence for peak I. The second measurements followed preheating to 100°C to remove peak I and then, to 220°C to remove peak II and showed only the background signal (figure 5.13; open circles). The results show that the loss of electrons at room temperature due to phosphorescence is the cause of thermal fading in peak I.

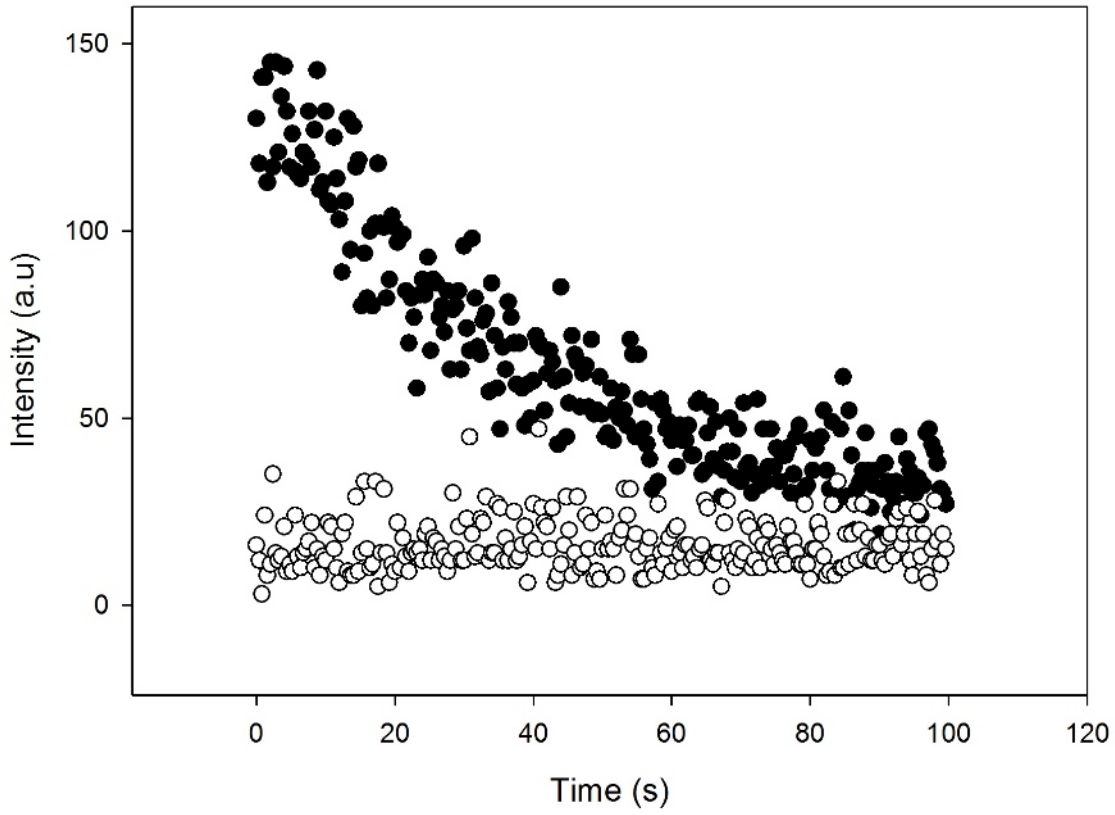

Figure 5.13: Intensity versus time graphs. The solid circles show the phosphorescence measured from peak I and the open circles denote the background of signal from a preheated sample.

Figure 5.14 shows the TL intensity ratios of peaks II and III as a function of time as peak I faded. Figure 5.14 (a) shows the ratio of TL intensity of peak II to the intensity of peak I versus time and figure 5.14 (b) represents the ratio of TL intensity of peak III to the intensity of peak I versus time as peak I faded. The increase of the intensity ratios of peaks II and III as a function of time confirms that the lost electrons as peak I fades are captured by the more stable competitor traps corresponding to peaks II and III. The more interesting result, figure 5.14 (c), is that the rate of change of the intensity for both peaks II and III are identical.

Further analysis of thermal fading decay curve showed that peak I fades exponentially as a function of time as

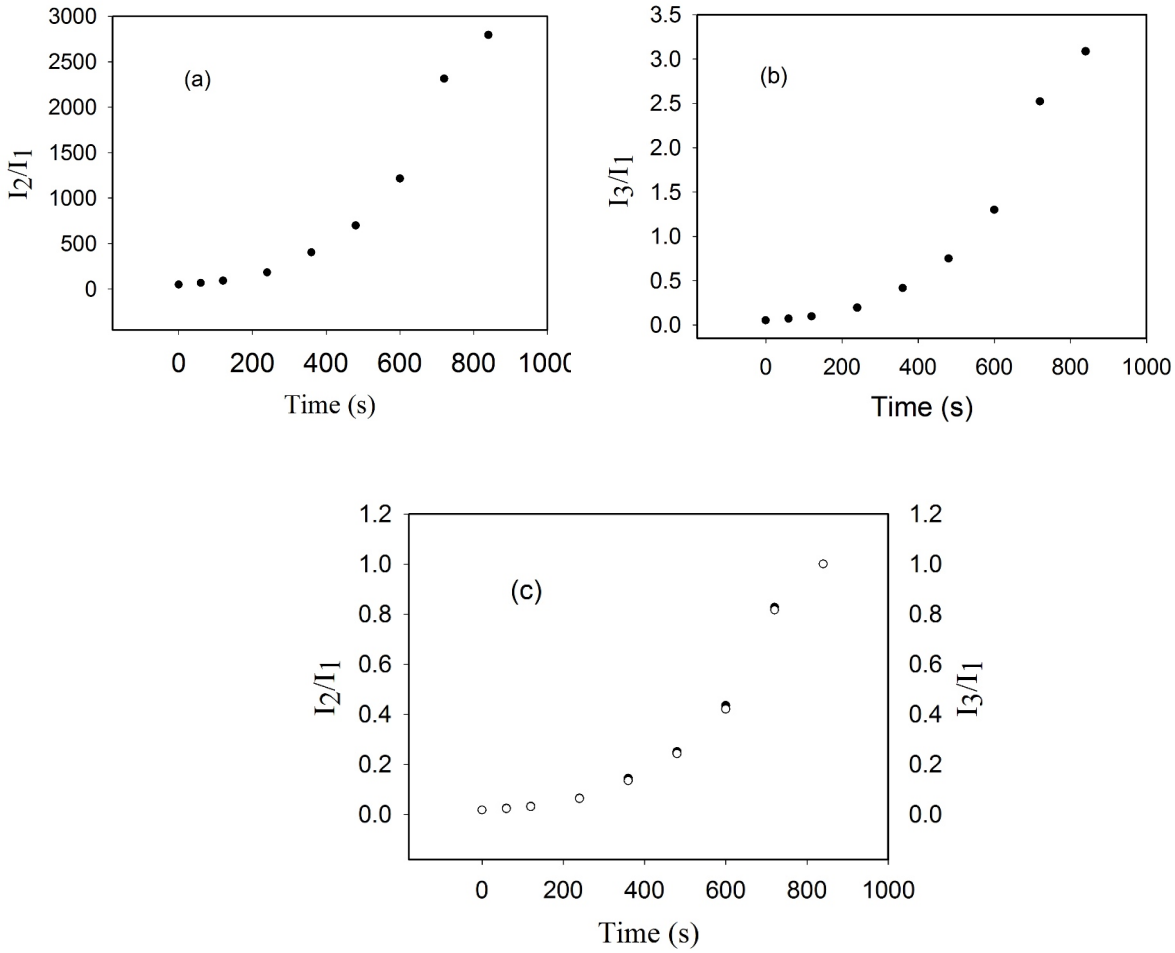

Figure 5.14: The ratios of change of TL intensity as function of time for peak II (a) peak III (b) and concurrent change of the normalized intensity in peaks II and III (c) as peak I fades.

$$\mathrm{I(t) = I_o \exp(-at)}, \tag{5.1}$$

where $I(t)$ is the TL intensity at time t and at a constant temperature T in kelvin; I_o is the initial intensity at $t = t_o$ and $a = 1/\tau$ is the decay constant; τ is the lifetime, that is, the mean time which an electron spends in the shallow trap. Figure 5.15 shows decay of the TL intensity of peak I as a function of time. The best fit to $I(t)$ using the experimental data for peak I is shown in figure 5.15 (a). The exponential decay feature of the fading of peak I was assessed by using a plot of $\ln(I)$ against t, figure 5.15 (b). The mean lifetime of $\tau = 180\,\mathrm{s}$ was calculated from the slope of a straight line in the plot of figure 5.15 (b) as well as from the best fit to $I(t)$ using equation 5.1. The obtained value of the lifetime shows that the TL intensity of peak I decreased with storage with a half-life of about 120 s. A previous study of thermal fading from peak I with storage reported a similar half-life of 150 s [9].

(a) Comparison between TL glow curves before and after fading of peak I

Figure 5.16 shows that peak I fades at room temperatures. The TL measured immediately after irradiation was dominated by phosphorescence and as such, peak I did not appear clearly (figure 5.16 a). In comparison, TL measured following a delay of 360 s between irradiation and measurements shows peak I better although its intensity has decreased due to fading (figure 5.16 b). The TL measurement used a heating rate of $2^{o}\mathrm{C\,s^{-1}}$ and a dose of 0.5 Gy. Further measurements on thermal fading of peak I showed that the peak decayed to half-maximum intensity within 120 s and faded completely after 840 s at room temperature. This attests to negligible retrapping at the trap associated with peak I.

(b) Effect of fading on E and s for peak I calculated using the peak shape method

The peak shape method was used to determine the values of E and s using TL data for peak I measured six minutes after irradiation. The peak was measured for various doses from 0.5 up to 2.5 Gy. Average activation energies were $E_\omega = 0.80 \pm 0.20$ eV, $E_\tau = 0.84 \pm 0.12$ eV and $E_\delta = 0.72 \pm 0.46$ eV. The corresponding frequency factors are $s = 2 \times 10^{12}\,\mathrm{s^{-1}}$, $s = 1.6 \times 10^{10}\,\mathrm{s^{-1}}$ and $s = 4 \times 10^{11}\,\mathrm{s^{-1}}$. The full results are shown in

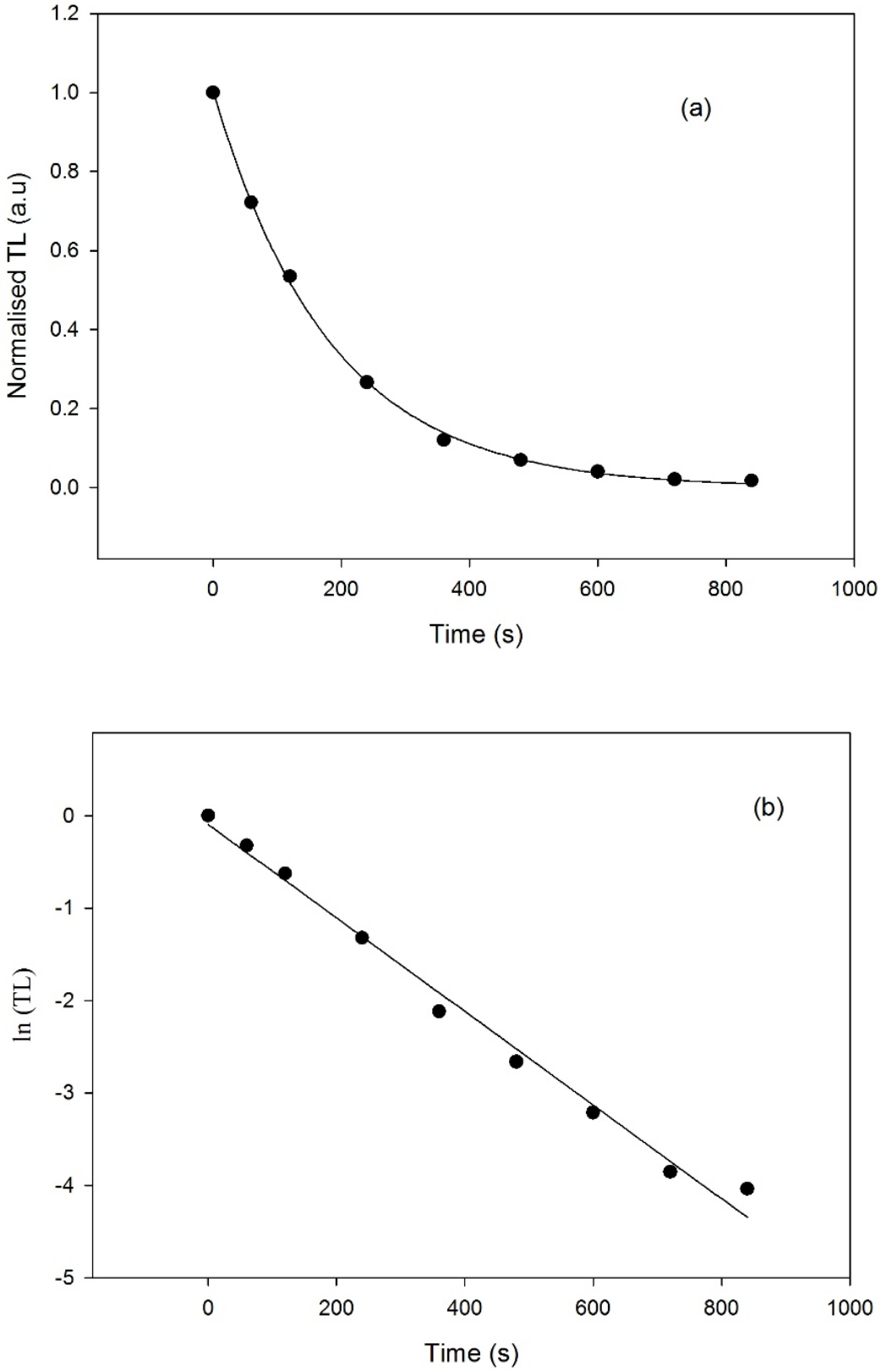

Figure 5.15: The best fit to TL data for peak I as a function of time (a) a straight line obtained from a plot of $\ln(I)$ against time for TL data as peak faded confirms the exponential decay of the fading of peak I (b).

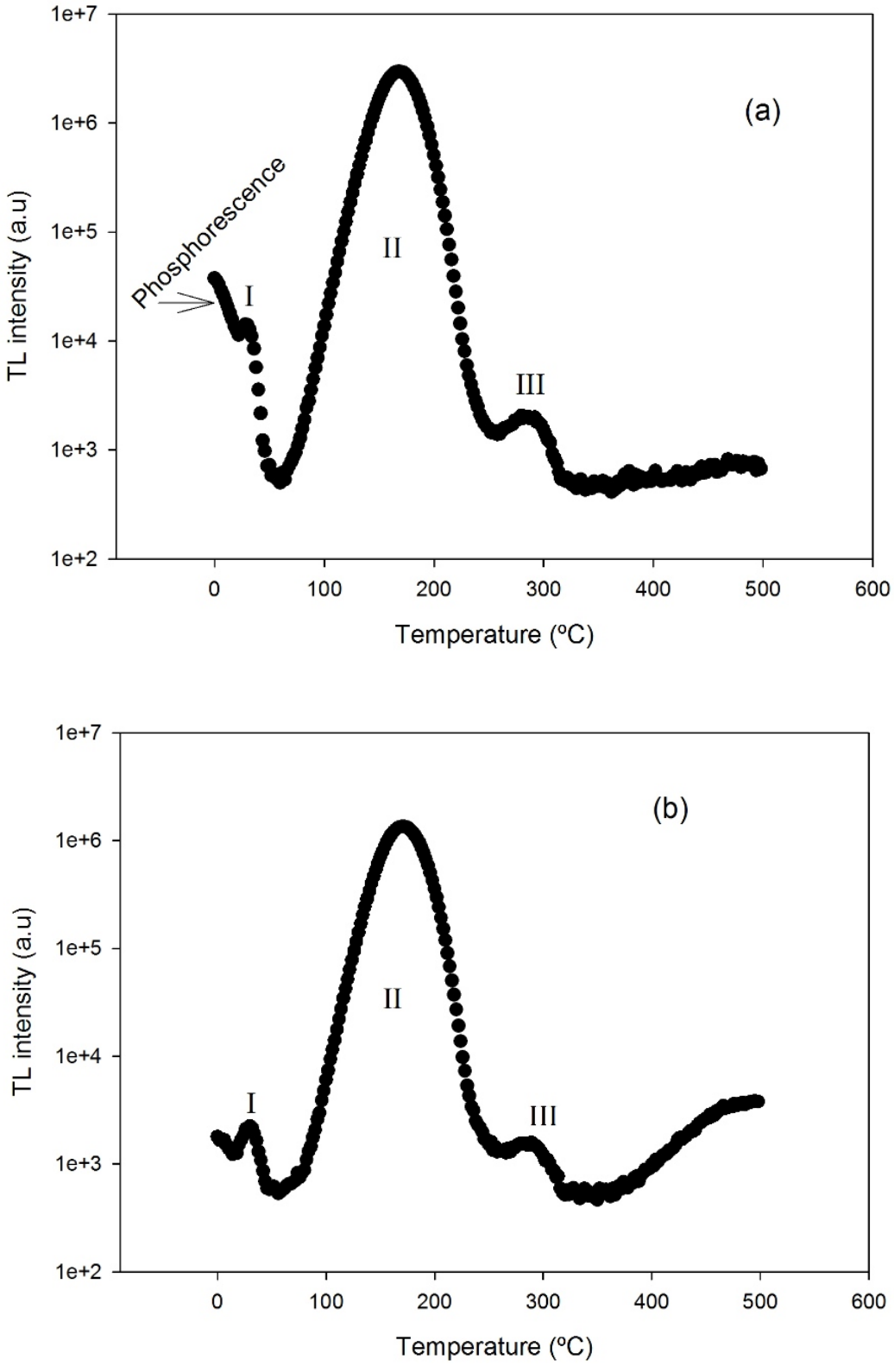

Figure 5.16: The comparison of thermoluminescence glow curves for peak I; one from the TL intensity measured immediately after irradiation to 0.5 Gy (a) and another measured six minutes following an irradiation dose of 0.5 Gy (b). The heating rate was $2^{o}\mathrm{C\,s^{-1}}$.

table 5.5. Results shown in the table are consistent and are in good agreement with values of E and s calculated using other methods. Nonetheless, $E_\delta < E_\omega < E_\tau$. This is because of non symmetry of peak I as it follows a first order kinetics where the theoretical error in calculating E and s is largest for τ, intermediate for ω and smallest for δ [2]. The largest error for τ causes the E_τ-method to give the worst result of estimated E and s. The best result is obtained using E_δ-method while the E_ω-method provides an intermediate accuracy result. However in the case of thermally cleaned first order kinetics peak, E_τ-method gives the best result since the lower half-width τ corresponds to the low temperature region of the thermally cleaned peak [2]. In comparison to thermal cleaning, thermal fading of peak I involves a loss of charge due to phosphorescence at the low temperatures region (τ region). The effect of removal of phosphorescence was to clean peak I, however its maximum intensity was then also affected. This means that E_τ-method cannot be judged to give a better result in this case. One can choose the method using ω that gives an intermediate result to avoid large error. In addition, the results of E and s calculated using the peak shape methods are reasonable because the value of s is close to the Debye vibration frequency. This is unlike the results from peak shape method applied on TL data for peak I in the presence of the phosphorescence (table 5.2) where E and s have got values greater than ones evaluated using other methods. The shape of the peak is affected by the phosphorescence. In turn, the trapping parameters for peak I calculated using the peak shape method may also have been modified by the phosphorescence in table 5.2.

Table 5.5: Activation energies calculated using the peak shape method for TL data from peak I measured 6 minutes following various beta doses from 0.5 up to 2.5 Gy using a heating rate of $1^{\circ}\mathrm{C\,s^{-1}}$.

β-dose (Gy)	E_ω (eV)	E_τ (eV)	E_δ (eV)
0.5	0.75 ± 0.28	0.82 ± 0.15	0.60 ± 0.57
1.0	0.75 ± 0.28	0.82 ± 0.15	0.60 ± 0.57
1.5	0.84 ± 0.27	0.87 ± 0.15	0.76 ± 0.49
2.0	0.85 ± 0.19	0.85 ± 0.08	0.83 ± 0.33
2.5	0.85 ± 0.19	0.85 ± 0.08	0.83 ± 0.33
Average	$\mathbf{0.80 \pm 0.20}$	$\mathbf{0.84 \pm 0.12}$	$\mathbf{0.72 \pm 0.46}$

5.1.3.2 Thermoluminescence dose response

The dose dependence of the thermoluminescence intensity of peak I was studied for low doses from 0.5 up to 2.5 Gy using a heating rate of $1^{o}\mathrm{C\,s^{-1}}$. In this dose range, the maximum TL intensity I_M at each dose D was noted and then, a graph of I_M against D plotted. The result is presented in figure 5.17. The dose dependence of the TL intensity is a linear function in this dose range. The linear increase of intensity as a function of dose suggests that the number of electrons in the electron trap that recombine in the recombination centre is proportional to the amount of absorbed dose within the sample. A general analytical function to describe the dose dependence of TL intensity can be written as

$$I_M = aD^k, \tag{5.2}$$

where I_M is the maximum TL intensity, D denotes the dose; a and k are constants [5]. The experimental TL data of figure 5.17 was fitted by a straight line of form

$$\mathrm{y = mx + c}, \tag{5.3}$$

as indicated by a solid line through TL data points. The linear growth curve of peak I was confirmed using a log-log plot of the I_M, from which yields a straight line with a slope of about $k = 1$ (figure 5.17 inset). In this case of the linear dependence of TL intensity on dose (k=1), equation 5.2 becomes

$$I_M(D) = aD. \tag{5.4}$$

A similar result was also be deduced from the superlinearity index $g(D)$. The index $g(D)$ is dimensionless quantity that measures the change in slope of the growth curve and is defined as

$$g(D) = [Dy''(D)/y'(D)] + 1, \tag{5.5}$$

where y' and y'' are the first and second derivatives of the analytical function of the growth curve [2, 5]. Either equation 5.3 (an expression which fitted experimentally

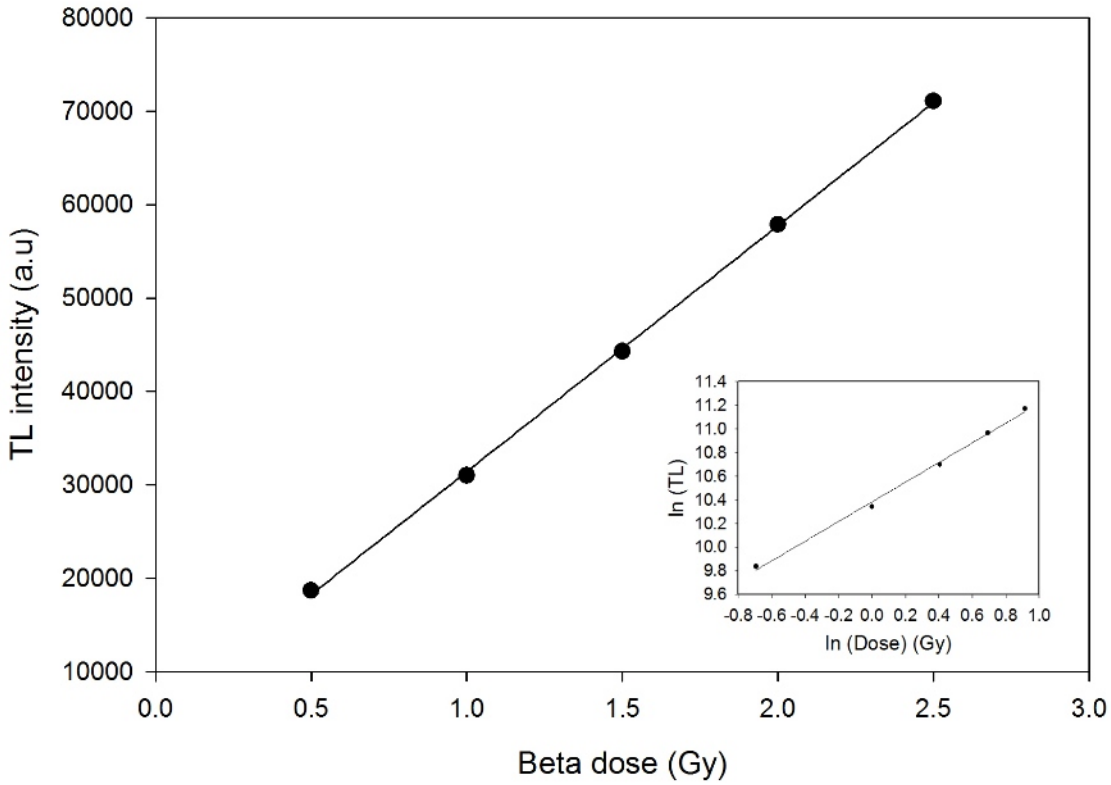

Figure 5.17: The dose dependence of TL intensity for peak I using a heating rate of $1^{o}\mathrm{C\,s^{-1}}$ for dose range from 0.5 to 2.5 Gy. The solid line indicates the best fit of a linear function. The inset is the log-log plot of the analytical function for the dose dependence.

the TL dose response for peak I) or equation 5.4 was used into equation 5.5 to get $g(D) = 1$. Hence, at low doses from 0.5 up to 2.5 Gy and at a heating rate of $1^{o}\mathrm{C\,s^{-1}}$ the TL dose response for peak I was linear. Therefore, the increase in TL intensity is proportional to the number of trapped electrons in the electron trap that eventually recombine in the recombination centre.

Figure 5.18 shows the dependence of the peak position T_M for peak I on dose. In figure 5.18 (a), T_M is plotted against dose. The peak position T_M is independent of dose. In other words, T_M for peak I remains in the same position for different values of trap filling n. Thus, that peak I is of first order kinetics is confirmed from the independence of T_M on dose. Figure 5.18 (b) shows a plot of glow curves for peak I measured following different doses. The TL intensity increased with dose but the peak position remained unchanged.

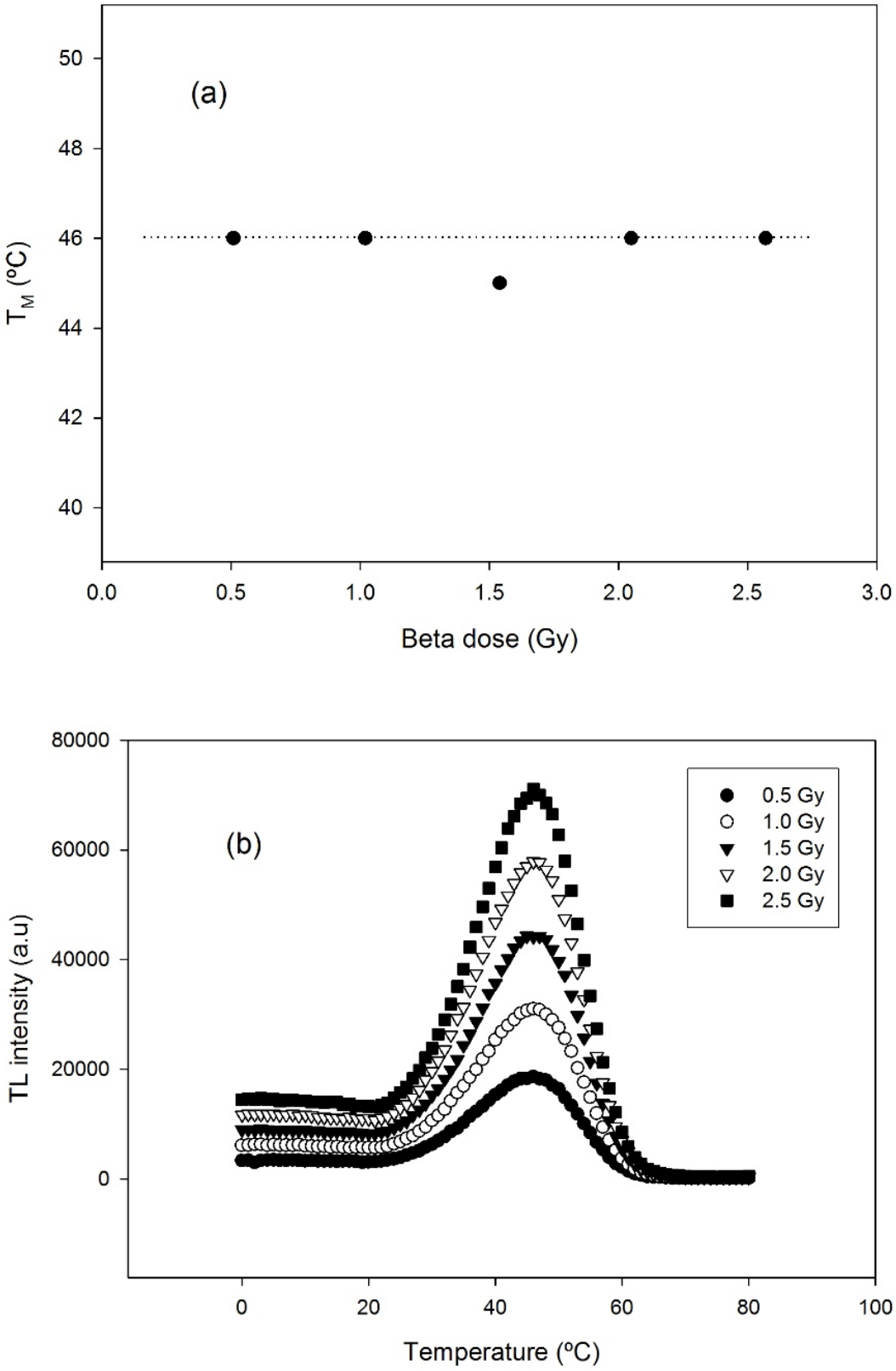

Figure 5.18: The dependence of the peak position T_M on dose for peak I for TL measured at a heating rate of $1^{\circ}\mathrm{C\,s^{-1}}$ (a) and glow curves of peak I (b). Doses from 0.5 up to 2.5 Gy were used.

5.1.4 Kinetic analysis for the higher temperature secondary peak: peak III

Thermoluminescence intensity for peak III measured at beta doses less than 3 Gy showed low intensity TL comparable to background signals. Figure 5.19 shows TL signals for peak III peaking at 268°C for a sample irradiated to 1 Gy and measured using a heating rate of $0.4^{\circ}\mathrm{C\,s^{-1}}$. The kinetic analysis of TL for peak III was therefore studied by increasing the dose up to 3 Gy in an annealed sample. Samples were annealed at 900°C for 15 minutes to remove residual charge before irradiation. After dose, the glow curve was thermally cleaned until a better resolved peak III was obtained but without affecting its maximum intensity much. Four methods were used to calculate trapping parameters for peak III including the heating rate, peak shape, whole peak and T_M-T_{stop} methods. Application of the glow curve deconvolution method will be reported later.

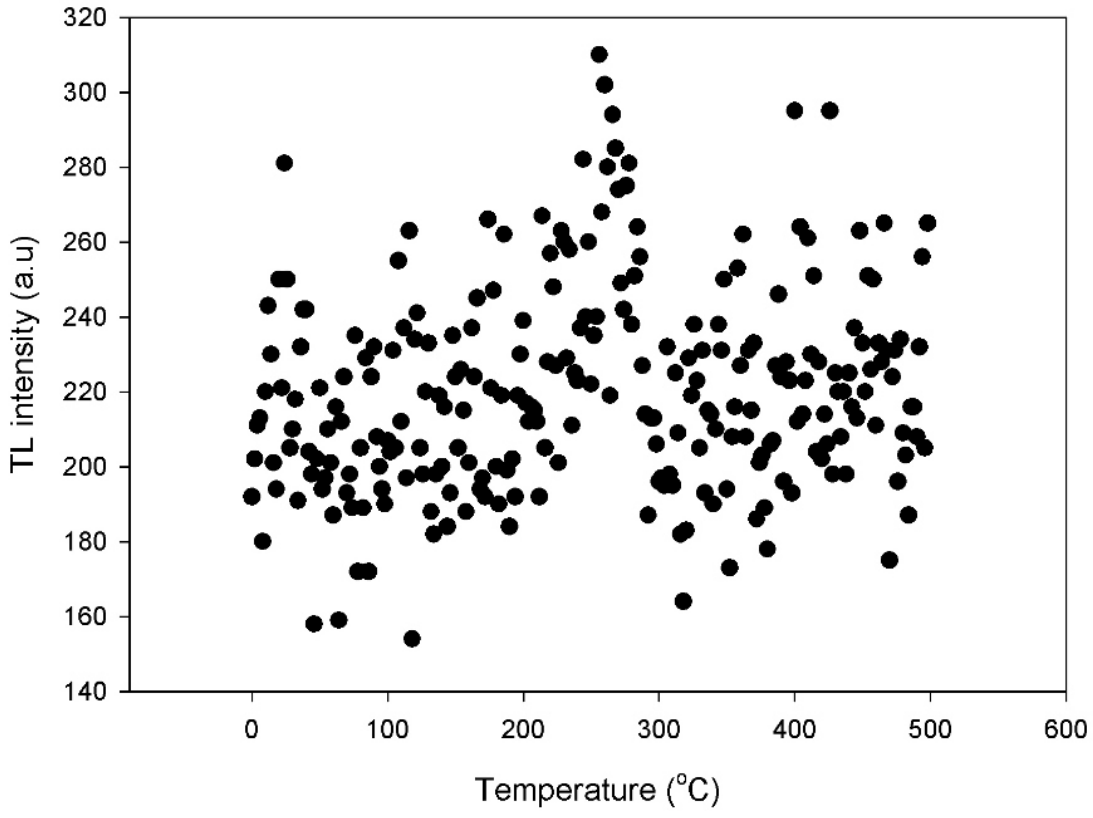

Figure 5.19: The glow curve measured at $0.4^{\circ}\mathrm{C\,s^{-1}}$ in a sample irradiated to 1 Gy. The peak position T_M for peak III can be found at 268°C.

5.1.4.1 Thermal cleaning to isolate peak III

The thermal cleaning method was first used as an an experimental procedure to produce isolated, non-overlapping, glow peaks. Here, the technique was also used to asses qualitatively the number of secondary glow peaks that appear at higher temperatures. Before cleaning, the positions of different peaks of the glow curve in $\alpha - Al_2O_3 : C$ are shown in figure 5.20, that is, peak I at 36°C, peak II at 156°C and peak III at 268°C. The TL was measured at $0.4^{o}C\,s^{-1}$ in a sample dosed to 3 Gy. Peak III was separated from the other peaks using the thermal cleaning technique. Firstly, an irradiated sample was preheated to a temperature of 180°C to remove peak I and peak II. The whole curve was then measured to 500°C. An overlapping peak of peak II was observed at 170°C while peak III appeared at 268°C. The procedure was repeated several times by changing the preheating temperatures above the maximum temperature of peak II. Figure 5.21 shows the properly resolved peak III used in the kinetic analysis obtained

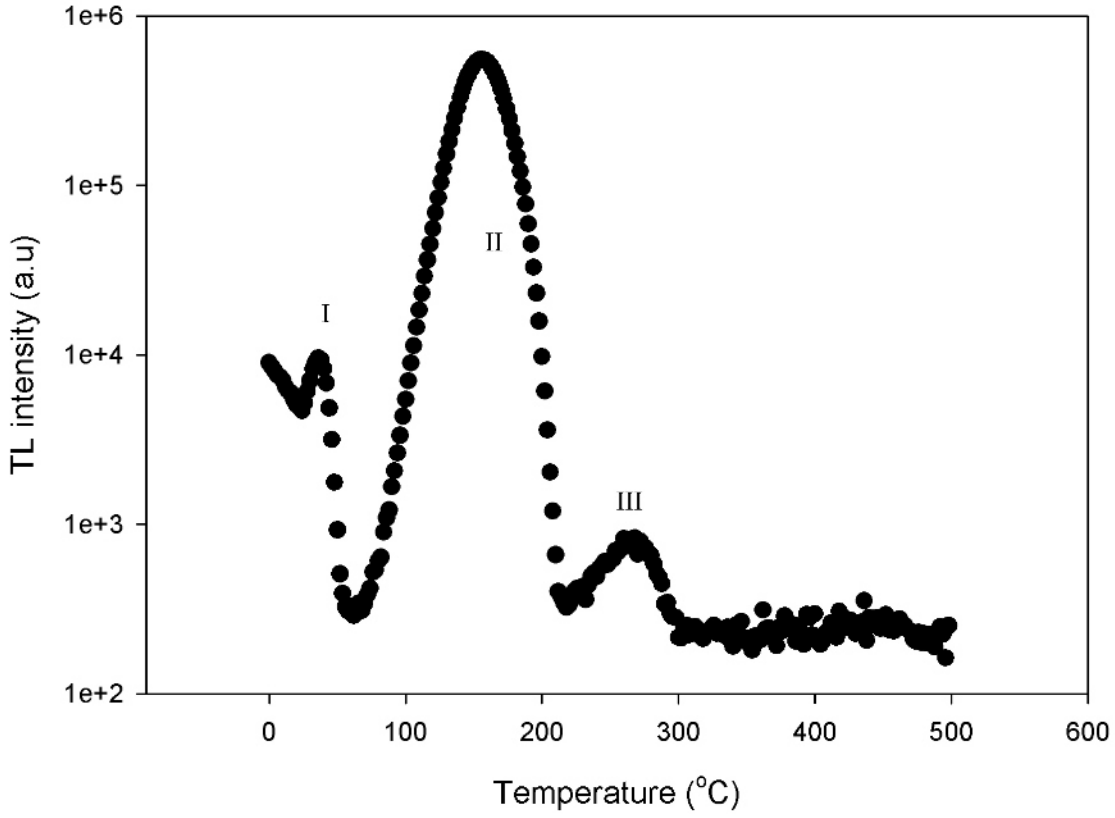

Figure 5.20: The glow curve measured using a heating rate of $0.4^{o}C\,s^{-1}$ following a dose of 3 Gy. The position of peaks I, II and III appeared at 36°C, 156°C and 268°C respectively.

after heating to 200°C. The peak at 170°C (peak IIA) disappeared only after preheating to 210°C. Also the thermal cleaning of peak III near its maximum temperature shown a third subsidiary glow peak, peak IV, associated with a deep trap. Figure 5.22 shows the position of peak IV at about 422°C following preheating to 265°C for TL measured using a heating rate of $0.4^{\circ}\mathrm{C\,s^{-1}}$ in a sample dosed to 3 Gy. Because its intensity was weak (about 0.5×10^{-3} of the intensity of the main peak), peak IV only appears after partial-heating above the maximum temperature of peak III. Nyirenda [25] reported similar results of two additional peaks for deep electron traps between 400°C and 500°C at a heating rate of $0.03^{\circ}\mathrm{C\,s^{-1}}$ and high dose of 6 Gy. Nikiforov et al. [26] reported three more visible peaks at 400°C, 430°C and 550°C.

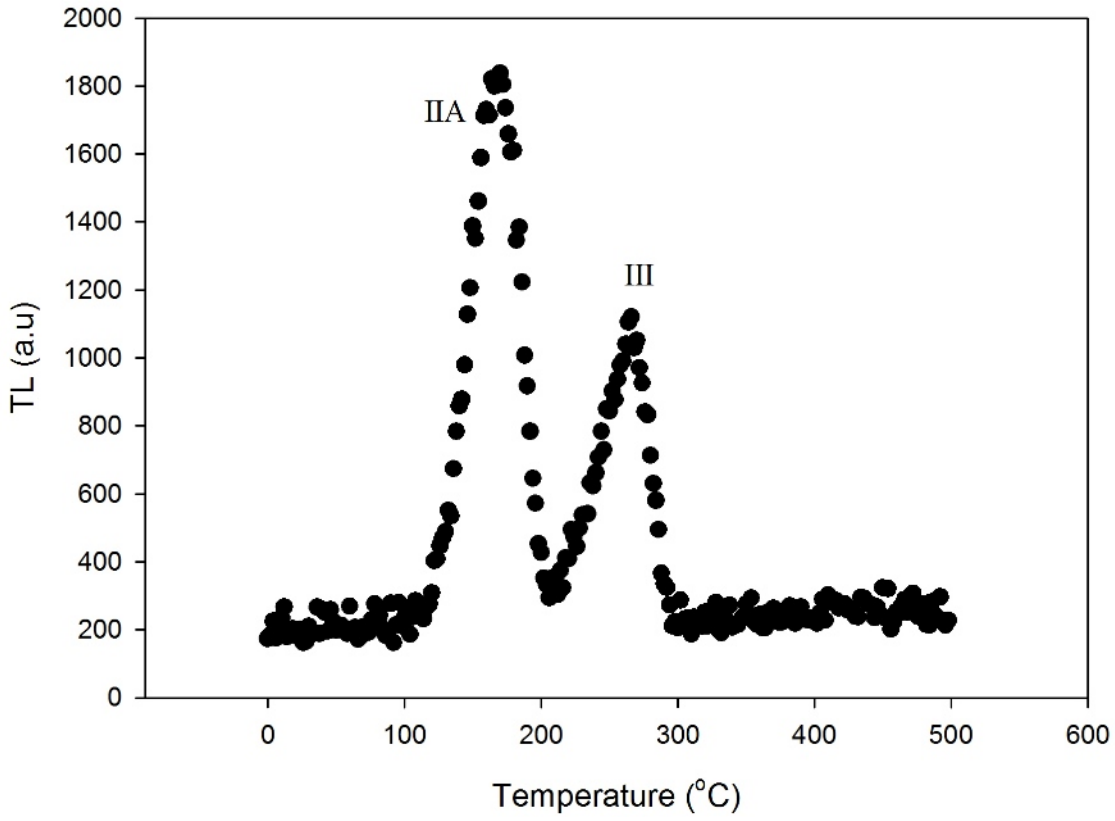

Figure 5.21: The TL for peak III after thermal cleaning to 200°C following an irradiation dose of 3 Gy. Using a heating rate of $0.4^{\circ}\mathrm{C\,s^{-1}}$, a peak at 170°C (labeled IIA) appeared before peak III at 264°C.

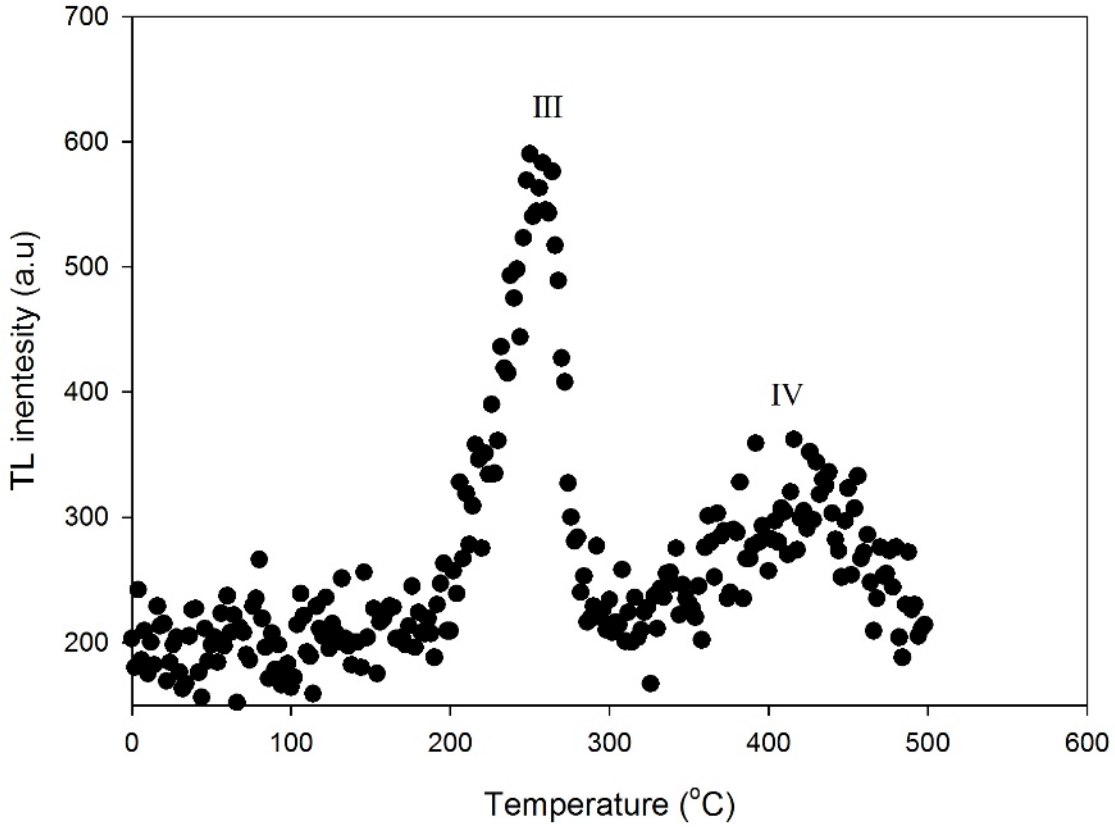

Figure 5.22: Peaks III at 264°C and IV at 422°C in a TL glow curve measured from 30°C after preheating to 265°C using a heating rate of $0.4^{\circ}\mathrm{C\,s^{-1}}$. A dose of 3 Gy was used.

5.1.4.2 The T_M-T_{stop} method

The order of kinetics for peak III was assessed using the T_M-T_{stop} method [5]. The sample was first preheated to 220°C following an irradiation of 3 Gy and we then noted the peak position T_M. After cooling, the whole TL was taken from room temperature. The experiment was repeated for various T_{stop} temperatures from 225 up to 265°C in steps of $\Delta\mathrm{T} = 5^{\circ}\mathrm{C}$. The results, figure 5.23 shows that the position of the peak T_M is essentially independent of T_{stop}. The result implies that the peak position is not affected by the initial concentration of trapped charge. Therefore, the T_M-T_{stop} technique suggested that peak III is a single peak that follows first order kinetics.

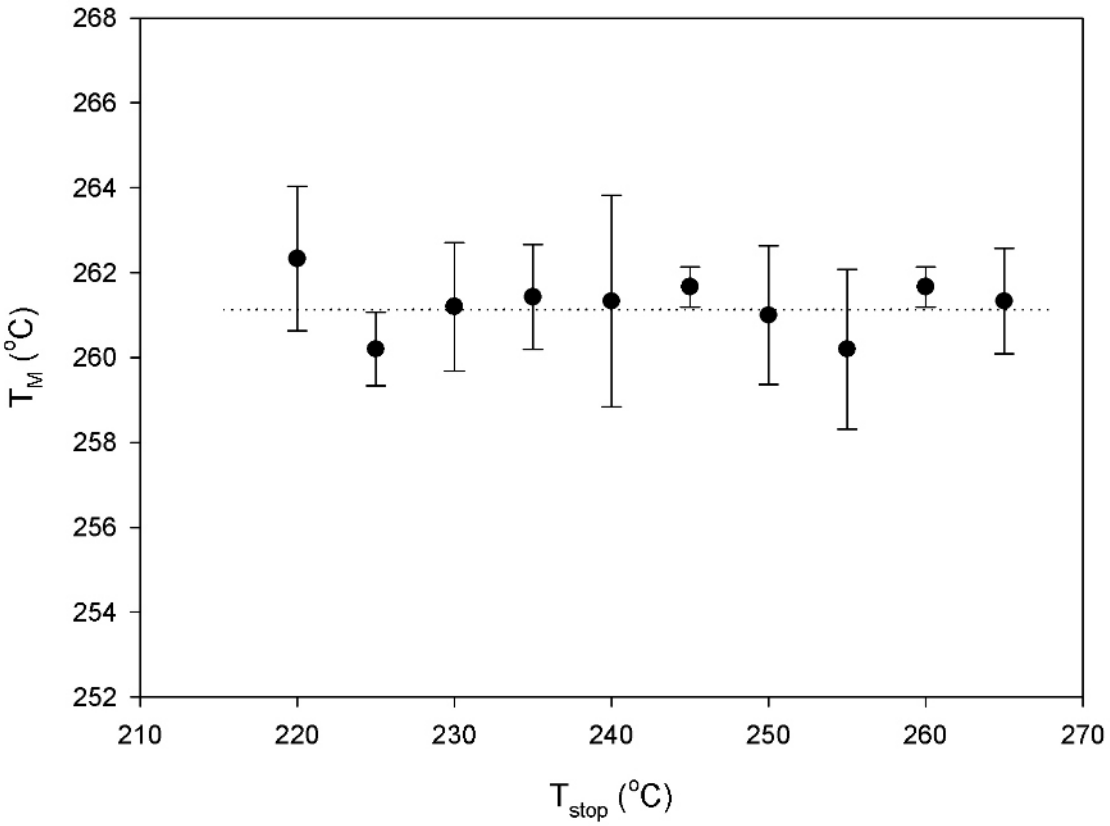

Figure 5.23: A plot of T_M-T_{stop} used to assess the order of kinetics for peak III. The dotted line through data points is only a guide to show the independence of T_M from T_{stop}.

5.1.4.3 The peak shape method

The geometrical shape of peak III was studied using T_M and full width half-maximum intensity from which three parameters (τ, δ and ω) were found. Equation 2.14 was used to determine the activation energy associated with each parameter in the peak shape method. Table 5.6 shows values of the activation energy from different forms of the peak shape method for a dose of 3 Gy calculated for three different heating rates. The values of the activation energy in the τ, δ and ω methods are consistent. For a first order peak, using a heating rate of $0.4^{\circ}\mathrm{C\,s^{-1}}$ with an average activation energy from each type of the peak shape method, the frequency factor was found as $s = 1 \times 10^{9}\,\mathrm{s^{-1}}$. The geometrical factor μ_g is nearly equal to 0.42, further confirmation of first order kinetics for peak III.

Table 5.6: The peak shape method applied on TL data for peak III using various heating rates of 0.4, 2, and 4°C s^{-1}. The dose was 3 Gy.

Rate (°C s^{-1})	T_M (°C)	μ_g	E_ω (eV)	E_τ (eV)	E_δ (eV)
0.4	264	0.42 ± 0.02	1.16 ± 0.10	1.15 ± 0.08	1.15 ± 0.20
2.0	292	0.40 ± 0.02	1.23 ± 0.12	1.23 ± 0.08	1.22 ± 0.25
4.0	304	0.40 ± 0.03	1.05 ± 0.15	1.11 ± 0.06	1.04 ± 0.27
Average		$\mathbf{0.41 \pm 0.02}$	$\mathbf{1.15 \pm 0.12}$	$\mathbf{1.16 \pm 0.07}$	$\mathbf{1.14 \pm 0.15}$

5.1.4.4 The whole curve method

The earlier expression (equation 2.32) used to calculate an activation energy using the whole curve method was used for TL data from peak III. Figure 5.24 shows the whole curve method applied on TL data of peak III.

Different regression lines from a plot of $\ln(I/area^b)$ versus $1/kT$ for various order of kinetics b between 0.9 and 1.2 are shown in figure 5.24 (a). Figure 5.24 (b) shows the best fit at $b = 0.9$. A plot of residuals for each fit was used to determine the best fit option. The scatter in points were most close to zero for the order $b = 0.9$ (figure 5.24 (b), inset). This also shows first order kinetics for peak III. The activation energy and the pre-exponential factor from the best fit are $\mathrm{E} = 1.10 \pm 0.04\,\mathrm{eV}$ and $s = 1 \times 10^9\,\mathrm{s}^{-1}$ respectively. The calculated parameters are in a good agreement with E and s for peak III obtained using the peak shape method.

5.1.4.5 The variable heating rate method

A plot of $\ln(T_M^2/\beta)$ against $1/kT_M$ for peak III is presented in figure 5.25. The slope E and intercept $\ln(E/sk)$ from a straight line of the figure yielded an activation energy of $\mathrm{E} = 1.51 \pm 0.06\,\mathrm{eV}$ and frequency factor $s = 6 \times 10^{12}\,\mathrm{s}^{-1}$ respectively.

The activation energy was also calculated by using a pair of maximum temperatures T_{M1} and T_{M2} which correspond to two heating rates β_1 and β_2. From $\beta = 0.4$ and 0.6°C s^{-1} corresponding to $T = 537\,K$ and $T = 543\,K$, $\mathrm{E}_1 = 1.6\,\mathrm{eV}$. Similarly, $\beta = 0.4$°C s^{-1} and $\beta = 0.8$°C s^{-1} produced $\mathrm{E}_2 = 1.4\,\mathrm{eV}$. Finally, several combinations of two different heating rates yielded an average activation energy of about $\mathrm{E} = 1.5 \pm 0.10\,\mathrm{eV}$. On the basis of first order kinetics, the frequency factor was $s = 3 \times 10^{10}\,\mathrm{s}^{-1}$.

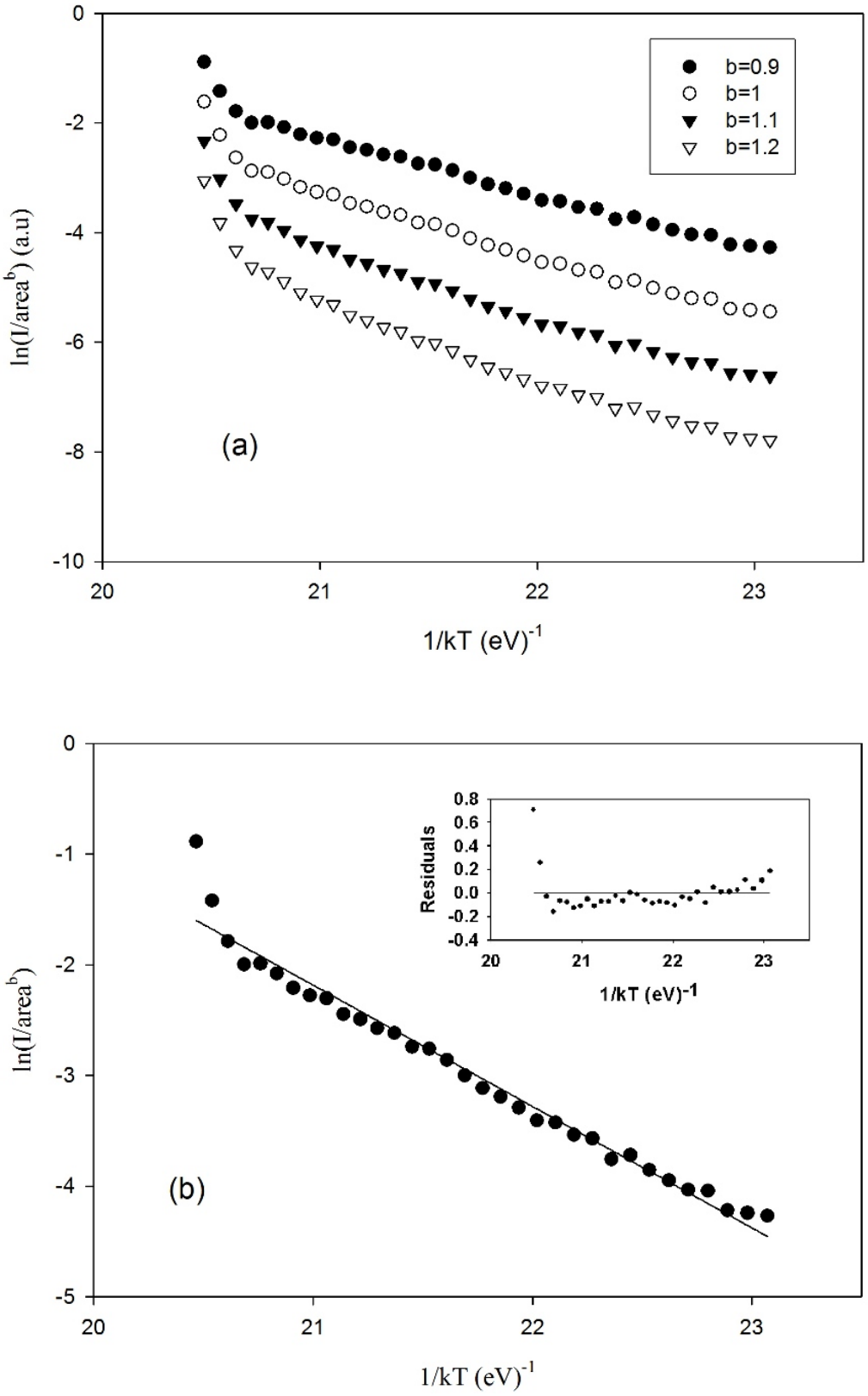

Figure 5.24: The whole curve method applied on TL data of peak III measured using a heating rate of $0.4^{\circ}\mathrm{C\,s^{-1}}$ for dose of 3 Gy. Different fits resulted from the dependence of $\ln(I/area^b)$ on $1/kT$ at various orders b (a) yields the best fit for the order $b = 0.9$ (b). The inset shows the residuals plotted as a function of $1/kT$.

The E and s values calculated from the variable heating rate method for peak III deviate, but not too much, from the other values calculated using the peak shape and the whole curve methods. In addition, the peak position T_M shifted to the higher temperature as the heating rate increased from 0.2 up to $6^{o}\mathrm{C\,s^{-1}}$, figure 5.25 inset.

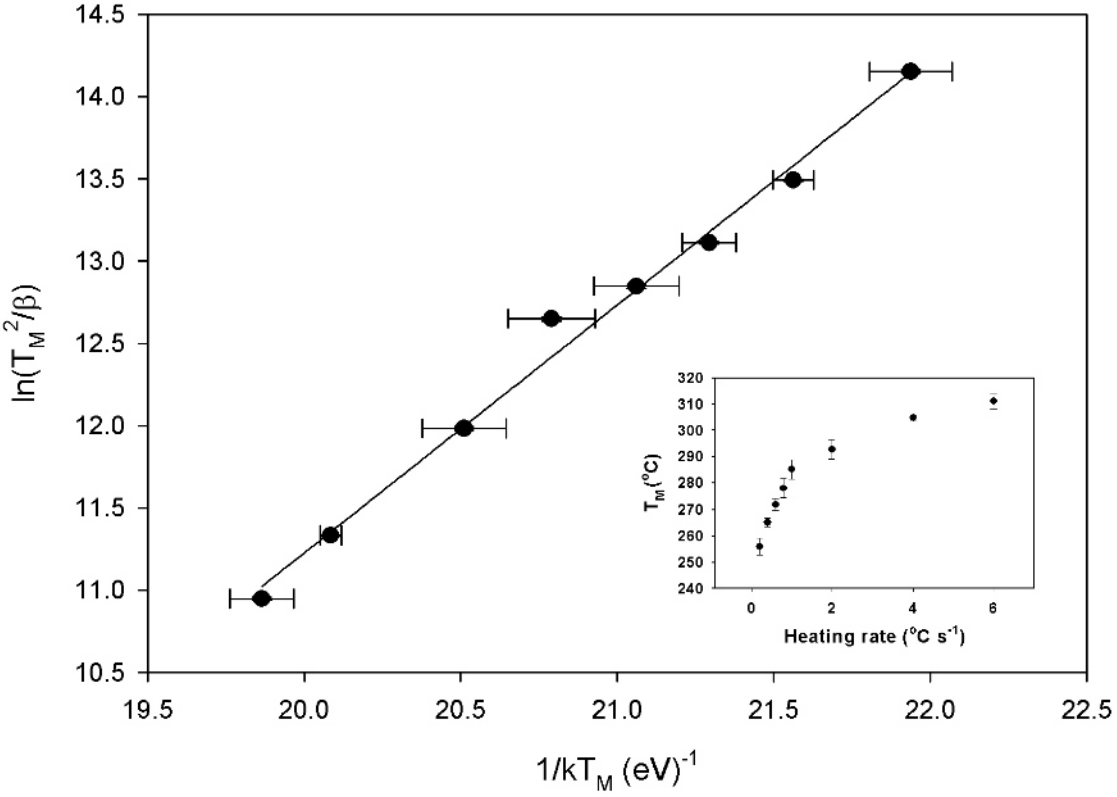

Figure 5.25: The variable heating rate method applied on peak III. Each data point is an average of five from which a shift in peak position T_M to the higher temperatures (inset) was observed as the heating rate increased from 0.2 to $6^{o}\mathrm{C\,s^{-1}}$. The sample was dosed to 3 Gy. The error bars for $\ln(T_M^2/\beta)$ dominates error bars for $1/kT_M$.

5.1.4.6 Thermal quenching effect

Unlike the TL intensity measured for peak I, the corresponding intensity for peak III decreases as the heating rate increases. The TL was measured five times using various heating rates from 0.2 to $6^{o}\mathrm{C\,s^{-1}}$ in a sample freshly irradiated to 3 Gy. Result in figure 5.26 shows that peak integral decreased as heating rate increased. This is an indication of thermal quenching. The normalized peak integral (in counts per ^{o}C) and maximum TL intensity also decrease as a function of a heating rate.

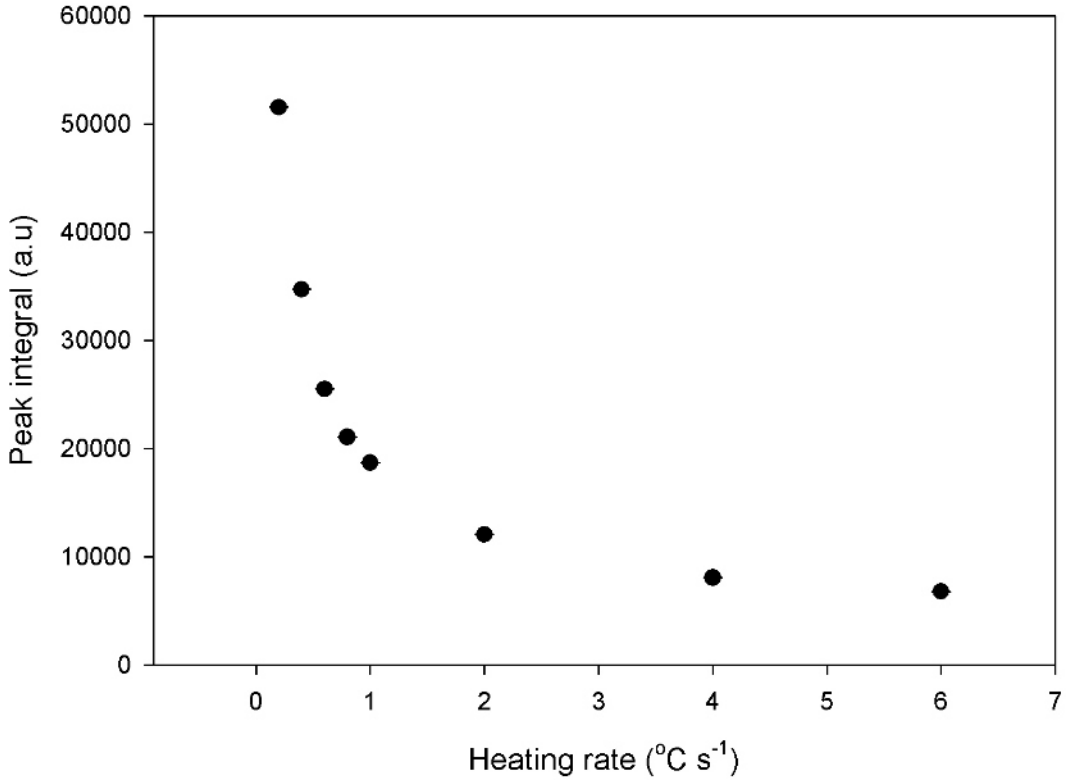

Figure 5.26: A decrease of peak integral (in a.u) as a function of heating rate. Heating rates from 0.2 to 6°C s^{-1} were used in a sample dosed to 3 Gy.

In addition, figure 5.27 shows that the decrease is identical for both normalized peak integral and maximum TL intensity when presented on the same plot. Figure 5.27 inset shows the quenched peaks IIA and III in a glow curve at various heating rates from 0.6 to 4°C s^{-1}. The thermal quenching feature for peak III was studied using an expression of quenched TL intensity [5, 27]

$$I_Q(\eta, T_M) = I_U \eta(T_M), \tag{5.6}$$

where I_Q and I_U are quenched and unquenched thermoluminescence intensities respectively. I_U is the intensity corresponding to the lowest heating rate used (0.2°C s^{-1} in this experiment). η is the luminescence efficiency whose expression is

$$\eta = 1/\left[1 + \mathrm{Cexp}\left(-\mathrm{W}/\mathrm{kT_M}\right)\right], \tag{5.7}$$

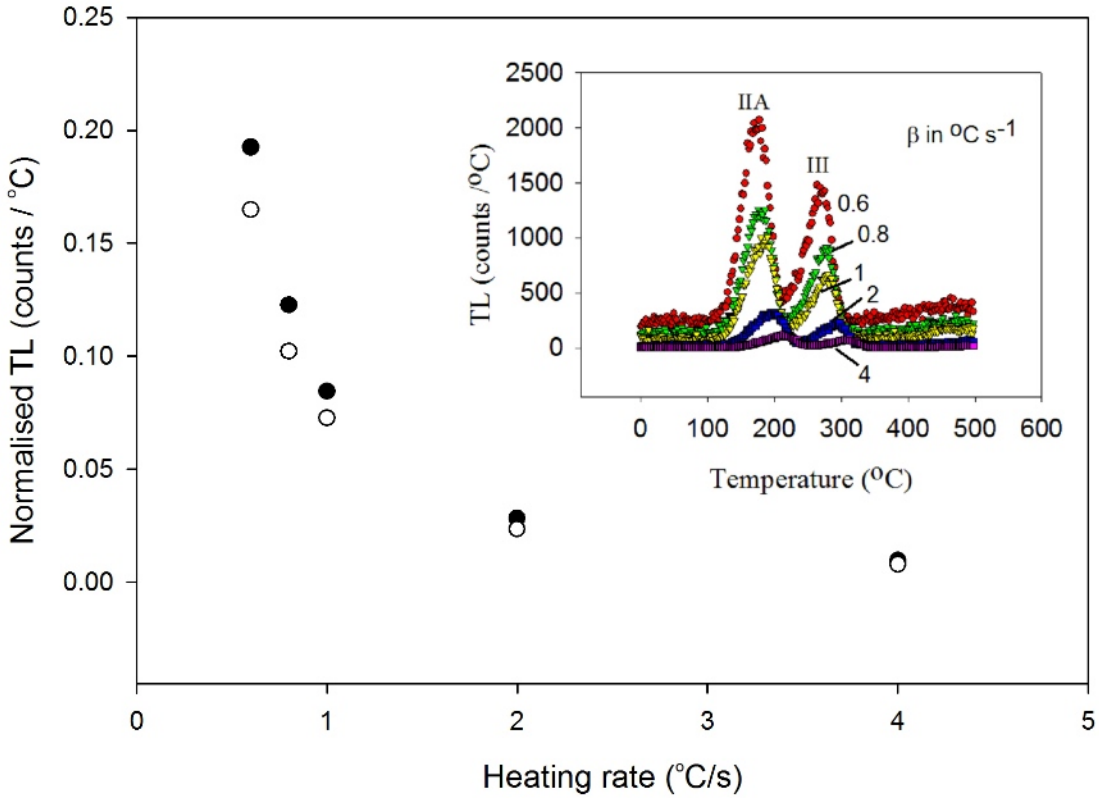

Figure 5.27: The normalized TL intensity and the peak integral (in counts/^{o}C) from peak III at the lower heating rate of 0.2°C s^{-1} versus heating rate. The inset is the TL (in counts/^{o}C) against temperature (^{o}C) using various heating rates from 0.2 to 6°C s^{-1}. The dosed of 3 Gy was used.

where W is activation energy for thermal quenching, C is a dimensionless constant and T_M is the maximum temperature in Kelvin [1, 28, 29]. Equations 5.6 can be rewritten as

$$\frac{\mathrm{I_U}}{\mathrm{I_Q}} - 1 = \mathrm{C}\exp\left(-\mathrm{W}/\mathrm{kT_M}\right), \tag{5.8}$$

from which a plot of $\ln\left[(I_U/I_Q) - 1\right]$ against $1/kT_M$ yields a straight line of a slope $(-W)$ and intercept $\ln(C)$. The parameters from the slope and intercept are shown in figure 5.28 were $\mathrm{W} = 1.48 \pm 0.10$ eV and $\mathrm{C} = 4 \times 10^{13}$ respectively. Previous findings reported similar quenching parameters using the main dosimetric peak. Examples are $\mathrm{W} = 0.96 \pm 0.05$ eV and $\mathrm{C} = 1.3 \times 10^{10}$ [30] from TL data for peak II; $\mathrm{W} = 1.1$ eV and $\mathrm{C} = 10^{11}$ [31] from TL/OSL modeling; $\mathrm{W} = 1.55$ eV and $\mathrm{C} = 10^{17}$ [27] using radioluminescence and photoluminescence and $\mathrm{W} = 1.08 \pm 0.03$ eV [32] using the time resolved photoluminescence spectroscopy. The energy level of thermal quenching is associated

with excited states of F-centres in $\alpha - Al_2O_3 : C$. That values of W that are close for all quenched electron traps suggests that one recombination centre is involved.

Thermal quenching characteristics in peak III is explained by the mechanism of TL process using an energy band model previously reported by many authors [9, 15, 21, 30]. The energy band model is given and discussed in section 5.1.6. Thermal quenching phenomenon is attributed to the decrease of the luminescence efficiency caused by increasing non-radiative transitions at the recombination centres.

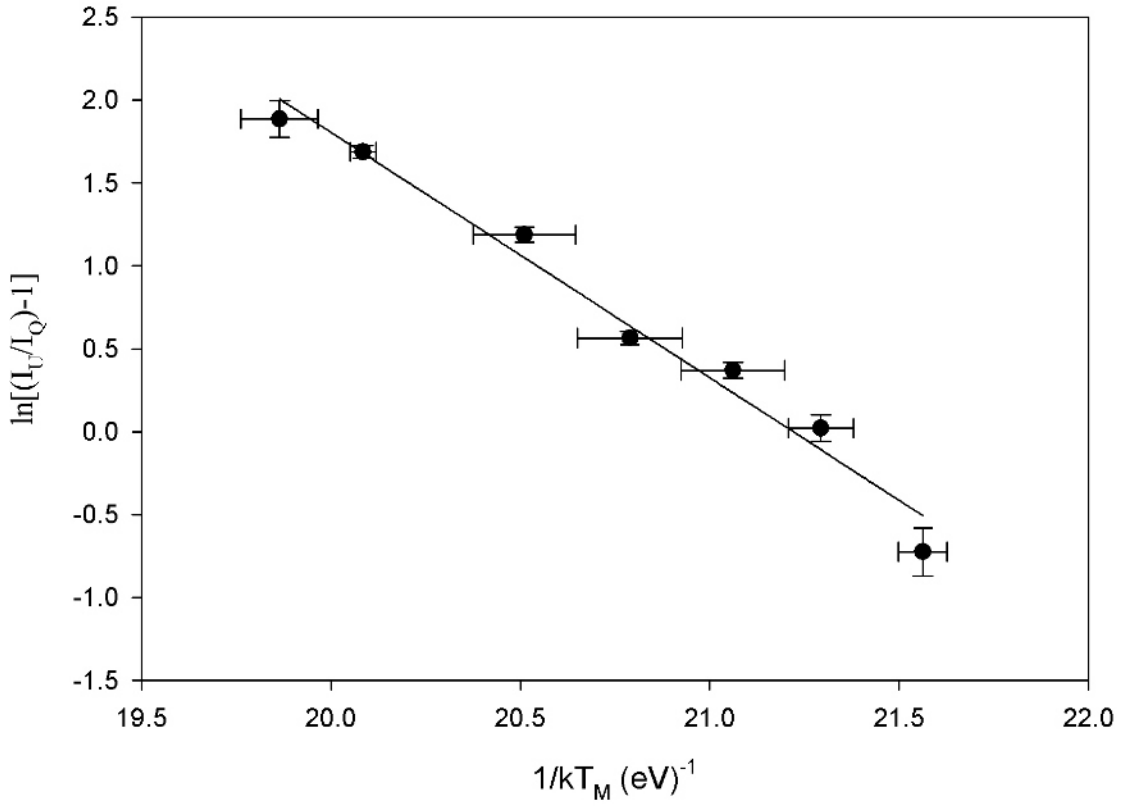

Figure 5.28: A plot of $\ln[(I_U/I_Q) - 1]$ against $1/kT_M$ at various heating rate from 0.2 up to $6^oC\,s^{-1}$. The sample was dosed to 3 Gy. Each data point is an average of five. Error bars are calculated from the standard deviation on TL intensity and on T_M.

5.1.4.7 Summary of kinetic analysis of TL for peak III

The trapping parameters of peak III were calculated using the peak shape, whole curve and variable heating rate methods. The results are summarised in table 5.7 and are consistent. The values of the activation energy and frequency factor for peak III are

generally similar and independent of the method used for kinetic analysis. First order kinetics was apparent for peak III from the peak shape and whole curve methods. This was confirmed by the T_M-T_{stop} method. In addition, peak III is affected by thermal quenching with $W = 1.48 \pm 0.10$ eV and $C = 4 \times 10^{13}$. Peak III was of weak intensity and this caused much scatter of data points. It follows that the maximum temperatures used in the peak shape and variable heating rate methods were chosen only by estimation. The thermal cleaning method could not separate completely peak III from other peaks without loss of some signal from peak III. The activation energy from the whole curve method was on this basis also only a good estimation for peak III.

Table 5.7: The activation energy and frequency factor for peak III calculated using the variable heating rate, the peak shape and the whole curve methods.

Method	E (eV)	s (s^{-1})
Peak shape in ω-form	1.15 ± 0.12	1×10^9
Peak shape in τ-form	1.16 ± 0.07	1×10^9
Peak shape in δ-form	1.14 ± 0.15	1×10^9
Whole curve	1.10 ± 0.04	1×10^9
Variable heating rate	1.51 ± 0.06	6×10^{12}

5.1.4.8 The kinetic analysis of peak IIA (component of peak II)

Peak IIA was observed at 170°C after thermal cleaning of peak III by preheating to 200°C to remove peak II (at 156°C). This was shown in the previous section (figure 5.21). The activation energy E for peak IIA was calculated using the initial rise, variable heating rate and peak shape methods. The E value is compared with the activation energy largely evaluated from a single main peak, for example the values of E ranging from 0.9 to 1.3 eV were reported by Ogundare et al [30]. The TL data for peak IIA was measured using a heating rate of $0.4^{o}C\,s^{-1}$ using a sample dosed to 3 Gy. A plot of $\ln(I)$ against $1/kT$ for data from peak IIA is shown in figure 5.29. The best fit gave $E = 0.85 \pm 0.04$ eV. Using the variable heating rate method (figure 5.30) it was found that $E = 0.92 \pm 0.08$ eV.

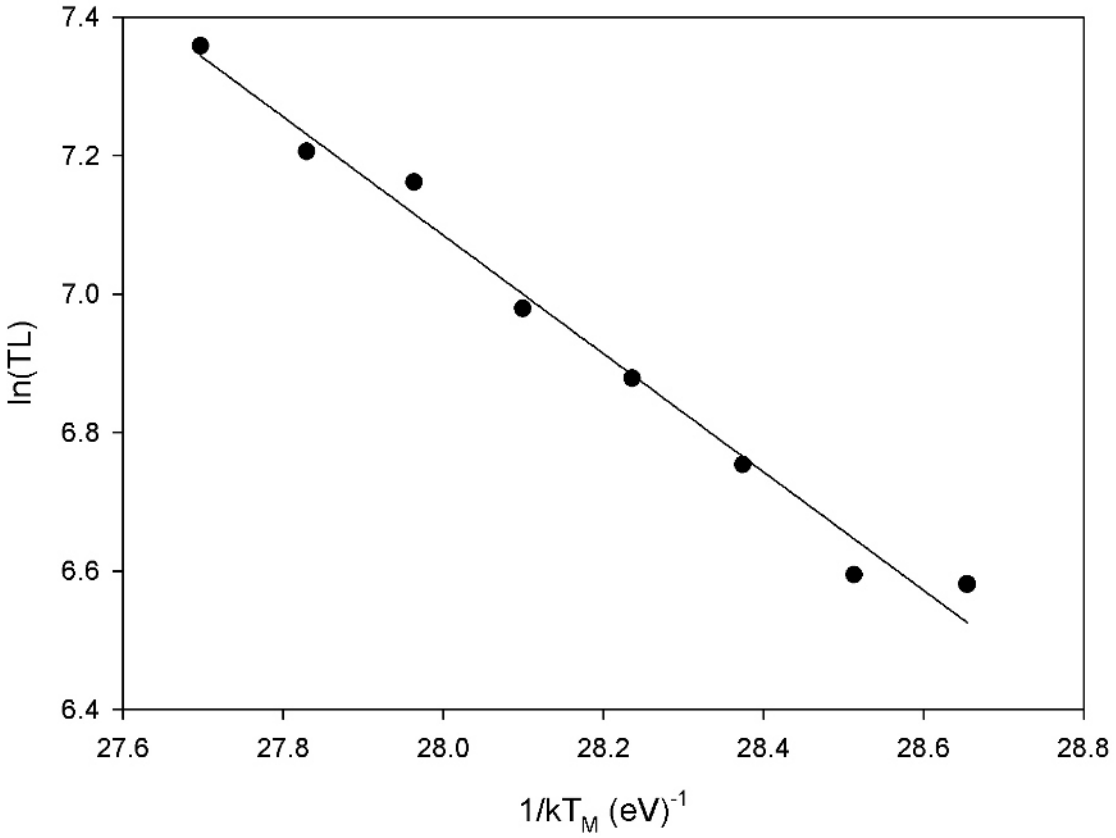

Figure 5.29: The initial rise method. The heating rate of $0.4^{\circ}\mathrm{C\,s^{-1}}$ was used and a sample was dosed to 3 Gy.

Equation 2.14 was used to calculate the activation energy from τ, ω and δ methods of the peak shape methods. Results are summarized in table 5.8. E_ω, E_δ and E_τ methods are consistent with the initial rise and variable heating rate methods. The geometrical factor μ_g was at about 0.42 which suggests that peak IIA follows first order kinetics. This is confirmed by using the glow curve deconvolution method as will be shown later.

Figure 5.31 shows a plot of TL intensity for peak IIA against heating rate. The maximum TL intensity decreases with heating rate for heating rate from 0.2 to $6^{\circ}\mathrm{C\,s^{-1}}$. This is an indication that the peak is subject to thermal quenching.

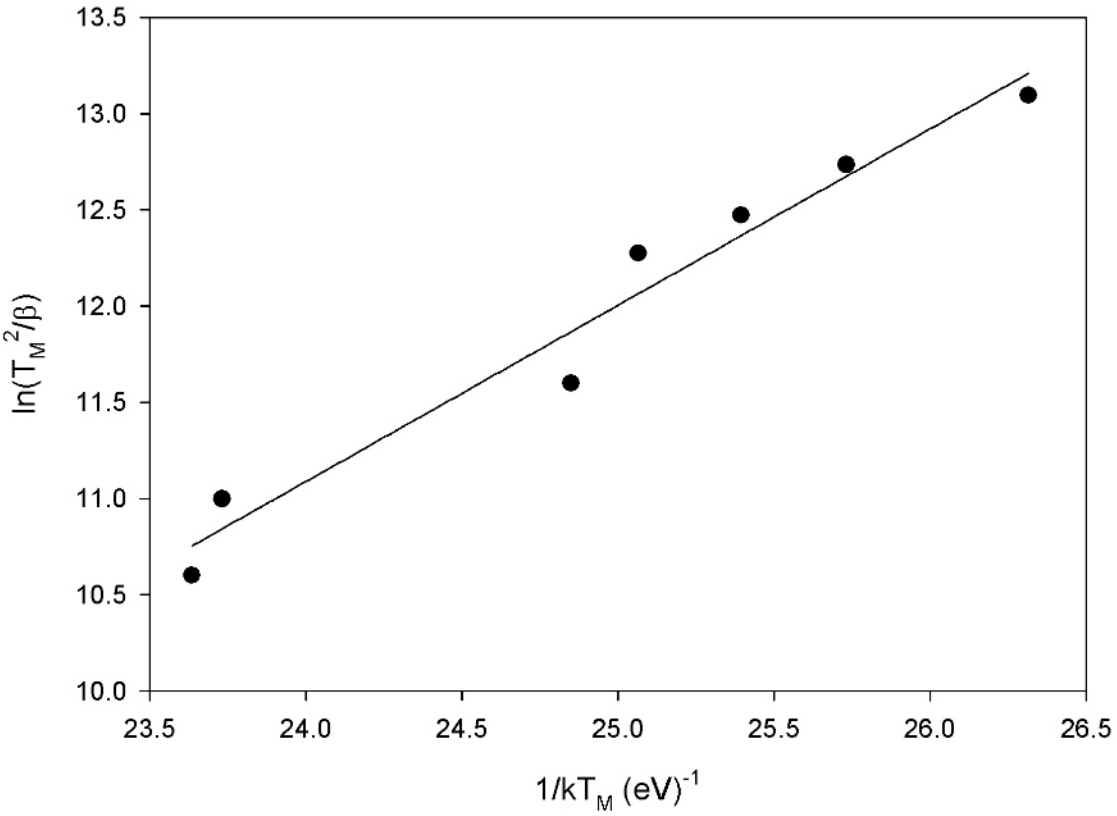

Figure 5.30: A plot of $\ln(T_M^2/\beta)$ against $1/kT_M$ for peak IIA. A dose of 3 Gy was used.

Table 5.8: The activation energy E and frequency factor s for TL data of peak IIA from various methods. The frequency factor s was calculated using equation 2.4 on assumption of first order kinetics.

Method	E (eV)	s (s^{-1})
Initial rise	0.85±0.04	1×10^8
Variable heating rate	0.92±0.08	1.0×10^{10}
Chen's ω-method	0.86±0.11	2.2×10^8
Chen's δ-method	0.86±0.20	2.2×10^8
Chen's τ-method	0.84±0.08	1.2×10^8

5.1.5 The glow curve deconvolution method

The TL data for the whole glow curve was fitted using five terms of the general order kinetics equation [15], equation 2.35. Figure 5.32 (a) shows attempt at fitting using equation 2.35. The glow curve was measured at a heating rate of $0.4^{\circ}\mathrm{C\,s^{-1}}$ following a dose of 3 Gy. The initial guesses for values of E and s used in the fitting were taken from the previous methods for each peak. The other initial parameters used were T_M

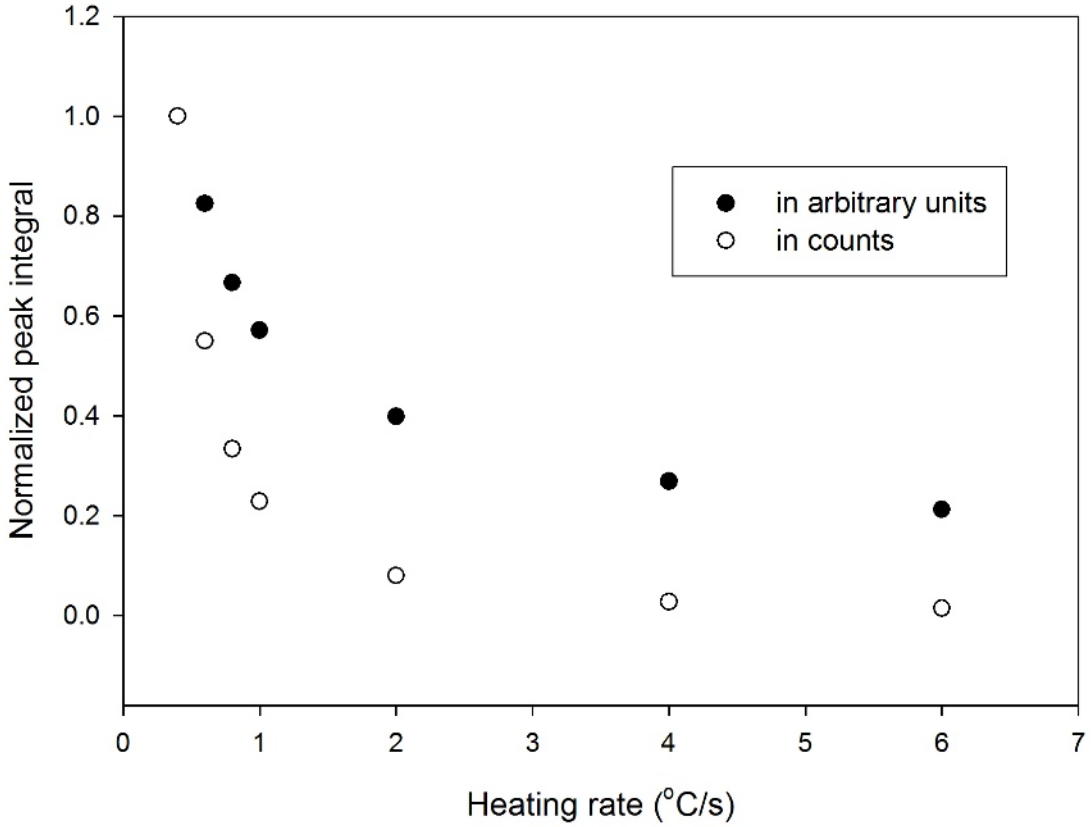

Figure 5.31: TL intensity against heating rate. The sample was dosed to 3 Gy.

and I_M from the experimental data. The glow curve is dominated by the intense main dosimetric peak as can seen in figure 5.32 (b) where the y-axis is on a logarithmic scale. The residuals plot (figure 5.32 c) shows that the fitting was only partially good. The fit for the main peak is poor. Some authors have reported peak II to be a superposition of many undistinguishable peaks as well as a satellite peak at the higher temperature end of the peak [24, 33, 34]. Thus, these possibilities are probably the cause of the poor fit for the main peak. In addition, unfitted data points from the initial part of peak I are due to phosphorescence. Peak IV is also undefined, so that the fitting could not be good at all due to the weak TL intensity for this peak with much scatter. The glow curve deconvolution method was therefore used only as a first estimate.

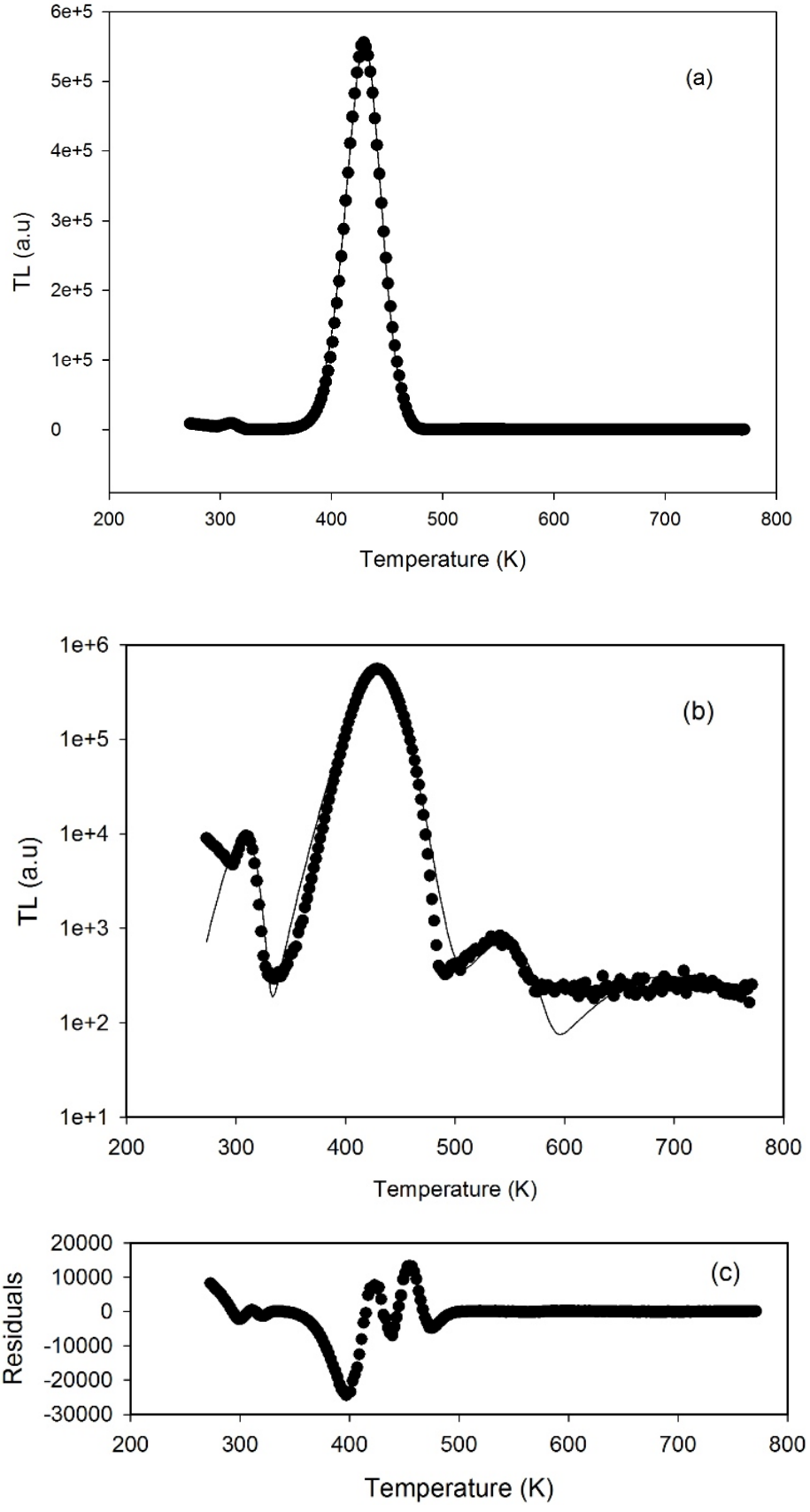

Figure 5.32: The fitting of a glow-curve for TL data measured using a heating rate of $0.4^{o}\mathrm{C\,s^{-1}}$ after a dose of 3 Gy (a) the TL data is shown on a logarithmic scale for better clarity (b) the bottom fgure shows a plot of the residuals versus temperature (c).

5.1.5.1 The deconvoluted peaks of the glow-curve in $\alpha - Al_2O_3 : C$

The parameters from the fit of section 5.1.5 were used to generate the individual peak and these are shown in figure 5.33. The TL for peaks of number I, IIA, III and IV have been scaled up for better clarity. The glow curve deconvolution method was used to assess two things. Firstly, to check the number of peaks of the glow curve following a dose of 3 Gy and a heating rate of $0.4^{o}C\,s^{-1}$. The kinetic parameters calculated using the method were compared with kinetic parameters evaluated using the other methods of TL analysis.

The number of peaks in a glow-curve of $\alpha - Al_2O_3 : C$ for TL measured using a heating rate of $0.4^{o}C\,s^{-1}$ for a dose of 3 Gy were determined following different steps. At the beginning, three clear peaks before thermal cleaning of peak III (peaks I, II and III) were fitted. The guessed initial parameters for peak I were inserted by keeping the order of kinetics $b_1 = 1.1$ constant and changing values of E_1 from 0.7 to 1 eV. For peak II, E_2 was changed from 0.9 up to 1.2 eV at $b_2 = 1.4$ while E_3 was changed between 0.9 and 1.3 eV for peak III at $b_3 = 1.1$. The kinetic order b_i of i^{th} peak in a glow curve was also changed at constant E_i. For each fit the FOM was noted until the best fit parameters corresponding to the minimum FOM were obtained. Another fitting considered peaks IIA and IV (appeared during thermal cleaning process to reveal peak III) in addition to peaks I, II and III. Values of E and s from fitted data for different number of peaks met the acceptance criteria of $C_b < 0.4$ but had different FOM values. A comparison of FOM values showed that the best fit parameters was found using five peaks with a minimum FOM of 5.5%. The second FOM was 7.2% for only fitting three peaks and the worst was 17.6% for 4 peaks. This means that the glow curve deconvolution method confirmed the presence of five peaks for a glow curve in $\alpha - Al_2O_3 : C$. Results are shown in table 5.9. It is also important to note that the two overlapping peaks of the main peak were previously reported by Yazici et al. [33] using glow curve deconvolution method on an isolated peak II. He assessed the overlapping nature of the main dosimetric peak by increasing dose from 0.02 up to 144 Gy. This work suggested that by increasing dose up to 3 Gy and heating rate to $0.4^{o}C\,s^{-1}$, the

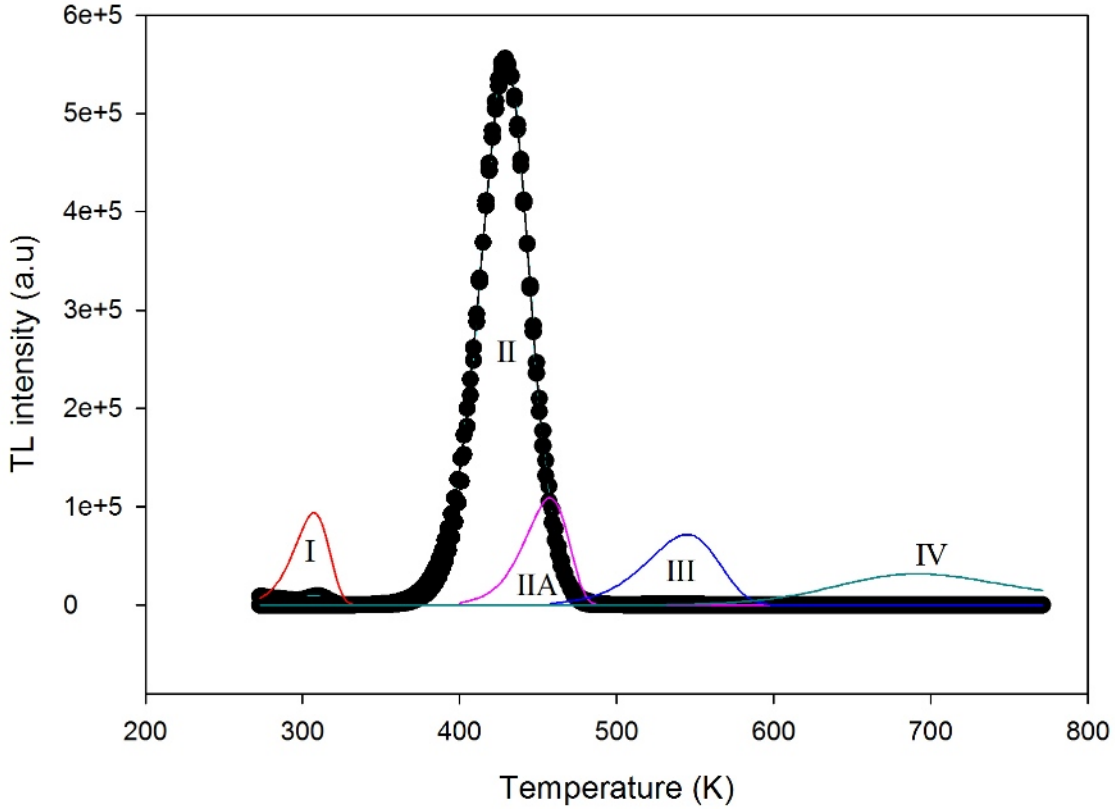

Figure 5.33: The glow-curve deconvolution method for TL data measured using a heating rate of $0.4^{o}\mathrm{C\,s^{-1}}$ following a dose of 3 Gy. The intensities of peaks numbers I, IIA, III and IV have been scaled up to be better seen. The deconvoluted peak number II overlaps with the experimental data of the main peak.

glow curve deconvolution showed another subsidiary peak at higher temperatures at about 422°C. Our glow curve deconvolution method showed first order kinetics for peaks I (309 K) and III (541 K). We have also shown that peak II is composed of two peaks at 429 K (a general order kinetics peak II) and at 443 K (a first order kinetics peak IIA). The peak at 695 K (peak IV) is not well defined (figure 5.22) and do not provide any significant value at this stage.

The main conclusion from this study is that the glow curve consists of five peaks. The activation energies of peaks I and II are acceptable but those of peaks IIA, III and IV are not due to their large errors caused by poor fitting. Other methods were used to improve the fit. These methods considered the fit of peaks IIA, III and IV following the thermal cleaning method to find peak III (figures 5.21 and 5.22). Firstly, a whole glow curve showing peaks IIA, III and IV after preheating to 200°C to remove peaks

Table 5.9: The best fit kinetic parameters (FOM of 5.5%) for five peaks evaluated using the glow curve deconvolution method. During TL experiment, a heating rate of $0.4^{o}\mathrm{C\,s^{-1}}$ following an irradiation dose of 3 Gy was used. The large errors in subsidiary peaks are caused by the dominant intense main dosimetric peak (peak II).

T_M (K)	E (eV)	s ($\mathrm{s^{-1}}$)	b	C_b
309 (peak I)	0.73 ± 0.47	3×10^{10}	1.03 ± 0.97	0.3907
429 (peak II)	1.19 ± 0.02	2.7×10^{12}	1.42 ± 0.15	0.3356
443 (peak IIA)	1.29 ± 30.5	1.4×10^{13}	1.00 ± 10.6	0.3905
541 (peak III)	1.13 ± 8.16	1.0×10^{9}	1.06 ± 11.1	0.3898
695 (peak IV)	1.07 ± 18.7	1.0×10^{6}	2.46 ± 97.6	0.2813

I and II from a sample previously irradiated to a dose of 3 Gy was fitted using three terms of equation 2.35. A heating rate of $0.4^{o}\mathrm{C\,s^{-1}}$ was used. Figure 5.34 shows the best fit option after several changes of the inserted initial guesses for values of E and b into equation 2.35. A plot of residuals versus temperature (top of figure 5.34) shows that the fitting was good. The values of E for peaks IIA and III are $E = 1.01 \pm 0.02$ eV and $E = 1.27 \pm 0.06$ eV respectively and are acceptable. The orders $b = 1.2 \pm 0.04$ and $b = 1.00 \pm 0.07$ obtained for peaks IIA and III respectively imply that these peaks are of first order kinetics. Peak IV is of weak intensity and as such, equation 2.35 does not properly fit the data in this case. The best fit obtained using two terms of equation 2.35 gave acceptable fitting parameters for peak IV only when the fitting was done to a glow curve measured after preheating to 265°C to remove peak IIA (figure 5.22). Figure 5.35 shows the best fit of a glow curve for peaks III and IV from which the E value was acceptable. $\mathrm{E} = 1.27 \pm 0.09\,\mathrm{eV}$ and $b = 1.00 \pm 0.11$ were obtained for peak III and are similar to those obtained in figure 5.34. The fitting at this stage, also gives an acceptable $\mathrm{E} = 1.25 \pm 0.27\,\mathrm{eV}$ for peak IV. In addition, peak IV follows a general order kinetics with $b = 1.48 \pm 0.52$.

5.1.5.2 Summary on the glow curve deconvolution method

The deconvolution method shows that a glow curve consists of five glow peaks (figure 5.33). For the first attempt at fitting, a complete glow curve measured without thermal cleaning was used. This fitting gave acceptable activation energies only for peaks I and

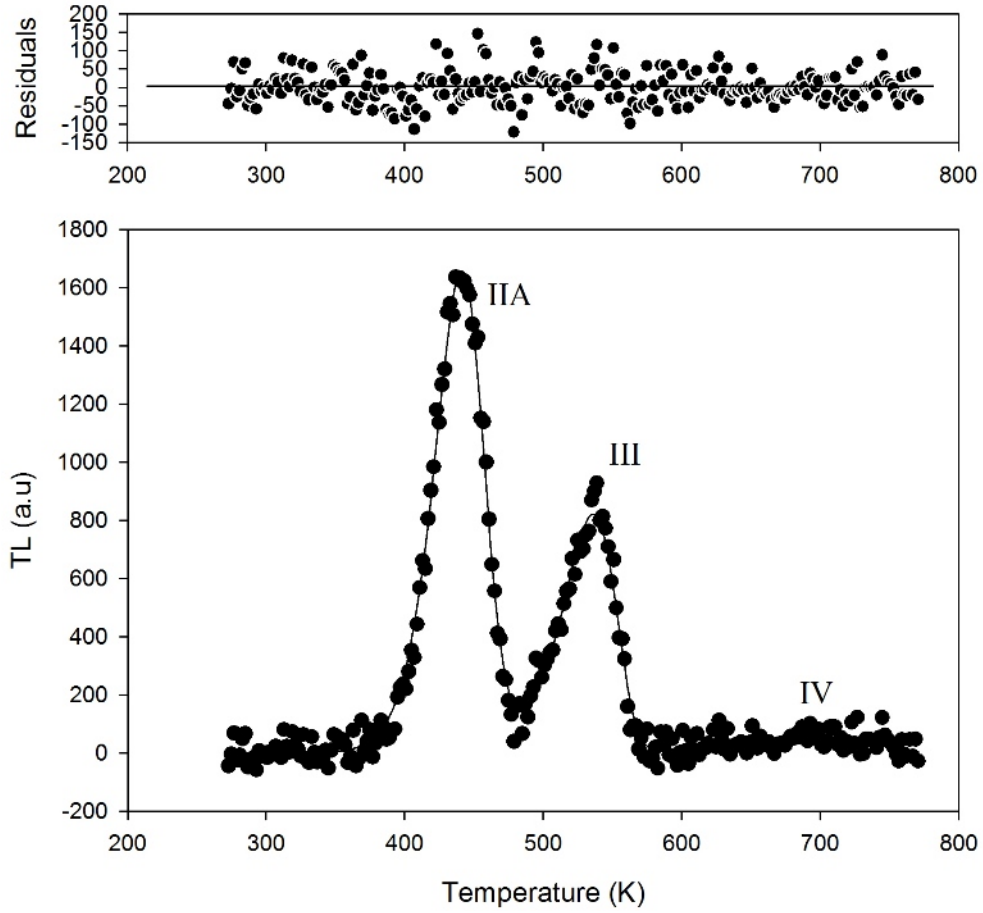

Figure 5.34: The fitting of a glow curve showing peaks IIA, III and IV for TL intensity measured following preheating to 200°C. The sample was heated at a rate of 0.4°C s^{-1} after irradiation to 3 Gy. A plot of residuals shows that the fitting was good.

II (table 5.9). The values of activation energy obtained for peaks IIA, III and IV were rejected because of the following reasons leading to the poor fit of a complete glow curve:

1. Peak II, which is very intense, overshadows peaks I, IIA, III and IV.

2. The possible overlaps of many peaks other than peak IIA to the main peak [24, 33].

3. The shape of peak I is affected by phosphorescence (figure 5.16 a); as such, the fit is not satisfactory in the low temperature region of the glow curve for peak I as shown in figure 5.32 (b).

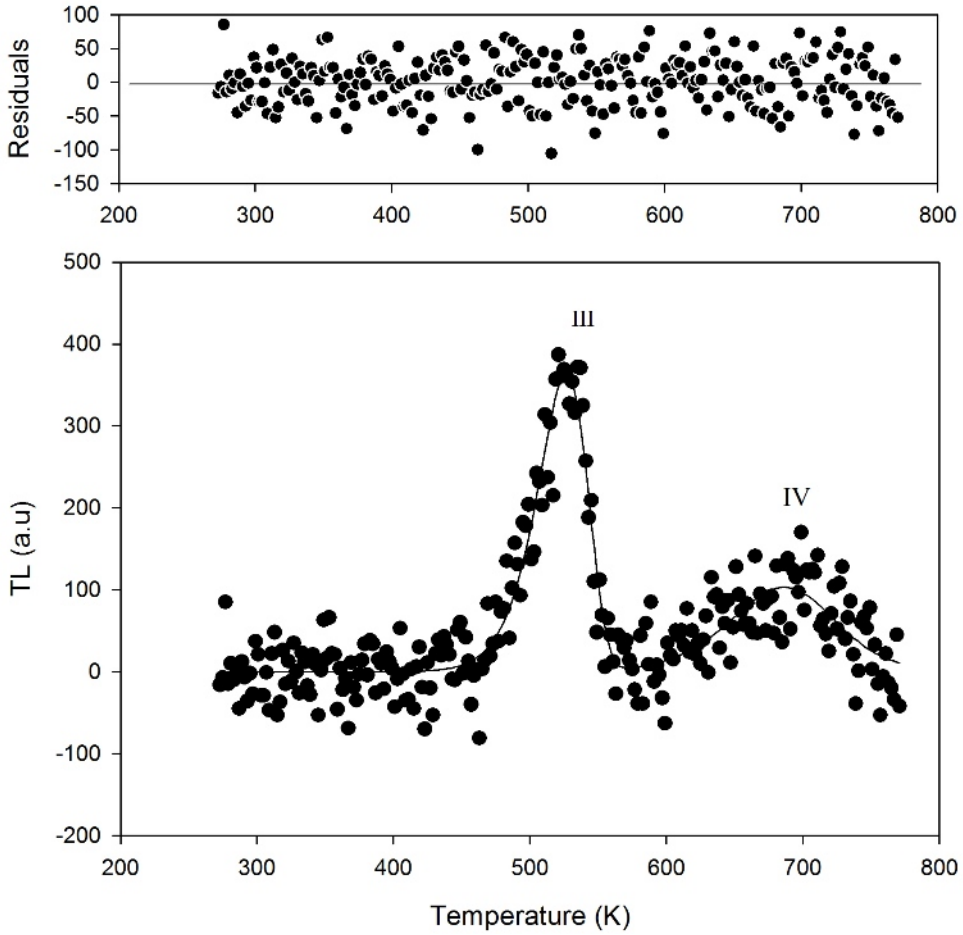

Figure 5.35: A glow curve showing peaks III and IV fitted using two terms equation 2.35. A preheating temperature of 265°C was used for thermal cleaning to find peak IV. The heating rate of $0.4^{\circ}\mathrm{C\,s^{-1}}$ and a dose of 3 Gy were used. The top of the figure is a plot of residuals.

Other attempts at fitting were performed on thermally cleaned glow curves (figures 5.34 and 5.35). These attempts at fitting thermal cleaned peaks gave acceptable parameters for all peaks. The summary of these results are shown in table 5.10. The first order kinetics equation (equation 2.33) was applied for peaks I, IIA and III to check the validity of equation 2.35 for $b = 1$. However, due to the inaccessibility of the fully well-resolved peak using peak-separation techniques the fit was poor based on the structures of the FOM and C_b in [1, 5, 15]. Here, the very correct values of E and b corresponded to the glow curve as being composed of five peaks and were only reported.

Table 5.10: The best fit values of the E and s acceptable for five peaks evaluated using the glow curve deconvolution method. For all measurements, the sample was irradiated to 3 Gy and heated to $0.4^{o}\mathrm{C\,s^{-1}}$ to record the TL glow curve. The best fit parameters for peaks IIA and III were found in a glow curve fitted after thermal cleaning to remove peaks I and II while those of peak IV were obtained from a glow curve measured after thermal cleaning to remove peaks I, II and IIA.

T_M (K)	E (eV)	s ($\mathrm{s^{-1}}$)	b	C_b
309 (peak I)	0.73 ± 0.47	3.0×10^{10}	1.03 ± 0.97	0.3907
429 (peak II)	1.19 ± 0.02	3.0×10^{12}	1.42 ± 0.15	0.3356
443 (peak IIA)	1.01 ± 0.02	1.0×10^{10}	1.2 ± 10.04	0.3905
541 (peak III)	1.27 ± 0.07	1.4×10^{10}	1.00 ± 0.07	0.3898
695 (peak IV)	1.25 ± 0.52	1.4×10^{7}	1.48 ± 0.27	0.2813

5.1.6 Mechanisms and summary of TL experiment

The experimental results observed during the thermoluminescence measurements in $\alpha - \mathrm{Al_2O_3 : C}$ can be discussed in terms of the dynamics of charge carriers from electron traps in the material to the recombination centres. Figure 5.36 shows the energy band model used to explain the dynamics of charge carriers during TL experiment in $\alpha - \mathrm{Al_2O_3 : C}$ [4, 22, 28]. Transitions in the diagram are used to explain the process involved during irradiation and heating. 1S denotes the ground state of the F-centres while 1P and 3P levels represent the excited states of F-centres. An electron may absorb an energy in the absorption band to move from 1S to 1P (transition 1) due to ionization of F-centres in a previously irradiated material. The ionizing radiation moves electrons to the excited 1P state leaving holes behind. Electrons excited to the 1P state may escape to the conduction band leading to the formation of F^+ centres. Being unstable in the conduction band, free electrons are captured into different energy traps (downward arrows). These electron traps are shallow (ST), main (MT) and intermediate (IDT) energy traps responsible for peaks I, II and III, respectively. The deep electron trap (DET) and deep hole trap (DHT) compete for the free electrons in the conduction band. The subsequent heating releases electrons from their respective energy traps (upward arrows) via the conduction band to recombine with existing F^+ centres leading to their conversion to F-centres [4]. The mechanism leading to thermoluminescence emitted at 420 nm in $\alpha - \mathrm{Al_2O_3 : C}$ is attributed to the radiative transitions of electrons from

the 3P excited state to the 1S ground state, transition 2. Non-radiative recombination, transition 3, is also possible. An electron in the excited 3P level can absorb energy from thermal ionization in transition P_F and follow transition 3. The energy produced after the relaxation of electrons in the ground state 1S, is dissipated as thermal vibration of the crystal lattice in the material. The increase of non-radiative recombination causes a decrease in the fraction of radiative recombination at the recombination centre. This is called thermal quenching of luminescence in a material and is temperature dependent [28, 32, 35, 36].

Thermal quenching was particularly observed from peak III at 266°C. We assume that a number of the released electrons to the excited 3P state were thermally ionized and followed transition 3. The activation energy of $W = 1.48 \pm 0.10\,eV$ and constant $C = 4 \times 10^{13}$ for this processes were calculated.

The analysis of the TL emission responsible for peak I showed that the thermal stimulation of trapped electrons was possible at ambient temperatures. Because peak I is associated with a shallow trap, a delay between irradiation and measurement of TL causes the fading of the peak at room temperature. However, the probability of producing non-radiative recombination for peak I is negligible. The dose response for this peak was studied at low doses between 0.5 and 2.5 Gy. An increase of dose in this range showed a linear dose response of TL. This means that the rate of production of F^+ centres by hole trapping at F-centres and their conversion to F-centres by an electron capture ($F \rightleftharpoons F^+$ centre conversion) is approximately equal at low dose. For further study of dose response at high doses, one may refer to the band model of the material reported previously [9, 28, 37]. The dose response for peak III was not studied. This can be properly performed at high beta doses greater than 3 Gy. This is due to the fact that deep traps are only filled appreciably at high doses. However, the dose assessment below 3 Gy for peak III helped to assess qualitatively the effect of deep trap filling on TL of $\alpha - Al_2O_3 : C$. The sample irradiated at low doses leaves deep traps unfilled. During heating, the empty deep electron trap competes for electrons that would otherwise combine with F^+ centres to produce luminescence and hence, reduces

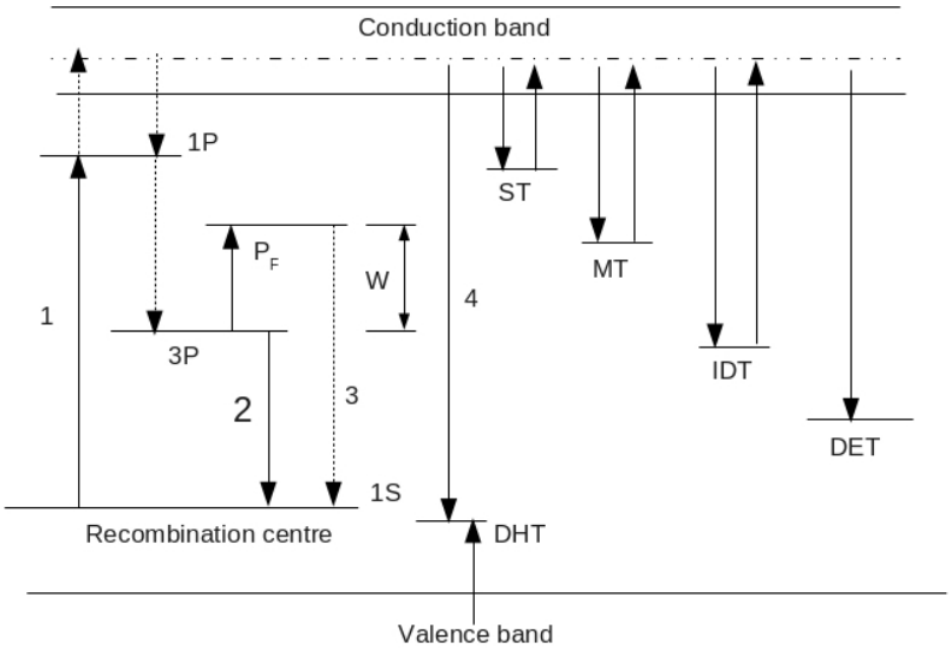

Figure 5.36: An energy band model used to describe the TL mechanisms of $\alpha - Al_2O_3 : C$. The model is a combination of models as reported previously [4, 28]. The band-model is shows the shallow, main and intermediate energy traps (ST, MT and IDT) associated with peaks I, II and III, respectively. Levels DET and DHT stand for deep electron and hole traps, respectively. 1S denotes the ground state of F-centres while levels 1P and 3P are assigned to the excited states of F-centres. Transition 1 denotes ionization and transition 2 shows the luminescence emission. P_F stands for thermal ionization transition leading to a non-radiative transition, transition 3. Transition 3 is actually a source of thermal quenching for peaks II and III with an activation energy of thermal quenching W. Transition 4 denotes electron-hole recombination at the DHT.

the luminescence emitted at the recombination centres. The increase of dose filled the more stable deep electron traps such that the competition was reduced and hence the luminescence is increased.

5.1.7 Summary of kinetics of secondary thermoluminescence

The best-fit parameters of secondary thermoluminescence in $\alpha - Al_2O_3 : C$ are shown in table 5.11. The values of E, s and b evaluated using the glow curve deconvolution method were in a good agreement with E, s and b values calculated from the initial rise, the whole curve, the isothermal analysis, the peak shape and the variable heating rate methods. The deconvolution method confirms first order kinetics for peaks I and

III, initially suggested in some of the methods and then attested to using the T_M-T_{stop} method. From the table, it can be seen that values of the activation energy E and frequency factor s evaluated from the initial rise, peak shape, variable heating rate, whole curve and isothermal analysis method are also verified using the glow curve deconvolution method. The kinetics of the charge-carrier transfer between traps during thermoluminescence process was described. A small deviation was observed from trapping parameters calculated using the peak shape method for peak I. The source of errors were explained as being due to guessing approximate temperatures used in the method. As previously discussed in the section on fading (section 5.1.3.1) the shape of peak I was modified by the phosphorescence. It follows that E, s values evaluated using the peak shape method were also affected by phosphorescence (as presented in table 5.5). The values of E and S calculated using the variable heating rate method for peak III are greater than the other values calculated using other methods. The cause was attributed to the thermal quenching effect.

Table 5.11: The comparison between values of trapping parameters evaluated using a variety of methods for secondary glow peaks.

(a) Peak I.

Method	E (eV)	s (s^{-1})	b
Initial rise	0.72 ± 0.01	3.0×10^{10}	
Variable heating rate	0.72 ± 0.04	2.7×10^{10}	
Peak shape in ω-form	1.05 ± 0.05	4.6×10^{15}	1
Peak shape in τ-form	1.05 ± 0.07	4.6×10^{15}	1
Peak shape in δ-form	0.99 ± 0.14	5.0×10^{14}	1
Whole curve	0.90 ± 0.02,	2.0×10^{13}	1
Isothermal analysis	0.72 ± 0.02	2.6×10^{10}	1
Glw-curve deconvolution	0.73 ± 0.47	3.0×10^{10}	1

(b) Peak III.

Method	E (eV)	s (s^{-1})	b
Variable heating rate	1.50 ± 0.08	3×10^{10}	
Peak shape in ω-form	1.15 ± 0.12	1×10^{9}	1
Peak shape in τ-form	1.16 ± 0.0	1×10^{9}	1
Peak shape in δ-form	1.14 ± 0.15	1×10^{9}	1
Whole curve	1.10 ± 0.04	2×10^{9}	1
Glow-curve deconvolution	1.27 ± 0.07	1.0×10^{10}	1

5.2 Phototransferred thermoluminescence from secondary glow peaks in α-$Al_2O_3 : C$

The aim of study in this section was to investigate the phototransferred thermoluminescence (PTTL) from α-$Al_2O_3 : C$. The influence of annealing and irradiation on PTTL from secondary peaks were also investigated on samples annealed at 900°C as well as unannealed. Samples used in the study of PTTL show generally three glow peaks (example figure 5.37). The study of PTTL focuses on peak I and peak III. Three groups of samples (samples A, A_1 and B) were studied in the PTTL from secondary glow peaks. Samples A and A_1 were not annealed at 900°C before use. The results obtained from samples A and A_1 were then compared to check if the characteristics of the PTTL peak vary from sample to sample. The PTTL in sample B was measured after annealing to 900°C for 15 minutes.

5.2.1 PTTL characteristics from shallow traps in unannealed samples: Sample A

The PTTL was studied, first, from a group of unannealed samples (sample A). The study was concerned with the effects of annealing and dose on PTTL from secondary peaks. Figure 5.37 shows the peak positions in a glow curve from samples used in the PTTL study. The position of peaks are 86°C (peak I), 240°C (peak II) and 360°C (peak III) using a heating rate of $5°C\,s^{-1}$ following a beta dose of 0.5 Gy. Samples were exposed to 470 nm blue light emitting diodes after preheating to various temperatures chosen to empty shallow traps.

5.2.1.1 PTTL from peak I following preheating to 100°C

Figure 5.38 shows the PTTL signal measured from peak I following preheating to 100°C. A heating rate of $5°C\,s^{-1}$ was used after a beta dose of 0.5 Gy and illumination for 30 s. The position of the PTTL peak is 90°C. Several measurements of PTTL signal corresponding to various illumination times from 0 to 60 s were done for the same dose

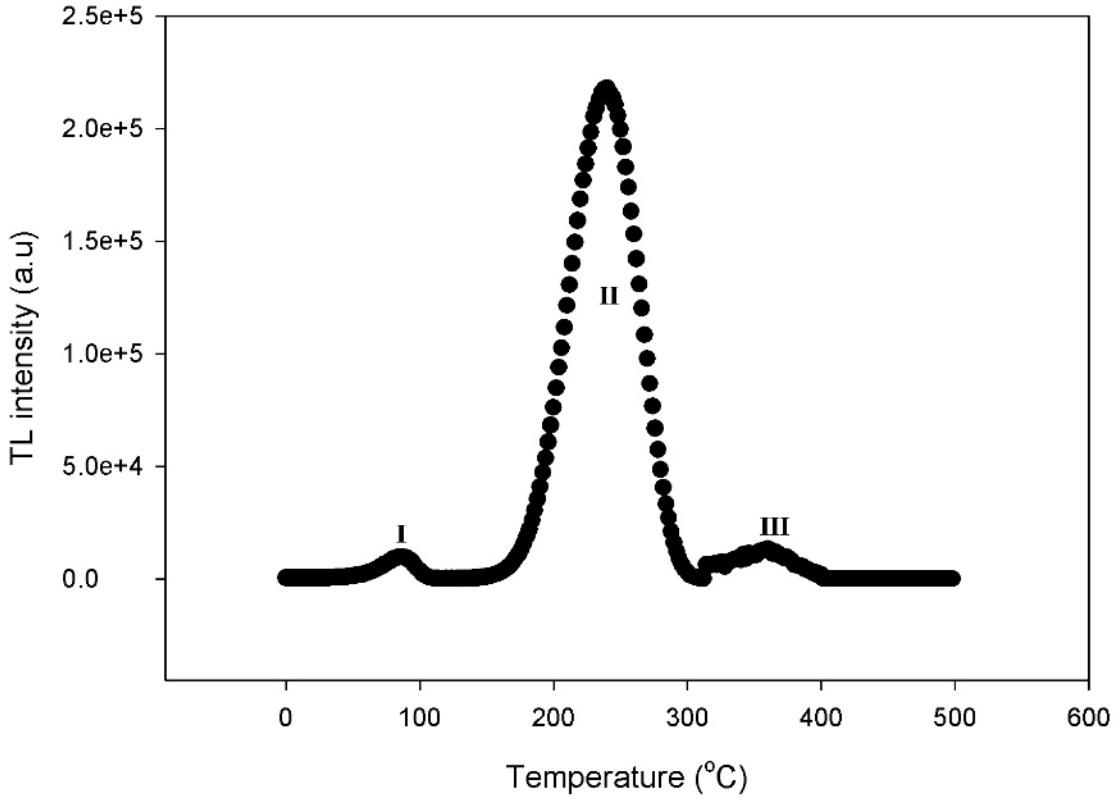

Figure 5.37: The temperature dependence of thermoluminescence following heating to $5^{o}C\,s^{-1}$ using sample irradiated to 0.5 Gy. Peak I appears at 86°C, peak II at 240°C and peak III at 360°C. Data for peak III has been magnified for better clarity.

of 0.5 Gy and heating rate of $5^{o}C\,s^{-1}$. Figure 5.39 shows a plot of PTTL intensity versus illumination time. The plot shows a peak-shaped structure with maximum at an illumination time of 7 s. The change of the intensity with time reflects the charge exchange between the shallow trap corresponding to peak I and deep traps due to optical stimulation. The increasing part of figure 5.39 implies that, at low illumination time, the trapping of electrons at the shallow trap exceeds any removal by optical stimulation. For long illumination times greater than 7 s, the PTTL intensity decreases. This means that the removal of electrons from the shallow trap by optical stimulation dominates the trapping of electrons.

5.2.1.2 The PTTL feature from peaks I and II after preheating to 290°C

An irradiated sample was pre-heated to 290°C to remove both peaks I and II. A PTTL signal was recorded directly after exposure to blue light for 30 s. Figure 5.40 shows

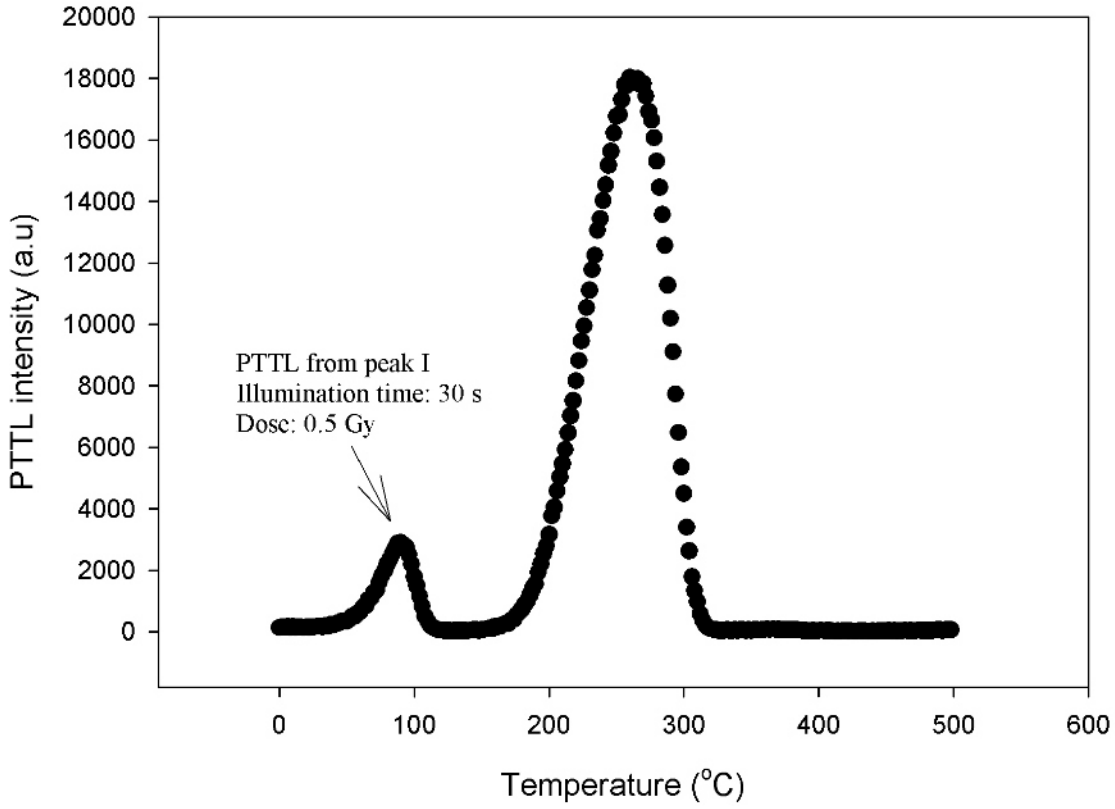

Figure 5.38: The PTTL peak I following preheating to 100°C for a dose of 0.5 Gy is shown at 90°C. A heating rate of $5^{o}\mathrm{C\,s^{-1}}$ after an illumination time of 30 s was used.

peaks I and II regenerated by phototransfer. Peak I and peak II were reproduced at 92°C and at 270°C respectively. The sample was heated using a heating rate of $5^{o}\mathrm{C\,s^{-1}}$ after a dose of 0.5 Gy.

The maximum intensities of PTTL from peaks I and II following light exposure at times from 0 to 600 s were recorded. Figure 5.41 (a) shows a plot of PTTL signal against illumination time for peak I. The plot shows that the maximum of intensity versus time graph is at an illumination time of 40 s. The time dependence of the PTTL signal from peak II after heating to the same temperature of 290°C is shown in figure 5.41 (b). As can be seen, the measured PTTL signal of peak II also has a peak-like form with a maximum at an illumination time of 30 s. The charge involved in the luminescence of PTTL from peaks I and II were optically transferred to these traps out of deep traps by the light exposure. The intensity of PTTL for peak II increases then decreases with time faster than the intensity for peak I. In addition, figure 5.41

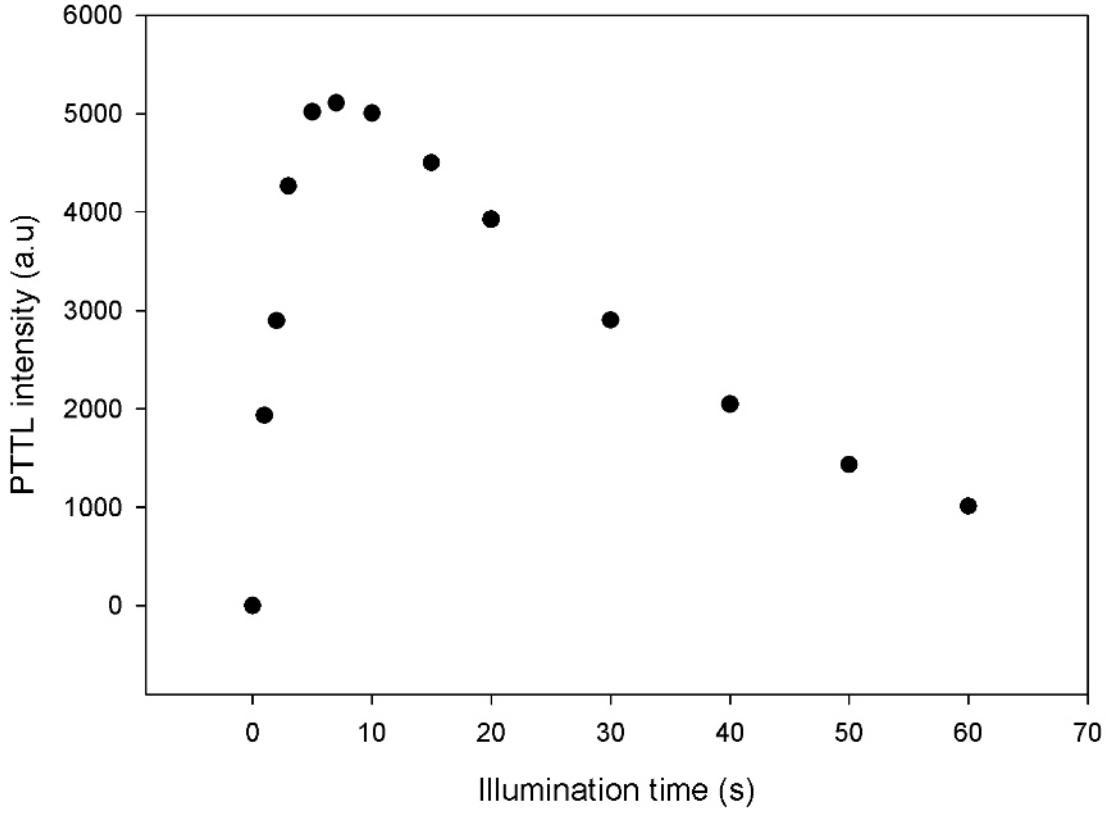

Figure 5.39: The dependence of PTTL intensity on illumination time for peak I. The sample was preheated to 100°C before each measurement.

(b) shows that the intensity is constant at illumination times about 300 s and more.

The high temperature peak, peak III, in figure 5.40 is not a PTTL peak produced after preheating to 290°C since the position of peak III is 366°C and is not removed by preheating to 290°C. This means that peak III is a normal TL peak.

Figure 5.42 shows the dependence of TL intensity on illumination time for peak III for sample preheated to 290°C. The intensity increases with illumination time, reaches its maximum at an illumination time of 20 s and then decreases thereafter to 600 s. This can be interpreted as that part of phototransferred charges from deeper traps go to the electron trap associated with peak III. However, after heating to 390°C to remove all peaks, peak III was not reproduced for any illumination time. This may be explained as the probability of optical removal of electrons from the trap is very much higher than its retrapping probability. It may also mean that the transfer of electrons to this trap is negligible. In addition, the increase of intensity up to its maximum

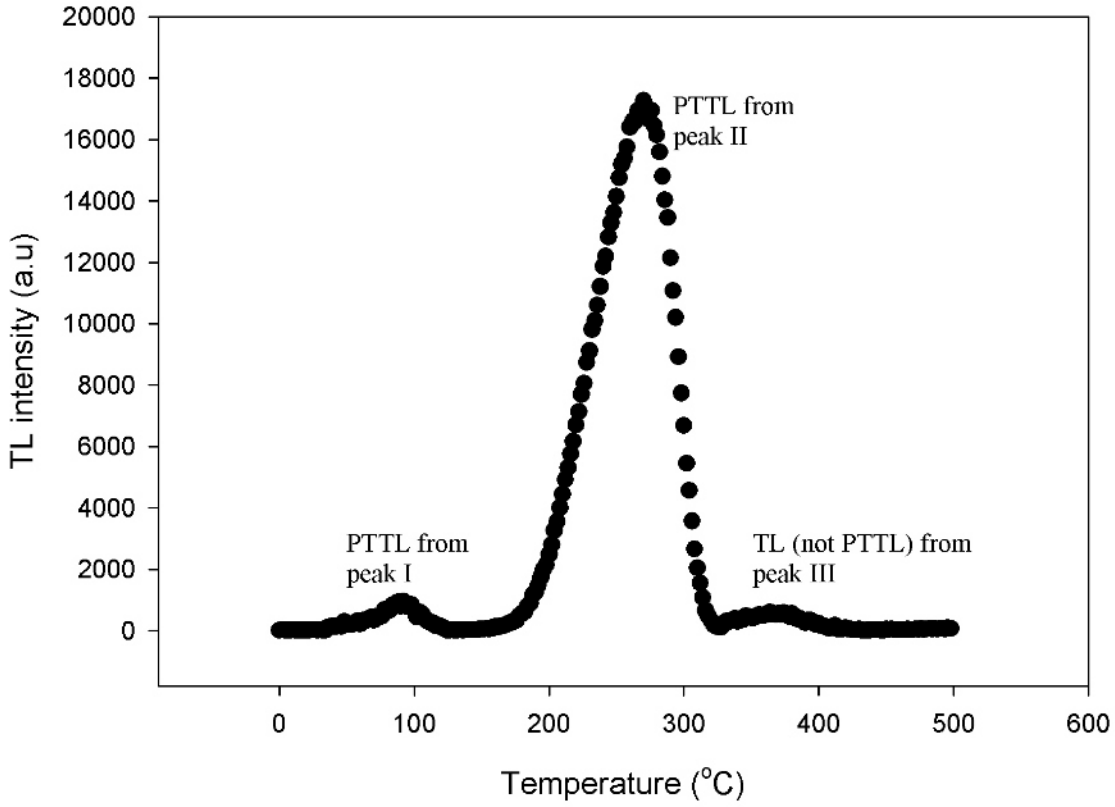

Figure 5.40: A glow curve showing PTTL peaks I and II following preheating to 290°C. Peak III had not been removed by the preheating as it appears at 366°C, that is, peak III in this figure is for normal TL not PTTL.

suggests that peak III is a competitor of photostimulated charges from deeper traps particularly when the main dosimetric trap is empty. The decrease of intensity with time from peak III for longer illumination times shows that the peak is also a donor trap of electrons to peaks I and II by optical stimulation.

5.2.1.3 The PTTL from peaks I and II following preheating to 390°C

All peaks (I, II and III) were removed by preheating samples to 390°C after an irradiation dose of 0.5 Gy. The PTTL signal was measured by subsequent heating to 500°C at a rate of $5^{\circ}\mathrm{C\,s^{-1}}$ following illumination times from 0 to 600 s.

An illumination time of 30 s following the preheating to 390°C gave rise to peaks at 84°C (peak I) and at 268°C (peak II) under PTTL. This is shown in figure 5.43. Peak III was not reproduced under PTTL. Figure 5.44 shows a TL glow curve (figure

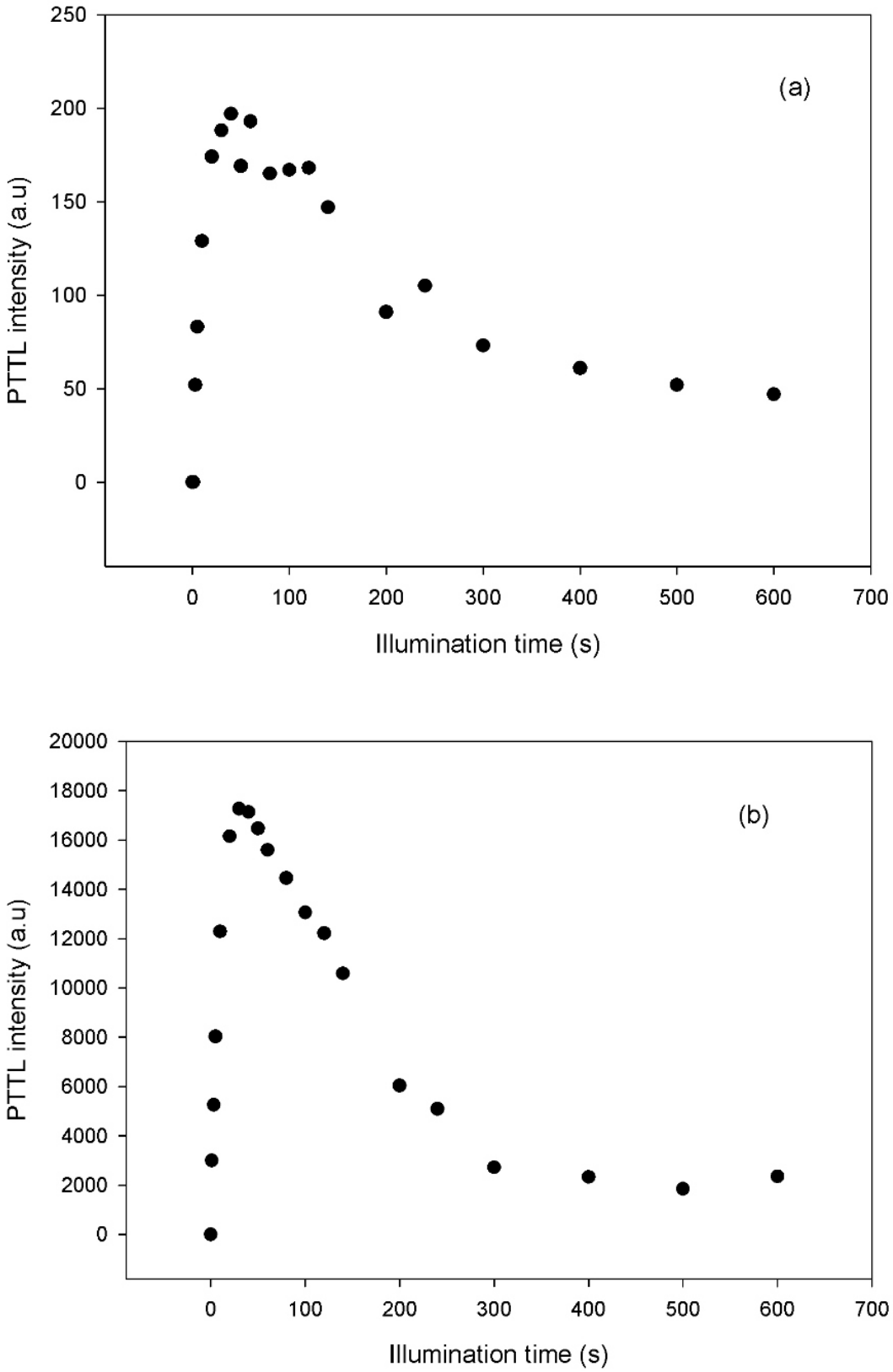

Figure 5.41: PTTL intensity versus illumination time for peak I (a) and for peak II (b) after preheating to 290°C. The sample was dosed to 0.5 Gy.

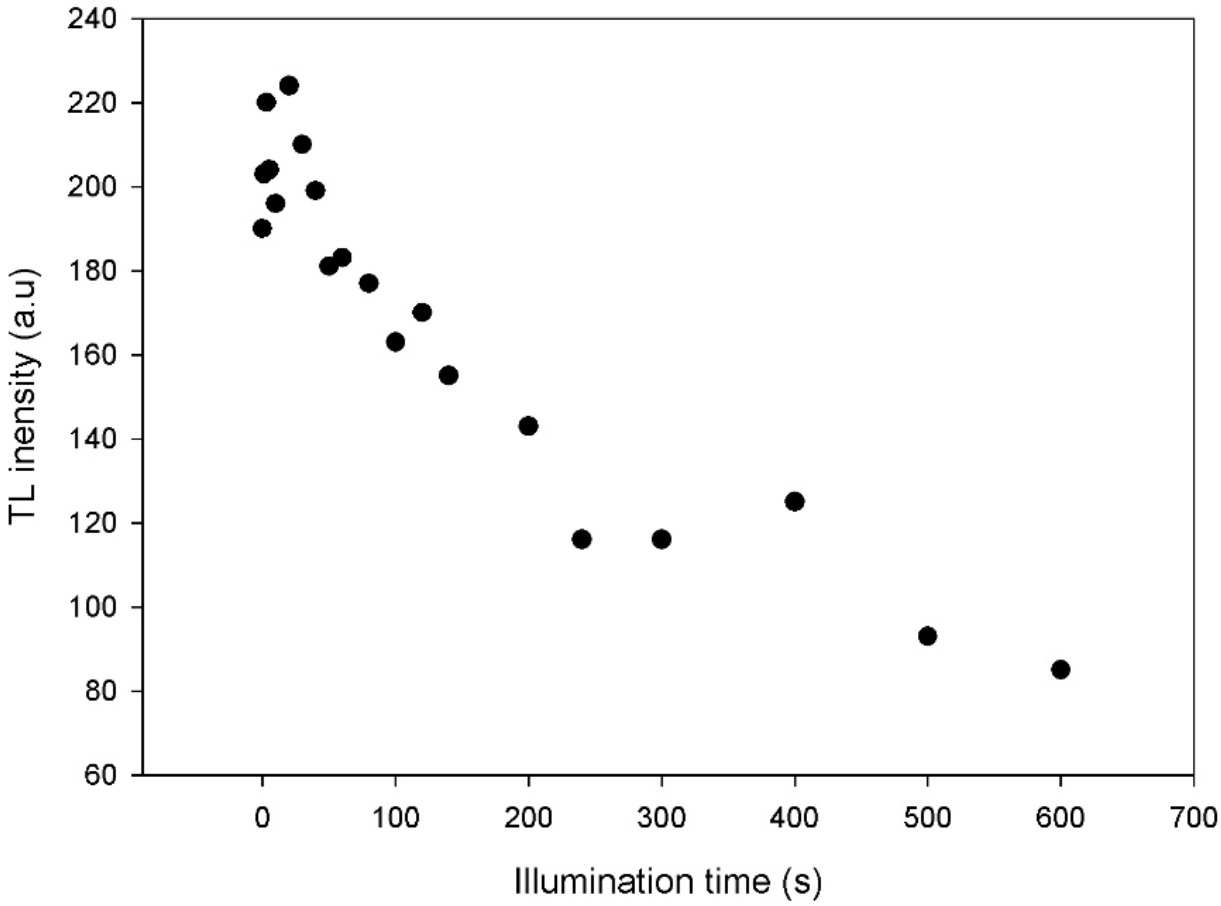

Figure 5.42: The illumination time dependence of TL intensity from peak III (at 366°C) after preheating to 290°C. The intensity of the initial part of the plot increases with time up to 20 s and then decreases from 20 s to the end of illumination (600 s). This shows that peak III is a competitor and a donor trap of electrons respectively.

5.37) comprised with PTTL glow curve (figure 5.43) in one graph for better clarity of PTTL results. As it can be seen, the PTTL for peak I is regenerated at the original position of TL peak I and the PTTL peak II is collocated to the normal TL peak II.

The dependence of PTTL intensity on illumination time for peak I is shown in figure 5.45. The intensity of the peak increases to a maximum at an illumination time of 120 s.

Comparing three graphs (figures 5.39, 5.41 (a) and 5.45) of the time dependence of PTTL for peak I after heating to various temperatures we can conclude the following:

1. The PTTL intensity from peak I following preheating to 100°C (figure 5.39) decays to half maximum in an illumination time of about 30 s,

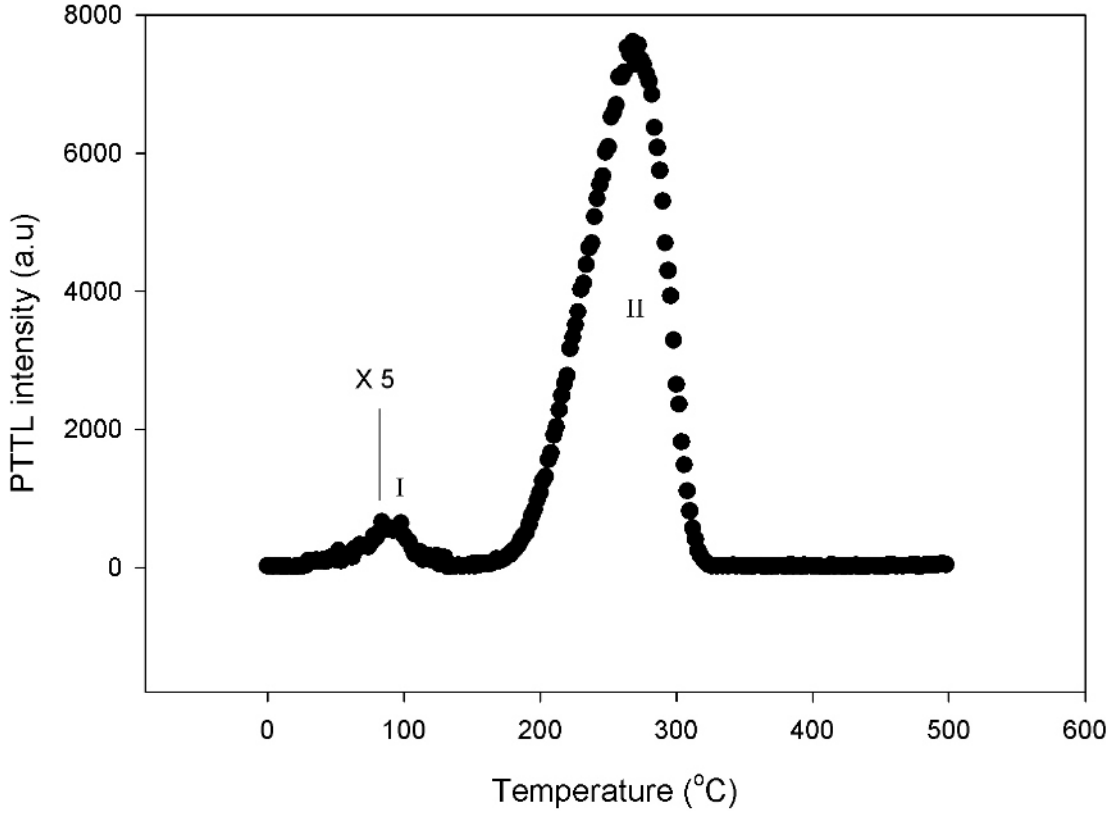

Figure 5.43: A glow curve after preheating to 390°C showing PTTL peaks I and II. Data for peak I has been scaled up for better clarity. No PTTL from peak III was observed.

2. In contrast, after preheating to 290°C and to 390°C, a slow PTTL decrease to half maxima intensity near 200 and 300 s were observed (figure 5.41 and 5.45 a).

The plot of PTTL intensity versus illumination time for peak II is shown in figure 5.46. The intensity of PTTL peak II goes through a peak with illumination for a sample illuminated at times from 0 to 600 s. Its maximum appeared at an illumination time of 60 s.

5.2.1.4 PTTL traps depopulated by preheating to 500°C

The pre-existing charges in traps associated with peaks I, II and III were emptied by preheating the sample to 500°C after an irradiation dose of 0.5 Gy. The PTTL signal was measured at a rate of $5^{o}\mathrm{C\,s^{-1}}$ after illumination time for 60 s.

Figure 5.47 shows the resulting glow curve where peak I appears at 94°C and peak II at 260°C. No PTTL signal was obtained from peak III. Figure 5.48 shows PTTL

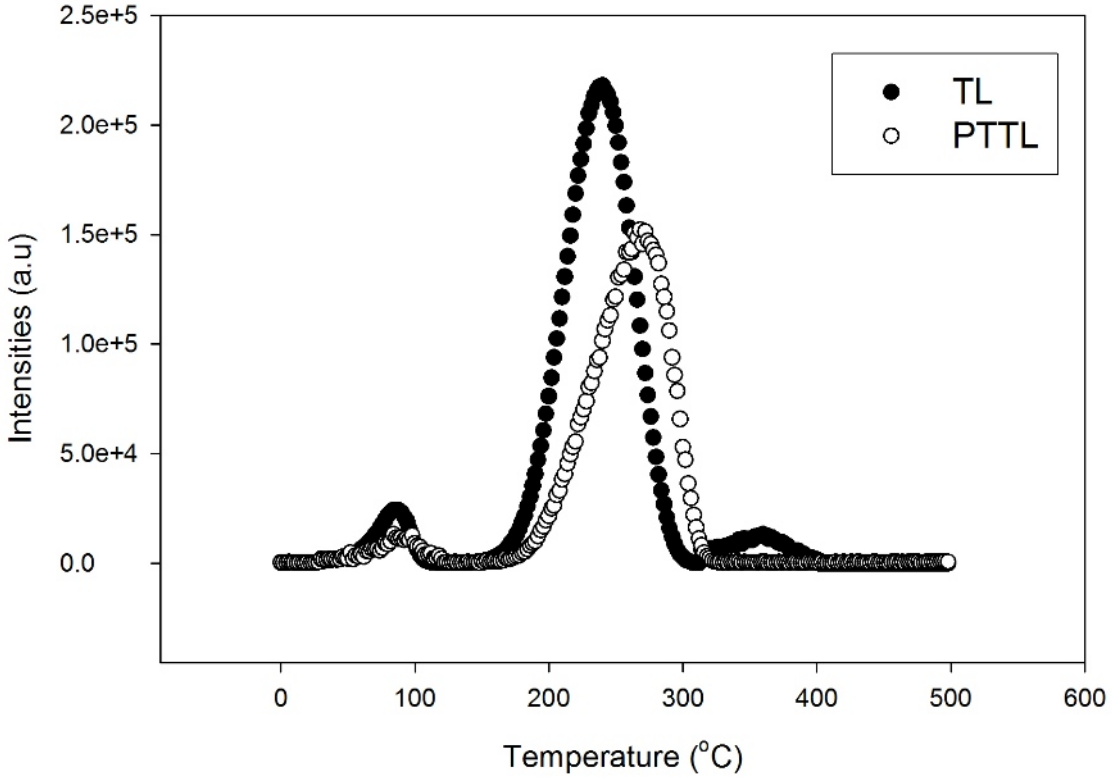

Figure 5.44: A comparison of a PTTL and a TL glow curves drawn in one figure. Only PTTL peaks I and II are regenerated after preheating to 390°C. Data for the PTTL curve has been scaled up for better clarity.

intensity against illumination time measured for peak I after preheating to 500°C. The PTTL plot has a maximum at an illumination time of 120 s. The PTTL was measured immediately after exposure to 470 nm blue light at times from 0 to 600 s. In contrast to PTTL from peak I following a preheat below 500°C (figures 5.39, 5.41 (a) and 5.45), figure 5.48 shows a slow increase followed by a much slower decrease. The different shapes of PTTL-time plots for peak I show that the PTTL from peak depends on preheating temperatures. For a preheating temperature low enough to remove peak I the trapping of electrons into the shallow trap responsible for peak I is very fast such that the intensity of the peak reaches its maximum at a shorter illumination time. However, the continuous illumination for long eventually evicts trapped electrons from the shallow trap and the intensity of the peak follows a rapid decrease. When the preheating temperature is higher enough, the slower increase of intensity of PTTL with illumination time from peak I is followed by a slower decrease.

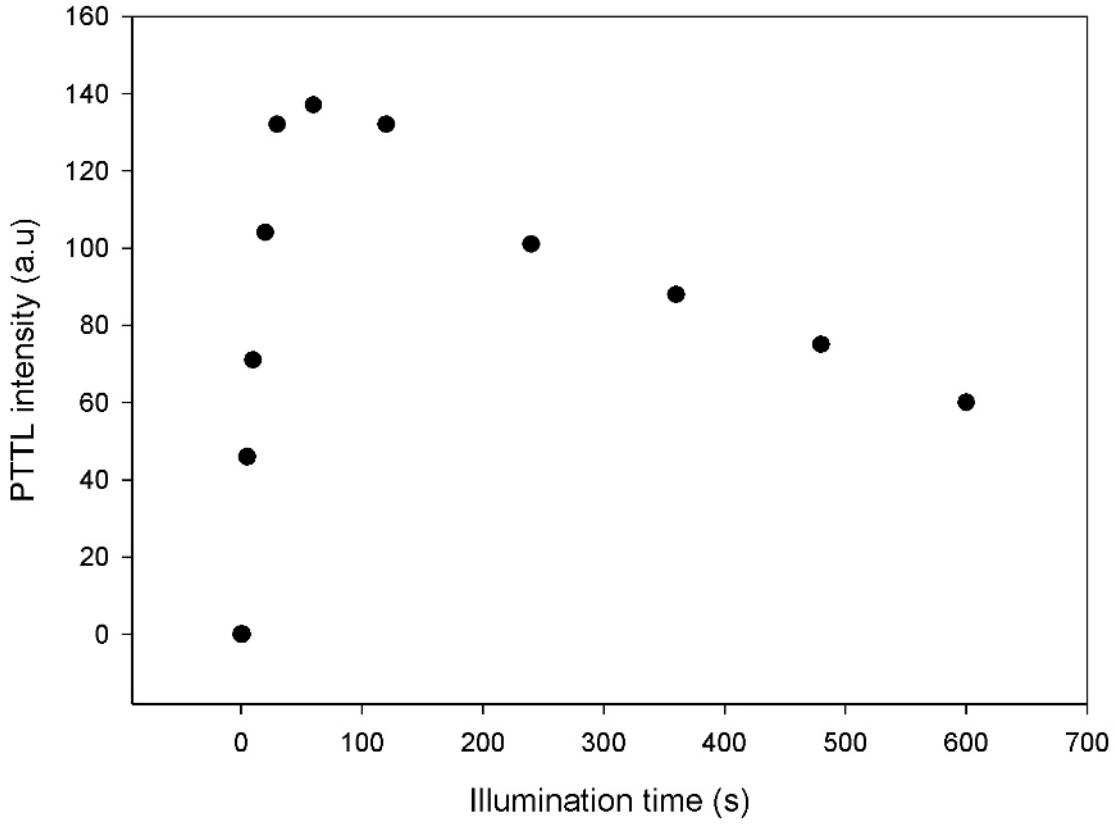

Figure 5.45: PTTL intensity versus illumination time for peak I in a sample preheated to 390°C. The maximum intensity of the peak was recorded for each illumination time between 0 and 600 s.

This variety of PTTL-time plots is associated with the PTTL sensitivity changes introduced by emptying deep electron traps at different preheating temperatures. Similar results were reported by Nikiforov et al. [26]. The TL sensitivity in α-$Al_2O_3 : C$ was explained by Yukihara et al. [37].

Figure 5.49 shows the PTTL intensity against illumination time for peak II following preheating to 500°C. The intensity is a monotonic function of illumination time from 0 up to a maximum at an illumination time of 80 s. The increase of PTTL signal to a maximum value is followed by a decrease. In contrast to the PTTL signals measured from peak II following preheating to 290°C (figure 5.41 b) and 390°C (figure 5.46), the PTTL after preheating to 500°C as shown in figure 5.49 decreases much slower to half maximum at about 350 s.

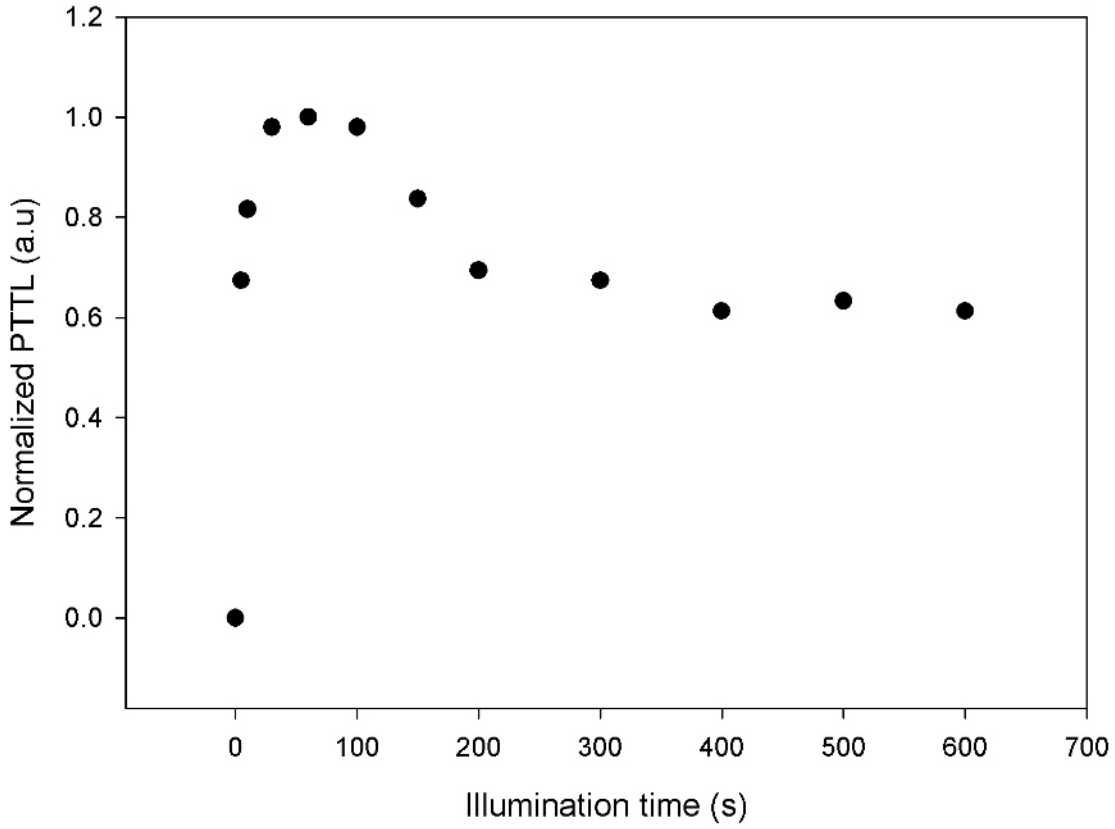

Figure 5.46: The dependence of PTTL on illumination time for peak II after preheating to 390°C. The intensity of PTTL was measured in a sample exposed to blue light for illumination times between 0 and 600 s.

5.2.1.5 PTTL from samples preheated to temperatures above 500°C

Preheating to temperature less than 500°C did not completely remove charge from deeper traps in sample A as can be seen from the observed PTTL signal for peaks I and II even after preheating to 500°C (figures 5.48 and 5.49). These deep traps responsible for peaks at temperatures higher than 500°C were previously reported [26, 37–40]. Some authors reported deep electron traps between 500 and 600°C [39]. Yukihara et al. [37] and Akselrod et al. [38] reported deep electrons traps that become unstable between 700 and 900°C. Figure 5.50 shows an example of a glow curve showing peaks I, II, III and the initial rise of peak V from the TL measured to 600°C at a heating rate of $0.4^{\circ}\mathrm{C\,s^{-1}}$ after a dose of 0.5 Gy. Peak IV is not well defined at a such dose of 0.5 Gy, however, increasing dose to 3 Gy for the same heating rate of $0.4^{\circ}\mathrm{C\,s^{-1}}$ it appears at 422°C (figure 5.22). The initial rise of peak V starting from 540°C is an indication

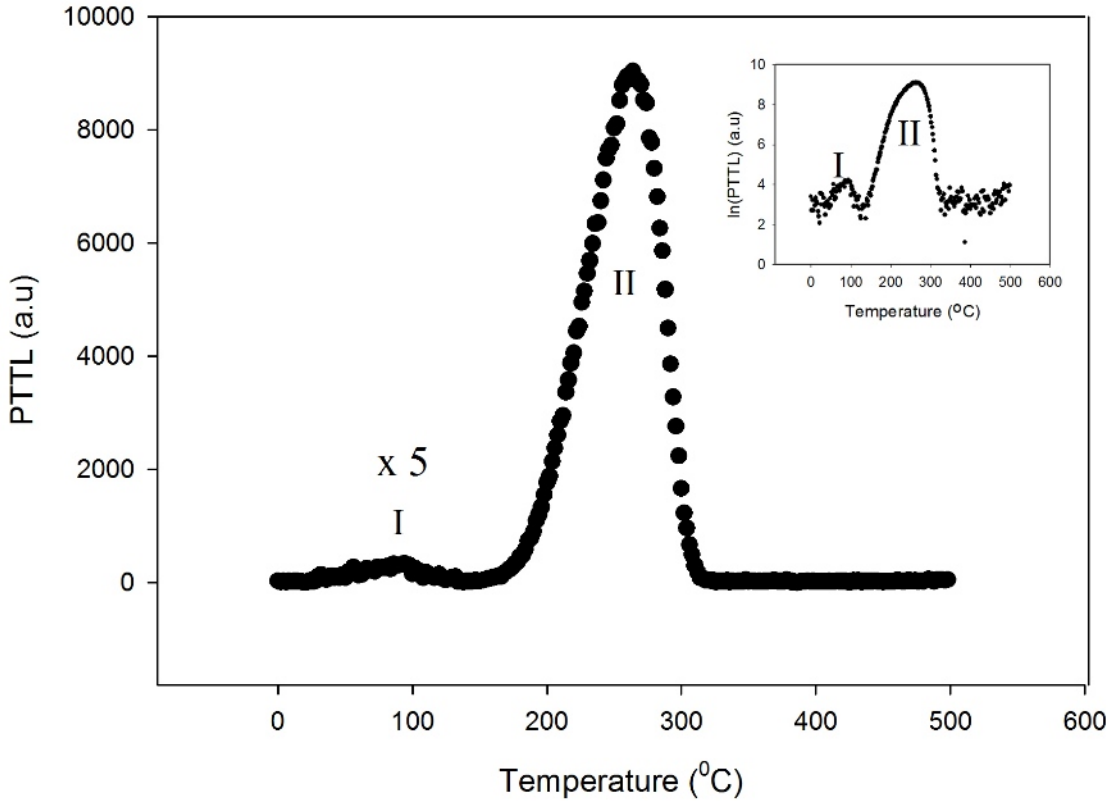

Figure 5.47: A PTTL glow curve from a sample pre-heated to 500°C. The PTTL signal at 94°C (peak I) and at 260°C (peak II) were measured after an illumination time of 60 s. The PTTL from peak I can be seen clearer when the PTTL signal is plotted on a log-scale (inset).

of the presence of a deep electron trap near 600°C which is emptied after preheating to above 600°C. A recent report by Nikiforov et al. [26] showed a peak visible at 550°C for a sample irradiated by a pulse electron beam.

A sample irradiated at 0.5 Gy was preheated to 600°C for 6 minutes in a furnace. The subsequent PTTL measurement following an illumination time of 60 s showed a signal for peak II. Therefore, because deep electron traps had not been emptied by preheating to 600°C for 6 minutes, we increased the time for the preheating from 6 to 15 minutes. Results of PTTL measurements are shown in figure 5.51.

5.2.1.6 PTTL from peak II for samples preheated at 600°C

Figure 5.51 (a) shows a glow peak from a sample preheated at 600°C for 6 minutes. This produced a PTTL peak at 222°C (peak II). A sample was irradiated to 0.5 Gy and heated at $5^{\circ}\mathrm{C\,s^{-1}}$ after an illumination time of 60 s. Figure 5.51 (b) shows a glow

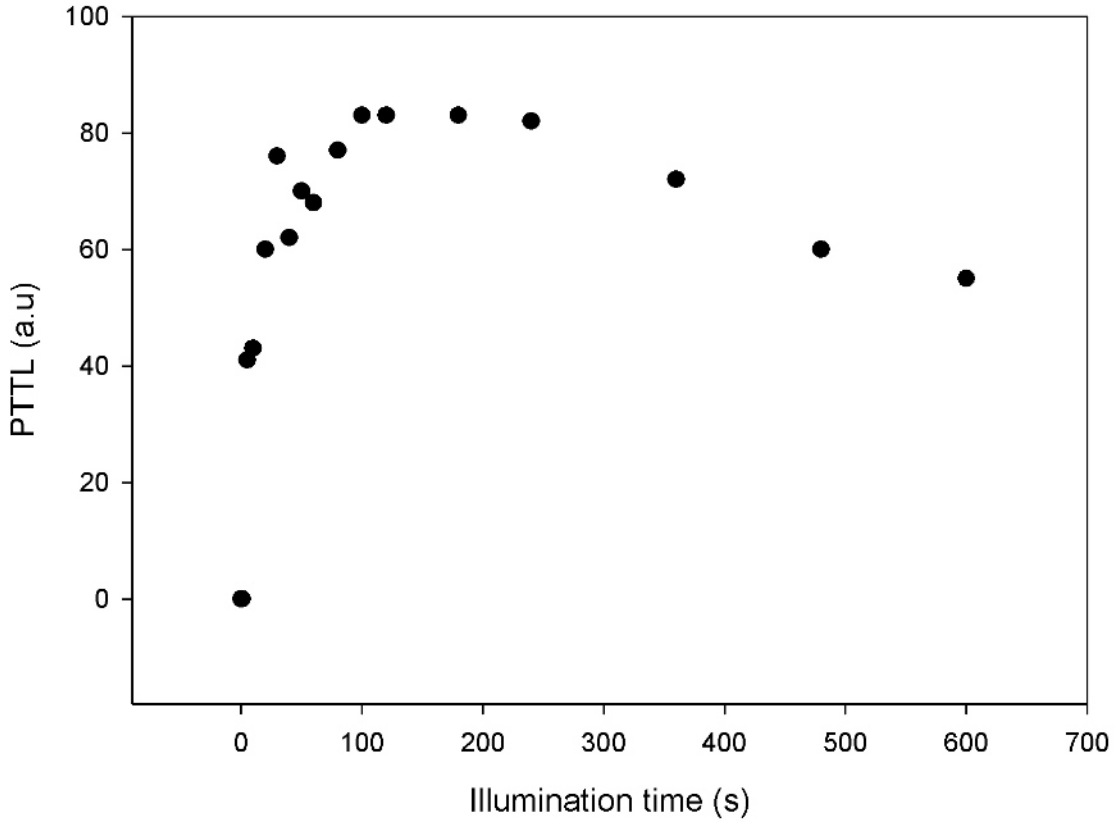

Figure 5.48: PTTL intensity versus illumination time for peak I following preheating to 500°C.

peak of PTTL from peak II of the same sample freshly dosed to 0.5 Gy and preheated to 600°C for 15 minutes. The peak position is 212°C for the same heating rate of $5^{o}C\,s^{-1}$ and at the same illumination time of 60 s. The intensity data of the PTTL peak produced in a sample pre-annealed to 600°C for 6 minutes (figure 5.51 a) does not have much scatter and is more intense than that produced in the same sample pre-annealed to 600°C for 15 minutes (figure 5.51 b).

Peak I was not regenerated under PTTL measured following preheating to 600°C. However, preheating for 6 minutes (figure 5.51 a) shows an increase of background signal which one may associate with a weak PTTL for peak I. It means that 6 minutes was not enough time for pre-annealing to empty completely the charges from deep traps responsible for peaks I and II. No peak III was observed under PTTL for samples pre-annealed at 600°C as also observed for other preheating to temperature under 600°C.

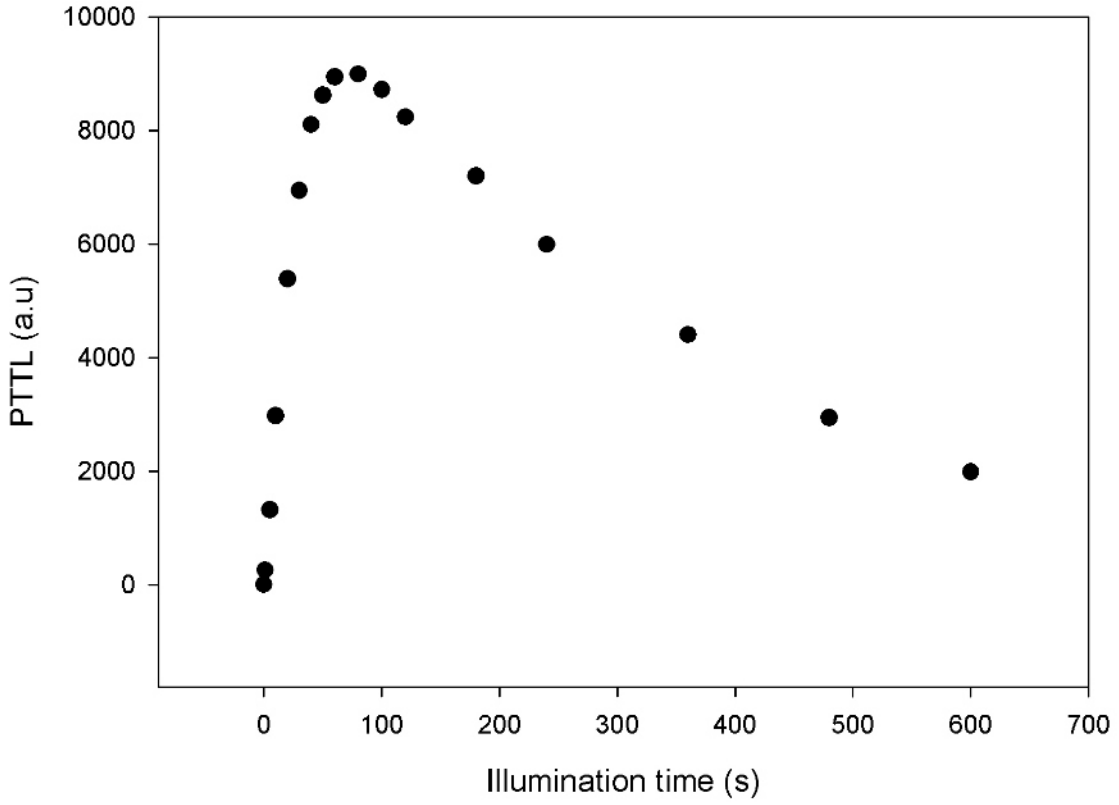

Figure 5.49: The PTTL intensity against illumination time for peak II after preheating to 500°C.

The maximum intensity of peak II was recorded for each illumination time between 0 and 600 s. The PTTL intensity versus illumination time for peak II is plotted for illumination times from 0 to 600 s. Figure 5.52 shows the dependence of PTTL intensity on illumination time for peak II for sample A preheated to 600°C for 6 minutes. The maximum intensity of PTTL is at an illumination time of 50 s. The decay part of the peak decreases much slower and did not reach its half-maximum at the end of illumination (600 s). Figure 5.53 shows the PTTL intensity against illumination time from peak II following preheating to 600°C for 15 minutes. The intensity increases to a maximum value at an illumination time of 240 s.

In contrast to the behaviour of the intensity of PTTL measured from peak II after pre-annealing to 600°C for 6 minutes (figure 5.52), the intensity measured following pre-annealing at 600°C for 15 minutes (figure 5.53) increases to saturation for longer illumination times. The saturation starts from the maximum intensity at an illumi-

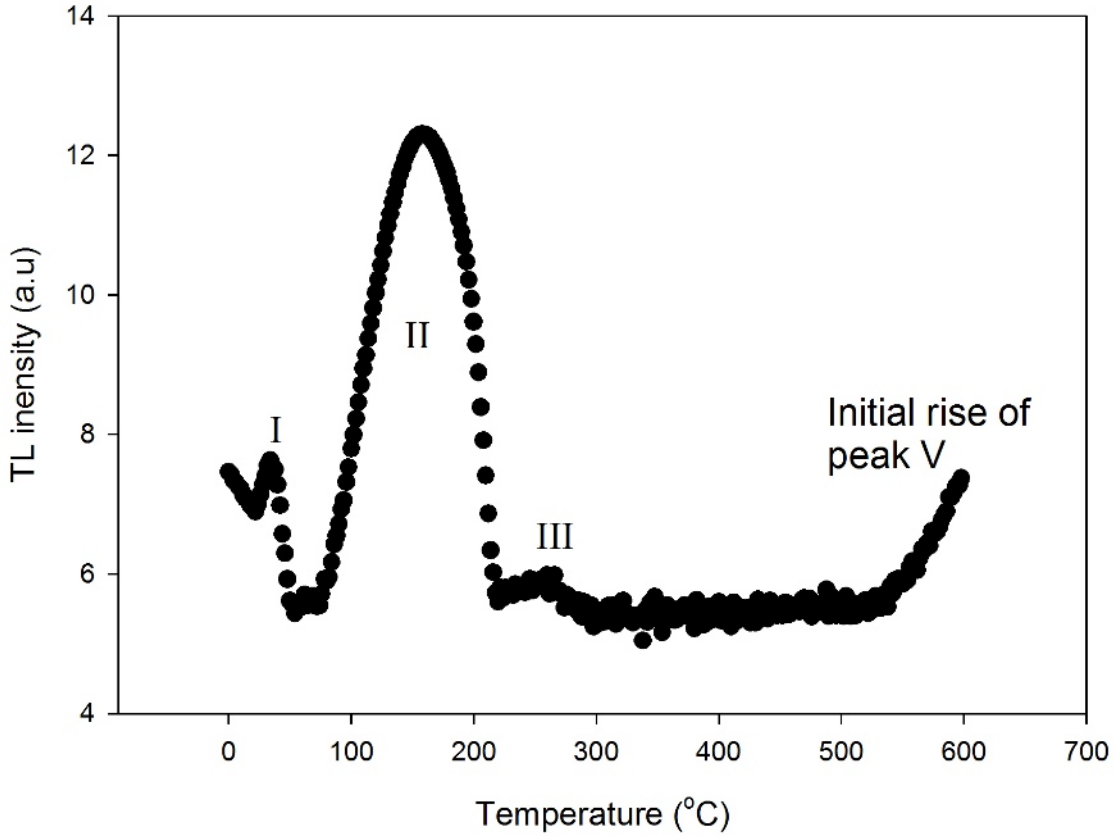

Figure 5.50: TL glow curve from α-$Al_2O_3 : C$ heated to 600°C using a heating rate of $0.4^{o}C\,s^{-1}$ at 0.5 Gy. The intensity is in logarithm scale for better clarity. An increase of intensity at the end of heating attests to the presence of another peak near 600°C, peak IV.

nation time of 240 s to the end of illumination time for 600 s used. The saturation can be interpreted as that at times corresponding to the maximum PTTL, transfer of charges from deep traps to the main trap responsible for peak II was at its maximum. Further illuminations did not release charge carriers from the main trap and the competition between centres might have been very weak so that there was no charge exchange between them. The possibility of an increase of PTTL intensity to a saturation for long illumination times was reported by Alexander and McKeever under certain assumptions on numerically solved rate equations describing PTTL [16].

5.2.1.7 The PTTL from peak II following preheating to 700°C

Figure 5.54 (a), a glow curve shows PTTL measured following pre-annealing to 700°C for 6 minutes after a dose of 0.5 Gy. The PTTL signal was measured in samples heated

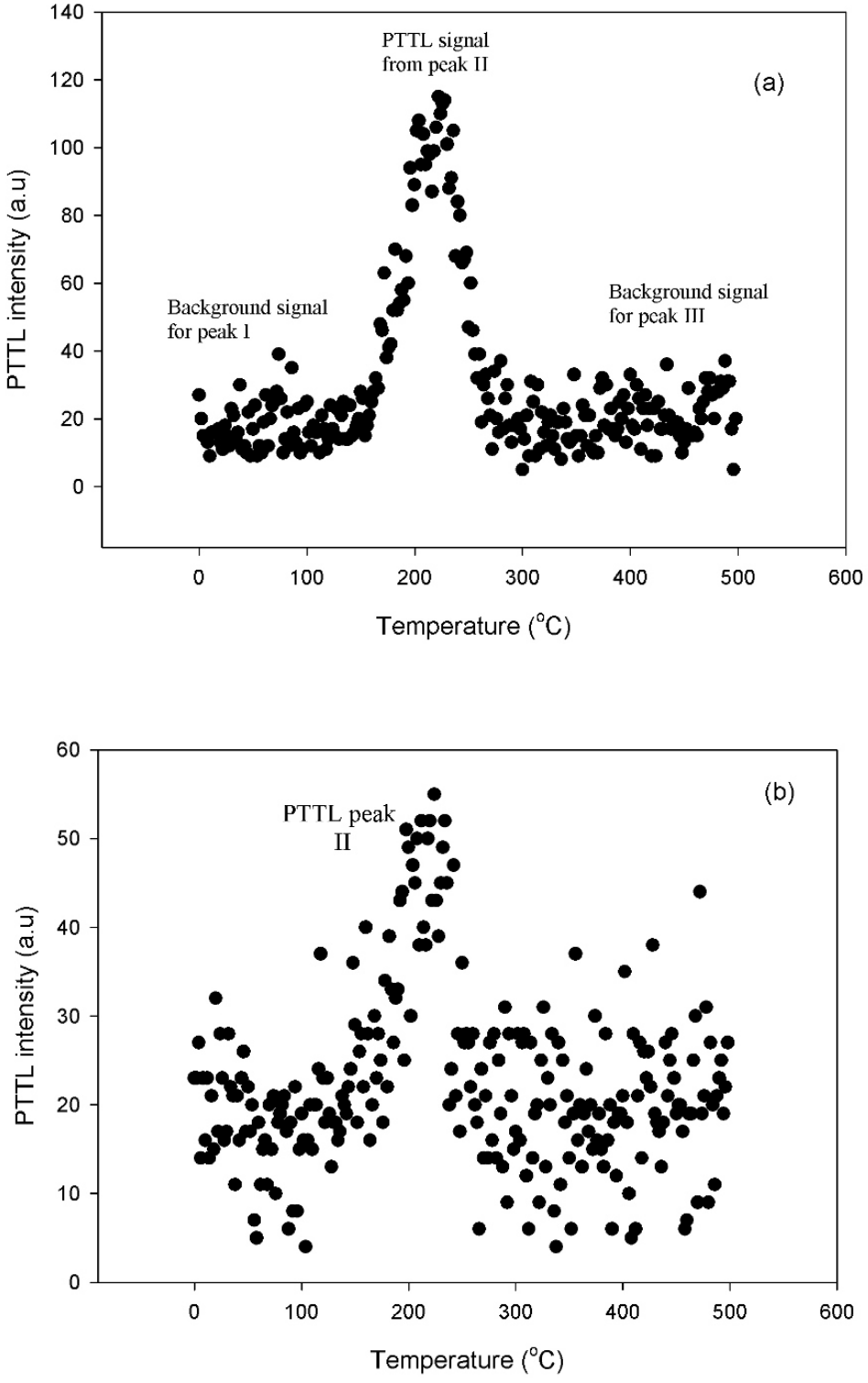

Figure 5.51: A glow-curve showing PTTL from peak II following pre-annealing to 600°C for 6 minutes and illumination for 60 s (a). The experiment was repeated by also pre-annealing to 600°C but for 15 minutes using the same sample A (b).

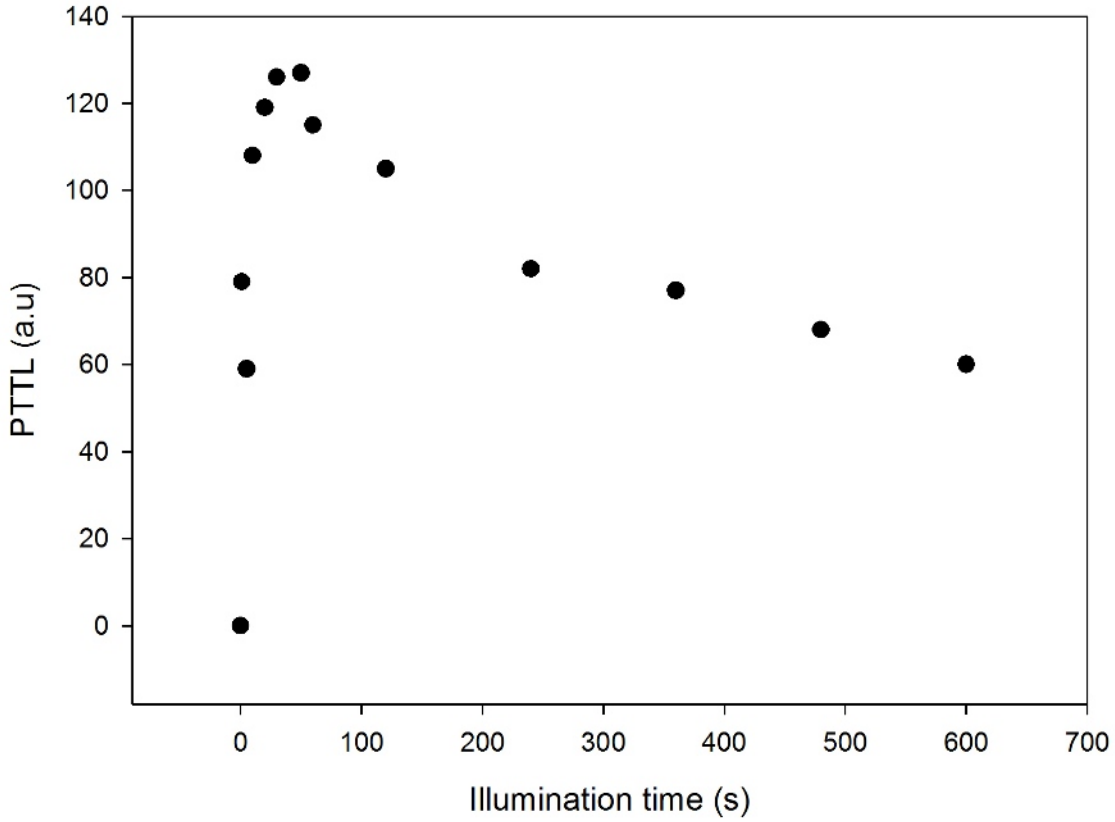

Figure 5.52: PTTL intensity versus illumination time for peak II after preheating to 600°C for 6 minutes. The sample was illuminated using 470 nm blue light for illumination times between 0 to 600 s.

at $5^{o}C\,s^{-1}$. The position of the peak was 212°C for an illumination time of 60 s. In figure 5.54 (b), the intensity of PTTL from peak II was measured in the same sample freshly dosed to 0.5y and preheated at the same heating rate of $5^{o}C\,s^{-1}$ but following pre-annealing to 700°C for 15 minutes. For an illumination time of 60 s, the position of the peak was 226°C. No PTTL was observed from peaks I and III.

Figure 5.55 (a) shows the integrated PTTL intensity versus illumination time for peak II from the sample pre-annealed at 700°C for 6 minutes. The heating rate of $5^{o}C\,s^{-1}$ and dose of 0.5 Gy were used in the measurements of the PTTL peak II after illumination times from 0 to 600 s. Its maximum intensity is at an illumination of 60 s. Similarly, figure 5.55 (b) shows the dependence of integrated PTTL signal on illumination time for peak II in the same sample but pre-annealed at 700°C for 15 minutes. The intensity of PTTL from peak II increases also to a maximum at an

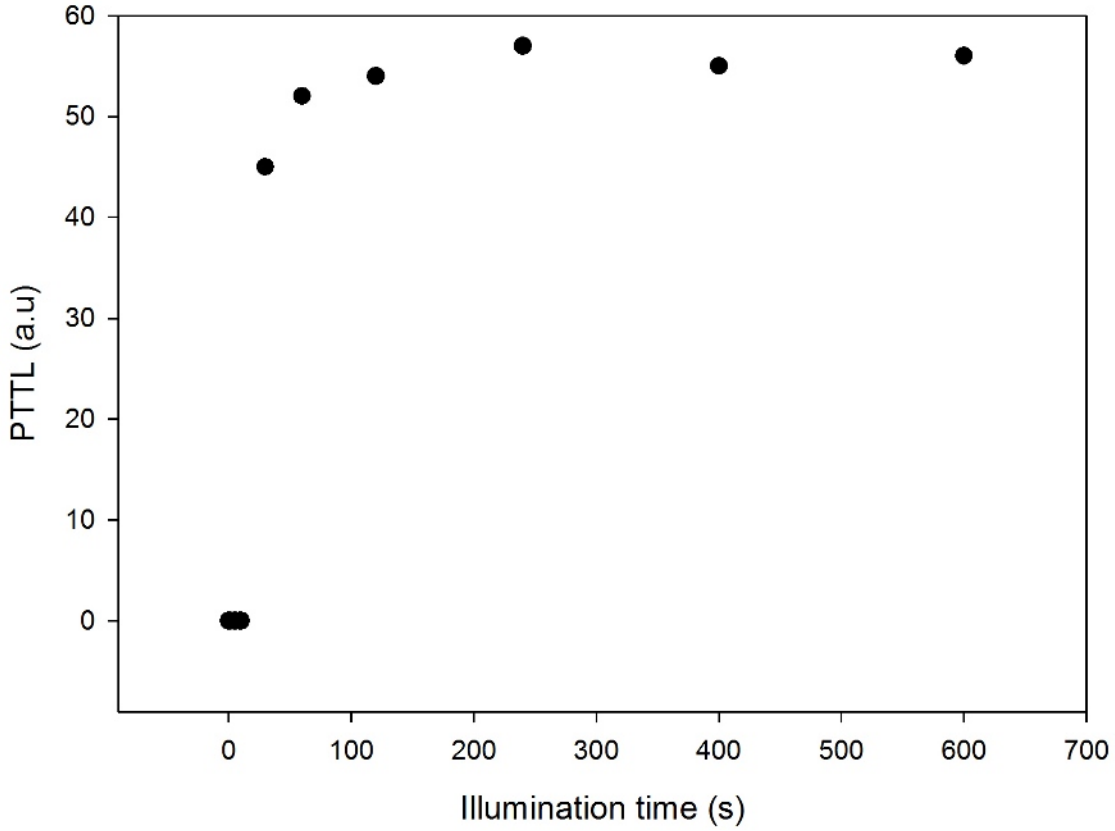

Figure 5.53: PTTL intensity versus illumination time for peak II following preheating to 600°C for 15 minutes.

illumination time of 60 s.

The observed PTTL from peak II in sample A after preheating to 700°C either for 6 minutes or for 15 minutes confirms that deep traps responsible for PTTL from peak II are thermally stable even for pre-annealing to 700°C. The PTTL feature of peak II observed in sample A does not seem to support the reported result [17] that the PTTL effect from peak II is removed after preheating to temperatures greater than 600°C.

5.2.1.8 PTTL signal from peak II after annealing at 800°C

Pre-annealing at 800°C for 6 minutes did not empty all deep traps responsible for PTTL of peak II. This is because we still observed PTTL signals which were distinguishable from background signals or blackbody radiation. An example of a PTTL glow curve measured after a dose of 0.5 Gy is shown in figure 5.56 (a). The position of the peak for PTTL peak II can be seen at 214°C using a heating rate of $5°C\,s^{-1}$ after an illumination

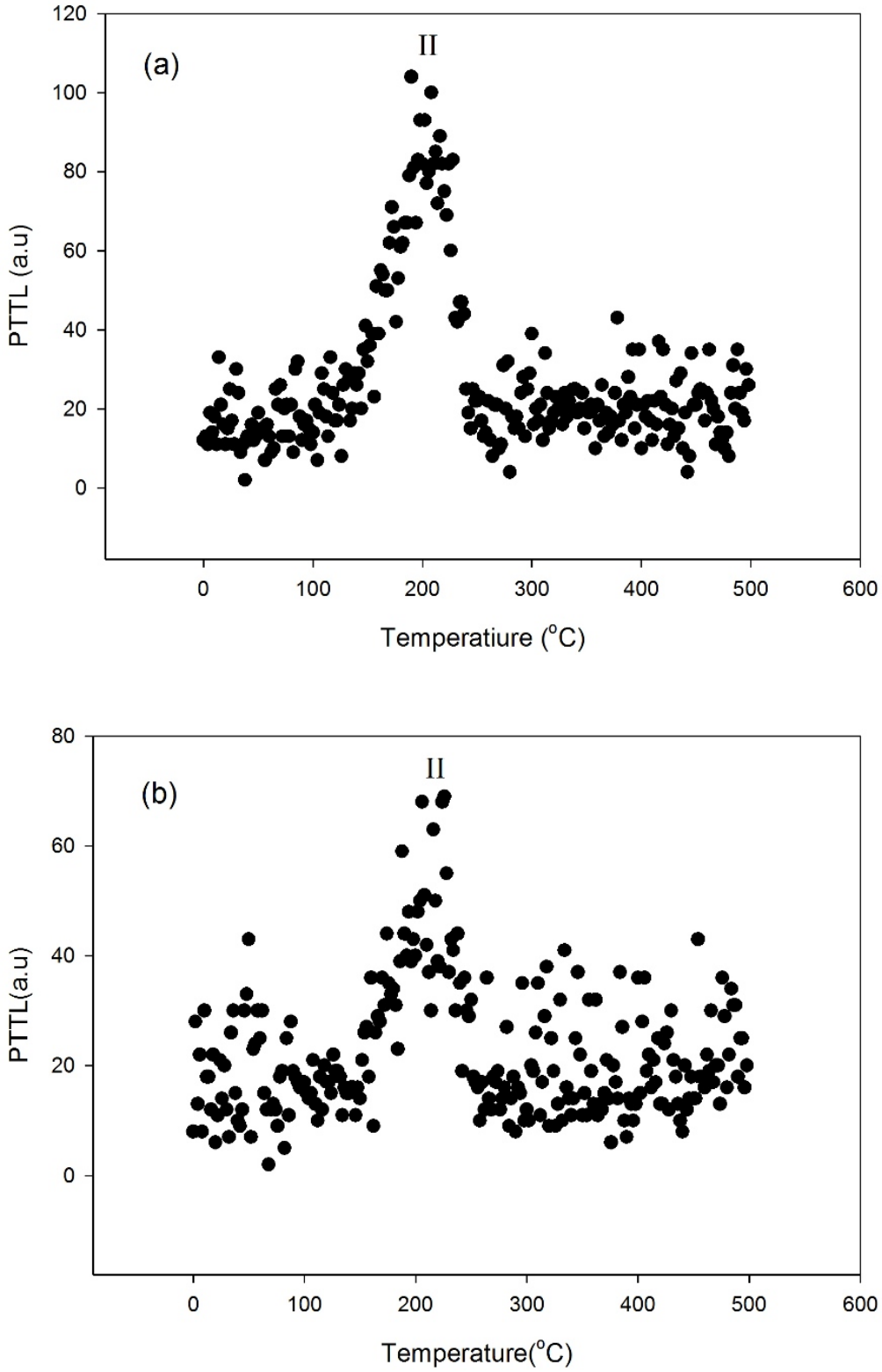

Figure 5.54: Glow curve showing PTTL from peak II in sample *A* pre-annealed at 700°C for 6 minutes (a). The measurement on PTTL intensity was repeated in the same sample freshly irradiated and following same pre-annealing to 700°C but for 15 minutes (b). An illumination time of 60 s was used in both cases.

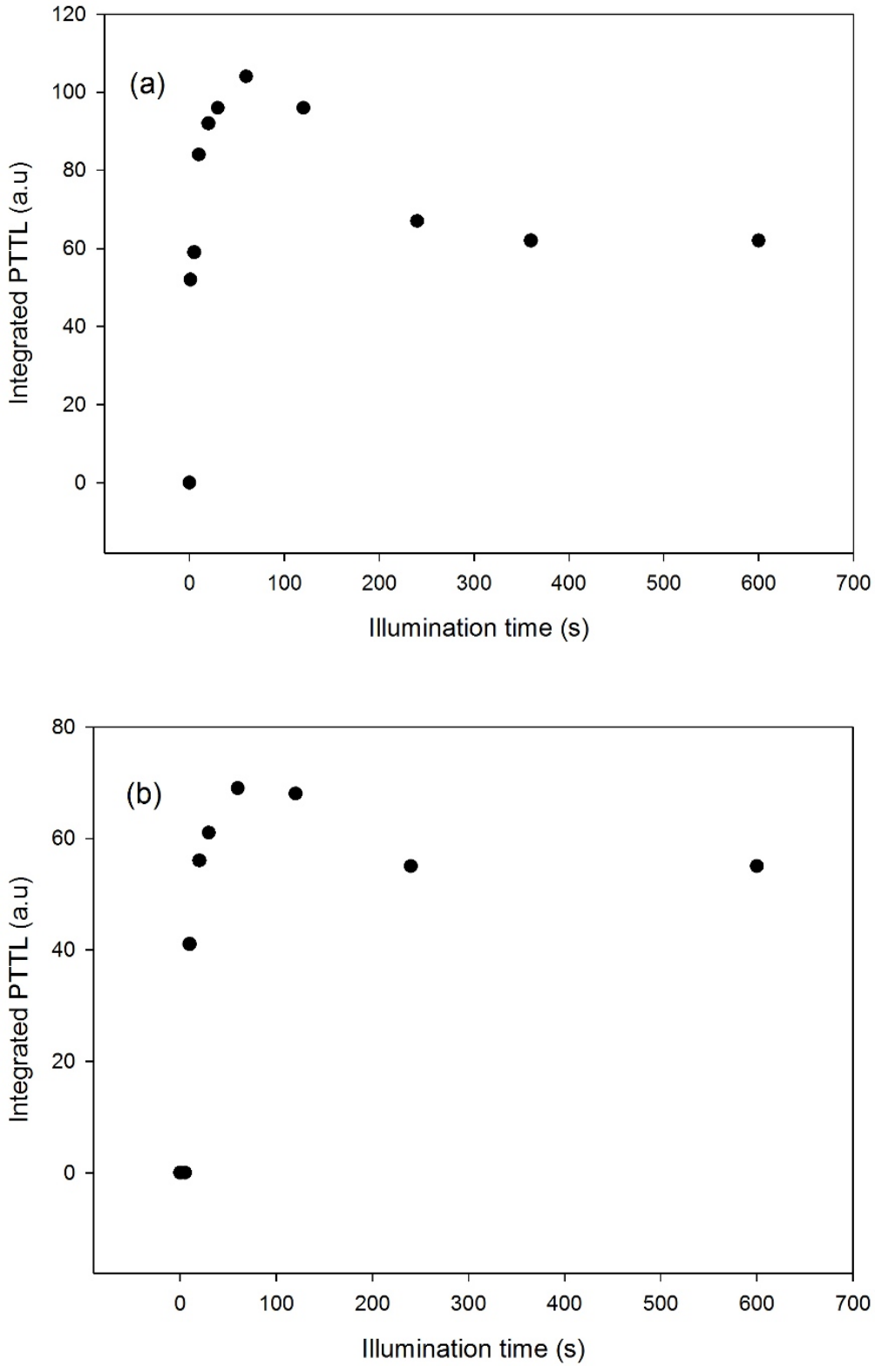

Figure 5.55: The integrated PTTL intensity against illumination time for peak II after pre-annealing to 700°C for 6 minutes (a). The PTTL experiment was repeated following the same pre-annealing to 700°C but changing the annealing time to 15 minutes (b).

time of 30 s. Figure 5.56 (b) shows the time dependence of the peak integral for PTTL intensity for peak II following preheating to 800°C for 6 minutes. The maximum peak integral of PTTL for peak II can be seen at an illumination time of 50 s when a dose of 0.5 Gy and a heating rate of $5^{o}\mathrm{C\,s^{-1}}$ were used.

In comparison, while PTTL measurements from a sample pre-annealed at 800°C for 6 minutes produced a PTTL signal for peak II (figure 5.56 a), pre-annealing at the same temperature of 800°C for 15 minutes did not produce any PTTL. This shows that for samples annealed beyond 700°C, 15 minutes was sufficient to empty deep traps responsible for PTTL. The existence of PTTL from peak II measured in sample *A* pre-annealed at 800°C for 6 minutes agrees with previous reports [37, 38] which confirmed the presence of deep electron traps with delocalization temperatures between 800 and 900°C. However, the PTTL measured following the same pre-annealing to 800°C but increasing the time for anneal to 15 minutes did not show any PTTL. This may be due to a negligible influence of these deep traps on peak II and hence the possibility of producing PTTL was not possible or may be the deep electron traps responsible for PTTL from peak II are delocalized with temperatures under 800°C which can be emptied by pre-annealing to 800°C for 15 minutes.

5.2.1.9 Kinetic analysis of PTTL glow peak I

The kinetic analysis of the PTTL from peak I was done in order to calculate the activation energy and frequency factor of the electron trap responsible for the PTTL peak I. The activation energy E was calculated for a PTTL peak measured following preheating to 100°C to remove peak I. The PTTL measurements used a heating rate of $5^{o}\mathrm{C\,s^{-1}}$ after an illumination time 60 s. The sample was dosed to 0.5 Gy. Four methods were used to calculate the activation energy. These are the initial rise, the peak shape, whole curve and variable heating rate methods.

(a) Initial rise method

Figure 5.57 shows a plot of $\ln(PTTL)$ against $1/kT$ as a means to calculate E using the initial rise method. The value of E and frequency factor s were computed from the slope

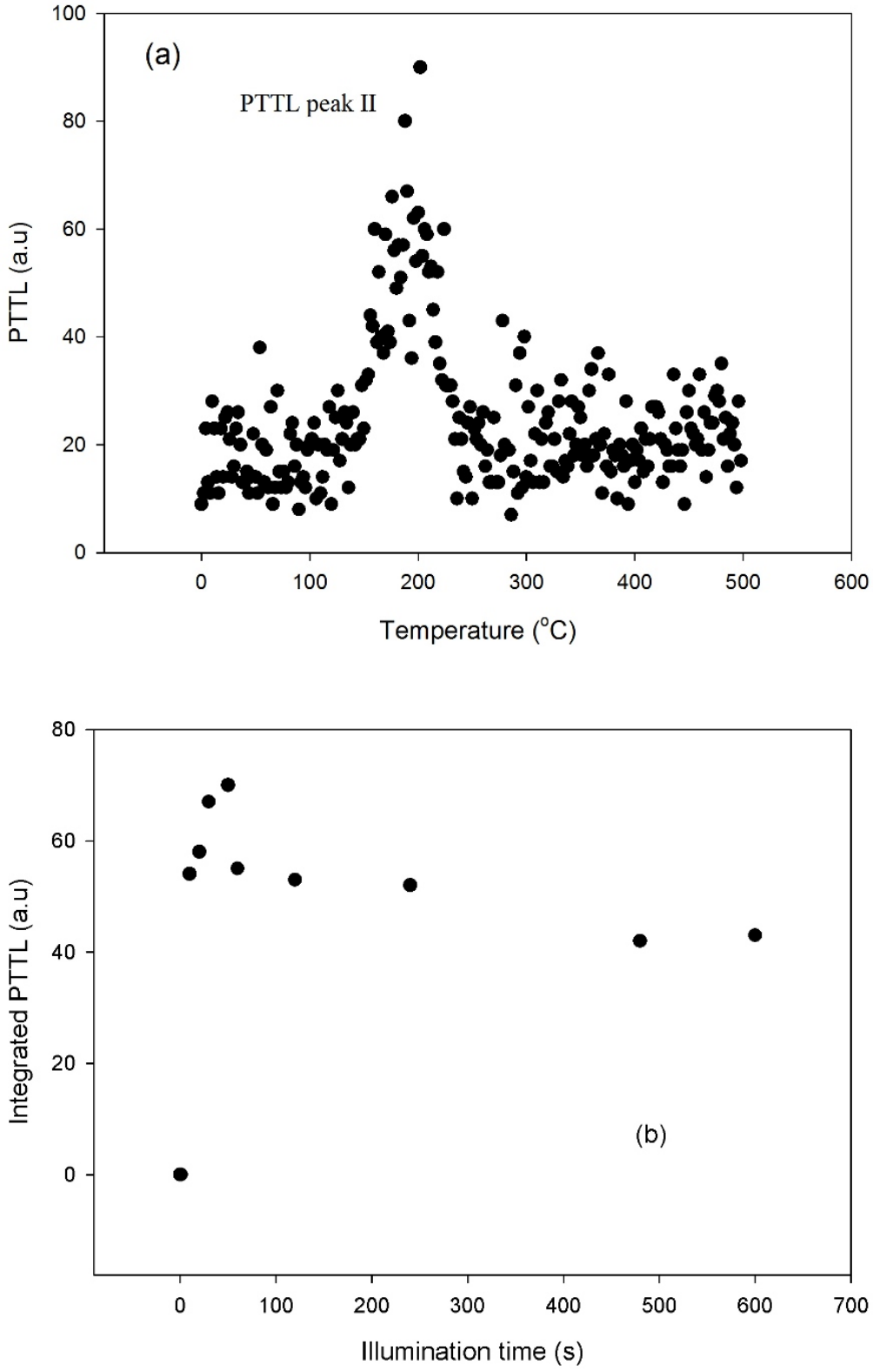

Figure 5.56: PTTL from peak II for samples annealed at 800°C for 6 minutes. A glow curve measured from PTTL for peak II (a) and the illumination time dependence of the PTTL intensity from peak II (b).

of straight line and y-intercept respectively. Results (figure 5.57) are $\mathrm{E} = 0.60 \pm 0.04\,\mathrm{eV}$ and $s = 1 \times 10^{12}\,\mathrm{s}^{-1}$. These E and s values calculated from PTTL for peak I are consistent with the $\mathrm{E} = 0.64 \pm 0.02\,\mathrm{eV}$ and $s = 5.5 \times 10^{13}\,\mathrm{s}^{-1}$ evaluated from normal TL (not PTTL) for peak I.

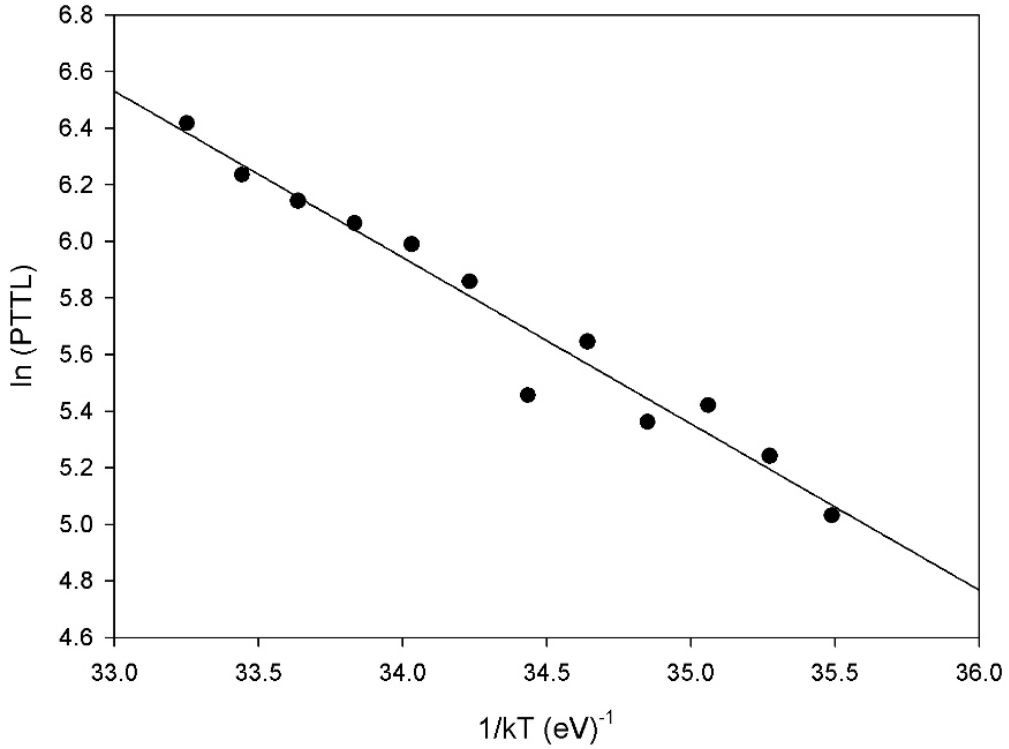

Figure 5.57: The dependence of $\ln(I)$ on $1/kT$ using the initial rise method. The activation energy found is for the electron trap responsible for the PTTL from peak I following preheating to 100°C. An illumination time of 60 s was used.

(b) Whole curve method

Equation 2.32 for general order kinetics used in the whole curve method leads to a plot of $\ln(PTTL/n^b)$ against $1/kT$. Figure 5.58 shows several options for order kinetics b between 0.9 and 1.2. A heating rate of $5^{\circ}\mathrm{C\,s}^{-1}$ was used after a beta dose of 0.5 Gy. The best fit is at $b = 1$ which suggests that first order kinetics apply. The slope of a straight line from the figure yielded the activation energy of $\mathrm{E} = 0.72 \pm 0.01\,\mathrm{eV}$. The y-intercept yielded a pre-exponential frequency factor for first order $s = 1.6 \times 10^{10}\,\mathrm{s}^{-1}$. Here too, the E and s values calculated from PTTL are consistent with those found from TL for peak I.

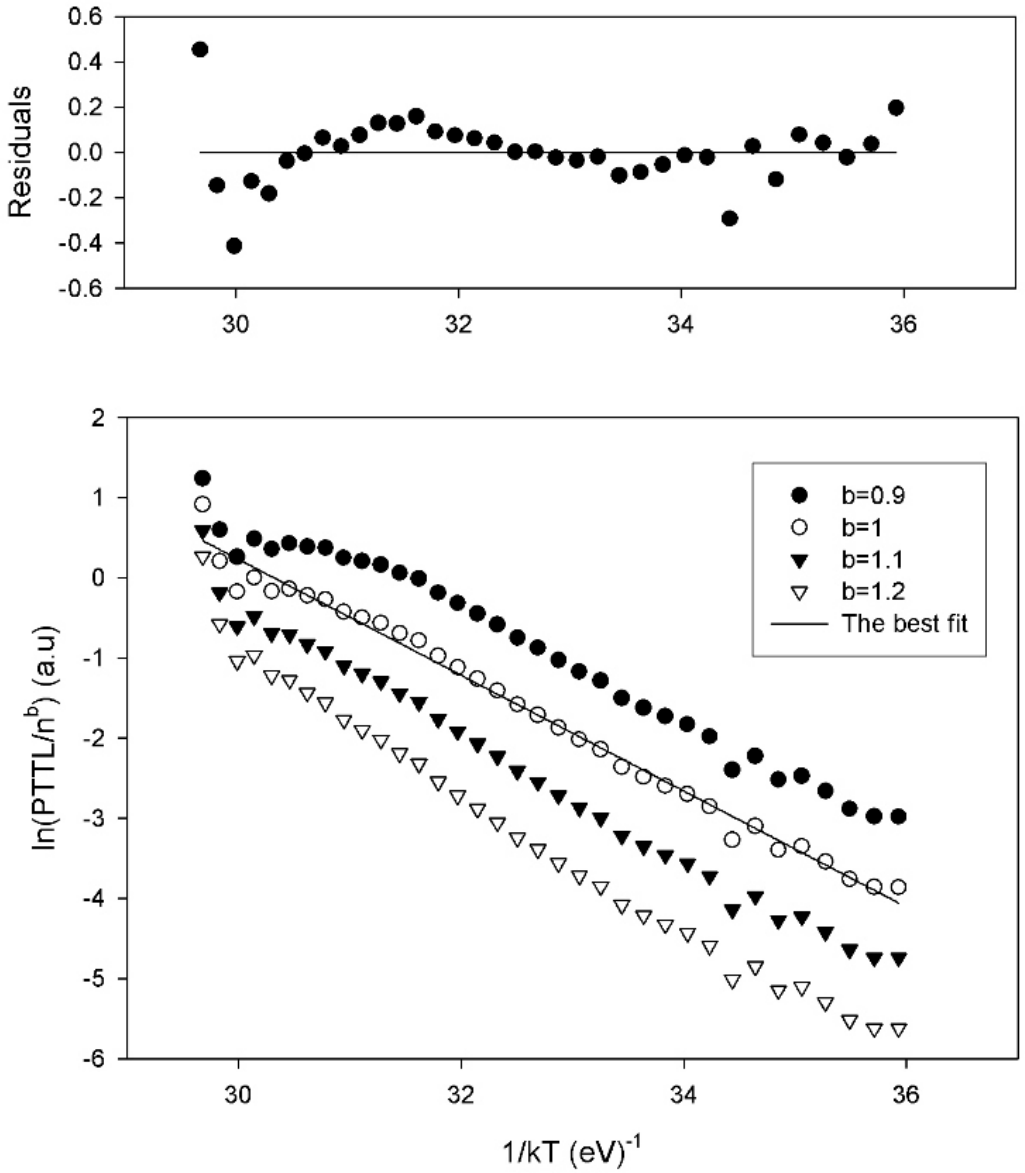

Figure 5.58: The dependence of $\ln(I/n^b)$ on $1/kT$ from PTTL peak I. The heating rate was $5^{\circ}\mathrm{C\,s^{-1}}$ and dose, 0.5 Gy. The best fit (solid line through the PTTL data for $b = 1$) was chosen on the basis of residuals being close to zero.

(c) The variable heating rate method

Figure 5.59 shows the dependence of $\ln(T_M^2/\beta)$ on $1/k_M T$ for PTTL from peak I in sample preheated at 100°C after a dose of 0.5 Gy. $\mathrm{E} = 0.5 \pm 0.02\,\mathrm{eV}$ and $s = 1 \times 10^7\,\mathrm{s^{-1}}$ were evaluated from the slope and intercept $\ln(E/sk)$ respectively of the plot. Equation 2.27 was also used to calculate the activation energy for various pairs of temperature corresponding to maximum PTTL intensity, T_{M1} and T_{M2}, giving an average activation energy of $\mathrm{E} = 0.7\,\mathrm{eV}$.

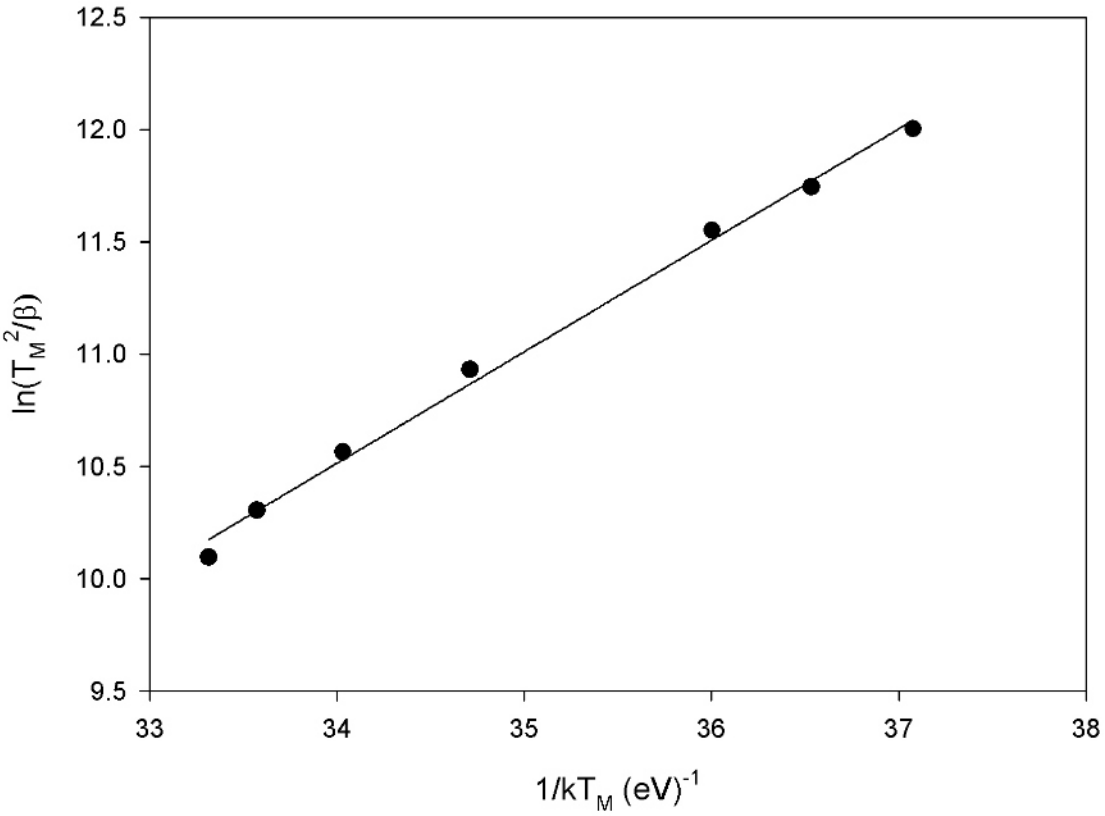

Figure 5.59: A plot of $\ln(T_M^2/\beta)$ against $1/k_M T$ for PTTL from peak I. The heating rates were from 0.6 to 5°C s^{-1} and the beta dose, 0.5 Gy.

Figure 5.60 shows the dependence of the peak position T_M on the heating rate β. As can be seen, an increase of the heating rate shifts the position of the peak to higher temperature.

(d) Peak shape methods

The position T_M of the PTTL for peak I used in the peak shape methods was 92°C. The full width was $\omega = 30^o$C and the geometrical factor was $\mu_g = 0.37 \pm 0.04$. The activation energy from the peak shape method was calculated using equation 2.14. Table 5.12 compares results from the peak shape method with the activation energy evaluated using other methods. Results shown in the table are consistent between methods. There is also consistency between parameters evaluated from TL peak I and from PTTL peak I. This confirms that the peak I reproduced under PTTL is the same as the original TL peak I. This means that the same emptied shallow trap associated with peak I following preheating to 100°C was filled by charges due to the optical

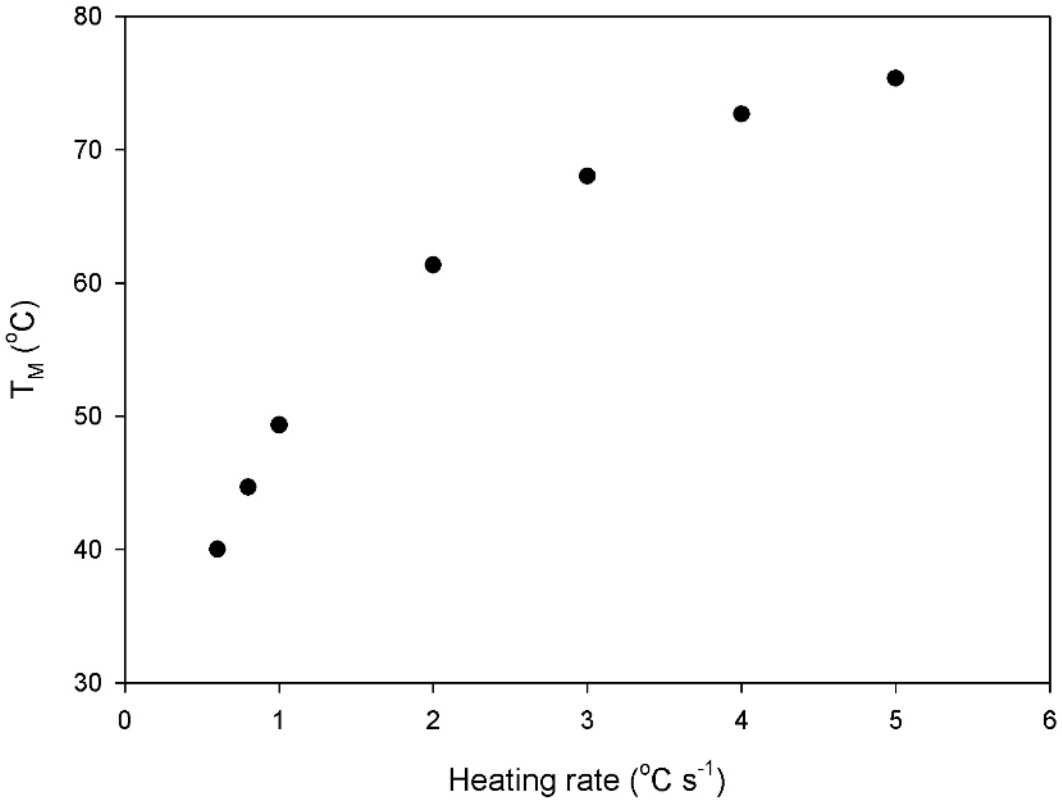

Figure 5.60: The peak position T_M versus heating rate. As can be seen, the peak shifts to higher temperature with increase of the heating rate from 0.4 up to 4°C s^{-1}. A beta dose of 0.5 Gy was used in the measurements.

stimulation of electrons from deeper traps to produce PTTL for peak I.

Table 5.12: Activation energies of PTTL and normal TL glow peaks for peak I from initial rise, peak shape in its three forms, whole curve and variable heating rate methods.

Method	TL E (eV)	PTTL E (eV)
Initial rise	0.64±0.02	0.60±0.04
Chen's E_ω	0.72±0.17	0.70±0.16
Chen's E_δ	0.62±0.36	0.64±0.32
Chen's E_τ	0.76±0.09	0.74±0.09
Whole curve	0.81±0.01	0.72±0.01
Variable heating rate	0.78±0.04	0.70±0.02

5.2.1.10 Summary

The phototransferred thermoluminescence technique has been used to investigate the existence of deep traps and their role in thermoluminescence from α-Al_2O_3 : C. A group

of unannealed samples labelled "sample A" were used. Experiments showed that peak I is reproduced under phototransfer after preheating from 100°C up to 500°C. Peak II is reproduced as a PTTL peak until the sample is annealed at 800°C for 6 minutes. Preheating to 800°C for 15 minutes from sample A irradiated to 0.5 Gy removed PTTL signal for all peaks. No PTTL was observed from peak III for all preheating temperatures from 100 to 900°C. However, the study of the time dependence of TL for peak III following the preheating to remove peak II showed that:

1. Peak III is a competitor trap for electrons transferred to the shallow electron traps responsible for peaks I and II.

2. For long illumination times, peak III loses a part of its trapped electrons to the shallower traps, that is, peak III acts as a donor trap.

The intensity of PTTL changes through a peak as a function of illumination time. The intensity of the PTTL peak for peaks I and II decreases from its maximum slowly as the preheating temperature is increased. Also, the increasing part of the PTTL intensity-time graph for peak I after preheating at higher temperatures has much scatter in data points.

The activation energy of the PTTL glow peak following preheating to 100^{o}C after an illumination time of 60 s was about $\mathrm{E} = 0.7\,\mathrm{eV}$. This value of activation energy of the PTTL for peak I was found to be consistent with the value calculated for its normal TL.

5.2.2 The effect of annealing on PTTL intensity from secondary glow peaks in α-$Al_2O_3 : C$

A glow curve from α-$Al_2O_3 : C$ comprises three glow peaks including the main (peak II) of high intensity and the two secondary peaks of low intensity (peak I and peak III). PTTL from the peaks was reported in subsection 5.2.1 in an unannealed group of samples, sample A. Experimental results for PTTL in sample A showed that peaks I and II are reproduced under phototransfer. No PTTL was observed from peak III.

However, further measurements of PTTL from sample A annealed at 900°C for 15 minutes in between measurements did not show any PTTL from peak I at a dose of 0.5 Gy. The same heating rate of $5^{\circ}\mathrm{C\,s^{-1}}$ and illumination times from 0 up to 600 s were used. This implies that deep traps responsible for PTTL from peak I are emptied following annealing to 900°C for 15 minutes and are not filled after an irradiation dose of only 0.5 Gy. To study the effect of annealing on PTTL from peak I we planned two tests:

(a) *Test 1: The assessment for the effect of annealing on PTTL from secondary peaks.* New PTTL measurements from peak I were done using two fresh samples, sample A_1 and sample B. Sample A_1 (not annealed to 900°C before use like sample A) was used to check if the characteristics of the PTTL from peak I observed in sample A at the end of PTTL measurement can vary from sample to sample. Sample B was annealed at 900°C for 15 minutes at the start and in between measurements.

(b) *Test 2: Test of the dose effect on PTTL from secondary peaks.* The effect of dose on PTTL from peak I was studied from samples A, A_1 and B after annealing all of them to 900°C for 15 minutes. The results from the PTTL measurements for peak I were compared at various doses from 0.5 to 5 Gy in each sample and between samples.

We proceeded to produce PTTL from peak I as follows. Electron traps were filled by an irradiation dose of 0.5 Gy. Shallow traps were emptied by preheating to different temperatures from 100°C to 900°C in sample A, A_1 and B. Samples were subsequently illuminated by 470 nm blue-LED light to transfer charges from deep trap to the pre-existing shallow traps. The PTTL was measured at a heating rate of $5^{\circ}\mathrm{C\,s^{-1}}$ after illumination times from 0 to 600 s.

5.2.2.1 PTTL characteristics in sample A_1

Sample A_1 was used for PTTL measured from peak I and was not annealed at 900°C for 15 minutes at the start of measurements. The effect of PTTL on peak I from the two unannealed samples A and A_1 are compared and then they will be compared to an annealed sample B later. Figure 5.61 shows a glow curve from sample A_1. A TL glow

curve from sample A_1 showed three peaks; at 56°C (peak I), at 180°C (peak II) and at 298°C (peak III) when a heating rate of $5^{\circ}\mathrm{C\,s^{-1}}$ and a dose of 0.5 Gy were used.

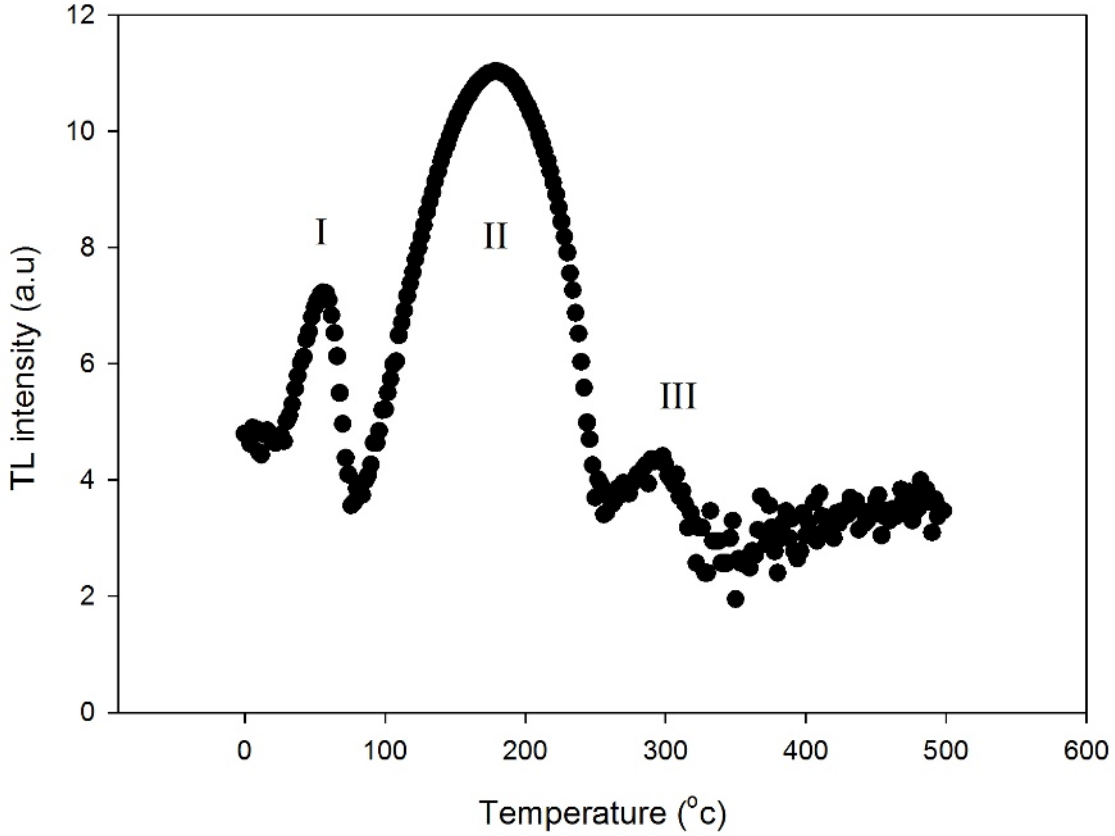

Figure 5.61: The TL glow curve of sample A_1 showing peaks I, II and III. y-axis is in a logarithmic scale in order to see clearer peaks I and III.

5.2.2.2 PTTL from peak I in sample A_1 after preheating to 80°C

Figure 5.62 (a) shows a PTTL peak measured from sample A_1 following preheating to 80°C. Preheating to 80°C was done to empty the shallow trap responsible for peak I after a dose of 0.5 Gy. The sample was heated at a heating rate of $5^{\circ}\mathrm{C\,s^{-1}}$ after an illumination time of 10 s. The PTTL peak I is reproduced at 52°C for an illumination time of 10 s. Figure 5.62 (b) shows The PTTL intensity against illumination time for peak I from sample A_1 dosed to 0.5 Gy. The PTTL signal was measured at a heating rate of $5^{\circ}\mathrm{C\,s^{-1}}$ after various illumination times from 0 to 60 s. The PTTL intensity goes through a peak with time. The peak has a maximum intensity at an illumination

time of 15 s.

Figure 5.63 shows a glow curve following preheating to 80°C before illumination time for 300 s. The figure shows that for long times of light exposure, traps responsible for peaks I, II and III were significantly depleted and no PTTL is observed at an illumination time of 300 s. The PTTL intensity measured from peak I in sample A_1 preheated to 80°C decreased with illumination time to zero after an illumination time of 300 s. This decrease of the PTTL signal is unlike the decrease to a steady value in the intensity of the PTTL from peak I in sample A following preheating to temperatures from 290 to 500°C (figures 5.41 (a), 5.45 and 5.48). The removal of all signal in sample A_1 for the PTTL measured from peak I following preheating to 80°C after long illumination times from 300 s and above can have different causes. One of the causes can be explained by a strong electron-hole recombination at an F-centre and negligible electron-retrapping in the shallow and deep traps for long illumination times. This means that the possibility of trapping electrons by optical transfer from deep electron traps to shallow electron traps may have dominated by removal of electrons to recombine with holes leading to OSL, inset of figure 5.63. At the end of illumination, electron traps responsible for peaks I, II and III are almost unfilled. Further heating to 500°C after long illumination times will then not produce any luminescence.

5.2.2.3 PTTL intensity from peak II in sample A_1 after preheating to 320°C

Traps corresponding to peaks I, II and III were emptied by preheating sample A_1 to 320°C. Unlike the PTTL intensity for peak II in sample A, where peaks I and II were regenerated under PTTL after preheating to 390°C that removed peaks I, II and III (figures, 5.45 and 5.46), only peak II was reproduced under PTTL after illumination times from 0 to 600 s in sample A_1. Figure 5.64 shows the dependence of PTTL intensity on illumination time for peak II after preheating to 320°C. The PTTL intensity goes through a peak in time with a maximum at an illumination time of 80 s when heating was done at $5^{\circ}\mathrm{C\,s^{-1}}$ after a dose of 0.5 Gy.

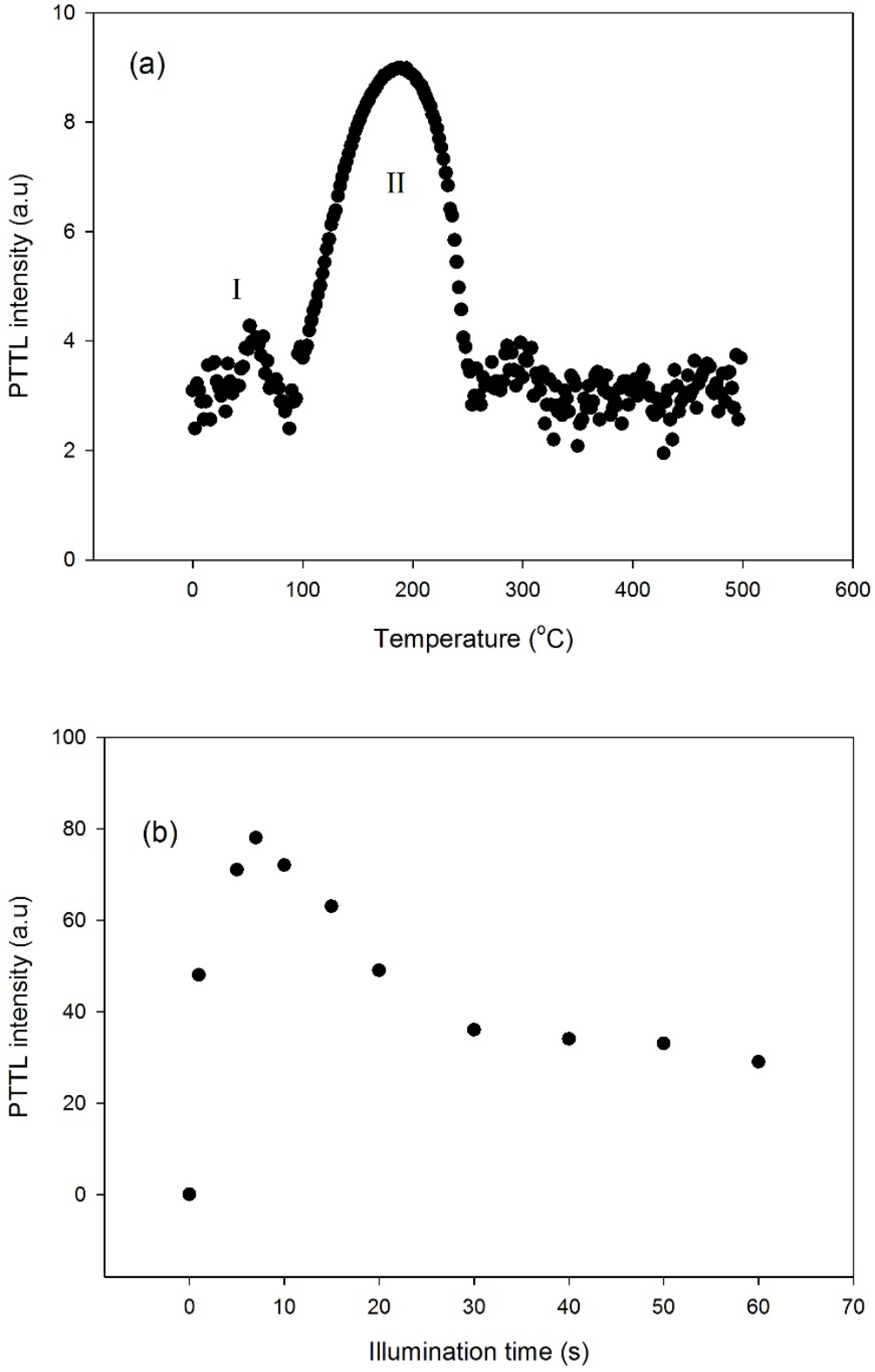

Figure 5.62: Glow curve showing PTTL peak I after an illumination time of 10 s (a) and illumination time dependence of PTTL for peak I in sample $A1$ (b). The intensity of PTTL was measured following preheating to 80°C at a heating rate of $5^{\circ}\mathrm{C\,s^{-1}}$ and a dose of 0.5 Gy. y-axis is in a logarithmic scale for visual clarity of peak I.

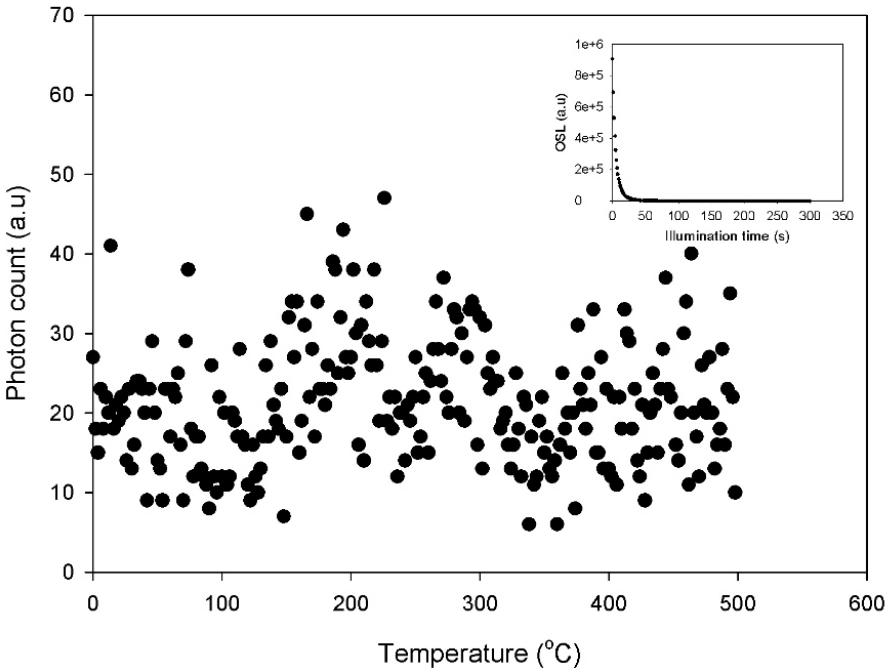

Figure 5.63: Glow curve from sample A_1 following preheating to 80°C followed by long illumination time of 300 s. All signal for peaks I, II and III in a glow curve are indistinguishable from the background signal. The inset is the OSL recorded as a function of time.

5.2.2.4 PTTL intensity versus illumination time from peak II in sample A_1 following preheating to 500°C

Figure 5.65 shows the illumination time dependence of PTTL for peak II following preheating to 500°C after a dose of 0.5 Gy. Sample A_1 was heated at $5°C\,s^{-1}$ after illumination times from 0 to 600 s. The PTTL intensity increases from zero to a maximum followed by a decrease to a non-zero constant value. The intensity has its maximum at an illumination time of 30 s. The PTTL intensity decreases slowly from its maximum to its half-maximum at an illumination time of about 500 s. This contrasts with the PTTL intensity for peak I following the preheating to 80°C that decays much faster to its half-maximum at an illumination time of 30 s (figure 5.62 b).

5.2.2.5 PTTL in sample A_1 following preheating to 600°C and 700°C

Samples A and A_1 were not annealed to 900°C before use. Effect of phototransfer on PTTL peak I from these samples are compared at the end of measurements (after sev-

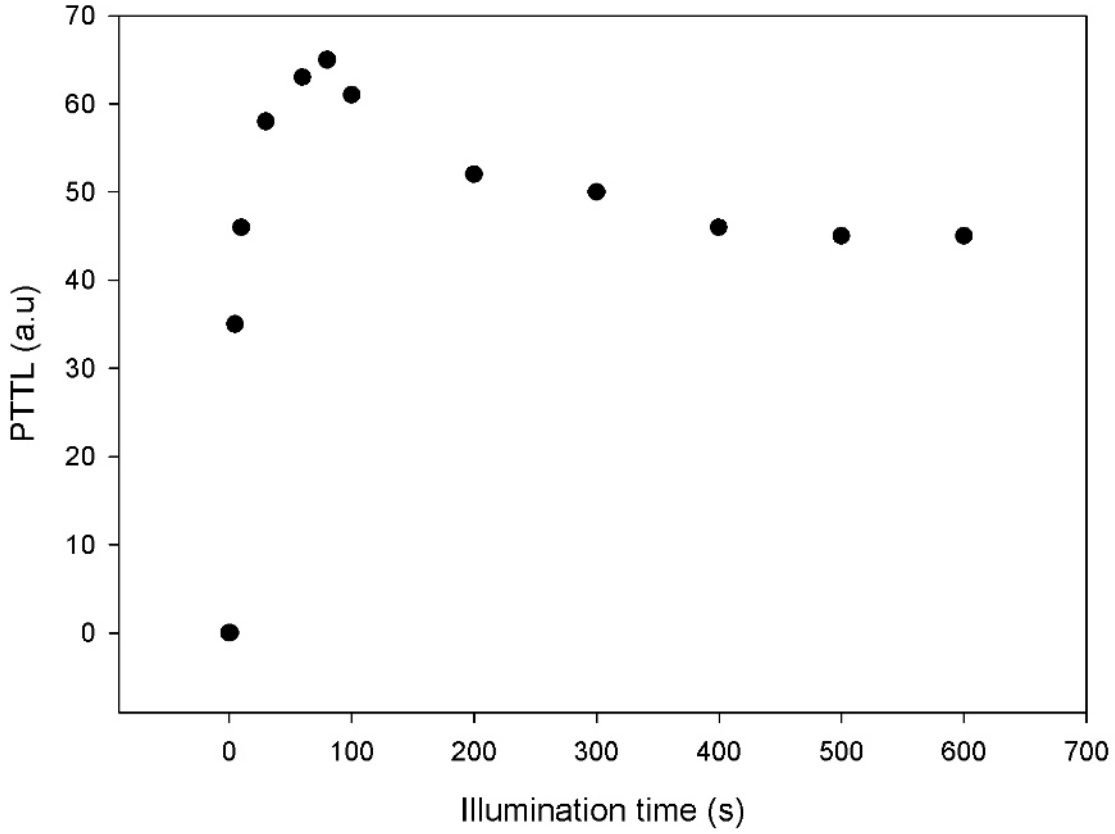

Figure 5.64: PTTL signal versus illumination time for peak II in sample A_1 after preheating to 320°C.

eral measurements done for PTTL following various preheats up to 900°C in annealed samples). The preheating to 600°C and 700°C in sample A_1 was done for 6 minutes. Figure 5.66 (a) is a glow curve showing PTTL from peak II in sample A_1 following the preheating to 600°C for 6 minutes. Figure 5.66 (b) shows a glow curve with PTTL from peak II after preheating to 700°C for 6 minutes. The plots show a weak signal but which is still distinguishable from the background. The PTTL maximum appeared at 202°C following preheating to 600°C (figure 5.66 a) while preheating to 700°C (figure 5.66 b) produces a peak at 194°C for an illumination time of 10 s. However, in sample A (first paragraph of subsection 5.2.1) a clear PTTL peak II was observed after heating to 700°C for 6 minutes. In addition, preannealing at 700°C for 15 minutes removed all effects of PTTL in peaks I, II and III in sample A_1 while in sample A peak II was reproduced under PTTL (figure 5.54). This result of the PTTL feature in sample A_1 is consistent with that previously reported by Bulur et al. [17] but that of sample A

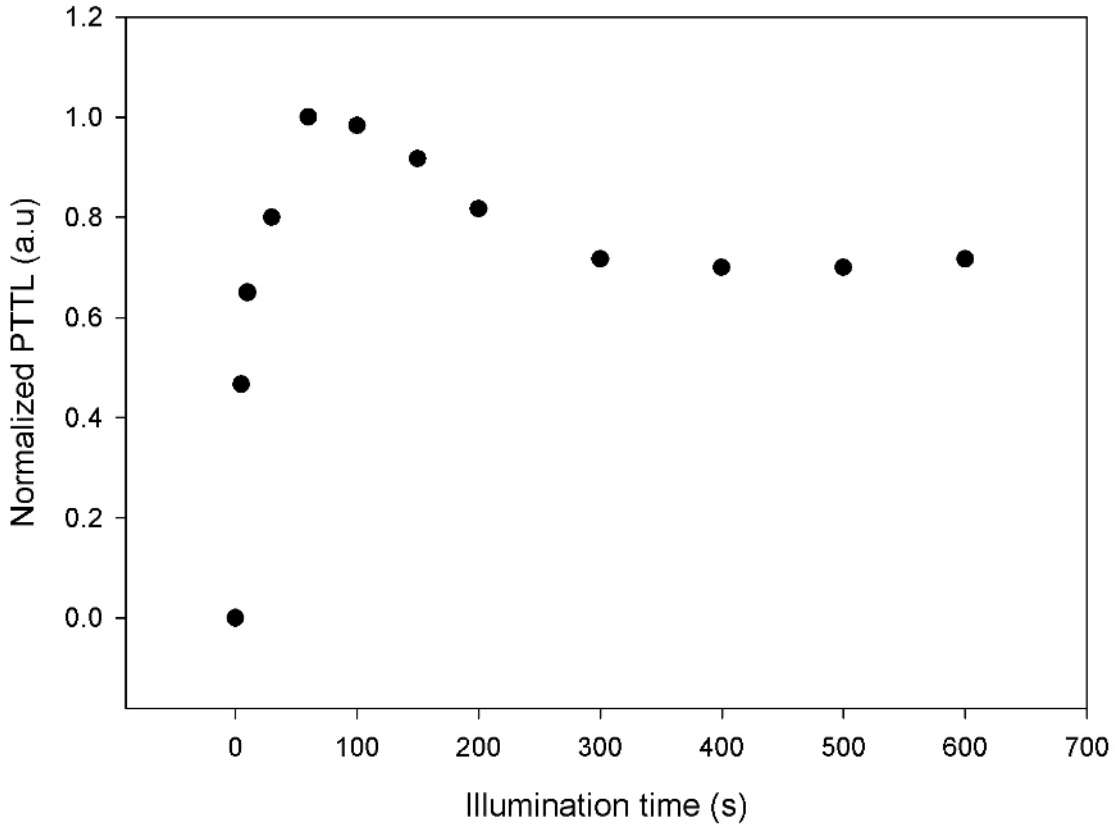

Figure 5.65: PTTL intensity against illumination time for peak II in sample C following heating to 500°C.

is not. They reported that deep electron traps responsible for PTTL in shallow traps are removed after preheating to 700°C. Further experiments on PTTL in an annealed sample A as in sample A_1 did not show any PTTL for peak I even after preheating to temperature to 100°C (to remove peak I from sample A) and to 80°C (to remove peak I from sample A_1) after a dose of 0.5 Gy.

5.2.2.6 The investigation of PTTL signal from peak I in sample B

Sample B was annealed at 900°C for 15 minutes before use for PTTL measurements. The effect of annealing on PTTL from peak I was analysed by comparing characteristics of PTTL from peak I in an annealed sample B to unannealed samples A and A_1. Figure 5.67 shows a glow curve of sample B. The glow curve consists of three TL glow peaks, peak I at 60°C, peak II at 184°C and peak III at 300°C. A heating rate of $5^{\circ}\mathrm{C\,s^{-1}}$ and a dose of 0.5 Gy were used.

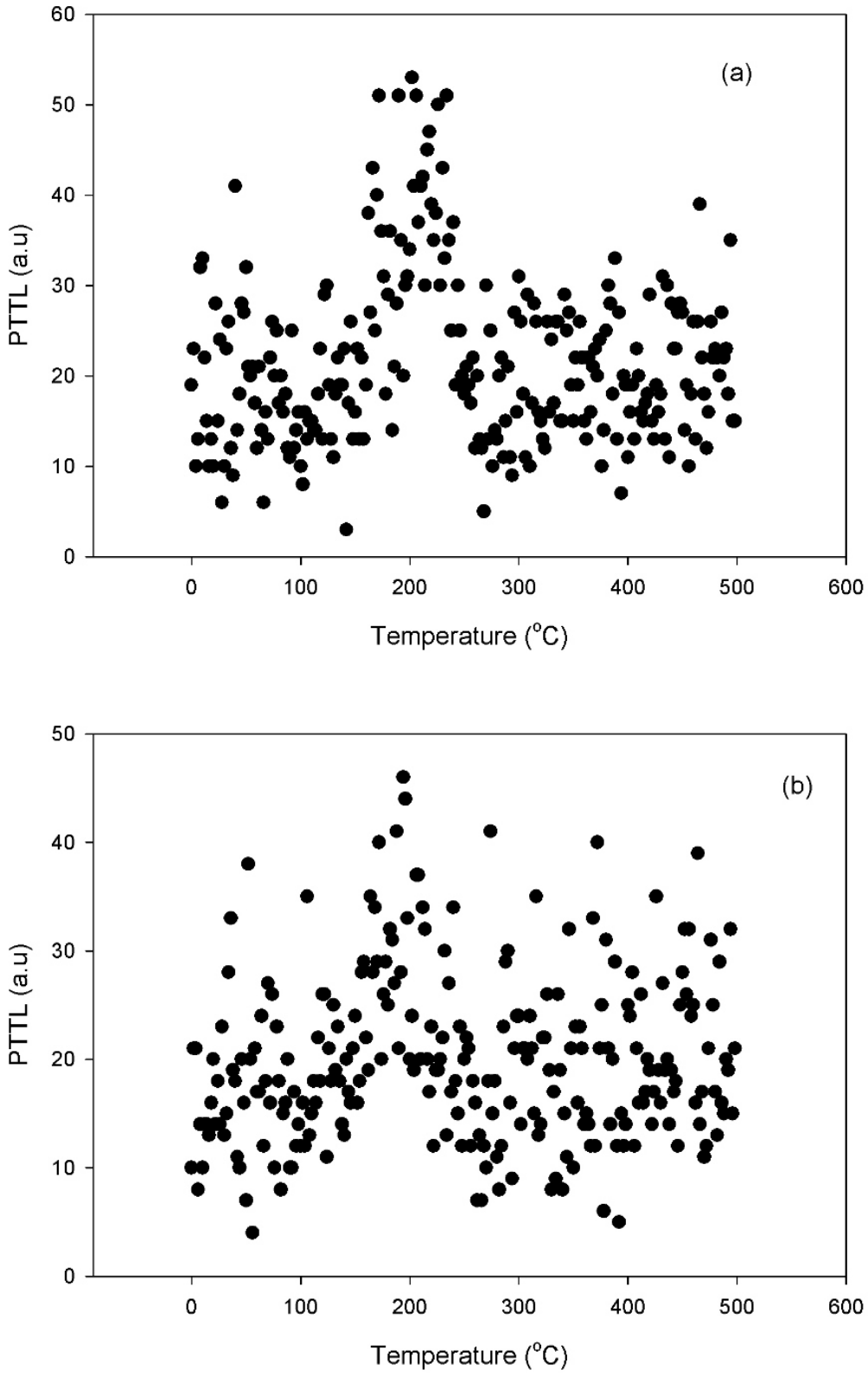

Figure 5.66: Glow curve from sample A_1 following preheating to 600°C (a) and to 700°C (b) for 6 minutes after illumination for 10 s.

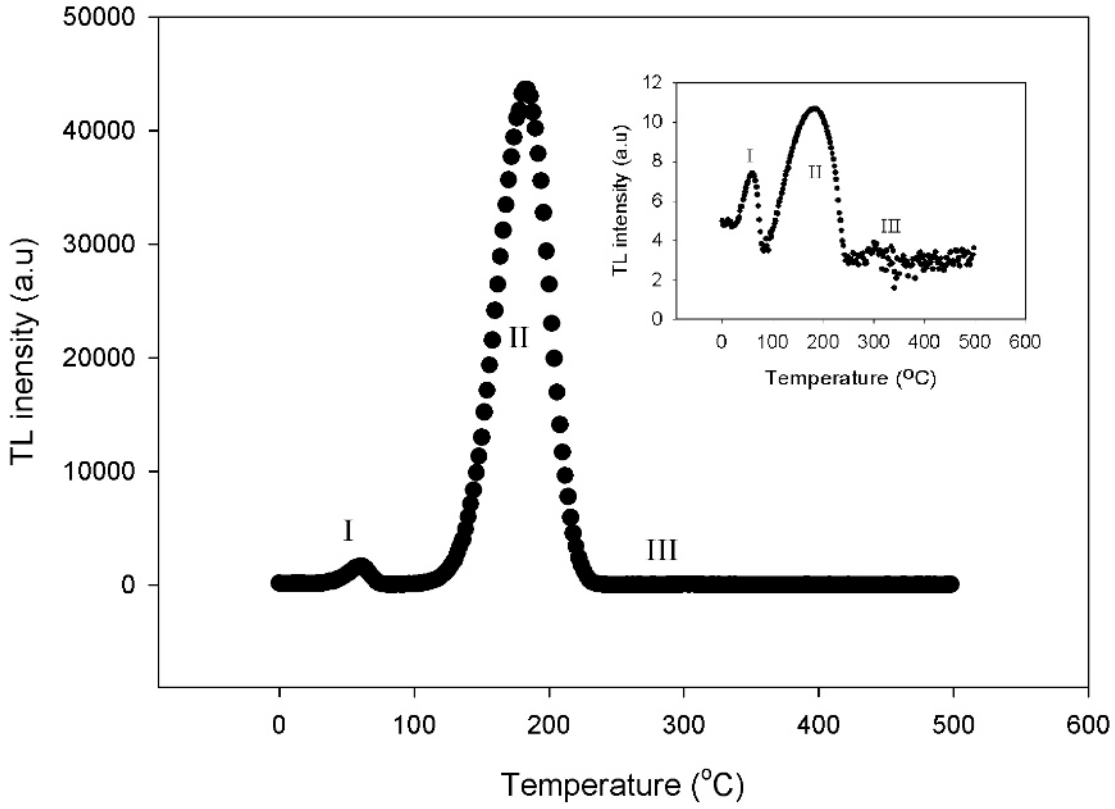

Figure 5.67: A TL glow curve of sample B showing three glow peaks I, II and III. The TL data in the inset is on a logarithmic scale for clear vision of peaks I and III.

5.2.2.7 PTTL from peak I in sample B annealed at 900°C for 15 minutes

The sample was annealed at 900°C for 15 minutes at the start of measurements to remove residual charge in deep electron traps before any irradiation. It should be noted that PTTL measurement following each illumination was followed by annealing at 900°C for 15 minutes.

Figure 5.68 shows a glow curve showing a PTTL signal from peak following pre-heating to 80°C. Peak I is reproduced under PTTL measured from sample B. The position of peak I can be seen at 70°C for the PTTL measured after an illumination of 10 s at a heating rate of $5^{o}\mathrm{C\,s^{-1}}$ for a dose of 0.5 Gy. PTTL intensity corresponding to illumination times from 0 to 10 s was investigated in peak I from sample B annealed at 900°C for 15 minutes following each preheating to 80°C. The inset of figure 5.68 shows the dependence of PTTL intensity on illumination time. The maximum intensity of the PTTL peak is at an illumination of 5 s. However, the PTTL signal was very weak

and disappeared rapidly after illumination times above 10 s. This is why there are no data points corresponding to times greater than 10 s.

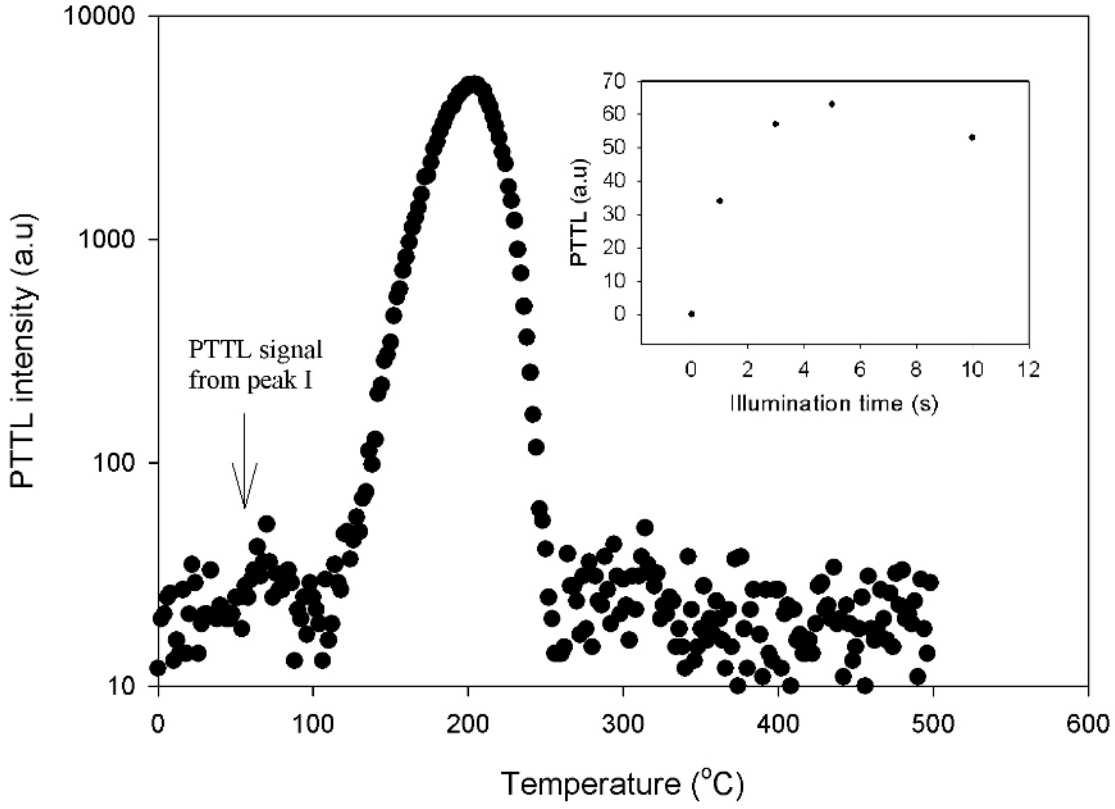

Figure 5.68: A PTTL glow curve measured from peak I following preheating to 80°C and illumination time for 10 s in sample B. The sample was annealed at 900°C for 15 minutes at the start and in between measurements. The inset shows the dependence of PTTL intensity on illumination time for peak I.

5.2.2.8 PTTL from peak II in sample B annealed at 900°C for 15 minutes

Further preheating of sample B to 320°C removed peaks I, II and III but only peak II was reproduced under phototransfer for illumination times below 100 s. Figure 5.69 (a) shows a glow curve showing the PTTL from peak II following preheating to 320°C after an illumination time of 10 s. The sample was heated at 320°C after a dose of 0.5 Gy. The position of the peak is 184°C. Figure 5.69 (b) shows the dependence of PTTL from peak II on illumination time. Sample B was annealed at 900°C for 15 minutes after each illumination time from 0 to 100 s. The intensity of the PTTL from peak II increases as a function of illumination time to a maximum at an illuminationn time of

30 s from which it decreases. The intensity of PTTL for illumination for more than 100 s was negligible. In contrast to unannealed samples A and A_1, preheating beyond 320°C did not lead to PTTL in peaks I, II and III from sample B.

5.2.2.9 Summary

PTTL experiments were performed on three different samples referred to as A, A_1 and B. Samples A and A_1 were not annealed before use, the purpose of measurements on two unannealed samples was to confirm that the characteristics of PTTL peak from α-$Al_2O_3 : C$ differ from sample to sample. Sample B was annealed at 900°C for 15 minutes at the start and after each PTTL measurement following each illumination time from 0 to 100 s. Measurements was done on an annealed sample B and unannealed samples A and A_1 to check the effect of annealing on PTTL from secondary peaks. Each sample was dosed to 0.5 Gy and heated at $5^{o}C\,s^{-1}$.

The following are conclusions on the effect of annealing on PTTL from peak I. The PTTL for peak I was regenerated in samples A and A_1 not annealed to 900°C for illumination times from 0 to 600 s. Sample A produced a PTTL signal for peak I even after preheating to 500°C while sample A_1 preheated to above 80°C did not produce any PTTL signal for peak I. Sample B showed PTTL intensity from peak I only when annealed once before the start of measurements. Generally the PTTL peak for peak I in sample B disappeared after annealing for several times at 900°C for 15 minutes in between measurements (4 or 5 consecutive times of annealing) corresponding to each illumination time from 0 to 30 s.

It is important to note that after reusing several times samples A and A_1 to measure PTTL were also annealed at 900°C for 15 minutes ($\sim$ 2 times in between measurements), the PTTL for peak I was completely removed. This means that PTTL measurements did not produce any PTTL for peak I following preheating to temperatures (100°C for sample A and 80°C for sample A_1) that removed peak I before. This suggests that the observed PTTL from peak I in unannealed samples was influenced by residual charges in the deep traps which are partially filled at low doses. This is

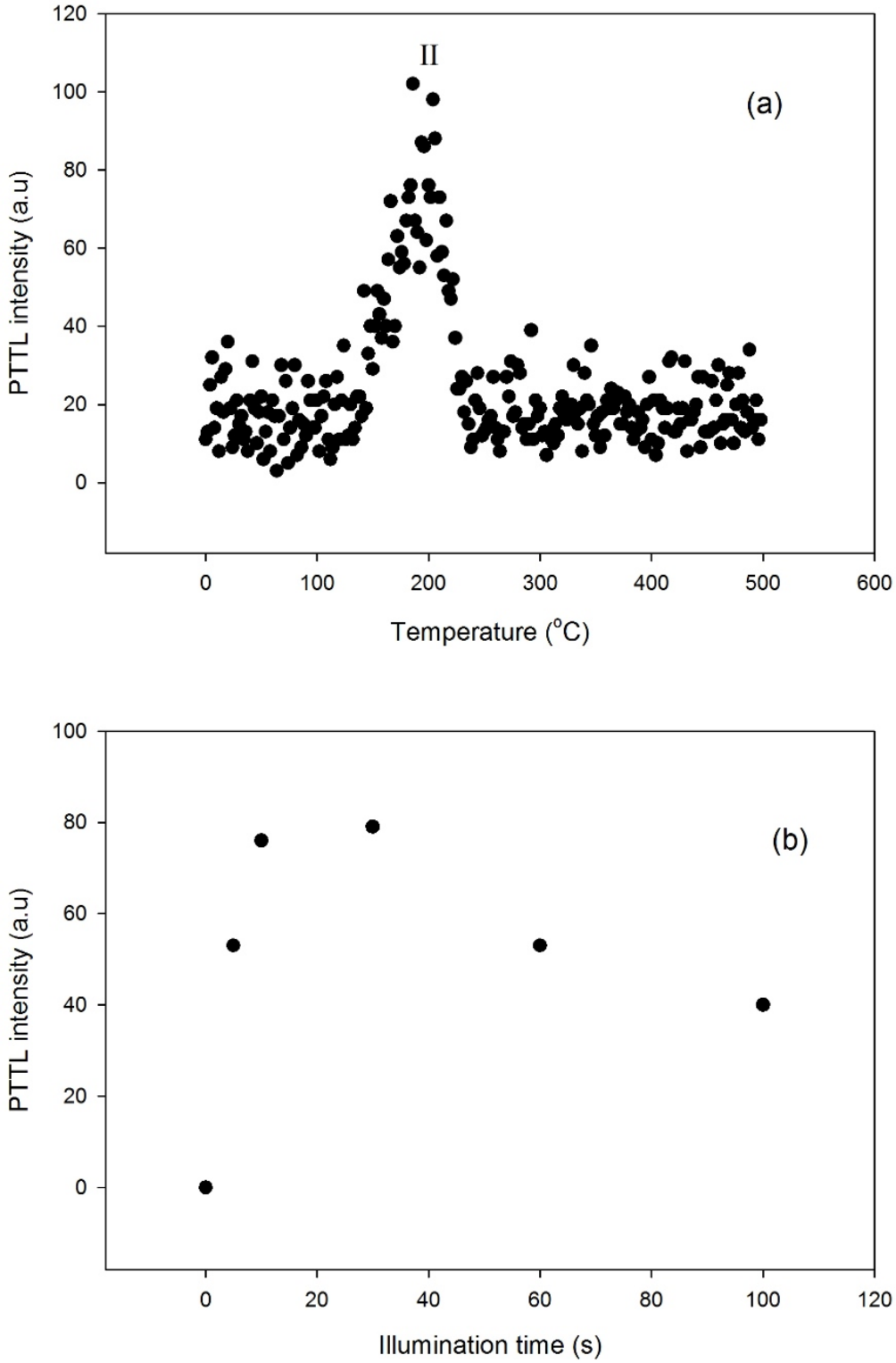

Figure 5.69: A glow curve measured from peak II in sample B following preheating to 320°C after an illumination time of 10 s (a). The evolution of a PTTL peak as function of illumination time (b). The sample was heated to $5^{o}\mathrm{C\,s}^{-1}$ after a dose of 0.5 Gy.

verified in the following section. No PTTL was observed from peak III in all samples A and A_1 and B, either annealed at 900°C for 15 minutes or not.

5.2.3 The effect of dose on PTTL intensity from secondary peaks

Peak I and peak III are of low intensity compared to the main one (peak II) in a glow curve of α-$Al_2O_3 : C$ and been referred to before as secondary peaks [9]. PTTL from peak I was studied for doses increased from 0.5 to 5 Gy in an annealed sample A and from 0.5 to 3 Gy for annealed samples A_1 and B. This is because for a dose of 0.5 Gy, peak I was not reproduced under PTTL in samples annealed at 900°C for 15 minutes more than once in between PTTL measurements. The annealing was done to remove residual charge in deep electron-traps which are the donors of electrons to the shallow electron trap responsible for peak I. The purpose of increasing dose was to verify if a filled deep electron trap can generate PTTL from peak I in a sample annealed at 900°C for 15 minutes after each illumination time from 0 to 100 s.

5.2.3.1 PTTL intensity for peak I in samples A, A_1 and B annealed at 900°C for 15 minutes

Samples A and A_1 were not annealed before use in PTTL experiments while sample B was annealed before and in between PTTL measurements executed after each illumination time between 0 and 100 s. In this study of the dose effect on PTTL from secondary peaks, samples A and A_1 (used in the first measurements as not annealed samples) were annealed once at 900°C for 15 minutes at the start of the second experiments.

Figure 5.70 shows a glow curve showing peak I obtained as PTTL measured in samples A, A_1 and B at $5°C\,s^{-1}$ and illumination for 10 s. In sample A (figure 5.70 a), the PTTL intensity for peak I following preheating to 100°C was observed from sample only after increasing dose up to 5 Gy (sample A irradiated to a dose less than 5 Gy did not show any PTTL from peak I). The peak position is 78°C. A PTTL glow curve for peak I in sample A_1 following preheating to 80°C for a dose of 3 Gy is shown in

figure 5.70 (b). The position of the peak is 61°C. Figure 5.70 (c) shows a glow curve of PTTL for peak I in sample B following preheating to 80°C after a dose of 3 Gy. The position of the peak is 60°C for the same illumination time of 10 s.

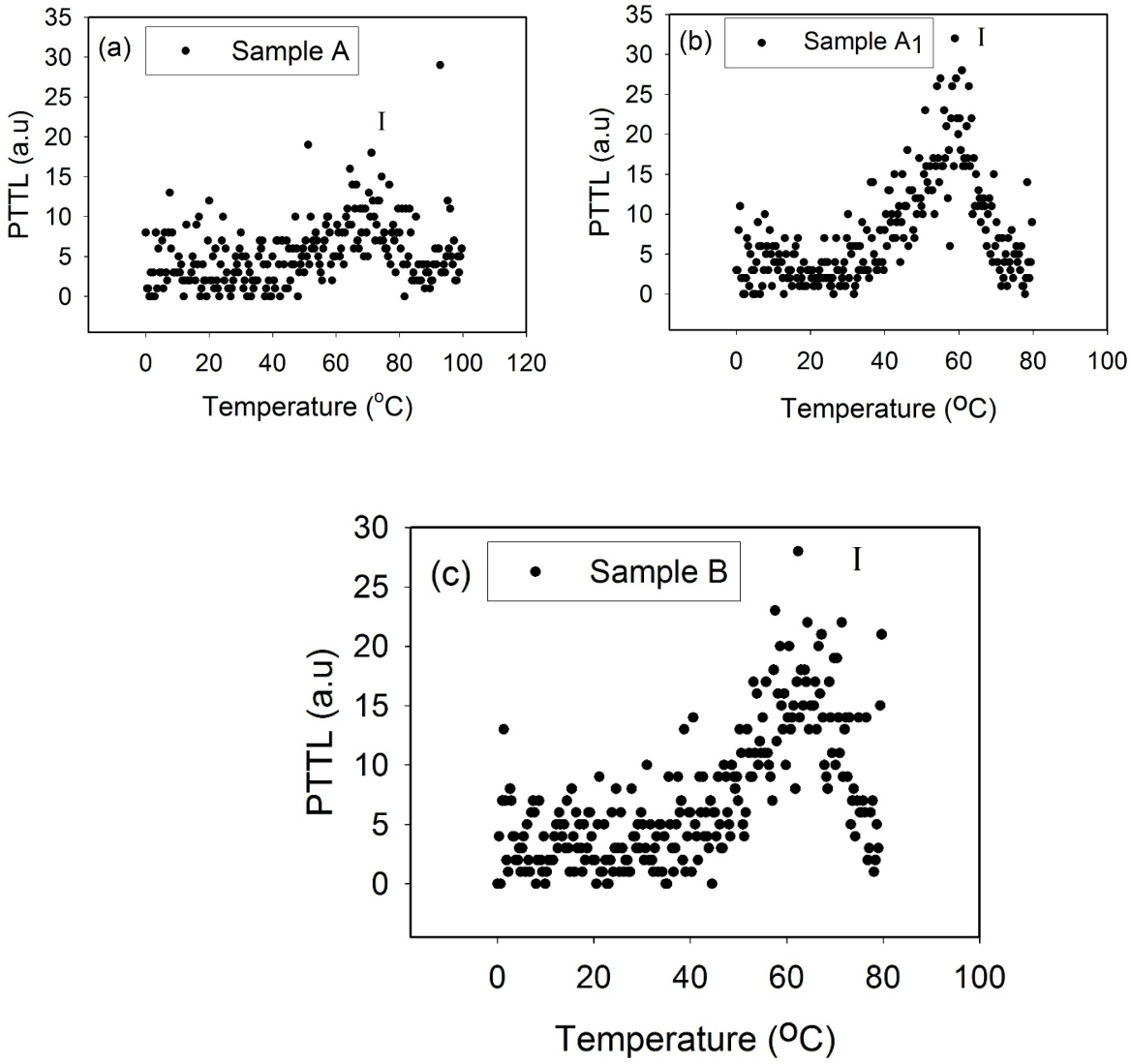

Figure 5.70: PTTL glow curve for peak I in an annealed sample A following preheating to 100°C after a dose of 5 Gy (a) PTTL glow curve for peak I in annealed samples A_1 (b) and B (c) were measured following preheating to 80°C and a dose of 3 Gy. Samples A, A_1 and B were heated at $5^{o}\mathrm{C\,s^{-1}}$ after illumination time of 10 s.

The area of PTTL glow peak I corresponding to illumination times from 0 to 100 s was recorded in samples A_1 and B following preheating to 80°C. The PTTL intensity from peak I in sample A was too weak to enable the dependence of PTTL intensity on illumination time to be studied (figure 5.70 a). Figure 5.71 shows the dependence of PTTL intensity on illumination time for samples A_1 and B . Results show that the

intensity goes through a peak with illumination time in samples A_1 (figure 5.71 a) and B (figure 5.71 b). The maximum of the peak is observed at an illumination time of 30 s in each sample A_1 or B.

The important conclusion from these results in figure 5.71 is that the dose increased up to 3 Gy in an annealed affects the intensity of PTTL from peak I. This implies that at low doses less than 3 Gy, deep electron traps responsible for peak I are partially-filled such the effect of PTTL from peak I are negligible in samples A, A_1 and B annealed to 900°C for 15 minutes. However, when the dose increases to 3 Gy in samples A_1 and B or to 5 Gy in sample A deep electron traps are filled enough such that a clear PTTL peak I is reproduced from further PTTL measurements (figure 5.70).

5.2.3.2 PTTL intensity versus illumination time for peak II in samples A, A_1 and B annealed at 900°C for 15 minutes

PTTL was also studied in annealed samples A, A_1 and B following preheating to temperatures above which all peaks I, II and III are removed. The annealing procedure was as follows.

Samples A, A_1 and B were first annealed at 900°C for 15 minutes and then irradiated to a beta dose of 3 Gy. After irradiation, the samples were taken back to the furnace to preheat them a second time at a temperature that removes all peaks I, II and III for 15 minutes. Sample A was preheated to 390°C for 15 minutes while samples A_1 and B were preheated to 320°C for 15 minutes. The PTTL was measured from the subsequent reheating to 500°C after each illumination time between 0 and 600 s. After the preheating, only peak II was observed under PTTL. A heating rate of $5^{o}\mathrm{C\,s^{-1}}$ was used in the measurements of PTTL.

Figure 5.72 shows the PTTL intensity versus illumination time for peak II in samples A, A_1 and B. Plots show a peak with maxima at an illumination time of 100 s for sample A (figure 5.72 a), at 60 s for sample A_1 (figure 5.72 b) and at 100 s for sample B (figure 5.72 c). A PTTL peak for sample A was measured for illumination times from 0 to 600 s. The length of illumination times for sample A_1 is 0 to 200 s

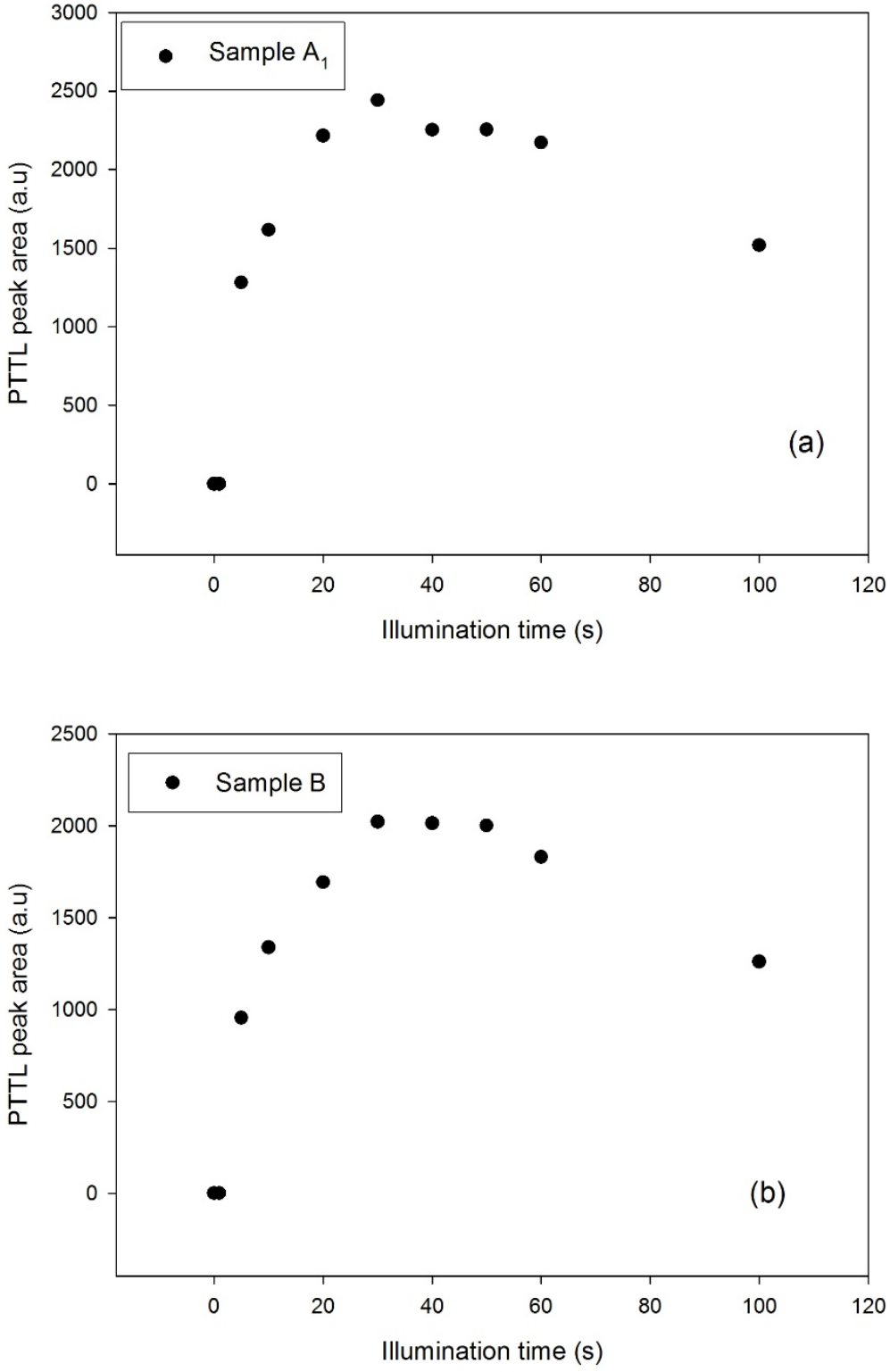

Figure 5.71: The PTTL peak area against illumination time for peak I in annealed sample A_1 (a) and B (b) following heating to 80°C for illumination times from 0 to 100 s. The samples were heated at $5^{\circ}\mathrm{C\,s^{-1}}$ after a dose of 3 Gy.

while that for sample B starts from 0 to 400 s. In all samples, the intensity of the peak slowly decreased from its maximum but did not reach its half maximum at the end of illumination. It should be recalled that in all samples annealed at 900°C for 15 minutes in between PTTL experiments and dosed to 3 Gy, no PTTL was observed after illumination following preheating to 500°C and above. This implies that there are deep electron traps which are unstable between 400 and 500°C which act as donors for electrons to the shallow electron traps. Examples are peak IV at 422°C (figure 5.22) and others reported in the literature at 400°C, 430°C and 550°C [26].

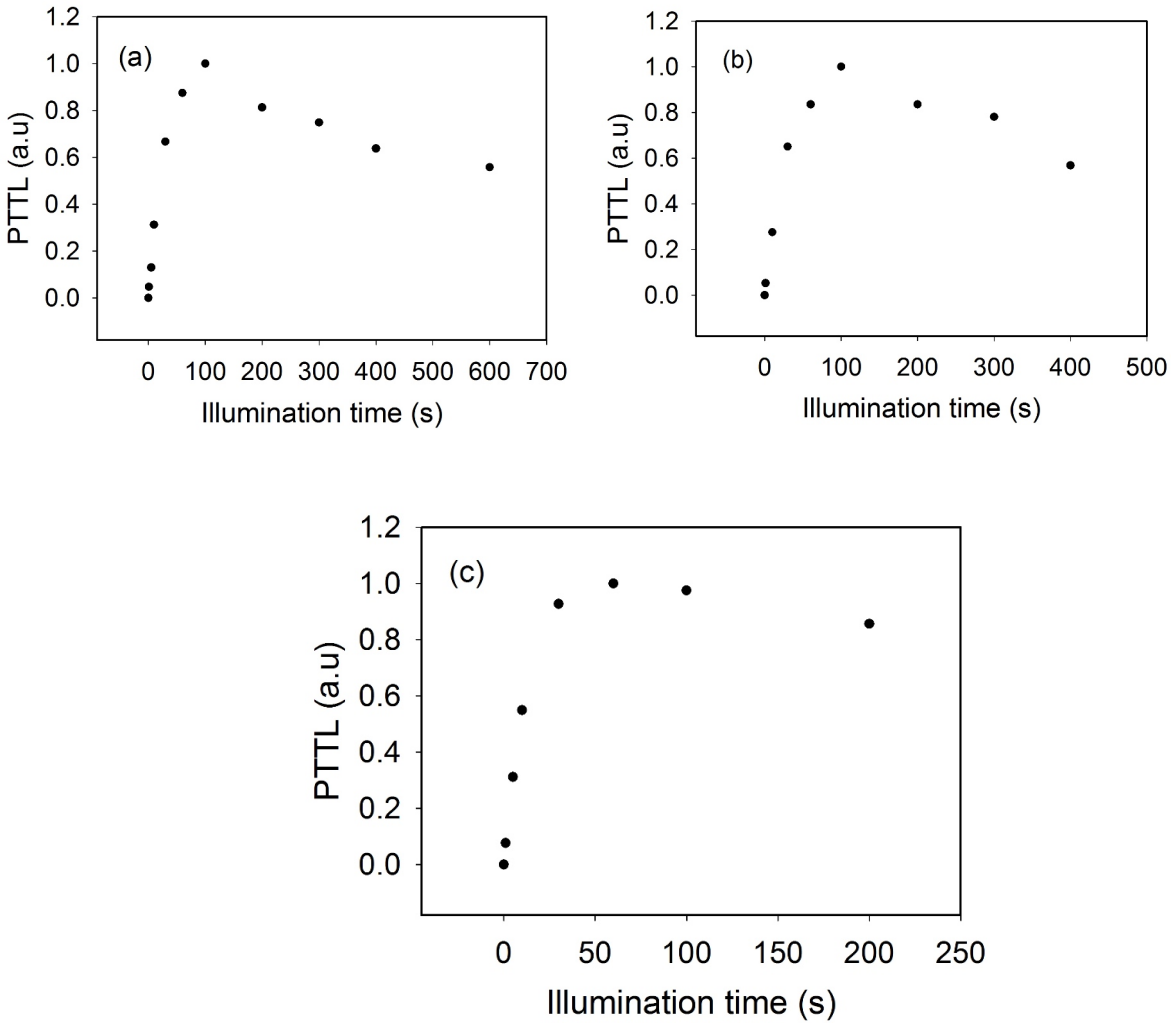

Figure 5.72: The PTTL (measured as peak area) against illumination time for peak II in annealed sample A following 390°C (a) and in annealed samples A_1 (b) and B (c) following heating to 320°C.

5.2.3.3 Summary

Residual charges in deep traps affect the PTTL signal produced from shallow traps. The deep traps are only emptied by annealing samples of α-$Al_2O_3 : C$ at 900°C for 15 minutes. This was attested to by the effect of annealing on PTTL signal observed for peak I. After a beta irradiation dose of 0.5 Gy, shallow and competitor deep traps are only partially-filled with free charges from ionization of the sample. The optical stimulation out of deep electron traps, following preheating to certain temperatures to empty shallow traps, transfers the few available trapped charges from deep traps to shallower traps. Because the main dosimetric trap responsible for peak II is the most competitive, most of the charge will be trapped in the main dosimetric trap at the low dose of 0.5 Gy. The subsequent heating after illumination stimulates electrons to recombine with F^+ centres at the recombination centres. This produces the PTTL for peak II. The shallow trap corresponding to peak I is filled if there are enough electrons in deep traps such that during illumination some of them are trapped in the main dosimetric traps, others in the shallower trap. This was experimentally observed in PTTL investigated from peak I in annealed samples A_1 and B for a dose of 3 Gy only. PTTL from peak I was observed from annealed sample A only by increasing dose to 5 Gy. In addition, filling deep electron traps increases the luminescence efficiency since the competition for electrons during heating is reduced [37].

5.2.4 The effect of heating rate on PTTL from peak I

Kinetic theory predicts a shift in position of a peak to higher temperature as a function of increase in heating rate [5]. This was experimentally verified in both PTTL and TL of peak I. Firstly, an unnealed sample A was heated to 500°C after an irradiation dose of 0.5 Gy. A TL of whole glow curve was recorded at a heating rate of $0.6^{\circ}C\,s^{-1}$. The experiment was repeated five times at various heating rates from 0.6 to $5^{\circ}C\,s^{-1}$ in the same sample freshly dosed to 0.5 Gy for each measurement. The average peak position from five measurements was then calculated. Secondly, the PTTL for peak I was recorded following preheating to 100°C after an illumination time of 10 s. The same

dose of 0.5 Gy was used. The intensity of a PTTL from peak I was recorded at various heating rates from 0.6 to 5°C s^{-1}. Similarly, the average peak position of a PTTL from peak I at each heating rate from 0.6 to 5°C s^{-1} was found. Figure 5.73 shows plots of the PTTL and normal TL peak positions for peak I against variable heating rate. The maximum temperature T_M for TL and PTTL shift to higher temperatures when heating rate is increased from 0.6 to 5°C s^{-1}, consistent with kinetic theory.

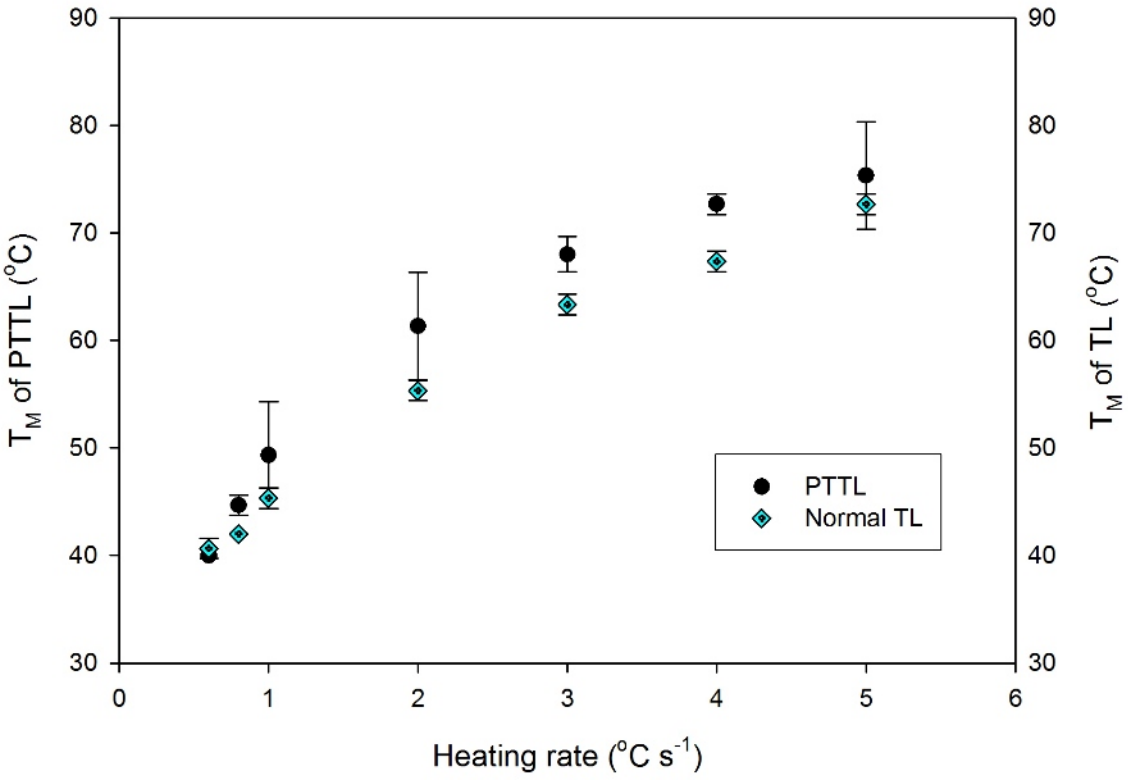

Figure 5.73: The dependence of the PTTL and normal TL peak positions for peak I on various heating rates from 0.6 to 5°C s^{-1} for a dose of 0.5 Gy. The PTTL intensity for peak I was measured after an illumination of 10 s. As can be seen, the increase of T_M for TL and T_M for PTTL as a function of heating rate is identical.

The influence of heating rate on PTTL intensity for peak I in α-Al_2O_3 : C is shown in figure 5.74. The PTTL intensity of peak I decreases when the heating rate is increased. From theory of kinetics, the opposite result would be expected [2]. The decrease of PTTL intensity with heating rate is an indication of a decrease of radiative recombinations at F^+ centre. However, normal TL intensity increases with heating rate (figure 5.74 inset). Similar opposite effects of heating rate on TL and PTTL processes

from peak II in α-$Al_2O_3 : C$ were reported by Kortov et al. [39]. This contrast needs further study. A decrease of the PTTL intensity as a function of heating rate can be explained in two ways:

1. PTTL emission from peak I involves interaction between active deep traps (traps responsible for the PTTL intensity) and the shallow trap during heating which is not the case for normal TL process [9]. This means that some electrons released from the shallow trap during heating are captured by competitor deep traps. The competition from deep traps for released electrons becomes strong at high heating rates which reduces the number of electrons that would recombine with holes to produce PTTL at the recombination centre.

2. The decrease of the PTTL intensity for peak I as the heating rate increases can also be explained as being due to an increase of non-radiative recombination (thermal quenching).

The activation energy W and the constant C for thermal quenching can be evaluated using equation 5.8 from the theory of thermal quenching [5, 27]. Figure 5.75 shows a plot of $\ln[(I_U/I_Q) - 1]$ versus $1/kT$ where all parameters were defined in the discussion of equation 5.8. Results from the fit are $W = 1.03 \pm 0.08\,\text{eV}$ and $C = 3 \times 10^{11}$. These parameters are similar to quenched parameters obtained in the kinetic analysis of normal TL peak III. This is another confirmation that all electron traps associated with peaks I, II and III in α-$Al_2O_3 : C$ have a common recombination centre.

5.2.5 Fading characteristics of the PTTL signal from peak I

The delay between illumination and the measurement of PTTL leads to a decrease of the PTTL intensity from peak I. The cause of this fading is the significant loss of charges from the shallow trap. The PTTL signal of peak I, in an annealed sample, was observed to decay completely within 2 minutes for PTTL measured at $5^{\circ}\text{C}\,\text{s}^{-1}$ after beta-irradiation dose of 0.5 Gy. Figure 5.76 shows the fading of PTTL intensity from peak I measured following preheating to 80°C after illumination for 10 s. PTTL data

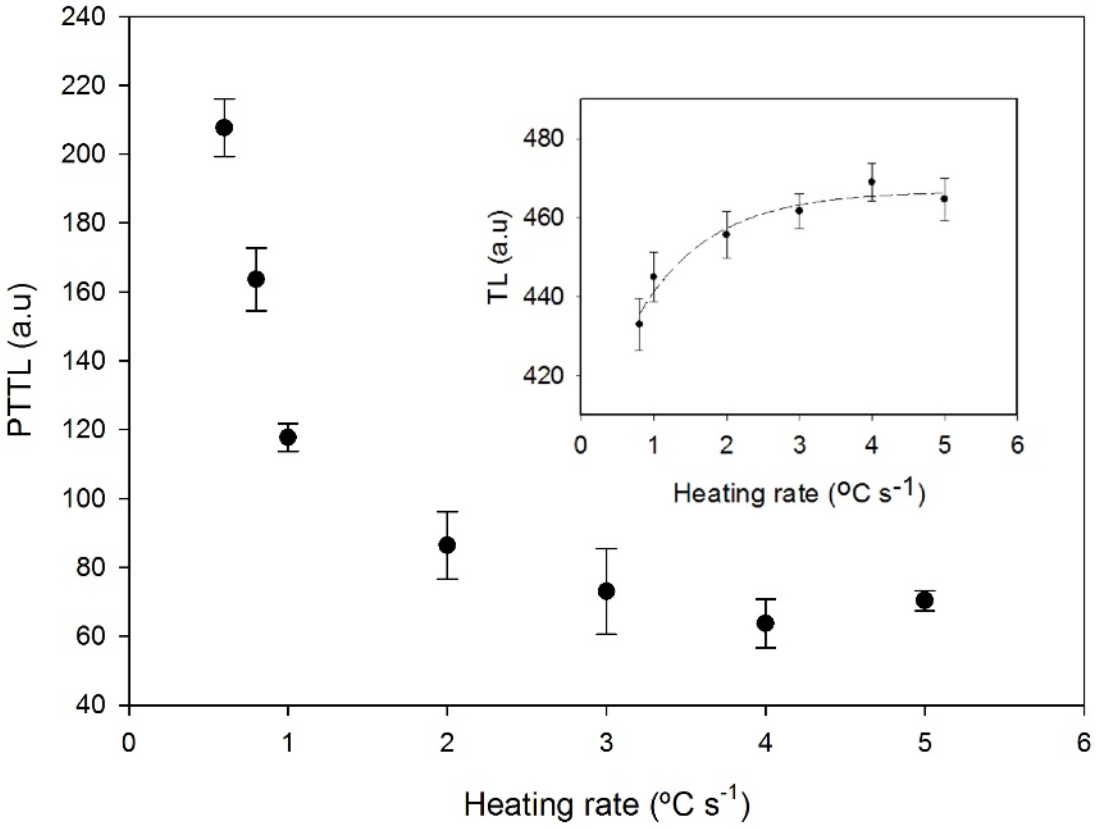

Figure 5.74: The dependence of PTTL intensity from peak I on heating rate. The intensity was measured after illumination with 470 nm blue light for 10 s at a dose of 0.5 Gy. The PTTL intensity decreases with the increase of heating rate from 0.6 to 5°C s^{-1}. In contrast, the TL intensity for peak I increases with the increase of heating rate (inset). The dashed line is include to improve clarity of the increase graphed.

were fitted by an exponential function plus a constant as

$$\mathrm{I(t) = C_0 + I_0 \exp(-\alpha t)} \tag{5.9}$$

where C_0 is the residual signal, I_0 is the maximum PTTL intensity at time $t = 0$ and α is a decay constant. The PTTL decays approximately exponentially as a function of delay time to its half intensity at an illumination time of 50 s with a half-life of about 10 s. The value of the half-life is related to the mean lifetime from the best fit to $I(t)$ using equation 5.9.

Fading of PTTL intensity from peak I was investigated in a sample not annealed at 900°C for 15 minutes because the annealing removed all residual charge in deep

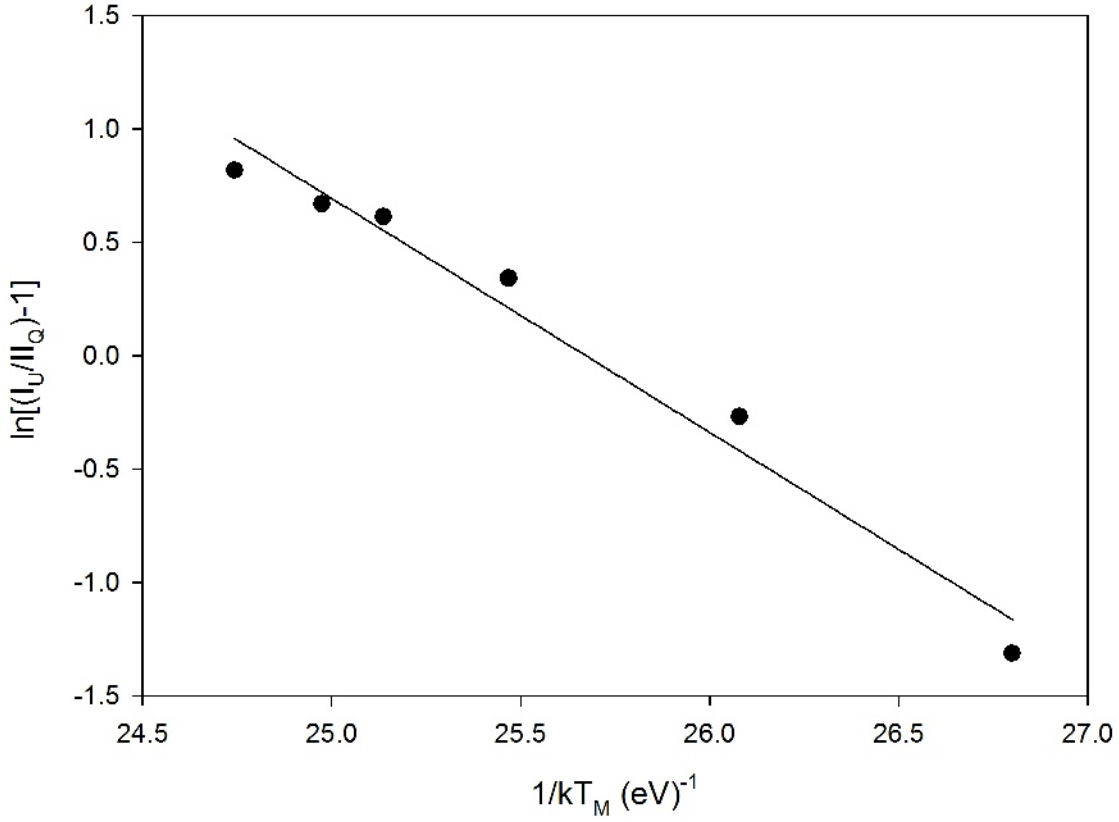

Figure 5.75: The dependence of $\ln[(I_U/I_Q) - 1]$ on $1/kT$ for PTTL peak I measured at various heating rates from 0.6 to 5°C s^{-1} after a beta dose 0.5 Gy. I_U and I_Q are unquenched and quenched intensities of the PTTL from peak I respectively; k is Boltzmann's constant and T is absolute temperature.

traps responsible for PTTL from peak I. A further measurement following the same preheating to 80°C after illumination for 10 s did not reproduce PTTL for peak I after a dose of 0.5 Gy. Subsequent irradiation to 0.5 Gy seems not to have filled all deep traps in an annealed sample. It is also important to mention that the fading in PTTL peak I is much faster with half-life of 10 s than the fading in normal TL intensity for peak I (figure 5.15) with half-life of 120 s.

5.2.6 General Mechanisms of PTTL in α-$Al_2O_3 : C$

The PTTL phenomenon, the dependence of PTTL intensity on illumination as well a thermal quenching in α-$Al_2O_3 : C$ can be explained by using the energy band model for shown in figure 5.77 [9, 21, 28, 37]. The band model contains electron traps respon-

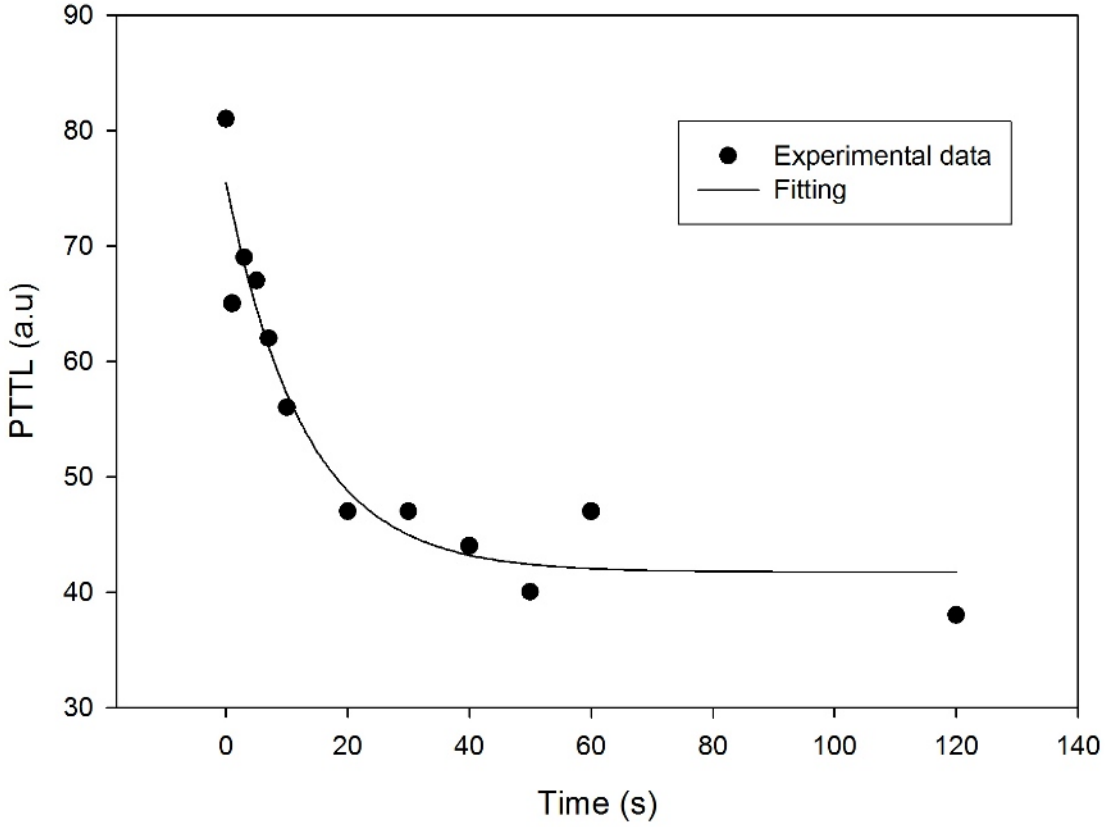

Figure 5.76: The PTTL intensity from peak I recorded as a function of time as peak I faded. The PTTL signal decay data was fitted by the equation 5.9.

sible for thermoluminescence. These are the shallow electron trap (ST), main electron trap (MT) and intermediate electron trap (IDT) corresponding to peaks I, II and III respectively. The deep electron trap (DET) only competes for free electrons from the conduction band with the deep hole trap (DHT). The DET and DHT populations affect the PTTL feature from peaks I, II and III. This is the same scheme shown in figure 5.36 but reproduced here for ease of reference.

The process of producing PTTL in a sample preheated to a temperature enough to empty the ST, MT and IDT traps after irradiation is considered. After illumination (transition 1) the ST, MT and IDT traps are refilled (transitions 2 to 4) with electrons transferred via the conduction band. These electrons come from deep electron traps during illumination. In this model we assumed that the probability of electrons leaving the trap is far greater than the probability of retrapping.

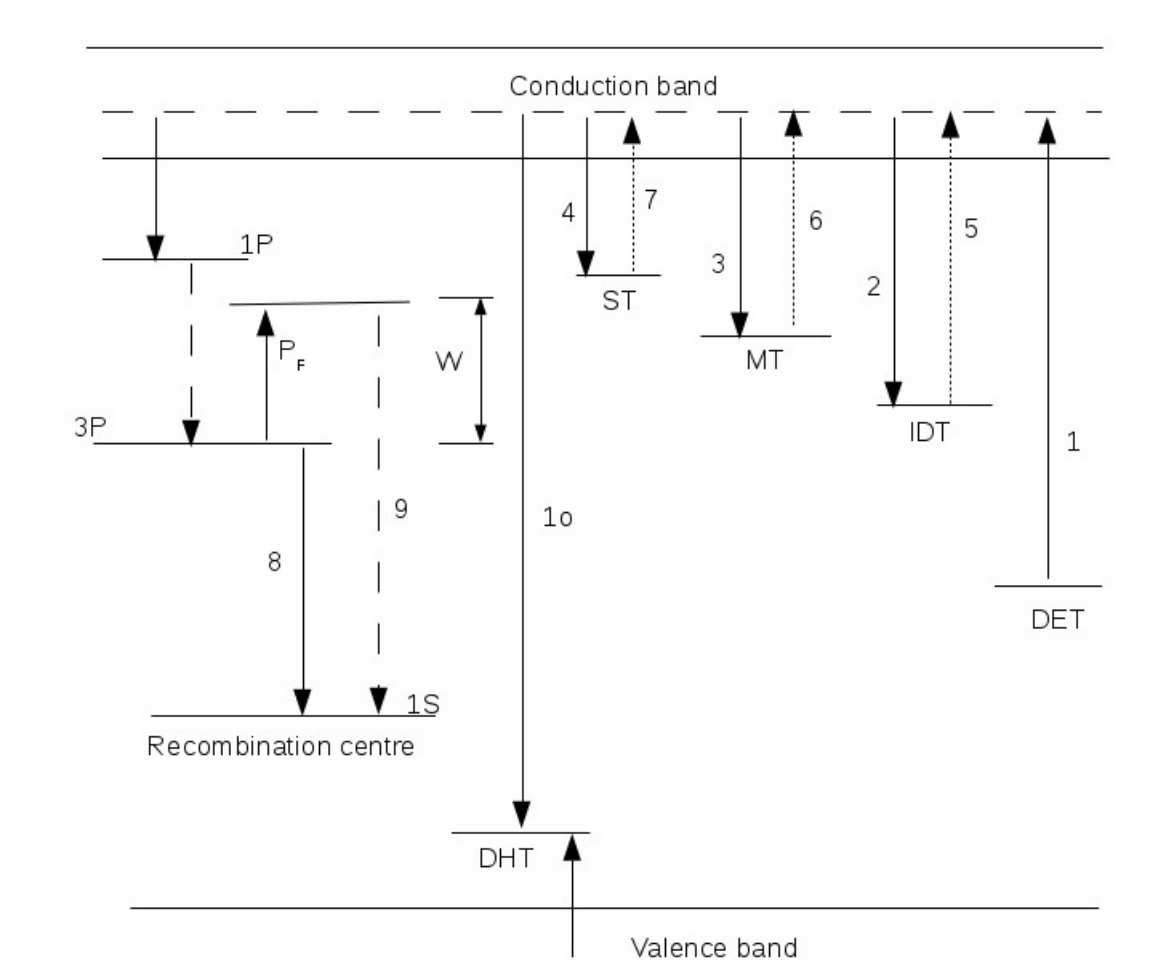

Figure 5.77: An energy band diagram used to explain the mechanisms of PTTL in $\alpha - Al_2O_3 : C$. The diagram shows the shallow, main and intermediate energy traps (ST, MT and IDT) associated with peaks I, II and III respectively. Transition 1 stands for the optical excitation from deep electron trap (DET). DHT is a deep hole trap. 1S is the ground state of F-centres while 1P and 3P are the excited states of F-centres. PTTL is produced via transition 8 (from 3P to 1S level). P_F stands for thermal ionization transition of electrons from the excited 3P level to the intermediate excited level between 3P and the low edge of the conduction band. W is the activation energy of thermal quenching. Transition 10 stands for hole-electron recombination at the DHT.

Heating to 500°C stimulates trapped electrons (dotted upward arrows, transitions 5 to 7) to recombine with F^+ centres in the recombination centres (transition 8). Once the F^+ centre has captured an electron, it becomes an excited F-centre. This excited F-centre relaxes with the emission of a photon at 410-420 nm. This is the PTTL. However, non-radiative recombination (thermal quenching, transition 9) is also possible. In the case of non-radiative transitions, electrons in the excited $3P$ level absorb energy from thermal ionization in transition P_F and then, recombine via transition 9. The relaxation

energy is dissipated in the crystal as phonons [1, 21].

If assumptions of quasi-equilibrium and negligible retrapping into deep traps during illumination hold in this model, the experimental data of PTTL peak area versus illumination time (example, figure 5.39) can be described by equation 3.33. However, the analysis of a PTTL peak I using equation 3.33 meet these assumptions only for the PTTL measured after preheating to a temperature high enough to remove peak I. Figure 5.78 shows an example of fitted data of PTTL intensity for peak I following preheating to 100°C after a dose of 0.5 Gy in unannealed sample A. The best fit using equation 3.33 yields the decay rate constants $f_1 = 0.03 \pm 0.01\,s^{-1}$ and $f_2 = 0.34 \pm 0.02\,s^{-1}$ corresponding to the rate of loss of electrons in the shallow and in the deep traps, respectively. At low illumination, the filling of the shallow trap exceeds any removal of electrons by optical excitation ($f_2 > f_1$). This explains the observed rapid increase of the PTTL peak intensity at an illumination time below 7 s in figure 5.78. When f_1 equals f_2, the increase of PTTL intensity reaches its maximum at an illumination time of 7 s. The continuous illumination removes some of trapped electrons from the shallow trap to recombine with F^+ centres and produce OSL or recombine non-radiatively. For long illumination, the emptying becomes greater than the filling in the shallow trap ($f_1 > f_2$) and the decreasing part of the PTTL intensity is observed.

Figure 5.79 shows an example of the best fit using equation 3.33 to PTTL data for peak I measured in annealed samples A_1 (a) and B (b) following heating to 80°C for a beta dose of 3 Gy. The reciprocal decay rate constants from the fit are $f_2 = 0.09 \pm 0.02\,s^{-1}$ and $f_1 = 0.01 \pm 0.01\,s^{-1}$. The same fit using equation 3.33 was done to PTTL data for peak I in an unannealed sample A after preheating to 290°C, 390°C and 500°C.

However, the equation does not fit the PTTL data for peak I measured following preheating to temperature beyond 100°C. An example is shown in figure 5.80 following preheating to 500°C, inset. Equation 3.33 does not properly fit the PTTL data for peak I after preheating to 500°C. This means that the assumptions made for this analytical function do not always apply during charge transfer in the PTTL process. Thermal

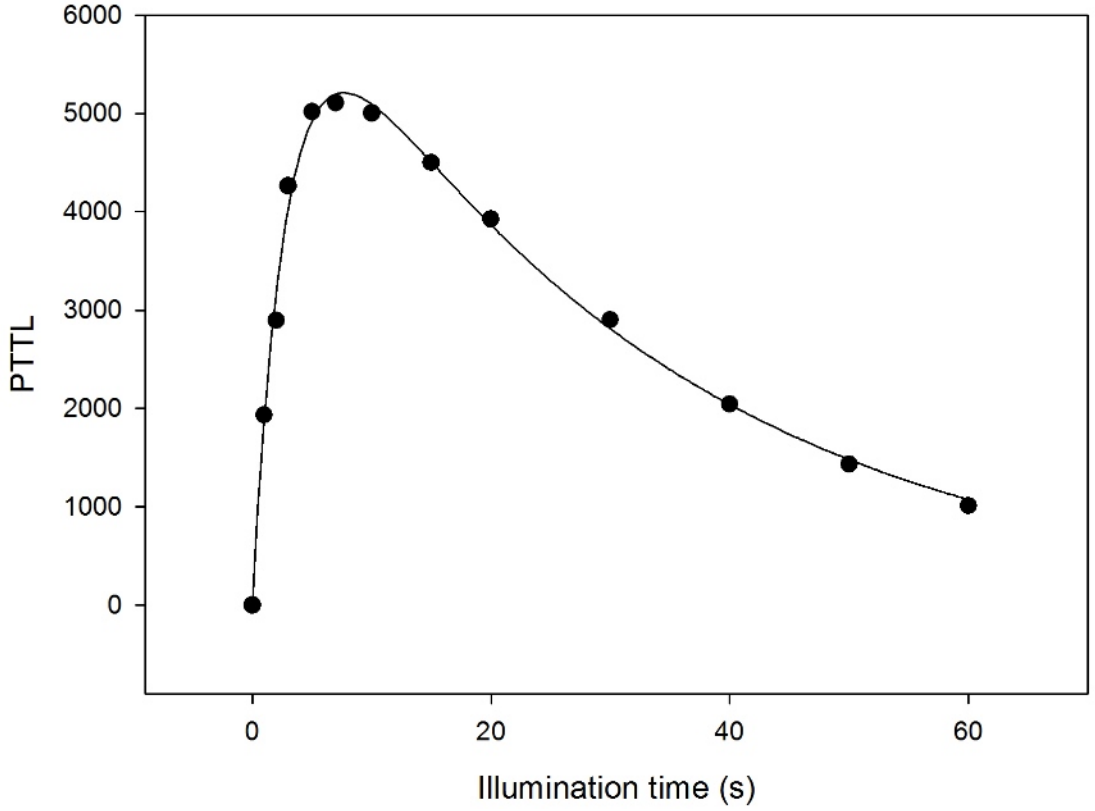

Figure 5.78: The PTTL peak intensity for peak I as a function of illumination time after preheating to 100°C for a beta dose of 0.5 Gy. A heating rate of $5^{o}\mathrm{C\,s^{-1}}$ was used in an unannealed sample *A*. The continuous solid line indicates the best fit using equation 3.33.

quenching and retrapping are observed at higher temperatures. An assumption of a quasi-equilibrium situation in PTTL measurements is not always true. Therefore, a systematic study of more complex models where the retrapping plays a bigger role is required to be compared with the general model presented in the band diagram shown in figure 5.77.

5.2.7 Summary on PTTL from secondary glow peaks

The PTTL characteristics from secondary glow peaks in α-Al_2O_3 : C have been studied. Peaks I and II are reproduced under phototransfer but peak III is not. The dependence of PTTL intensity on illumination time showed a peak-like structure. The PTTL peak nature reflects the dynamics of charge exchange from the deep traps to the shallow trap. This charge transfer is the result of optical stimulation of electrons from deep

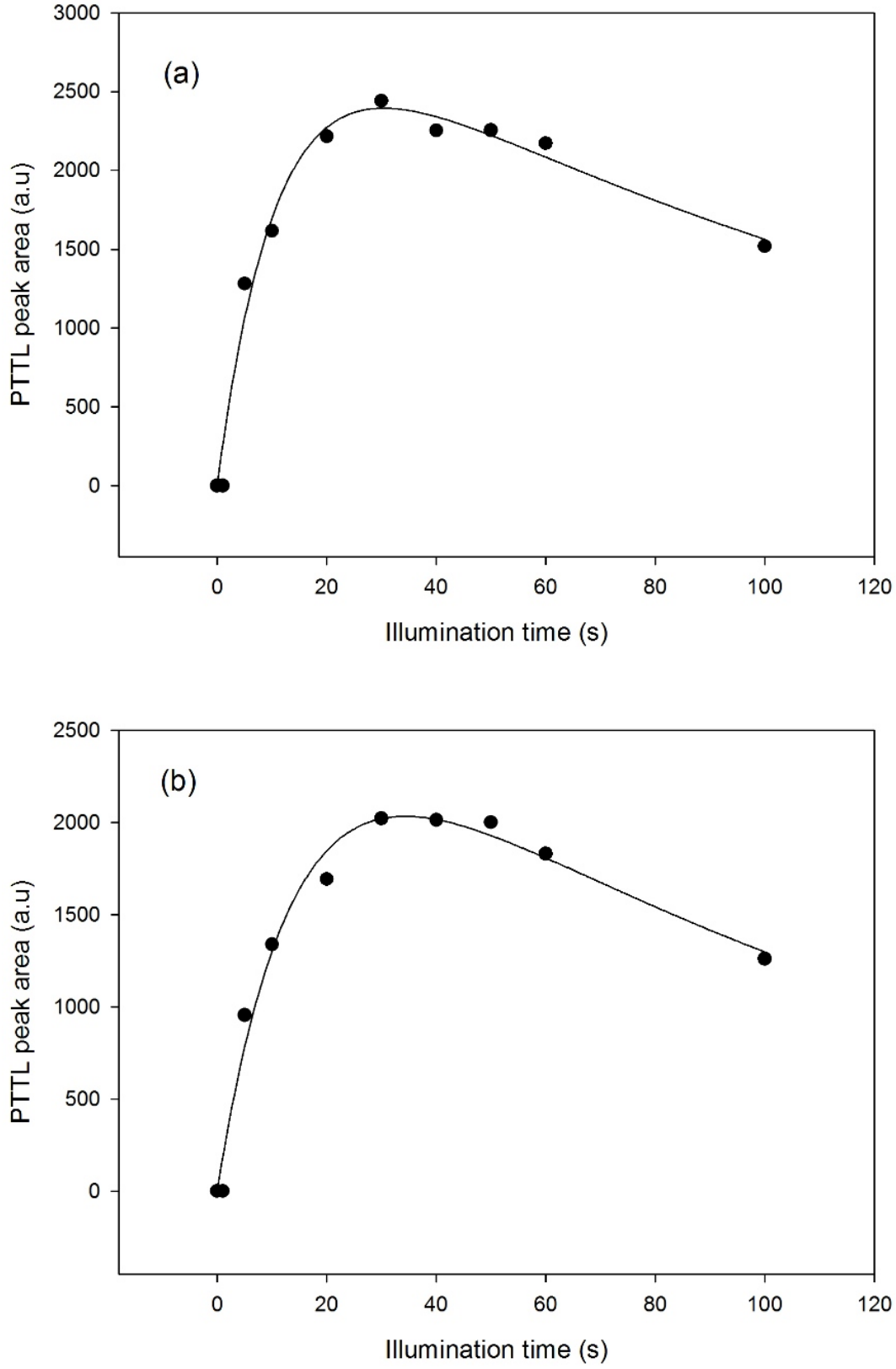

Figure 5.79: The best fit to the data from PTTL peak area for peak I as a function of illumination time after preheating to 80°C using equation 3.33. PTTL intensity for peak I was measured using a heating rate of $5^{\circ}\mathrm{C\,s^{-1}}$ in annealed samples A_1 (a) and B (b) previously irradiated to a beta dose of 3 Gy.

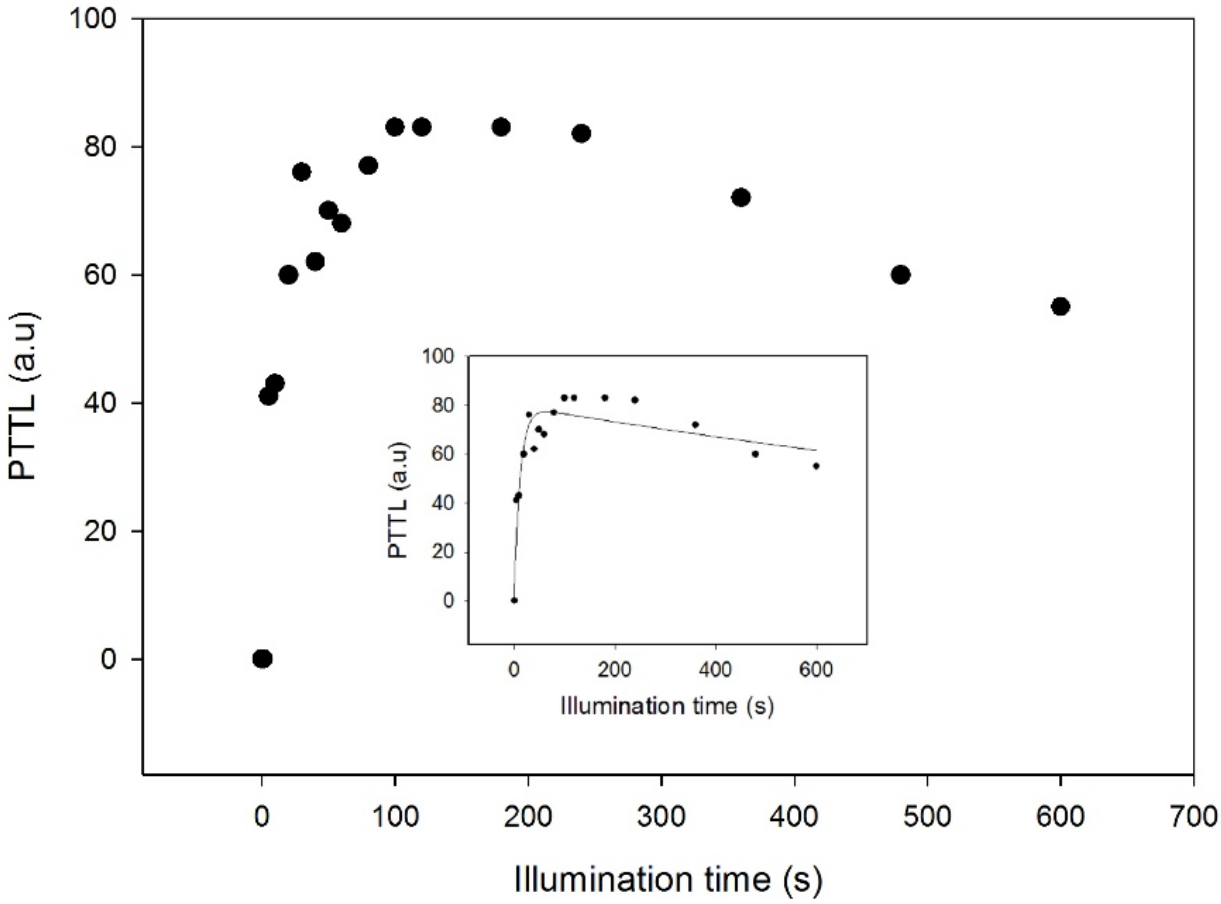

Figure 5.80: PTTL peak area against illumination time for peak I following preheating to 500°C in an unannealed sample *A*. PTTL data are not properly fitted by using assumptions of equation 3.33 (inset). The sample was previously dosed to 0.5 Gy and the heating rate of $5^{o}\mathrm{C\,s^{-1}}$ was used.

traps in a sample illuminated with 470 nm blue light for a given illumination time after preheating to certain temperatures to empty shallow traps.

The intensity of PTTL changed as a function of illumination time in three ways. These are:

1. Increasing to saturating exponential.

2. An increase from zero to a maximum followed by a decrease to zero.

3. Other PTTL peaks showed an increase followed by a decrease to non-zero constant.

The more preheating was increased to high temperatures, the much slower was the

decrease of intensity observed. Annealing at 900°C for 15 minute removes residual charges from deep traps. It follows that PTTL intensity for peak I disappears in annealed samples for low beta dose less than 3 Gy due to partially-filled deep traps during irradiation.

Kinetic analysis showed that the activation energy of PTTL peak I is about 0.7 eV, the same value for the normal TL from peak I. In addition, PTTL peak I suffers from thermal quenching with activation energy and pre-exponential factor of thermal quenching equal to 1.03 ± 0.08 eV and constant $C = 3 \times 10^{11}$ respectively. However, the normal TL peak I is not affected by thermal quenching. This contrasting effect between TL and PTTL for peak I suggests a further study. The PTTL peak I fades with storage with the lifetime of about 14 s. A slow fading of normal TL peak was also observed from peak I with the lifetime of 180 s.

A future study on PTTL from secondary glows peaks may consider the dose response of PTTL at higher doses, identifying the donor traps and the study of luminescence properties of deep traps. The dosimetric features of secondary PTTL peaks may also be studied at high doses greater than 3 Gy. It is also important to develop a general model which can be used to explain any PTTL behaviour observed in many PTTL experiments in α-$Al_2O_3 : C$. This may be compared with a general model under the assumption of quasi-equilibrium and non-retrapping of electrons using some experimental results from PTTL that were accounted for.

Chapter 6

Conclusion

The aim of our project was to study the thermoluminescence (TL) and phototransferred thermoluminescence (PTTL) from secondary peaks in α-$Al_2O_3 : C$ and to interpret results in terms of the physics of point defects involved. A TL glow curve measured in a sample heated from 30 to 500°C after irradiation to a dose of 0.5 Gy showed three peaks at a heating rate of $1^{o}C\,s^{-1}$. There is a peak at 46°C (peak I), the main dosimetric peak at 186°C (peak II) and a high temperature peak at 314°C (peak III) corresponding to the shallow, main and intermediate deep traps respectively.

The thermal cleaning method showed that peak II is a superposition of two overlapping peaks. Peak III was separated from others by preheating to a given temperature to remove peak II. The subsequent TL glow curve then showed a new peak, peak IIA, at the low temperature side of peak III. The position of peak IIA was different from the original position of peak II. We conclude that peak IIA overlaps the main peak (II). Another secondary peak at 422°C (peak IV) was also observed. However, the kinetic analysis of peak IV was not done due to its weak intensity. The peak is not well defined even at the relatively high dose level of 3 Gy.

Kinetic analysis of TL for peak I yielded values of the activation energy between 0.7 and 1 eV using different methods. The frequency factor s varied from 10^{10} to $10^{15}\,s^{-1}$. Sources of errors include overestimation made in choosing parameters used to calculate the activation energy in some methods such as the peak shape and variable heating rate methods. The peak position for peak I shifts to higher temperatures as the heating rate

increases from 0.2 to 6°C s^{-1}. The TL intensity for peak I also increases as a function of a heating rate. Peak I is affected by thermal fading following a delay between irradiation and TL measurements. This implies that the electron trap responsible for peak I is unstable at room temperature and its retrapping probability is negligible. Peak I fades exponentially as a function of time with a half-life of about 120 s.

The dose dependence of TL for peak I from 0.5 to 2.5 Gy was linear. The linear dependence of TL on dose was confirmed by a supralinearity index g(D) = 1. This means that at low doses between 0.5 and 2.5 Gy, peak I can be used in dosimetry. In addition, the position of peak I did not change with dose from 0.5 to 2.5 Gy. This means that the peak position for peak I was not affected by the change of the concentration of electrons in the corresponding trap, further confirmation that peak I is of first order kinetics. The $T_M - T_{stop}$ method showed that peak I is free of overlapping peaks and that it is a first order peak.

The kinetic analysis of peak III was done after increasing the dose to 3 Gy in a sample annealed at 900°C for 15 minutes. A heating rate of 0.4°C s^{-1} was used. A glow curve of the TL showed peak I at 36°C, peak II at 156°C and peak III at 268°C. An overlap of peak II at 170°C (peak IIA) and another secondary peak at 422°C (peak IV) were also observed after thermal cleaning to observe peak III. Peak IIA is affected by thermal quenching.

In contrast to peak I, the intensity of the TL from peak III decreased as the heating rate increased from 0.2 to 6°C s^{-1}. This decrease was due to thermal quenching. The activation energy and the constant of thermal quenching were W = 1.48 ± 0.10 eV and C = 4×10^{13} respectively. The W and C values obtained for peak III are consistent with the values previously calculated for peak II confirming that all electron traps in α-Al_2O_3 : C use one recombination centre. As peak I, peak III was also found to follow first order kinetics.

The PTTL from secondary peaks was first investigated in samples not annealed at 900°C for 15 minutes. At a second step, the PTTL measurements were done in annealed samples. Only peaks I and II were regenerated under PTTL. The plot of the

PTTL intensity against illumination time showed a peak-like structure. The following PTTL features were observed from peaks I and II at a heating rate of $5^{o}C\,s^{-1}$ after a dose of 0.5 Gy as follows:

(a) Samples A and A_1: Not annealed at 900°C *for 15 minutes in first PTTL measurements*

Two samples A and A_1 were used for PTTL measurements to compare the effects of PTTL from secondary peaks in this group of unannealed samples. Sample A showed that the PTTL is produced from peak I following preheating between 100°C through 500°C. The PTTL from peak II was observed even after annealing at 700°C for 15 minutes. In sample A_1, peak I was regenerated under PTTL only in measurements following preheating to 80°C, a temperature that removes peak I. The PTTL from peak II was observed in sample A_1 preannealed at a temperature less than 600°C for 15 minutes.

(b) Sample B: Annealed at 900°C *for 15 minutes in between measurements*

The PTTL measurements in sample B showed that the PTTL intensity for peak I disappeared after annealing 4 times in between measurements after each illumination time from 0 to 30 s. In contrast to unannealed samples A and A_1, sample B preheated to temperature beyond 320°C to remove peaks I, II and III did not produce any PTTL signal after a dose of 0.5 Gy.

Samples A, A_1 and B annealed many times (3 times and more) in between measurements at 900°C for 15 minutes did not produce any PTTL signal from peak I after a dose of 0.5 Gy. This confirms the fact that the residual charge in deep traps which can be removed after annealing at 900°C for 15 minutes contributed in producing PTTL from peak I in unannealed samples. Also, dosing a sample to 0.5 Gy did not fill deep traps responsible for PTTL from peak I. After increasing the dose to 3 Gy, the PTTL intensity measured following preheating to certain temperatures to remove peak I had showed that peak I is reproduced under PTTL. In all samples A, A_1 and B annealed at 900°C for 15 minutes many times in between measurements, no peak was regenerated as PTTL after preheating to 500°C and above.

The kinetic analysis of the PTTL from peak I showed that the activation energy of PTTL for peak I is about 0.7 eV, similar to the activation energy of the normal TL for peak I. PTTL of peak I suffers from thermal fading with storage between the end of illumination time and PTTL measurements. Peak I fades rapidly to its half-maxmum intensity at 50 s. Thermal fading of PTTL from peak I follows an exponential-like decay with a half-life of about 10 s. In contrast to the normal TL, the PTTL intensity increases when the heating rate increases from 0.2 to $6^{o}\mathrm{C\,s^{-1}}$. The cause of this difference is not clear. The decrease of the intensity of the PTTL from peak I as a function of a heating rate is attributed to thermal quenching. The activation energy of the thermal quenching was calculated as $1.03 \pm 0.08\,\mathrm{eV}$.

Suggestions for further research

Although delocalised energy levels corresponding to the TL from different peaks have been identified, the nature and types of these energy levels (electron or hole traps) are not well defined. The dynamics of charge exchange between defect levels leading to the TL emission was observed but the mechanisms involved in the luminescence have to be refined. The following areas are may be further studied.

1. Kinetic analysis of deep (electron and hole) traps and their influence on TL.

2. Study the influence of the shallow trap on the dosimetric trap.

3. Comparative study on luminescence of α-Al_2O_3 : C using time-resolved and TL.

Bibliography

[1] S.W.S. McKeever. *Thermoluminescence of solids*. Cambridge University Press, UK, 1985.

[2] R. Chen and S.W.S. McKeever. *Theory of Thermoluminescence and Related Phenomena*. World Scientific Publishing, 1997.

[3] S.W.S. McKeever, M. Moscovitch and P.D. Townsend. *Thermoluminescence Dosimetry Materials: Properties and Uses*. Nuclear Technology, UK, 1995.

[4] G.E. Yukihara and S.W.S. McKeever. *Optically Stimulated Luminescence: Fundamentals and Applications*. John Wiley and Sons Ltd, 2001.

[5] V. Pagonis, G. Kitis and C. Furetta. *Numerical and Practical Exercises in Thermoluminescence*. Springer, 2006.

[6] Claudio Furetta. *Questions and Answers on Thermoluminescence and Optically Stimulated Luminescence*. World Scientific Publishing Ltd, 2008.

[7] S.W.S. McKeever and R. Chen. Luminescence models. *Radiat. Meas.*, 27:625–661, 1997.

[8] M.L. Chithambo and C. Seneza. Kinetics and dosimetric features of secondary thermoluminescence in carbon-doped aluminium oxide. *Physica B*, 439:165–168, 2014.

[9] M.L. Chithambo. Concerning secondary thermoluminescence peaks in α-Al_2O_3:C. *S. Afric. J. Sci.*, 100:524–527, 2004.

[10] D.R. Mishra, M.S. Kulkarni, K.P. Muthe, C. Thianahara, M. Roy, S.K. Kulshreshtha, S. Kannan, B.C. Bhatt, S.K Gupta and D.N. Sharma. Luminescence properties of α-Al_2O_3:C with intense low temperature TL peak. *Radiat. Meas.*, 42:170–176, 2007.

[11] V.S. Kortov, S.V. Nikiforov and E.Z. Sadykova. Competing processes with participation of shallow traps in an-anion defective aluminium oxide. *Russ. Phys. J.*, 49:221–224, 2006.

[12] Y. Kirsh. Kinetic analysis of thermoluminescence. theoretical and practical aspects. *phys. stat. sol. (a)*, 129:16–45, 1992.

[13] M. Karmakar. On initial rise method for kinetic analysis in thermoluminescence. *INDJST*, 5:3674–3677, 2012.

[14] G.Kitis, J. Papadopoulos, S. Charalambousn and J.N. Tuyn. The influence of heating rate on the response and trapping parameters of α-$Al_2O_3 : C$. *Radiat. Prot. Dosim.*, 55:183–190, 1994.

[15] G.Kitis. TL glow-curve deconvolution for various kinetic orders and continous trap distribution: Acceptance criteria for E and s values. *J. Radioanal. Nucl. Chem.*, 247:697–703, 2001.

[16] C.S. Alexander and S.W.S. McKeever. Phototransferred thermoluminescence. *J. Phys. D: Appl. Phys.*, 31:2908–2920, 1998.

[17] E. Bulur and H.Y. Göksu. PTTL from α-Al_2O_3:C using blue LED. *Radiat. Meas.*, 30:203–206, 1999.

[18] C.S. Alexander, M.F. Morris and S.W.S. McKeever. The time and wavelength response of photontransferred thermoluminescence in natural quartz. *Radiat. Meas.*, 27:153–159, 1997.

[19] A.G. Wintle and A.S. Murray. The relationship between quartz TL, PTTL, and OSL. *Radiat. Meas.*, 27:615, 1997.

[20] L. Bøtter-Jensen, N. Agersnap Larsen, V. Mejdahl, N.R.J. Poolton, M. F. Morris and S.W.S. McKeever. Luminescence sensitvity changes in quartz as a result of annealing. *Radiat. Meas.*, 24:535–541, 1995.

[21] V. Pagonis, R. Chen, J.W. Maddrey and B. Sapp. Simulations of time-resolved photoluminescence experiments in α-Al_2O_3 : C. *J. Lumin.*, 131:1086, 2011.

[22] S.V. Nikiforov, I.I. Milman and V.S. Kortov. Thermal and optical ionization of F-centres in the luminescence mechanism of anion-defective corundum crystals. *Radiat. Meas.*, 33:547–551, 2001.

[23] Technical University of Denmark. *User manual of the Risø TL/OSL-DA-20 Reader*. Risø National Laboratory, DTU, Denmark, 2011.

[24] M. Zahedifar, L. Eshraghi and E. Sadeghi. Thermoluminescence kinetics analyis of α-Al_2O_3:C at different dose levels and populations of trapping states and a model for its dose response. *Radiat. Meas.*, 47:957–964, 2012.

[25] A. Nyirenda. Mechanisms of luminescence in α-Al_2O_3:C: Investigations using time-resolved optical stimulation and thermoluminescence techniques. *Unpublished MSc thesis*, 2012.

[26] S.V. Nikiforov, V.S. Kortov, S.V. Zvonarev, E.V. Moiseykin, M.G. Kazantseva. Basic luminescence and dosimetric properties of α-Al_2O_3:C irradiated by pulse intensive electron beam. *Abstract. 17th international conference on solid state dosimetry. Recife-Brasil*, 2013.

[27] V.S. Kortov, I.I. Milman, V.I. Kirpa and Ja. Lesz. Thermal quenching of tl in α-Al_2O_3:C dosimetric crytals. *Radiat. Prot. Dosim.*, 65:255–258, 1996.

[28] V. Pagonis, C. Ankjaergaard, M. Jain and R. Chen. Thermal dependence of time-resolved blue light stimulated luminescence in α-Al_2O_3:C. *J. Lumin.*, 136:276, 2013.

[29] M.L. Chithambo. The analysis of time-resolved obtically stimulated luminesence:II. computer simulations and experimental results. *J. Phys. D: Appl. Phys.*, 40:1880–1889, 2007.

[30] F.O. Ogundare, S.A. Ogundale, M.L. Chithambo and M.K. Fasasi. Thermoluminescence characteristics of the main glow peak in α-$Al_2O_3 : C$ exposed to low environmental-like radiation doses. *J. Lumin.*, 139:143, 2013.

[31] V. Pagonis, R. Chen, J.W. Maddrey and J.L. Lawless. A quantitative kinetic model for Al_2O_3:C: TL response to ionizing radiation. *Radiat. Meas.*, 42:200, 2007.

[32] M.S. Akserlod, N. Agersap, V. Whitley and S.W.S. McKeever. Thermal quenching of F-center luminescence properties in Al_2O_3:C. *J. Appl. Phys.*, 84:3364–3373, 1998.

[33] A.N. Yazici, S. Solak, M. Topasksu and Z. Yegingil. The analysis of dosimetric thermoluminescent glow peak of Al_2O_3:C after different dose levels by beta-irradiation. *J. Phys. D: Appl. Phys.*, 36:181–191, 2003.

[34] G.S. Polymeris and G. Kitis. Thermally assisted photo transfer OSL from deep traps in Al_2O_3:C grains exhibing different TL peak shapes. *Appl. Radiat. Isot.*, 70:2480, 2012.

[35] M.L. Chithambo. Dependence of the thermal influence on the luminescence lifetimes from quartz on the duration of optical stimulation. *Radiat. Meas.*, 37:167–175, 2003.

[36] A. Wintle. Thermal quenching of thermoluminescence in quartz. *Geophys. J.R. Astr. Soc.*, 41:107, 1975.

[37] E.G. Yukihara, V.H. Whitley, J.C. Polf, D.M Klein, S.W.S. McKeever, A.E. Akselrod and M.S. Akselrod. The effects of deep trap population on the thermoluminescence of α-$Al_2O_3 : C$. *Radat. Meas.*, 37:627–638, 2003.

[38] M.S. Akserlod and E.A. Gerelova. Deep traps in highly sensitive α-Al_2O_3:C TLD crystals. *Nucl. Tracks Radiat. Meas.*, 21:143–147, 1993.

[39] V.S. Kortov, I.I. Milman, Nikiforov, and E.V. Moiseykin. The role of deep traps in the luminescence mechanism of anion-defective single crystals of aluminium oxide. *Phys.Stat.Sol.(c)*, 2:515–518, 2005.

[40] E.G. Yukihara, V.H. Whitley, S.W.S. McKeever, A.E. Akselrod and M.S. Akselrod. Effect of high-dose irradiation on the optically stimulated luminescence of $Al_2O_3 : C$. *Radat. Meas.*, 38:317–330, 2004.